1-6-2017

Part I Convergent Total Synthesis of Bioactive Dipeptide–Lipids Isolated from Porphyromonas gingivalis: Possible Biomarker for Multiple Sclerosis Part II Synthesis of Nitroimidazole Indocyanine Green Dye Conjugates for Targeting Hypoxia in Tumor Cells for Near Infrared Fluorescence Frequency Domain Optical Tomography

Christopher James Dietz
christopher.dietz@uconn.edu

Part I

Convergent Total Synthesis of Bioactive Dipeptide–Lipids Isolated from *Porphyromonas gingivalis*: Possible Biomarker for Multiple Sclerosis

Part II

Synthesis of Nitroimidazole Indocyanine Green Dye Conjugates for Targeting Hypoxia in Tumor Cells for Near Infrared Fluorescence Frequency Domain Optical Tomography

Christopher James Dietz, Ph.D.

University of Connecticut 2017

Mankind's greatest attribute is the capability of higher order intellect being applied to prolonging life and improving one's overall health. Modern medicine and the research therein has created opportunities to understand and combat disease at incredible levels. Yet, some of the most befuddling diseases are ones that our own bodies inheritably produce. Autoimmune disease is a condition in which the body's own defense mechanisms begin to target healthy cells as if they were foreign threats. Cancer is a condition in which abnormal cell growth can spread throughout the body and begin to shut down vital bodily functions. Medicinal chemistry has difficulty combating and understanding such diseases due to the fact that intervention targets of the disorders are derived from human anatomy. The research presented within aims to aid in the scientific understanding of the two diseases discussed.

Part I: Lipids isolated for *Porphyromonas gingivalis* have been recently implicated in possible development and/or progression of multiple sclerosis. The lipids are produced in bacteria, which are found throughout the GI track, and are shown to invade into the body. First, this study is intended as a structural proof and stereochemical elucidation of the proposed lipid compounds labeled lipid 430 and 654. Second, synthesis of stereochemically pure material is needed for further biological testing to establish a greater understanding of disease implications. We present

the details of the convergent synthesis of lipids 430 and 654, which confirm the proposed structure of *P. gingivalis* lipid 654 to be (3*R* and 3*S*)-L-serine. The bis(fatty acid) (3*R*)-L-serine **2** was prepared as well as the synthetic precursor, serine dipeptide mono-fatty acid (3*R*)-L-serine **1**, which is the structure of lipid 430. We also synthesized the (3*S*)-L-serine diastereomer **2** as well as (3*S*)-L-serine **1**. Using these synthetic standards, we confirmed that phospholipase A2 (PLA2)-mediated hydrolysis of lipid 654 is enantioselective in that only the (3*R*)-L-serine **2**, but not (3*S*)-L-serine **2** is enzymatically hydrolyzed.

Part II: Cancerous tumors have been shown to have a hypoxic microenvironment that creates resistance to radiation therapy and ineffectiveness of common chemotherapy drugs. There is a need for improved noninvasive imaging techniques that detect hypoxic tumors and monitor the effects of administered cancer treatments. To do this we have synthesized hypoxic targeting fluorescence probes derived from FDA approved Indocyanine green dye to be used for optical imaging. Extending our previous work with 2-nitroimidazole-piperazine-indocyanine dye-conjugate **3**, we prepared the 4-nitroimidazole-piperazine-indocyanine derivative **12**. We also prepared imidazole derivative **14** as a control. We compared the *in vivo* hypoxia targeting performance of both with the previously tested 2-nitro dye conjugate, and the 4-nitro derivative showed a higher fluorescent intensity after 15 min post-injection. All findings were supported with fluorescence images of histological sections of tumor samples an immunohistochemistry technique for tumor hypoxia. New generations of the dyes are being created to increase the efficiency of the imaging technique.

Part I

Convergent Total Synthesis of Bioactive Dipeptide–Lipids Isolated from *Porphyromonas gingivalis*: Possible Biomarker for Multiple Sclerosis

Part II

Synthesis of Nitroimidazole Indocyanine Green Dye Conjugates for Targeting Hypoxia in Tumor Cells for Near Infrared Fluorescence Frequency Domain Optical Tomography

Christopher James Dietz

B. S. Niagara University

2008

A Dissertation Submitted
in
Partial Fulfillment of the Requirements
for the
Degree of Doctor of Philosophy
at the
University of Connecticut
2017

Approval Page

Doctor of Philosophy Dissertation

Part I

Convergent Total Synthesis of Bioactive Dipeptide–Lipids Isolated from *Porphyromonas gingivalis*: Possible Biomarker for Multiple Sclerosis

Part II

Synthesis of Nitroimidazole Indocyanine Green Dye Conjugates for Targeting Hypoxia in Tumor Cells for Near Inferred Fluorescence Frequency Domain Optical Tomography

Presented by

Christopher Dietz

Major Advisor _____

Michael B. Smith

Associate Advisor _____

Christian Brückner

Associate Advisor _____

Mark Peczuh

Associate Advisor _____

Edward Neth

Associate Advisor _____

Frank C. Nichols

2017

Acknowledgements

Dr. Michael Smith

Thank you for everything that you have done for me in the last four years, you're the perfect mentor. I arrived at UCONN with every intention of joining the Smith lab, and confirmed that intuition after the first time we spoke. I hope you and Sam enjoy retirement and I look forward to see all the great places you travel to.

Family

Mom and Dad, you're the greatest. Everything I do is to try and make you proud for all the things you have done for me. I could have never done this without you.

Amanda, I have basically followed you throughout my entire life. My academic career can be attributed to following in your footsteps. I love that you're my sister.

Emily, Dietz Nation has gained its first recruit! Thank you for staying by myside and doing all that you have done for me this past four years. The distance was hard but now we have the rest of our life together. I can't wait!

Friends

Thanks to all of you that have put up with me and for some reason still liking me. We will see each other.

Table of Contents

List of Figures

List of Schemes

List of Tables

Convergent Total Synthesis of Bioactive Dipeptide–Lipids Isolated from Porphyromonas gingivalis: Possible Biomarker for Multiple Sclerosis

1.1 Introduction

1.1.1 Disease, introducing the human microbiome

Chemistry, the study of matter, and biology, the study of life, can be linked in a number of ways. Medicinal chemistry is the nexus of modern chemistry and biology. Today, nothing is more important than the collaboration between the two sciences and how this plays in the development, progression, and regression of human disease.

Disease is classified as a disorder in the structure or function of a living organism. The causes of such conditions are seemingly endless. However, the vast majority of diseases are caused by either viruses or bacteria. Viruses, often with extremely complicated pathology, are seemingly simple to understand as to how they can cause disease. They infect human cells and force their exponential reproduction. The chemistry behind this can be extremely complex, but the underlying fact that the infecting agent is on the inside of the cell gives almost definite cause to why or how a viral disease can exist. On the other hand, bacteria produce disease through a wider group of pathogenic mechanisms, some of which are progressively being studied and befuddling researchers as to how they can interact with the human body and its anatomy.

It is easy to understand how a disease can develop from a bacterial infection including invasion and proliferation within the human body. It is like an invader behind enemy lines. On the contrary, the human microbiome, "the ecological community of commensal, symbiotic and pathogenic microorganisms that literally share our body space", has begun to grasp the attention

of scientists due to the extreme complexity of the relationship between the human body and its symbiotic partners.[1] For this reason, the human microbiome has become an area of utmost interest in disease relations over the past few decades.

The Human Microbiome Project (NMP) can be looked at as a continuation of the Human Genome Project. Its Goals include: (1) characterize the human microbiome and (2) Determine the relationship between heath/disease and changes in the biome.[2] The ratio of bacteria to human cells of an average human has been estimated to 1.3. The vast majority reside on internal and external surfaces of the human body including the; gastrointestinal track, urinary track, skin, saliva, oral mucosa, and conjunctiva.[3] This microbial community has been associated with the heath and disease of host multicellular organisms with roles in physiology, metabolism, immunodeficiency, and hypersensitivity.[4]

1.1.2 Multiple Sclerosis (MS)

Autoimmune disorders incorporate nearly 80 different diseases and are considered a leading cause of death and disability, with nearly 24 million reported cases in Americans.[5] This number could be much higher due to the number of undiagnosed patients. Such disorders are a result of the human immune system becoming unable to recognize self from non-self. Normally the immune system responds to foreign materials and has built in safe ways to avoid attacking its own tissues.[6] When this mechanism breaks down, the body begins to combat healthy cells/tissues of various organs including the pancreatic beta cells in diabetes, the joint synovia in rheumatoid arthritis and the central nervous system in multiple sclerosis, resulting in autoimmune disease.

Multiple sclerosis (MS) is one of the more severe autoimmune diseases, as it affects more than 2.3 million people worldwide. The disorder is considered chronic as symptoms range from blurred vision or poor coordination, to more severe effects such as paralysis or blindness. The symptoms differ in every patient, can be permanent or episodic, and often worsen overtime. The disease is found in patients of all ethnicities and can be diagnosed at any age as symptoms develop.[7]

One of the most significant problems with MS is the difficultly of diagnosing the disease. To date, no single laboratory test is available for disease identification. This is extremely problematic because most common treatments aim to suppress the body's immune system which can drastically increase the risk of further illness and infection. Instead of testing for the MS, one is evaluated for common symptoms and cross examined to rule out any other possibile explanations of causality. Physicians test mental functions, movement mobility, and vision for insight into the disease. When significant abnormal neurological findings are apparent, the use of magnetic resonance imaging (MRI) and invasive techniques are used to provide confirmatory evidence that MS is the cause. In 2010, the Revised McDonald Criteria was published by the international panel on diagnosis of multiple sclerosis.[8] This gives the most accurate test to date, as it gives strict guidelines for using the MRI to speed up the process of diagnosis. However it is far from a positive test, as it simply aims to visualize damage that may be the result of MS.

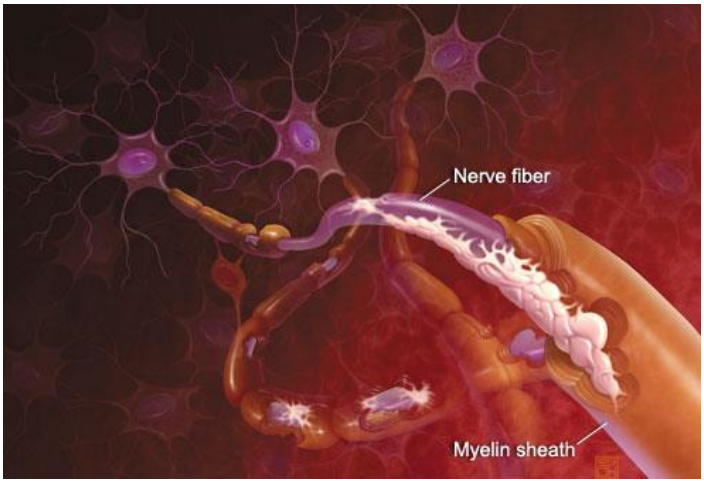

Figure 1. Example of myelin destruction resulting from autoimmune disease.[63]

Within the human body, Multiple Sclerosis is characterized as the immune system producing an inflammatory

response within the central nervous system.[9] This causes damage to cells that make up the signaling pathways of this delicate system. Though there is many theories discussed, the onset and progression of the process remains poorly understood. The universally accepted belief is that MS results from the body's self-produced T cells, a subclass of white blood cells, attack the CNS myelin surrounding nerve cells.[10] The biochemistry for the inflammatory response is unknown but can be facilitated by a number of factors, including environmental factors.

The causes of MS are not exactly established, however researchers have suggested several possibilities of factors that could contribute to disease progression. Genetic factors are thought to play a small roll but there is evidence that the illness isn't directly inherited.[11] Habits and environment are thought to play a larger roll. Populations further from the equator have increased frequencies of MS and attribute this to vitamin D deficiencies. Cigarette smoking has also proven to increase the possibility of developing symptoms of the disease. In totality, the disease is thought to be contributed to 4 causes: immunology, genetics, environmental, and infection factors. Understanding the reason for the autoimmune response could shed light onto the prevention, treatment, and/or detection of the disease.[12] Reading further will shift focus towards the role that human microbiome might play in the pathology of the disease and what evidence this might suggest.

1.1.3 Porphyromonas gingivalis

Inflammatory periodontal disease in adults is initiated with the accumulation of specific bacteria in the sulcus around the teeth, followed by a chronic inflammatory reaction by the host against the colonizing microorganisms. Periodontitis is labeled as an oral inflammatory gum disease that effects the tissues needed to support the teeth.[13] Often, progression of periodontitis

leads to loss of bone in the jaw and eventually tooth loss. The disease is proceeded by certain forms of gingivitis that may be directly caused from bacterial biofilms, or plaques, that buildup on tooth surfaces. Several microorganisms are associated with gingivitis/periodontitis, but substantial studies have implicated *Porphyromonas gingivalis* as a major pathogen in the destructive form of periodontal disease.[14]

P. gingivalis is an anaerobic, rod-shaped, non-motile, Gram-negative bacteria found in the oral cavity and the digestive track.[15] Expanding upon the implications *P. gingivalis* displays in dental disease, evidence has suggested that this bacterium may play a role in autoimmune disorders.[16] Rheumatoid arthritis is another such autoimmune disease associated with periodontal disease. *P. gingivalis* has been shown to contain an enzyme arginine deiminase (ADI) that can modify protein amino acid arginine to citrulline.[18] This transformation is called citrullination. Citrullinated proteins are recognized/attacked by the immune system and can be considered a direct cause of autoimmune diseases that result from the body trying to defend itself from its own proteins.

Several studies have reported findings of *P. gingivalis*' role in pathogenesis of the central nervous systems inflammatory response, leading to the aggravation of MS.[18] It is not understood exactly how or why this happens, but it has been shown that peripheral bacteria in the gastrointestinal track can trigger autoimmune reactivity. This is thought to be the result of the body recognizing agonists that are produced by the bacteria, not necessarily bacterial infection per se. These agonists can be bound to receptors of external tissue cells. Our work leads to the idea that *P. gingivalis* activates in the innate immune system and in such a way to lead to multiple scleroses.

1.1.4 Toll-Like Receptors (TLRs)

The innate immune system, or non-specific immune system, is an important part of the overall immune system. It protects the body from developing infection from microorganisms. Sentinel cells are the body's first line of defense verses pathogens derived from microorganisms that pose potential threats. There is a class of receptor proteins that are embedded in the sentinel cell's membranes that are designed to recognize such structural molecules. The general receptor class is known as Toll-like receptors (TLRs).[19] Their mode of action is triggered by binding pathogen's, small molecules, located on the exterior of the bacteria and are produced by a wide range of microbes. The interaction with these stimuli cause a cascade of signaling pathways inside tissues to activate the innate immune system to fight the foreign invading microbes.[20]

A total of 13 TLRs are known to exist, conveniently labeled TLR1- TLR13, with the first 11 being found in humans. Each receptor has the ability to recognize certain aspects of structurally similar molecules that are shared by a broad range of pathogens. A recent study has shown that TLR2 and TLR4 can play a direct role in CNS damage associated with multiple sclerosis.[21] Ligation to these receptors causes a cascade effect in the immune system that ultimately leads to leukocyte migration across the blood-brain barrier. This is problematic to the nervous system as white blood cells begin to destroy the protective coating, myelin, of nerve cells. Worse yet, through a similar mechanism, differentiation of regulatory T cells is inhibited. The regulatory T cells play an important role in suppressing CNS autoimmunity.[22]

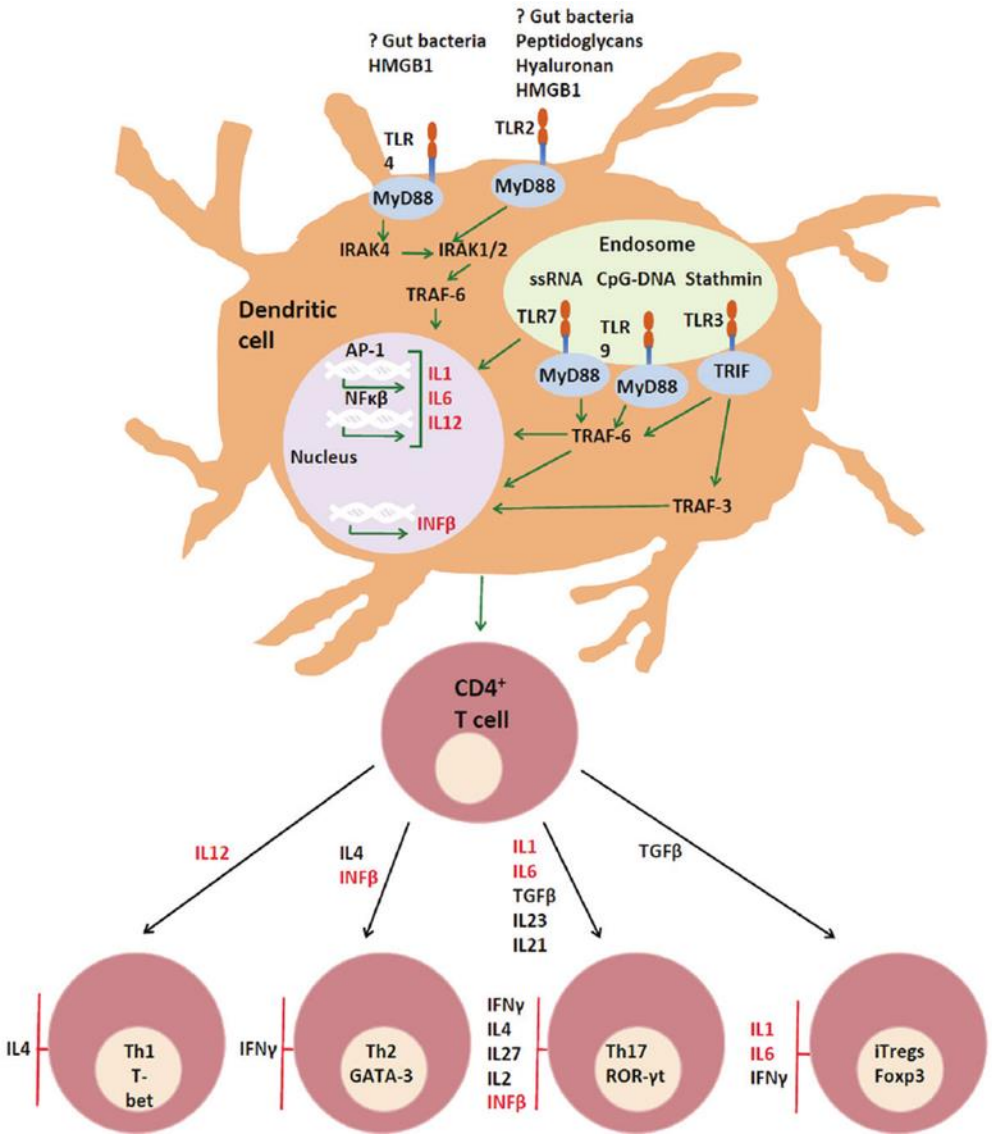

Figure 2. Toll-like receptors in Multiple Sclerosis.

Ligation of TLR2 and TLR4 induces the production of IL1, IL6 and IL12, which induce the differentiation of naïve T cells into Th1 and Th17 cells. Th17 and Th1 cells secrete IL17 and INFγ respectively. IL17/INFγ-producing cells facilitate leukocyte migration across the blood-brain barrier and contribute to CNS damage. IL1 and IL6 also inhibit the differentiation of induced regulatory T cells (iTregs). Tregs are a major source of IL10, a cytokine that plays a critical role in suppressing CNS autoimmunity. Activation of TLR3, TLR7 and/or TLR9 can lead to the production of IFNβ, which activates T suppressor cells and inhibits the production of IL17 and IL23.[21]

Reprinted directly from Miranda-Hernandez, S.; Baxter, A. G. *Am. J. Clin. Exp. Immunol*. **2013**, 2, 75-93**.**

Toll-like receptor 2 (TLR2) is known to recognize a broad class of structures from micro bacteria. Many of the substrates that do this closely resemble lipoproteins or fatty acids.[23] A recent report revealed that the lipid extract from *P. gingivalis* promotes activation of mouse dendritic

cells and inhibits osteoblast-mediated bone deposition through engagement of TLR2.[24] Studies originally claimed that *Porphyromonas gingivalis* lipoprotein, lipopolysaccharide (LPS), and fimbriae were the cause for TLR2 activation.[25] However, the extent these products mediate such reactions is disputed.[26] Upon further investigation, specific serine containing lipids isolated from *P. gingivalis* were structurally characterized and proven to be TLR2 ligands.[27]

1.1.5 Potential Serum Biomarker for MS

The role that *P. gingivalis* plays in the progression of gingivitis and periodontal disease can be directly correlated to the ligation of the bacteria's pathogens to TLR2. Inflammation of the gums is a major part of the disease. However, as stated earlier, *P. ging*ivalis and similar commensal bacteria may be contributing to the inflammatory response of the central nervous system in MS. This potential etiologic environmental factor can give definite evidence towards a mechanism or causality. But the study of the bacteria populating the GI tract could lead to a diagnostic aid, progression predictor, and/or possible target for therapeutic intervention for multiple sclerosis.

Recently, lipidomic work done by Clark et al at the University of Connecticut Health Center, showed that one of the serine lipids of *P. Gingivalis*, Lipid 654 (**2**), is detectable in the blood serum of all individuals.[28] This was done using multiple-reaction-monitoring (MRM) mass spectrometry. The most important finding in this work was that this lipid was found at significantly lower levels in patients diagnosed with MS. This was compared to the serum of healthy individuals and patients with Alzheimer's disease. This result, along with the involvement the serine lipids have in TLR activation, create a need for structural validation and stereochemical elucidation

1.1.6 Serine Lipid Targets

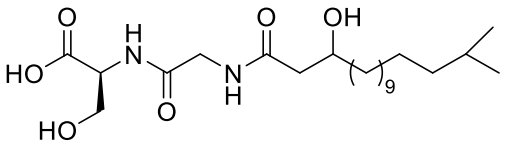

Lipid 430 (**1**)

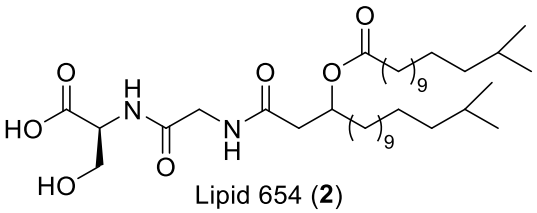

Lipid 654 (**2**)

Lipid **1** and **2** are the hypothesized structures of the bioactive ligands responsible for TLR2 activation and are commonly observed in chronically inflamed human tissues.[27] They were deduced using nuclear magnetic resonance (NMR) and tandem mass spectroscopy (MS/MS). The lipids are composed of a serine glycine dipeptide in an amide linkage to a 3-OH isobranched (iso) $C_{17:0}$ fatty acid. This base compound is labeled lipid 430 (**1**) which is indicative of its mass. The 3-OH iso-$C_{17:0}$ fatty acid moiety may form a 3-OH ester linkage to a saturated fatty acid, most frequently to iso-$C_{15:0}$. This esterified lipid is labeled lipid 654 (**2**).

A search of the literature indicated that this structure was originally proposed for a serine lipid product isolated from a limited number of Flavobacteria and was termed flavolipin.[29-32] We have also observed that lipid 430 was produced by enzymatic hydrolysis of lipid 654 and was, therefore, a logical synthetic precursor. Other fatty acids can substitute into these lipid classes, but they are less abundant relative to branched $C_{15:0}$ and 3-OH iso $C_{17:0}$.[33] Both of the serine dipeptide lipids, lipid 430 and lipid 654, are recovered in lipid extracts of *P. gingivalis*, but lipid 430 is recovered in low levels compared with lipid 654. Chiral GC-MS analysis showed that the serine lipids only contained L-serine stereochemistry. The absolute configuration of the β carbon of 3-OH iso $C_{17:0}$ fatty acid portion of the lipids was not as easy to elucidate. To do this the lipids would need a high level of quantification and difficult derivations to run 2D NMR experiments.

1.1.7 Phospolidase A2

Previously, catalytic deesterification of *P. gingivalis* derived lipid 654 to lipid 430 was observed using commercially available preparations of phospholipase A2 (PLA2).[33] PLA2 is an important enzyme in the release of arachidonic acid from glycerol-based phospholipids and levels of this enzyme are increased in chronically inflamed tissues. However, it was noted that a portion of lipid 654 isolated from *P. gingivalis* was not hydrolyzed by PLA2. Chiral fractionations show about 10-15% of one isoform and 85-90% of the other 654 isoform. In the *P. gingivalis* derived 654, recent HPLC analysis with direct infusion into the mass spectrometer suggest that the one isoform is less than 10%. These results suggest that enzymatic hydrolysis is stereospecific. Identification of the stereochemistry of **1** and **2**, as well as confirmation of which isoform is selectively hydrolyzed, required verification by total synthesis for enzymatic hydrolysis studies.

1.1.8 Literature Synthetic Approaches to Target Lipids

This investigation aimed to prepared both (3*R*) and (3*S*)-L-serine-lipid 430 and thereby both (3*R*) and (3*S*)-L-serine-lipid 654 and to ascertain if only one diastereomeric form of synthetic lipid 654 was susceptible to PLA2 enzymatic hydrolysis. If selective hydrolysis is observed, the diastereospecificity of the partial hydrolysis of *P. gingivalis* lipid 654 by PLA2 would be confirmed. This could be accompanied by the role that the diastereomers play in TLR2 ligation. The biological activity associated with lipid 654 and lipid 430 is sufficiently important that synthesis is a priority for structural verification, the accumulation of synthetic standards, and the preparation of each lipid in sufficient quantity for further biological evaluation.

Structure **2** has been reported as an isolate from several natural products. Uchida and coworkers isolated dipeptide lipids from *Flavobacterium* sp. No. 3559, and the compound labeled WB-3559 D.[29] In this work, WD-3559 D was shown to be a platelet aggregation inhibitor, and stimulated mouse plasma euglobulin clot lysis time. Kawai and coworkers identified a serine-containing lipid along with ornithine containing lipids from extractable cellular lipids in *Flavabacterium meningosepticum* and *F. indologes*, which are opportunistic pathogens.[30] The serine-containing lipid was identified and shown to be an immunoactivator that exhibited immuomodulator activity, and it was also identified as a blocking agent against endotoxemia.[31] Finally, Andoh and coworkers isolated a dipeptide lipid from strain B-572 of *Flexibacter topostinus* sp. nov. and it was named topostin D640.[32] Topostins are inhibitors of mammalian DNA topoisomerase I (topo I). All of these isolated compounds were deduced a structure of what we call lipid 654 (**2**). To date, these biological results have led to three synthetic strategies for structural validation and stereochemical correlation of the lipid.

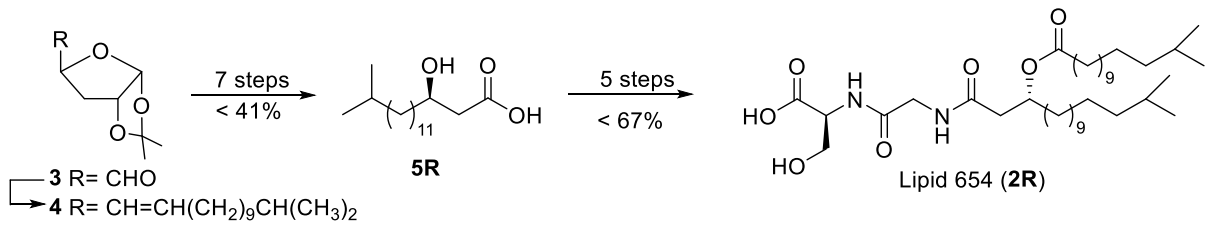

Scheme 1. Synthesis from Uchida et al.[34]

Uchida and coworkers were the first to isolate and synthesize Lipid 654 (**2**).[29,34] Their synthetic strategy started with aldehyde **3**, (3aR,5S,6aR)-2,2dimethyltetrahydrofuro[2,3-d][1,3]dioxole-5-carbaldehyde, functionalized from D-glucose in 10 steps.[35] The isobranched lipid chain was built into the complexity of the molecule via Wittig reaction with separately prepared

11-methyl dodecyltriphenyl- phosphorane to produce olefin **4**. Hydrogenation over Adam's catalyst and cleavage of the isopropylidene ketal, afforded the cyclic diol that was cleaved with sodium periodate and oxidized to produce (3R)-hydroxy-15-methylhexadecanal (**5R**). This sequence of reactions led to an overall yield as high as 41% in 7 synthetic steps.

Uchida and coworkers then reported a linear synthesis of lipid 654 from the crucial intermediate **5R**. Glycine benzyl ester and 13-methyltetradecanoic acid were coupled via amidation using N-hydroxy succinimide to activate the acid moiety and simple acid chloride acylation of the β hydroxy group respectively. The stepwise elongation was finished by hydrolysis deprotection of the benzyl ester and similar acid activation coupling with L-serine. From the steps that were reported, lipid **2R** was produced in 27% yield over 13 steps, from complex starting material **3**.

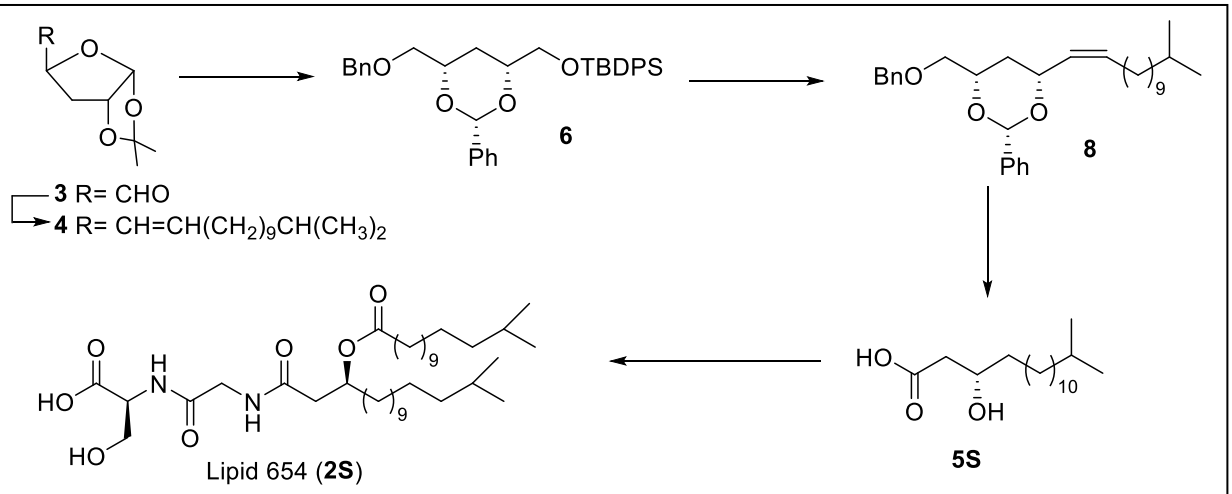

Scheme 2. Synthesis from Shiozaki et al.[36]

Shiozaki and coworkers prepared β hydroxy acid **5S** in 7 steps from the same aldehyde (**3**) as Uchida, however this was done in a different schematic manner.[36] Reduction of the aldehyde

and benzyl protection led to compound **6**. This 3-deoxy-pentose derivative was deprotected to the hemiacetal before treatment with sodium borohydride to open the ring between the oxygen and carbon 1 to produce the triol backbone for compound **7**. Protection of this triol ultimately yielded **7**. Sequential silyl ether cleavage, followed by Swern oxidation and a Wittig reaction with prepared 11-methyldodecyltriphenylphosphorane gave olefin **8**. This produced the scaffold for isobranched lipid chain in a similar manor as the previous synthesis, but utilized the oxygen atoms in a different orientation to produce the opposite enantiomer.

Compound **8** was subjected to hydrogenation conditions, reduction of the alkene and a global deprotection. Then the vicinal diol was cleaved with sodium periodate before ultimately being oxidized to β hydroxy fatty acid **3S**. The acid was esterified with diphenyl diazomethane, the hydroxyl group was acylated with 13-methyltetradecanioic acid, then hydrogenolysis yielded acid **9**. Tandem coupling/hydrogenolysis of glycine benzyl ester and then L-serine benzyl ester respectively, yielded lipid **2S**. The 19 step synthesis from D-glucose produced the product lipid in a reported 4% overall yield.

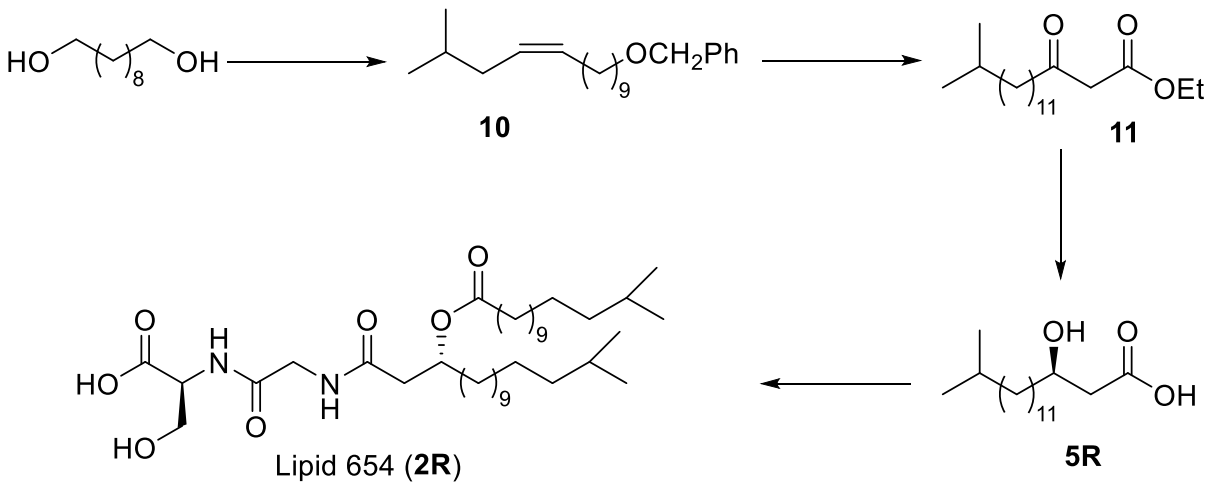

Scheme 3. Synthesis from Shioiri et al.[37]

Shioiri and coworkers synthesized lipid **2R** from economically friendly 1,10-decanediol.[37] Starting by stoichemetric benzylation followed by Swern oxidation of the free alcohol, allowed for the production of olefin **10** via Wittig reaction with isoamyltriphenylphosphonium bromide. Therefore the isobranched lipid chain was built into the molecule very efficiently. Catalytic hydrogenation over palladium-carbon would result in the reduction of the alkene and deprotection of the benzylated alcohol. Then oxidation to the carboxylic acid proceeded a magnesium enolate anion coupling of ethyl hydrogen malonate to afforded β keto ester **11**.[38] Asymmetric hydrogenation via ruthenium (II) catalyst system with (*R*)-BINAP as a ligand produced β hydroxy acid **5R** after saponification.

Much like the other syntheses, the final steps utilized a stepwise elongation of the molecule. First, condensation with glycine *tert*-butyl ester and *O*-acylaation with 13-methyltetradecanoic acid. Then, acid deprotection of the *tert*-butyl ester before coupling with L-serine benzyl ester and sequential deprotection, yielded lipid **2R**. This was the most efficient and nearly enantiomerically pure synthesis, achieved in 13 steps in a linear sequence that utilized asymmetric hydrogenation of a β-keto ester intermediate in an overall yield of about 11%. It also should be noted that this procedure is the only one that could yield both enantiomers of **5** with identical procedures.

Each synthesis incorporated unique and creative transitions throughout. The major goal was to produce intermediate **5** as efficiently and stereospecifically as possible. Chiral starting materials allow for the production of this lipid chain enantiomerically pure. However stereospecific production in the later stage of shiori's work, allowed for the production of both enantiomers. All three strategies chose to build the tagets in a stepwise elongation from the produced lipid chain. Since the β-hydroxy acid **5** is valuable material, a convergent synthesis could be utilized to increase yields, as it would carry material through less synthetic steps.

1.1.9 Retro Synthesis of Target Lipids

The synthetic goal was to verify the structural identity of lipid 654 (**2**), which would correlate with the previously identified and synthesized flavolipin. The previous syntheses produced hydroxy acid **5**, which could be converted to serine-glycine derivative **1**, which we believed to be lipid 430. While the stereochemistry of our lipid 430 and lipid 654 were unknown, our previous work indicated that the serine dipeptide lipids of *P. gingivalis* are primarily constituted with L-serine. This assumption is also consistent with previous reports of 2 by Uchida, Shiozaki, and Shioiri.

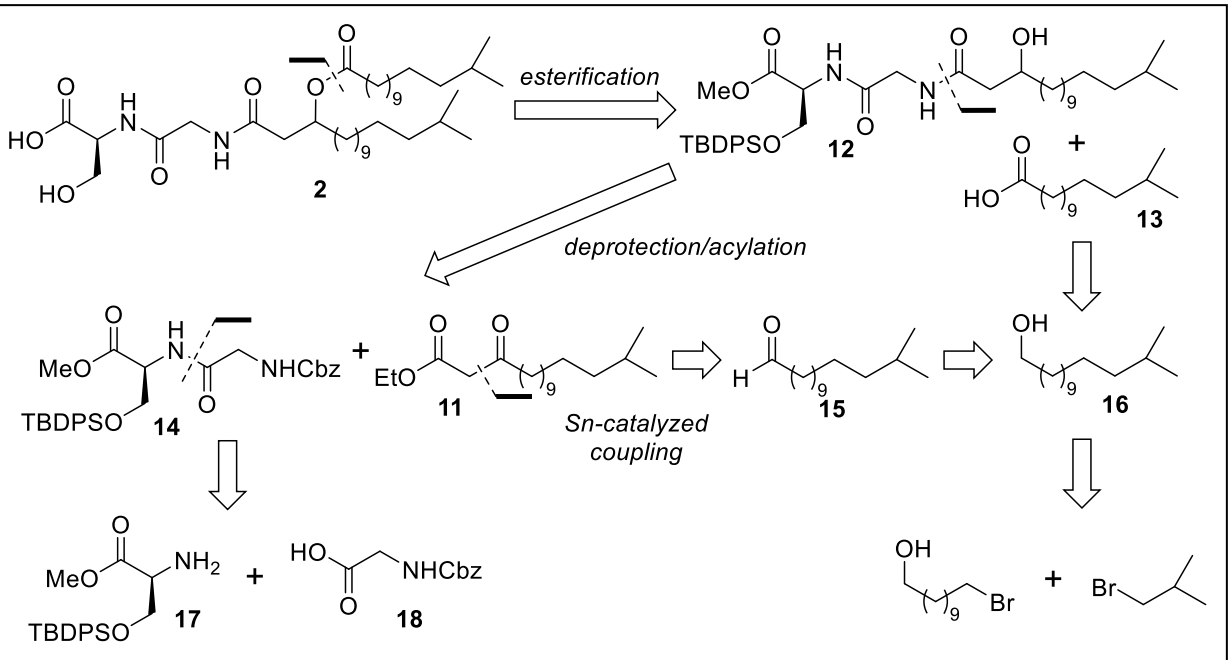

Scheme 4. Retro synthesis of L-serine lipids

Our retrosynthesis began with cleavage of the labile ester linkage from the putative structure for lipid 654 (**2**), which generated the putative structure of lipid 430 (**1**) and 13-

methyltetradecanoic acid (**16**). Disconnection of the peptide linkage to the β-hydroxy fatty acid moiety in **12** gave the L-serine-glycine dipeptide **14** and β-hydroxy acid derivative **11**. We therefore envisioned a convergent strategy that utilized elements of our previous work that would take advantage of the previously published syntheses to prepare **1** and then **2** using a protected L-serine-glycine dipeptide **14**. We believed that this approach would allow us to generate both diastereomers of L-serine **1** and of L-serine **2**, and in a shorter linear synthesis than previously reported.

Disconnection of **11** led to an acetate surrogate and 13-methyltetradecanal, **15**. Disconnection of **14** led to protected serine and glycine derivatives **17** and **18**. Aldehyde **15** can be prepared from 13-methyltetadean-1-ol (**16**) using previously published coupling of the Grignard reagent prepared from 1-bromo-2-methylpropane with 11-bromoundecan-1-ol.[39] We planned a coupling reaction of ethyl diazoacetate with **15** to give a β-keto ester **11**.[40] Subsequent reduction of the ketone, followed by saponification, would generate the racemic β-hydroxy acid, **5**. One approach could use the asymmetric hydrogenation procedure reported by Shioiri.[37] Alternatively, a classical resolution of this β-hydroxy fatty acid would yield each enantioenriched product.

1.2 Results and Discussion

1.2.1 Synthesis of Lipid 430 and Lipid 654

The initial steps of the synthesis focused on the fatty acid portion of the targeted lipids and the preparation of **16**, based on our published synthesis of dihydroceramides isolated from *P. gingivalis*.[41] The Grignard reagent prepared from 1-bromo-2-methylpropane was coupled to 11-bromoundecanol, in the presence of a lithium tetrachlorocuprate complex. A large excess of Grignard reagent was used to convert the alcohol to an alkoxide in situ, thus avoiding the use of a protecting group. The use of excess reagent can be avoided if 11-bromoundecanol is protected prior to the coupling reaction and additives are incorporated. In the latter case, however, there was a decrease in overall yield mainly attributed to the handling over the three steps. The fact that 2-methylbromopropane is much cheaper than the other reagents led us to use the unprotected alcohol in the coupling step. Oxidation of alcohol **16** with an oxoammonium reagent "Bobbitt's salt" (4-acetamido-2,2,6,6-tetramethylpiperidine 1-oxyl) yielded aldehyde **15** with no over-oxidation to the acid.[42] Upon exposure to air at ambient temperature, this aldehyde proved to be rather unstable, with rapid oxidation to the carboxylic acid **13**. If aldehyde **15** was maintained in wet THF solution until needed, the yield was near quantitative for the oxidation step and 91% from starting material 11-bromoundecanol.

The β–Keto ester **11** was prepared by the reaction of **16** with ethyl diazoacetate in the presence of catalytic tin (II) chloride, using the protocol developed by Roskamp et al.[40] Under these conditions, ester **11** was obtained in 80-90% yield under very mild conditions, although small amounts of carboxylic acid **13** were also observed. Reduction of the ketone moiety with sodium borohydride generated racemic β–hydroxy ester **19**. Saponification using lithium hydroxide

yielded racemic β-hydroxy acid **20** in an overall yield of 62% from starting material 11-bromoundecanol.

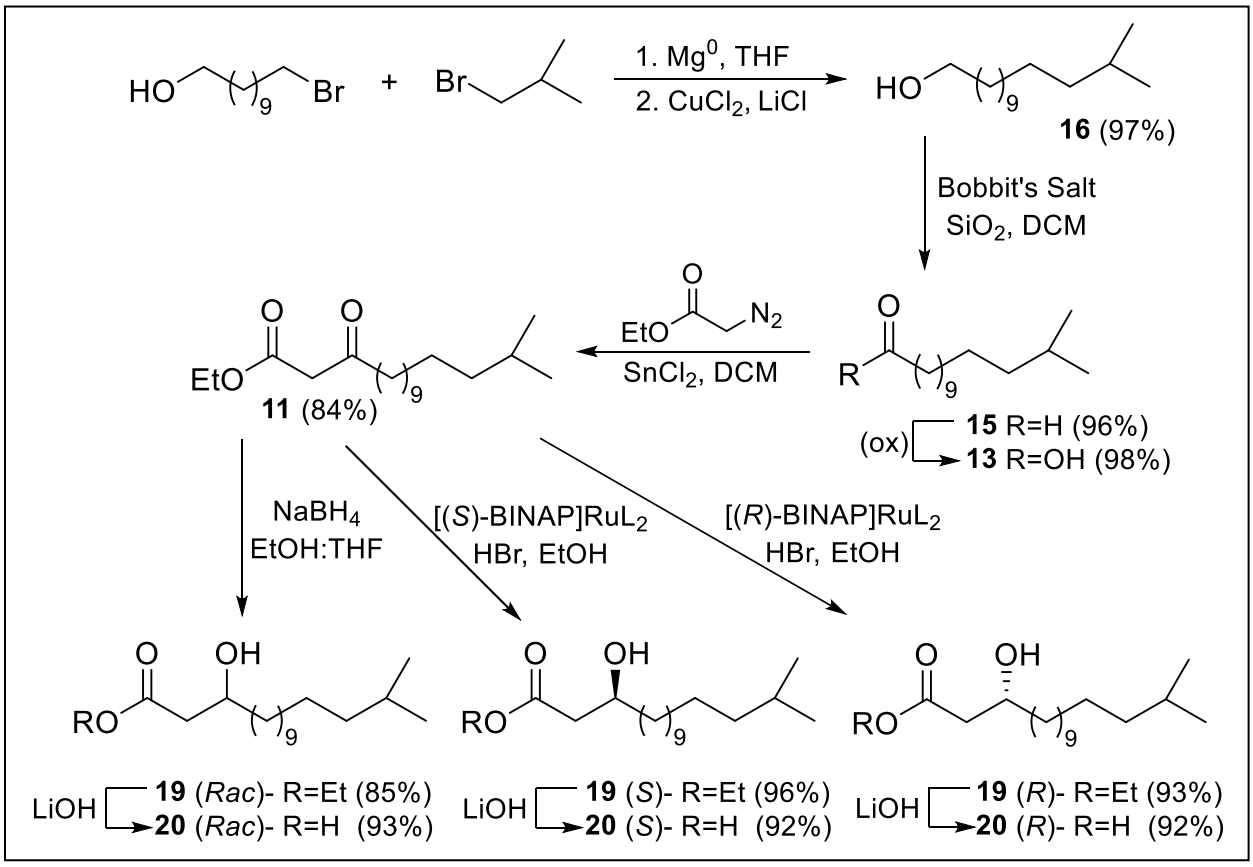

Scheme 5. Synthesis of β-hydroxy acids.

Our first attempt to generate enantiopure or enantioenriched β-hydroxy acid relied on an enzymatic resolution of racemic **20**. Sugai and Ohta reported the use of a *Pseudomonas* lipase with vinyl acetate for the enzymatic transesterification of 2-hydroxytetracosanoic acid.[43] Mori and coworkers used lipase PS and vinyl acetate to resolve 3-hydroxy-15-methylhexadecanoic acid (**20**), and used the (3*R*)-hydroxy-15-methylhexadecanoic acid provided by this procedure in a synthesis of sulfobactin.[44] We applied this enzymatic resolution technique to compound **20**, using commercially available Amano lipase PS. After several attempts, our best result provided (3*R*)-

20 in about 77% ee and (3*S*)-**20** in about 79% ee, based on the conversion to the respective Mosher's ester followed by ^{1}H NMR analysis that showed a 84*R*:15*S* mixture and a 11*R*:89*S* mixture.[45] We modified the exposure time of racemic **20** to the lipase, but we observed no improvement in enantiomeric enrichment.

A traditional resolution of the acid using brucine was also attempted. Racemic β-hydroxy acid **20** was heated at reflux with brucine in different polar solvents (methanol, ethanol, acetone, and chloroform). We obtained crystals from the reaction in chloroform, but all attempts to separate the diastereomeric salts failed because the resolving agent co-crystallized with both diastereomers under all conditions examined. We therefore abandoned this approach.

We obtained **20** in high enantiopurity using the asymmetric hydrogenation approach reported by Shioiri with β–keto ester **11**.[37] Catalytic hydrogenation of the ketone moiety in **11** using ruthenium catalyst complexed with (*S*)-BINAP or (*R*)-BINAP as chiral ligands led to β-hydroxy esters (3*S*)-**19** and (3*R*)-**19** respectively. The specific rotation of each β-hydroxy acid revealed $[\alpha]_D^{21}$ +14.5 and $[\alpha]_D^{21}$ –10.5 (c 1.0, $CHCl_3$) for the (*R*) and (*S*) enantiomers respectively. Shioiri reported the specific rotation of (3*R*)-**10** to be $[\alpha]_D^{21}$ –12.5° (c 1.02, $CHCl_3$).[37] To confirm our results, we prepared Mosher's esters of these compounds, and 1H NMR analysis indicated that (3*R*)-**19** was formed in 98 % ee and (3*S*)-**19** was formed in 98 %ee.[45] These samples were subjected to the LiOH saponification conditions to yield (3*R*)-**20** in 68 % and (3*S*)-**20** in 70 %, respectively, over 5 steps from 11-bromoundecanol.

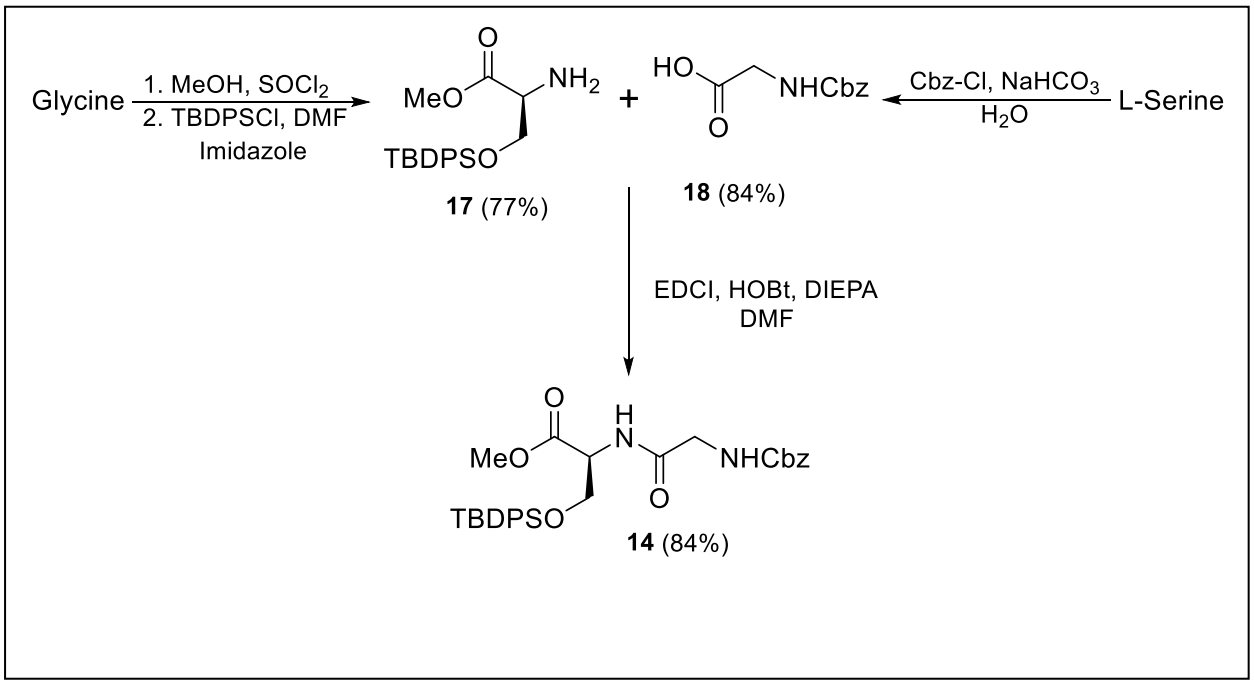

Scheme 6. Synthesis protected serine-glycine dipeptide.

The glycine-serine dipeptide portion of lipid 654 was prepared using standard methodology. The amino group of glycine was protected as the benzyl carbamate to produce amino acid derivative **18**. Both the carboxylic acid and alcohol moieties of L-serine required protection to avoid undesired byproducts in the planned couplings. The reaction of L-serine with thionyl chloride in methanol gave the L-serine methyl ester, which reacted with tert-butyldimethylsilyl chloride to give the protected derivative **17**. Dipeptide **14** was prepared by coupling the amino portion of **17** to the carboxyl group of **18** using DCC, where HOBt was used to generate the needed activated ester.

The coupling reaction of deprotected **14** and **20** proved challenging. Peptides with free amines, especially ones containing glycine, are known to undergo cyclisation to form a diketopiperazine derivative.[46] Dipeptides substituted with an amine at one terminus and an ester at the other can spontaneously cyclize to form a 2,5-DKP at a range of pH. Deprotection of the amino

moiety by hydrogenation of dipeptide **14** using a palladium catalyst gave almost exclusively the DKP product and little coupling to give **12**. Formation of this unwanted product could be partially suppressed with the addition of methanolic HCl to protonate the amine, but we were unable to isolate 14 free of DKP. Attempts to couple the HCl salt of **14** with β–hydroxy acid **20** failed and coupling was only observed upon neutralization of the amine salt. The addition of a stoichiometric amount of base led to the DKP and the yield of our coupling product was only 30-40%.

Methodology developed by Shute and Rich for the coupling of dipeptides to tetrapeptides provided a solution to the coupling problem Activation of acid **20** with N-hydroxysuccinimide formed the reactive ester and this crude product was added to the hydrogenolysis reaction of dipeptide **14**.[47] The presence of the activated ester gives a competitive reaction against the formation of undesired DKP product and facilitated the production of (*Rac*)-**12**. When **12** was obtained, deprotection with TBAF followed by LiOH saponification gave (*Rac*)-**1** (75% yield). Using an identical procedure beginning with (3*R*)-**20**, we obtained (3*R*)-**1** in 68% yield, and using (3*S*)-**20** in the sequence gave (3*S*)-**1** in 71% yield. Spectroscopic evaluation demonstrated that **1** correlates with the proposed structure of lipid 430 and the biological evaluation confirmed this conclusion.

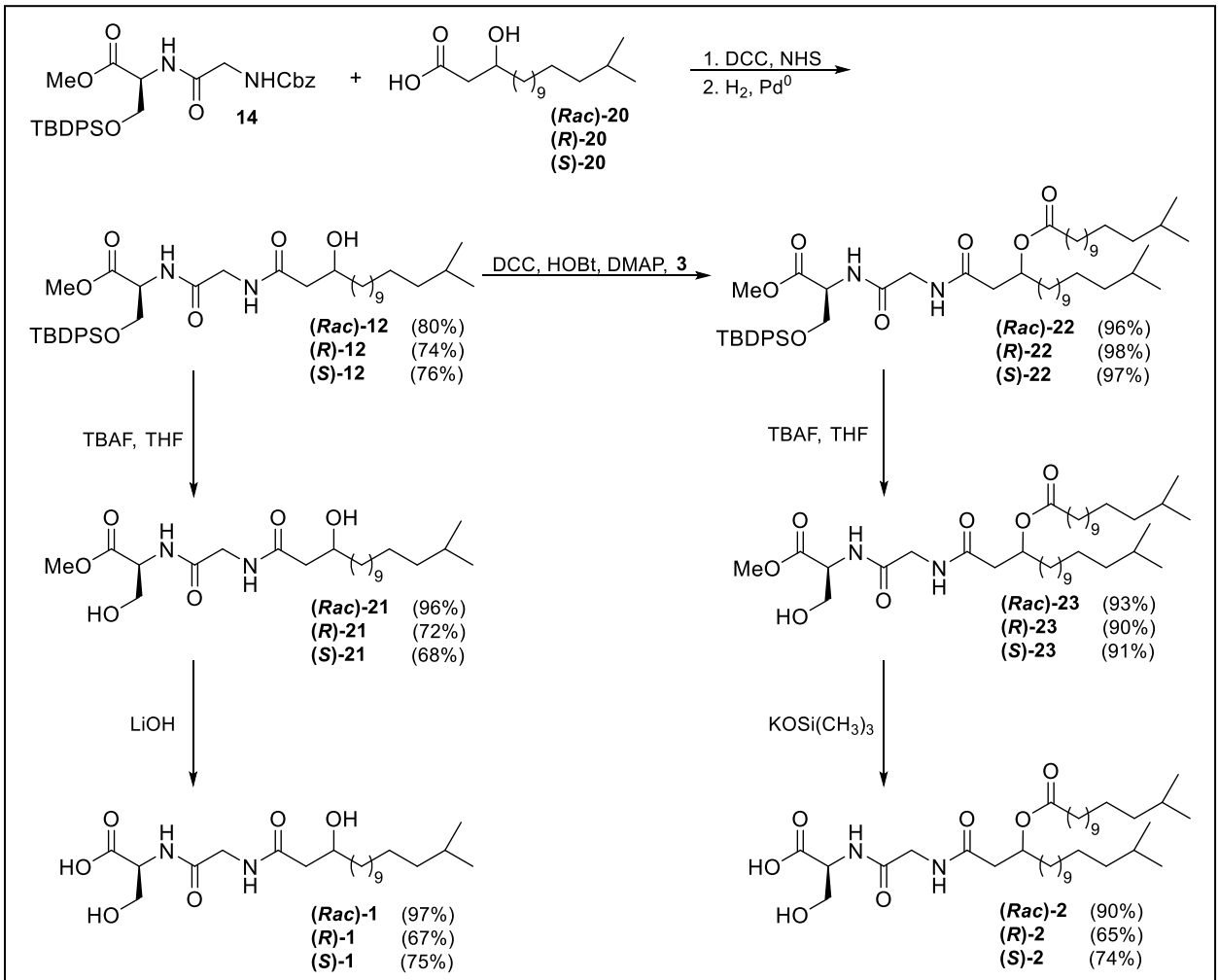

Scheme 7. Synthesis of Lipid 430 and 654.

The final synthetic step was esterification of the alcohol moiety in (*Rac*)-**12** with fatty acid **13**. A DCC mediated coupling gave product (*Rac*)-**22** in > 90% yield. The use of EDC did prove to make the ease of purification easier but did lower yields of the transformation. The sensitivity of the ester linkage in the lipid 654 derivatives led to deprotection of **12** and **22** using two different methods. First, the silyl ether was removed using tetrabutylammonium fluoride to liberate the hydroxyl derivative of the serine moiety. The desilylation of lipid derivative **22** was done in the same manner as before but a different hydrolysis of the methyl ester was used because

saponification of the fatty acid occurred under basic conditions. After treatment with TBAF, reaction with potassium trimethylsilanolate led to (*Rac*)-**2**.[48] This S_N2 type of deprotection was successful, but the yield was lower over the two steps, giving 66% of (*Rac*)-**2**. In an identical manner, (3*R*)-**22** gave (3*R*)-**2** (58%) and (3*S*)-**22** gave (3*S*)-**2** (67%). Spectroscopic analysis of (3R)-L-serine-2 showed that it correlates structurally with lipid 654.

1.2.2 Synthesis of Deuterium Labeled Lipids

In order to implicate this lipid class in human disease, accurate quantification of Lipid 654 requires supplementing biological samples with a stable isotope internal standard for subsequent quantification using conventional mass spectrometric approaches. For this reason the preparation of a deuterated serine lipid internal standard (**25**) for use in quantifying **2** in biological samples. In addition to quantifying the bacterial lipid **2** in biological samples, the deuterated lipid standard **24** can also be used for the evaluation of enzymatic hydrolysis of the parent lipid by known esterases as well as peptidases. In addition, the deuterated lipid **25** can be used for evaluation of metabolic breakdown of **2** by cells important in chronic inflammatory disease processes associated with the accumulation of bacterial serine dipeptide lipids.

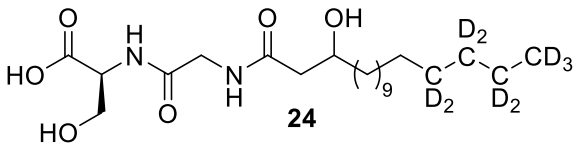

24

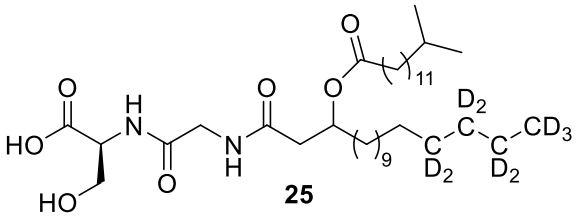

25

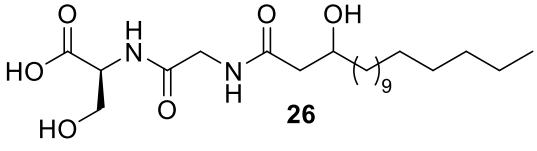

26

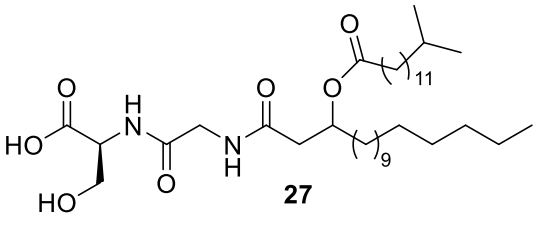

27

Deuterium labeled serine dipeptide lipid was successfully prepared for use in the analysis of biological samples. The first step was to prepare the non-deuterated straight chain fatty ester dipeptide via procedures that mimic the convergent synthesis of lipids 430 and 654 mentioned previously.[49] The straight chain non-deuterated lipids **26** and **27** were used as a control to correlate the spectral data for the production of deuterated lipids. We first protected the commercially available 11-bromoundecanol as the dimethyl(*t*-butyl)silyl derivative, **28**, in 61% yield. The Grignard reagent prepared from 1-bromobutane was coupled to **28**, in the presence of a lithium cuprate complex with *N*-methylpyrrolidone (NMP) as an additive. The use of NMP as well as a catalytic amount of lithium tetrachlorocuprate is an alteration to the previous synthesis and will be elaborated upon in the deuterium labeled production. Deprotection of **28** and oxidation with the oxoammonium salt known as Bobbitt's reagent provided pentadecanal **31** in 80% yield. Coupling with ethyl diazoacetate gave **32** (89.6%), using our standard methodology and reduction with $NaBH_4$, followed by deprotection with LiOH, afforded β-hydroxy acid **34** in 65% yield. Coupling of **34** and the previously prepared protected dipeptide **14** using *N*-hydroxy succinimide activated ester in the presence of hydrolysis of the N-Cbz group by catalytic hydrogenation, gave **35** in 67% yield. Deprotection of the ester of serine protecting groups afforded **26** in 68% yield, whereas esterification with 13-methyltetradecanoic acid gave **36** in 63.4% yield. Deprotection gave **27** in 50% yield. The overall conversion for the linear sequence of 9 steps to **26** was 6% overall yield, whereas the linear sequence of 11 steps gave **27** in 3% overall yield.

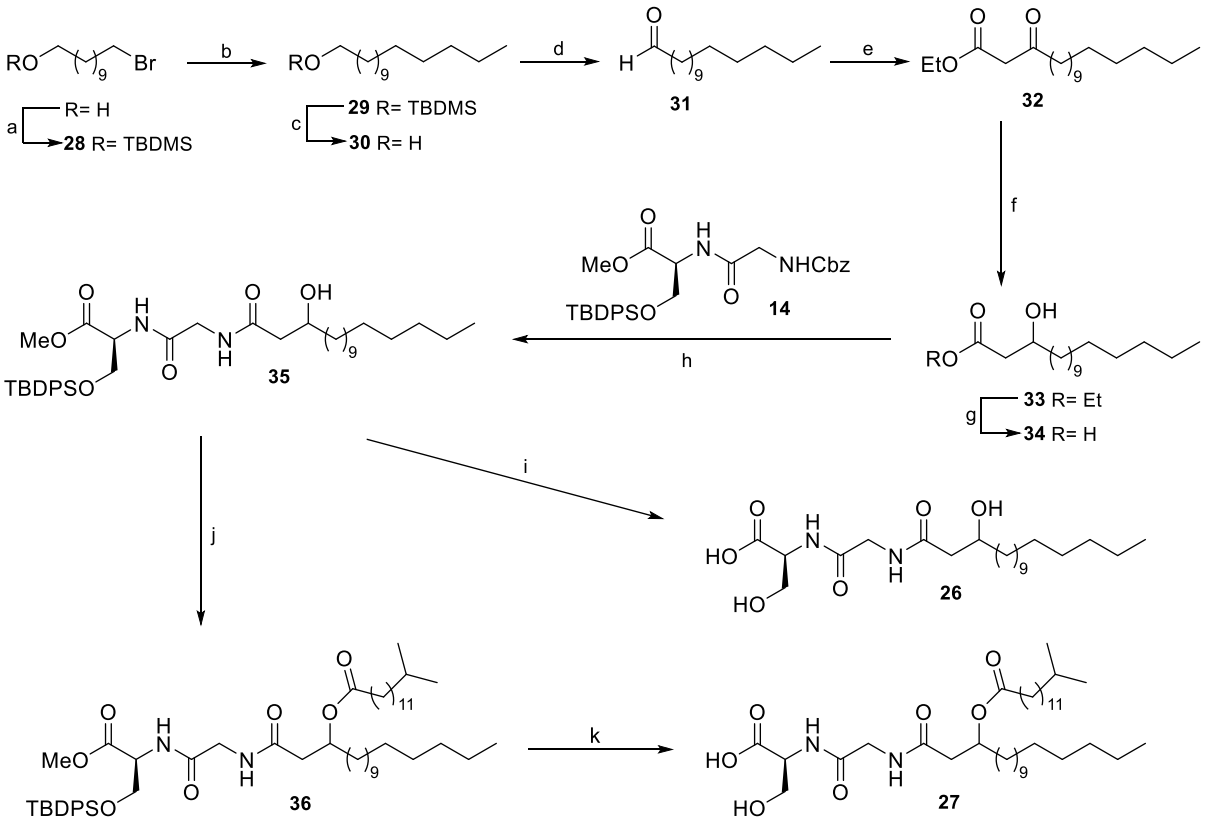

Scheme 8. Synthesis of non-deuterated straight chain lipid 654.

Reagents: (a) TBDMSCl, imidazole, 97.7%; (b) (i) 1-bromobutane, Mg^0, THF (ii) $CuCl_2$, LiCl, NMP, 93%; (c) TBAF, 87.4%; (d) Bobbitt's salt, SiO_2, 90.8%; (e) $SnCl_2$, ethyl diazoacetate, 89.6%; (f) $NaBH_4$, 77.6%; (g) LiOH, 83.6%; (h) (i) NHS, EDC, DMAP (ii) Pd/C, H_2, 67%; (i) (i) TBAF, 80.5% (ii) LiOH, 84%; (j) 13-methylpentadecanoic acid, EDC, DMAP, 63.4%; (k) (i) TBAF, 76.1% (ii) $KOSi(CH)_3$, 65%.

Following a similar synthetic methodology, the synthesis of deuterated lipids initially focused on the fatty acid portion of the lipid and the preparation of **42**. To avoid undesired reactivity of expensive deuterated Grignard reagent with the acidic hydroxy proton, commercially available 11-bromoundecan-1-ol was protected with *tert*-butyl dimethyl silyl chloride to form silyl ether **28**. This was coupled with the Grignard derivative of **37,** prepared by bromination of the commercially available d_9-butan-1-ol, in the presence of a lithium tetrachlorocuprate complex with *N*-methylpyrrolidone (NMP) as an additive.[50] The use of NMP as well as a catalytic amount of

lithium tetrachlorocuprate insured that a minimum amount of d_9-1-bromobutane was used to produce deuterated silyl ether **37**. Deprotection using tetrabutylammonium fluoride generated alcohol **38**. Oxidation of the alcohol with the oxoammonium reagent Bobbitt's salt yielded aldehyde **39** with no over-oxidation to the acid and in excellent yield. *β*–keto ester **40** was prepared by the reaction of the aldehyde with ethyl diazoacetate in the presence of catalytic tin (II) chloride. Selective reduction of the ketone moiety with sodium borohydride generated racemic *β*–hydroxy ester **41**. Saponification of this ester using lithium hydroxide yielded racemic β-hydroxy acid **42** in an overall yield of 42% from 11-bromoundecanol.

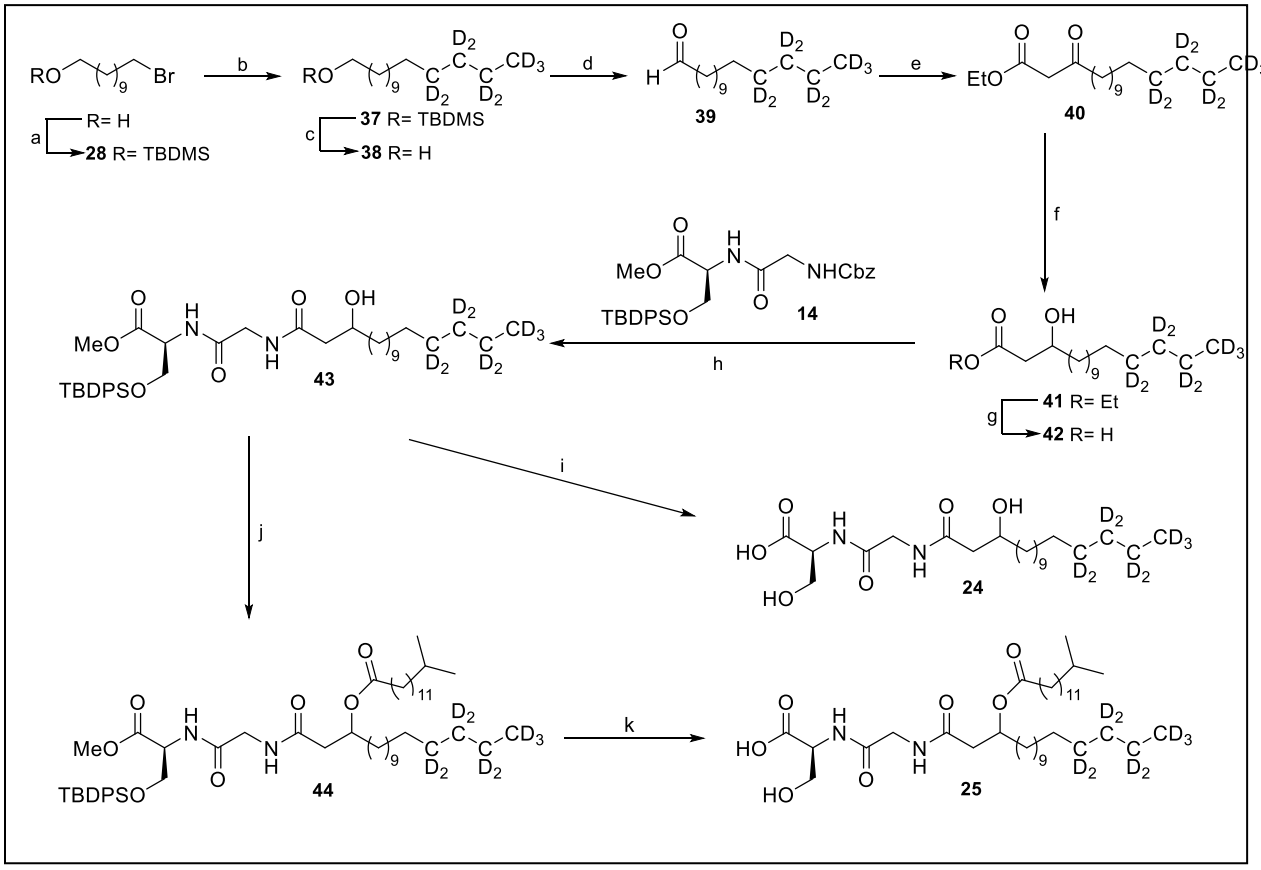

Scheme 9. Synthesis of deuterated L-serine lipid 654

Reagents: (a) TBDMSCl, imidazole, 97.7%; (b) (i) d_9-1-bromobutane, Mg^0, THF (ii) $CuCl_2$, LiCl, NMP, 98.3%; (c) TBAF, 99.1%; (d) Bobbitt's salt, SiO_2, 75.6%; (e) $SnCl_2$, ethyl diazoacetate, 80.6%; (f) $NaBH_4$, 79.7%; (g) LiOH, 89.3% (h) (i) **10**, NHS, EDC, DMAP (ii) Pd/C, H_2, 78.2%; (i) (i) TBAF, 85.1% (ii) LiOH, 73%; (j) 13-methylpentadecanoic acid, EDC, DMAP, 79.6%; (k) (i) TBAF, 85.1% (ii) $KOSi(CH)_3$, 58%.

With d_9-β-hydroxy acid **42** prepared, the convergent synthesis proceeded by amidation coupling with protected dipeptide **10**. Activation of the acid with *N*-hydroxysuccinimide combined with the hydrogenolysis product from the dipeptide facilitated the protected lipid **43**. Subsequent deprotection with TBAF followed by LiOH saponification gave d_9-lipid **24** in 49% yield from the C_{17} fatty acid.

The other targeted lipid utilized esterification of the alcohol moiety of **43** with 13-methylpentadecanoic acid. An EDC/DMAP mediated coupling gave d_9-protected lipid **44**. Deprotection proceeded via removal of the silyl ether using tetrabutylammonium fluoride to liberate the serine hydroxyl group. The sensitivity of the ester linkage in the lipid led to liberation of the methyl ester in a different method. Reaction with potassium trimethylsilanolate led to **25**. This S_N2 type of deprotection was successful, but the yield was lower over the two steps, giving 27% from synthetic fragments **42** and **14**.

1.2.3 MS/MS Fragmentation of Synthetic Lipids

The analysis via MS/MS of synthetic lipids was correlated with isolated lipid 654 from P. gingivalis to confirm proposed structure (Figure 3). The fragmentation pattern of L-serine (*rac*)-654-(**2**) matched identically and proved the hypothesized structure of bioactive compounds. Both diastereomers, (*R*)-**2** and (*S*)-**2**, were also evaluated by MS/MS. The diastermically enriched lipids showed identical fragmentation patterns. Therefore, no stereoisomer-specific precursor-to-fragment transitions available for differential quantitation of the (*R*) and (*S*) isoforms by MRM MS. That is not an unexpected result, however it is disappointing since the stereochemistry of future isolated lipid batches cannot determined solely by mass spectrometry. The deuterated lipid

25 showed the same MS/MS spectrum as the parent lipid **2** and indicating that it is a viable internal standard for accurate quantitation of L-serine-Lipid 654 stereoisomers.

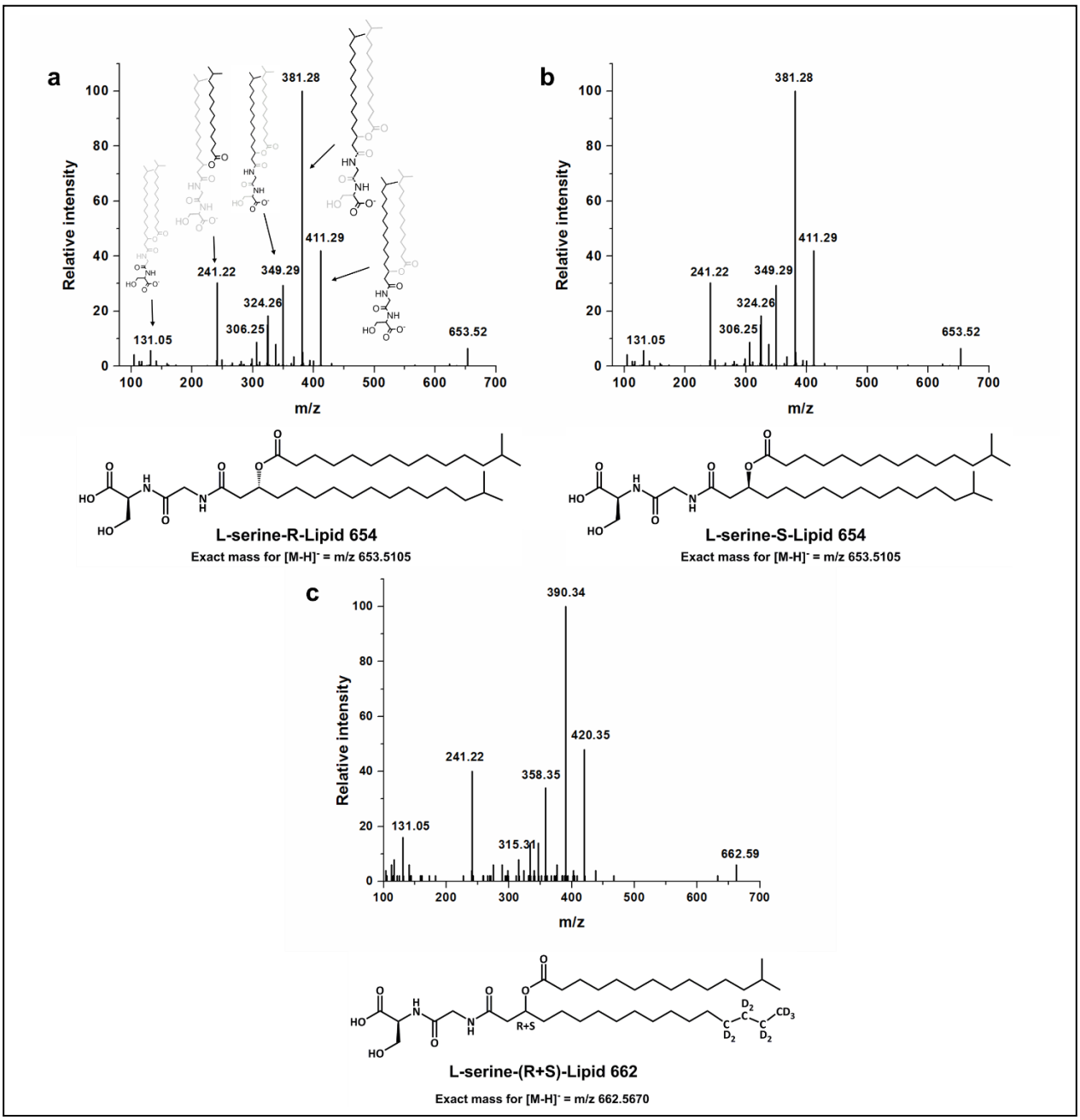

Figure 3. MS/MS spectrum of synthetic lipids.

1.2.4 Enzymatic Hydrolysis of Synthetic Lipid 654 (2).

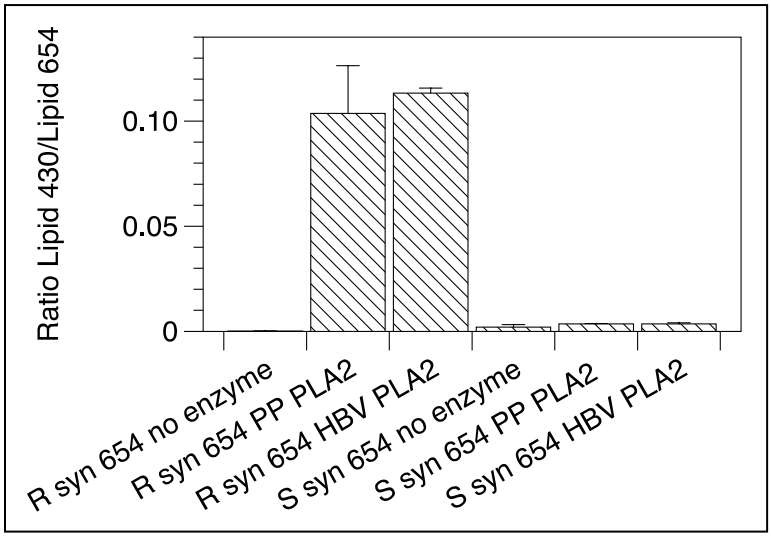

Figure 4. Hydrolysis of (3*R*)-L-serine-2 and (3*S*)-L-serine -2 by PLA2 enzyme preparations.

Each lipid preparation was aliquoted (250 ng/sample) and were dried. Samples were processed as described in the text. Multiple Reaction Monitoring (MRM) was performed using a Sciex QTrap 4000. The 654.3-381.3 or 430.3-382.3 *m/z* transitions were used to calculate the lipid 430/lipid 654 ratios.

HPLC purified synthetic (3*R*)-L-serine-**2** and (3*S*)-L-serine-**2** were subjected to enzymatic hydrolysis using commercially available PLA2 preparations. Approximately 250 ng of each synthetic lipid was sonicated in Tris buffer (10 mM, pH 7.5, 1 mL) containing 150 mM NaCl and 2.5 mM $CaCl_2$. Control samples received no enzyme. Approximately 100 U of either porcine pancreatic PLA2 or honey bee venom PLA2 (both from Sigma) was added and all samples were stirred for 5 days at 25°C. At 5 days, the samples were acidified with glacial acetic acid and extracted with $CHCl_3$ (1 mL x 3 extractions). The pooled extracts were dried and suspended in HPLC solvent (hexane:isopropanol:water, 6:8:0.75, v/v/v). The samples were evaluated using MRM-MS and the ratio of lipid 430 to lipid 654 was determined for both control and enzyme treated samples. The results in Figure 1 show that the (3*R*) diastereomer of synthetic lipid 654, (3*R*)-L-serine-**2**, is hydrolyzed by PLA2 but the (3*S*)-L-serine-**2** is not. This evidence suggests that

the partial hydrolysis of *P. gingivalis* lipid 654 results from the presence of both (3*R*) and (3*S*) diastereomers of lipid 654 in this organism where only the (3*R*) form is hydrolyzed. Of note, it was recently reported that the lipid 430 recovered following porcine pancreatic PLA2 hydrolysis of *P. gingivalis* lipid 654 is a potent inhibitor of osteoblast function both *in vivo* and *in vitro*.[33]

1.2.5 Conclusions

We have prepared (3*R*)-L-serine-**2** and (3*R*)-L-serine **1**, as well as (3*S*)-L-serine-**2** and (3*S*)-L-serine **1** by a convergent synthetic route that is significantly shorter than other published routes, producing the targeted compounds in higher yield. In summary, the convergent synthesis described herein confirms the proposed structures of lipid 654 produced from *P. gingivalis*. Our convergent synthesis gave lipid 430, (*R*)-**1**, in 8 linear steps and 24% overall yield, using the protected dipeptide **13** prepared separately. We similarly prepared (*S*)-**1** in 8 linear steps and 27% overall yield. Lipid 654, (*R*)-**2**, was prepared in 9 linear steps and 28% overall yield. We similarly prepared (*S*)-**2** in 8-linear steps and 34% overall yield. Using the same approaches, (*rac*)-**1** was prepared in 8 linear steps and 46% overall yield and (*rac*)-**2** was prepared in 9 linear steps ad 40% overall yield.

We have also successfully incorporated nine deuterium atoms into **24** and **25** from the commercially available 11-bromoundecan-1-ol using commercially available d_9-butan-1-ol as the deuterium source. The convergent synthesis prepared **24** in 9 linear steps and 13% overall yield from 11-bromoundecan-1-ol and **25** in 10 linear steps and 6% overall yield. Using an identical route we have prepared **26** in 9 linear steps and 12% overall yield and **27** in 10 linear steps and 3% overall yield. The d_9-**24** will be used as a standard for the lipid 430 isolated from *Porphyromonas gingivalis* and d_9-**25** will be used as a standard for 654 isolated from *P. gingivalis*.

Demonstration that there is a difference in enzymatic reactivity with the different diastereomers allows us to use the (*R*) and (*S*) synthetic preparations of lipid 654 to evaluate biological properties of enantioenriched or enantiopure lipids to engage the innate immune system, including the engagement of Toll-like receptor 2. Furthermore, it is important to determine the levels of (*R*) and (*S*) lipid 654 present in other members of the *Bacteroidetes* phylum as well as the levels of these isoforms in diseased tissues where lipid 654 is known to accumulate. These studies have begun, and the results will be the subject of a future communication.

1.3 Experimental

General

All glassware was oven-dried, and all reactions were performed under a nitrogen atmosphere. All chemicals were purchased from the Sigma-Aldrich Chemical Co., and used without further purification unless otherwise noted. Tetrahydrofuran (THF) was distilled from sodium benzophenone ketyl, methylene chloride (dichloromethane, DCM) was distilled from calcium hydride, and dimethylformamide (DMF) was distilled *in vacuo* from calcium hydride. Ethyl acetate (EtOAc), methanol (MeOH), and diethyl ether were used as obtained from the vendor. Bobbitt's salt[42] was provided as a gift from Dr. James Bobbitt (Department of Chemistry, The University of Connecticut)), but it is commercially available from Sigma-Aldrich as 4-acetamido-2,2,6,6-tetramethylpiperidine 1-oxyl. d_9-Butan-1-ol was purchased from Sigma-Aldrich.

Thin-layer chromatography was done on Sorbent Technologies aluminum-backed TLC plates with fluorescent indicator and 0.2 mm silica gel layer thickness, and *p*-anisaldehyde or phosphomolybdic acid were used as developing agents. Column chromatography was done using 60 Å porosity, 32-63 μm silica gel. ^{1}H and ^{13}C NMR were collected on a Bruker Avance 300 (300.13 MHz ^{1}H, 75.48 MHz ^{13}C), Bruker DRX-400 (400.144 MHz ^{1}H, 100.65 MHz ^{13}C) or a Bruker Avance 500 (500.13 MHz ^{1}H, 125.65 MHz ^{13}C). Chemical shifts are reported in ppm downfield from tetramethylsilane (TMS) in the following format chemical shift, multiplicity (s=singlet, d=doublet, t=triplet, q=quartet, m=multiplet). Coupling constants are reported in Hz. Mass spectrometry data was collected on a HP 5870B GC/MSD mass spectrometer with an HP-1 column, and high resolution MS and MS/MS spectra of synthetic **2** and **1** were obtained by direct infusion of the target lipids into a QTOF mass spectrometer, QSTAR Elite from Sciex (Foster City,

CA) or directly by using AccuTOF™ DART, JEOL (Peabody, MA). Multiple reaction monitoring (MRM) transitions were selected based the MS/MS spectra of **2** and **1**. Lipid samples were injected into a triple quadrupole mass spectrometer, 4000 QTrap from Sciex (Foster City, CA). IR spectra were taken on FT/IR-410/C031560585 JASCO and Nexus 670 FT-IR E.S.P, neat, unless otherwise stated. All melting points to an upper limit of 270 °C were obtained using a Uni-melt capillary melting point apparatus or Digimelt MPA160. Perfect. For products described as waxy solid or semi-solids, melting points could not be obtained.

Methyl L-serinate

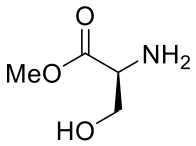

Thionyl chloride (2.75 mL, 37.8 mmol) was added, dropwise, to a suspension of L-serine (4.015 g, 38.2 mmol) in 50 mL of dry methanol. The solution was heated at reflux with stirring for 5 h and then cooled to ambient temperature. The solvent was removed *in vacuo* and the crude white solid was redissolved in a minimal amount of methanol. This solution was treated with an equal volume of toluene and the flask was swirled periodically to induce crystallization. Filtration yielded methyl L-serinate as a crystalline solid (3.9675 g, 33.3 mmol, 87.2%).[51] MP, 161-162 °C. ^{1}H NMR (400 MHz, Methanol-d_4) δ 4.14 (t, *J*=3.9 Hz, 1H), 4.01 (dd, *J*=11.8, 4.5 Hz, 1H), 3.93 (dd, *J*=11.8, 3.1 Hz, 1H), 3.85 (s, 3H). ^{13}C NMR (101 MHz, Methanol-d_4) δ 169.4, 60.7, 56.1, 53.71.

Methyl *O*-(*tert*-butyldiphenylsilyl)-L-serinate, (17)

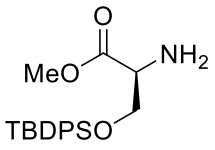

17

A stirring solution of methyl L-serinate (2.003 g, 16.8 mmol) in 15 mL of DMF was treated with imidazole (3.435 g, 50.4 mmol).[52] (*tert*-Butyl)diphenylsilyl chloride (4.80 mL, 18.5 mmol) was added, dropwise, and the reaction was stirred overnight at ambient temperature. At this time, the solvent was removed *in vacuo* and the resulting oil was dissolved in 100 mL of diethyl ether. This solution was washed with water (5 X 400 mL), 10 % LiCl (2 X 100), and brine (50 mL). Drying with $MgSO_4$, filtering, and concentration under reduced pressure yielded methyl *O*-(*tert*-butyldiphenylsilyl)-L-serinate, **17**, as a yellow oil (5.331 g, 14.9 mmol, 88.7%). ^{1}H NMR (400 MHz, $CDCl_3$) δ 7.64 (td, *J* = 7.7, 1.6 Hz, 4H), 7.50-7.35 (m, 6H), 3.98 (dd, *J* = 9.9, 4.3 Hz, 1H), 3.89 (dd, *J* = 9.9, 3.8 Hz, 1H), 3.71 (s, 3H), 3.58 (t, *J* = 4.1 Hz, 1H), 1.04 (s, 9H). ^{13}C NMR (101 MHz, $CDCl_3$) δ 135.6, 133.1, 133.0, 129.9, 127.8, 127.7, 66.1, 56.5, 52.1, 26.8, 19.3. HRMS (AccuTOF): [MH]+ Calc'd for $C_{20}H_{28}NO_3Si$ *m/z* 358.1838. Found: *m/z* 358.1819.

((Benzyloxy)carbonyl)glycine [*N*-Cbz-Glycine], (18)

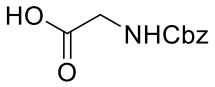

18

Glycine (3.000 g, 40.0 mmol) and sodium bicarbonate (6.710 g, 79.9 mmol) were dissolved in 100 mL of H_2O at ambient temperature and this solution was cooled to 0 °C using an ice bath. Benzyl chloroformate (8.56 mL, 59.9 mmol) in 25 mL of dioxane was added, dropwise. This solution was slowly warmed to ambient temperature and stirred overnight. The reaction mixture

was transferred to a separatory funnel and washed with EtOAc (2 X 50 mL). The aqueous layer was acidified with 10 % HCl to a pH=1 (to pH paper) and extracted with EtOAc (3 X 50 mL). The later organic layers were dried, filtered, and solvents evaporated at reduced pressure to yield ((benzyloxy)carbonyl)glycine, **18**,[53] as a white solid (6.982 g, 33.4 mmol, 83.5 %), MP, 112-114 °C. ^{1}H NMR (400 MHz, Methanol-d_4) δ 7.40–7.24 (m, 5H), 5.10 (s, 2H), 3.84 (s, 2H). ^{13}C NMR (101 MHz, Methanol-d_4) δ 173.6, 159.1, 138.1, 129.4, 129.0, 128.8, 67.7, 43.1.

Methyl *N*-(((benzyloxy)carbonyl)glycyl)-*O*-(*tert*-butyldiphenylsilyl)-L-serinate, (14)

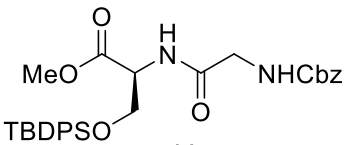

14

A solution of ((benzyloxy)carbonyl)glycine (1.748 g, 8.36 mmol) in 10 mL of DMF was cooled to 0°C using an ice bath. 1-Ethyl-3-(3-dimethylaminopropyl)carbodiimide (EDCI, 1.603 g, 8.36 mmol), HOBt (1.280 g, 8.36 mmol) and then diisopropylethylamine (DIPEA, 1.46 mL, 8.36 mmol) were added in that order. The solution was stirred for 15 min before the addition of methyl *O*-(*tert*-butyldiphenylsilyl)-L-serinate, **12** (2.988 g, 8.36 mmol). The reaction was warmed to ambient temperature and stirred for 48 h. At that time, the DMF was removed *in vacuo* and the resulting oil was dissolved in 100 mL of diethyl ether. The ether was washed with water (5 X 400 mL), saturated $NaHCO_3$ (3 X 100) mL, and brine (50 mL). The organic layer was dried, filtered, and solvents evaporated at reduced pressure. Purification by column chromatography (1 % MeOH:DCM) yielded (((benzyloxy)carbonyl)glycyl)-*O*-(*tert*-butyldiphenylsilyl)-L-serinate**, 14**, as a clear oil (3.390 g, 6.18 mmol, 73.9%). ^{1}H NMR (400 MHz, $CDCl_3$) δ 7.59 (t, *J* = 7.6 Hz, 4H), 7.49–7.34 (m, 6H), 6.77 (d, *J* = 6.9 Hz, 1H), 5.36 (s, 1H), 5.12 (q, *J*= 12.3, 7.6 Hz, 2H) 4.68 (dt, *J* = 8.3, 2.9 Hz, 1H), 4.13 (dd, *J* = 10.3, 2.8 Hz, 1H), 3.93–3.75 (m, 3H), 3.74 (s, 3H), 1.04 (s, 9H).

^{13}C NMR (101 MHz, $CDCl_3$) δ 170.5, 168.6, 156.4, 136.1, 135.5, 132.8, 132.6, 130.1, 128.6, 128.2, 128.1, 127.9, 127.8, 67.3, 64.2, 54.1, 52.5, 44.4, 26.7, 19.3. HRMS (AccuTOF): [MH]+ Calc'd for $C_{30}H_{37}N_2O_6Si$ *m/z* 549.2421. Found: *m/z* 549.2423.

13-Methyltetradecan-1-ol, (16)

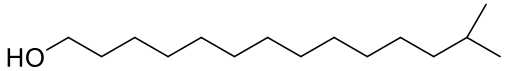

16

Magnesium turnings (2.90 g, 0.119 mol) were added to a 500 mL round bottom flask with a stirbar and flame-dried under a nitrogen atmosphere. After cooling, the Mg turnings were suspended in dry THF (50 mL) and 1-bromo-2-methylpropane (8.00 mL, 0.0736 mol) was rapidly added with vigorously stirring. Upon initiation, dry THF (50 mL) was added and the flask was immersed in an ice bath to modulate the exothermic reaction. The reaction was stirred until the flask cooled to ambient temperature and the temperature was lowered to -78 °C using dry ice acetone bath. 11-Bromoundecan-1-ol (4.005 g, 0.0172 mol) dissolved in THF (20 mL) and LiCl (1.53 g, 0.036 mol) and copper (II) chloride (2.54 g, 0.019 mol), dissolved in THF (30 mL), were added. The mixture was slowly warmed to ambient temperature and stirred overnight. The reaction was quenched with satd NH_4Cl (100 mL) before being transferred to a separatory funnel with diethyl ether (200 mL) and H_2O (100 mL). The layers were separated and the organic layer was washed with satd $NaHCO_3$ (50 mL X 3) and brine (50 mL). The organic phase was dried with $MgSO_4$, gravity filtered, and solvents removed *in vacuo*. The crude product was purified by column chromatography on silica gel (10% EtOAc:hexane) to yield 13-methyltetradecan-1-ol, **16**,[37,54] as a white solid (3.793 g, 0.017 mol, 96.7%), MP, 26-27 °C. ^{1}H NMR (400 MHz, $CDCl_3$)

δ 3.64 (t, 2H), 1.63–1.44 (m, 3H), 1.27 (m, 18H), 1.17 (m, 3H), 0.86 (d, J = 6.6 Hz, 6H); ^{13}C NMR (101 MHz, $CDCl_3$) δ 63.3, 39.2, 33.0, 30.1, 29.9, 29.8, 29.8, 29.6, 28.1, 27.6, 25.9, 22.8.

13-Methyltetradecanal, (15)

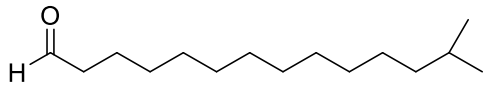

15

4-(Acetyamino)-2,2,6,6-tetramethyl-1-oxo-piperidinium tetrafluoroborate[42] (Bobbit's salt, 5.285 g, 0.0176 mol) was added to 13-ethyltetradecanol (**7**, 3.498 g, 0.0153 mol) dissolved in 250 mL of dry DCM. An equal mass of silica was slowly added to the stirring mixture. The bright yellow solution stirred at ambient temperature until the color faded, giving a solution with a pale yellow tint. The solution was filtered to remove the silica, and the filtrate was concentrated *in vacuo.* The crude product was purified by column chromatography (5% EtOAc:hexanes) to yield 13-methyltetradecanal, **15**,[41] as a clear solid, (3.319 g, 0.0147 mol, 95.8%), MP, ~25 °C. ^{1}H NMR(400 MHz, $CDCl_3$) δ 9.76 (t, *J* = 1.9 Hz, 1H), 2.41 (td, *J* = 7.4, 1.9 Hz, 2H), 1.63 (quin, *J* = 7.2 Hz, 2H), 1.51 (sep, 1H), 1.36–1.22 (m, 16H), 1.15 (m, 2H), 0.86 (d, *J* = 6.6 Hz, 6H) ^{13}C NMR (101 MHz, $CDCl_3$) δ 13C NMR (101 MHz, $CDCl_3$) δ 203.0, 44.0, 39.1, 30.0, 29.8, 29.7, 29.6, 29.5, 29.4, 29.2, 28.0, 27.5, 22.7, 22.2.

13-Methyltetradecanoic acid, (13)

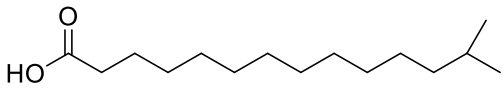

13

13-Methyltetradecanal (**15**, 1.251 g, 5.53 mmol) was dissolved in 50 mL of THF, and 5 mL of H_2O and 0.5 mL of 1M HCl were added. The reaction mixture was stirred for 72 h at

ambient temperature. The resulting solution was concentrated under reduced pressure, the residue dissolved in 15 mL of H_2O, and extracted with DCM (15 mL X 3). The resulting solution was filtered through a small plug of silica gel and rinsed with DCM before being concentrated *in vacuo* to yield 13-methyltetradecanoic acid[32,37,55] (**13**) as a white solid (1.307 g, 5.39 mmol, 97.6%), MP, 48-49 °C. ^{1}H NMR (400 MHz, $CDCl_3$) δ 2.35 (t, *J* = 7.5 Hz, 2H), 1.63 (quin, *J* = 7.4 Hz, 2H), 1.51 (sep, *J* = 6.6 Hz, 1H), 1.39–1.18 (m, 16H), 1.15 (q, *J* = 6.7 Hz, 2H), 0.86 (d, *J* = 6.6 Hz, 6H). ^{13}C NMR (101 MHz, $CDCl_3$) δ 13C NMR (101 MHz, $CDCl_3$) δ 179.6, 39.1, 34.0, 30.0, 29.8, 29.7, 29.7, 29.5, 29.3, 29.1, 28.0, 27.5, 24.8, 22.7.

Ethyl 15-methyl-3-oxohexadecanoate, (11)

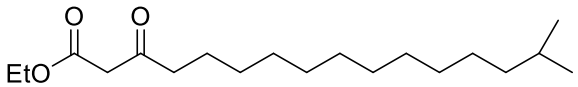

11

Tin (II) chloride dehydrate (0.417 g, 1.85 mmol) was suspended in 15 mL of dry DCM. Ethyl diazoacetate (2.60 g, 19.4 mmol) was added, dropwise via syringe, and the reaction was stirred for 15 min. 13-Methylpentadecanal (**15**, 4.186 g, 18.5 mmol) was dissolved in 10 mL of DCM and added to the reaction, dropwise, via cannula. The mixture was stirred at ambient temperature for about 6 h, until nitrogen evolution ceased. The reaction mixture was diluted with 100 mL of DCM and washed with a satd brine solution (2 X 50 mL). The aqueous layers were combined and extracted with DCM (2 X 25 mL). All organic layers were combined, dried with $MgSO_4$, filtered, and solvents evaporated at reduced pressure. The resulting crude product was purified via column chromatography (5% EtOAc:hexanes) to yield ethyl 15-methyl-3-oxohexadecanoate,[37,56] **11**, as a clear solid (4.871 g, 0.0156 mol, 84.3%), MP, ~25 °C. ^{1}H NMR (400 MHz, $CDCl_3$) δ 4.20 (q, *J* = 7.1 Hz, 2H), 3.42 (s, 2H), 2.53 (t, *J* = 7.3 Hz, 2H), 1.60 (quin, *J*

= 7.2 Hz, 2H), 1.50 (sep, *J* = 6.5 Hz, 1H), 1.30-1.20 (m, 20H), 1.15 (q, *J* = 7.3, 6.8 Hz, 2H), 0.86 (d, *J* = 6.6 Hz, 6H). ^{13}C NMR (101 MHz, $CDCl_3$) δ 203.0, 167.3, 61.4, 49.4, 43.1, 39.1, 30.0, 29.8, 29.7, 29.7, 29.5, 29.4, 29.1, 28.0, 27.5, 23.5, 22.7, 14.2.

Ethyl 3-hydroxy-15-methylhexadecanoate, (19)

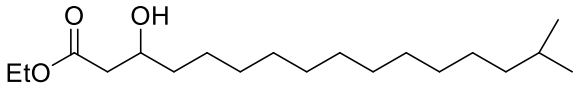

(*rac*)-19

A solution of ethyl 15-methyl-3-oxohexadecanoate (**11**, 3.114 g, 0.001 mol) in 2.5 mL of ethanol and 22.5 mL of THF was cooled to 0 °C on an ice bath. Sodium borohydride (0.301 g, 0.008 mol) was added and the resulting slurry was stirred vigorously for 1 h. The reaction was quenched by the slow addition of 50 mL of a 10 % aq citric acid solution. Subsequent neutralization with satd K_2CO_3 solution was followed by extraction with EtOAc (3 X 50 mL). The organic layers were washed with 25 mL of satd brine solution, dried with $MgSO_4$, filtered, and the solvents were removed at reduced pressure. The crude product was purified by column chromatography (10% EtOAc:hexanes) to yield ethyl 3-hydroxy-15-methylhexadecanoate,[37] **19** as a clear oil (2.674 g, 0.0085 mol, 85.3 %). ^{1}H NMR (400 MHz, $CDCl_3$) δ 4.17 (q, *J* = 7.1 Hz, 2H), 4.06–3.93 (m, 1H), 2.91 (d, *J* = 3.9 Hz, 1H), 2.50 (dd, *J* = 16.4, 3.1 Hz, 1H), 2.39 (dd, *J* = 16.4, 9.0 Hz, 1H), 1.60–1.20 (m, 23H), 1.15 (q, *J* = 6.6 Hz, 2H), 0.86 (d, *J* = 6.6 Hz, 6H). ^{13}C NMR (101 MHz, $CDCl_3$) δ 173.2, 68.1, 60.7, 41.4, 39.1, 36.6, 30.0, 29.8, 29.7, 29.6, 29.6, 28.0, 27.5, 25.5, 22.7, 14.2.

Ethyl (3*R*)-hydroxy-15-methylhexadecanoate, ((3*R*)-19)

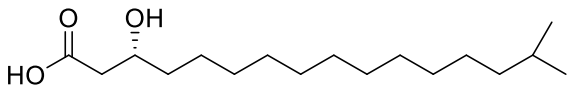

(3*R*)-19

In a nitrogen atmosphere glove box, (*R*)-BINAP (45 mg, 0.072 mmol) and bis(2-methylallyl)(1,5-cyclooctadiene)ruthenium(II) (20 mg, 0.063 mmol) were dissolved in 9 mL of freshly distilled acetone. Methanolic HBr (0.22 mL, 0.73 M, 0.16 mmol) was added, and the solution was stirred for 1 h. The reaction was concentrated to dryness *in vacuo* before being redissolved in 15 mL of ethanol and *β*-keto ester **11** (0.962 g, 3.08 mmol) was added. The system was flushed with hydrogen and heated at reflux for 48 h. The resulting solution was filtered and the solvents removed at reduced pressure. Subsequent purification via column chromatography (10% EtOAc:hexanes) yielded ethyl (3*R*)-hydroxy-15-methylhexadecanoate, (3*R*)-**19**[37] as a clear solid (0.901 g, 2.86 mol, 93.0 %), MP, ~25 °C. ^{1}H NMR (400 MHz, $CDCl_3$) δ 4.17 (q, *J* = 7.2 Hz, 2H), 4.05–3.94 (m, 1H), 2.91 (d, *J* = 4.0 Hz, 1H), 2.50 (dd, *J* = 16.4, 3.1 Hz, 1H), 2.39 (dd, *J* = 16.4, 9.0 Hz, 1H), 1.60–1.20 (m, 23H), 1.15 (q, *J* = 6.6 Hz, 2H), 0.86 (d, *J* = 6.6 Hz, 6H). ^{13}C NMR (101 MHz, $CDCl_3$) δ 173.2, 68.1, 60.7, 41.4, 39.1, 36.6, 30.0, 29.8, 29.7, 29.6, 29.6, 28.0, 27.5, 25.5, 22.7, 14.2. A ^{1}H NMR analysis that showed a 97*R*:03*S* mixture for (3*R*)-**19**.

Ethyl (3*S*)-hydroxy-15-methylhexadecanoate, ((3*S*)-19)

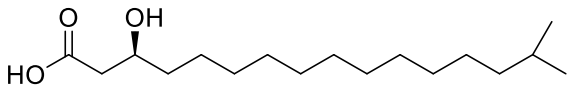

(3*S*)-19

In a nitrogen atmosphere glove box, (*S*)-BINAP (45 mg, 0.072 mmol) and bis(2-methylallyl)(1,5-cyclooctadiene)ruthenium(II) (20 mg, 0.063 mmol) were dissolved in 9 mL of freshly distilled acetone. Methanolic HBr (0.22 mL, 0.73 M, 0.16 mmol) was added, and the

solution stirred for 1 h. The reaction was concentrated to dryness *in vacuo* before being redissolved in 15 mL of ethanol and *β*-keto ester **11** (0.954 g, 3.05 mmol) was added. The system was flushed with hydrogen gas and heated at reflux for 48 h. The resulting solution was filtered and the solvents removed at reduced pressure. Subsequent purification via column chromatography (10% EtOAc:hexanes) yielded ethyl (3*S*)-hydroxy-15-methylhexadecanoate, (3*S*)-**19**[37] as a clear solid (0.917 g, 2.92 mol, 95.5 %), MP, ~25 °C. $[\alpha]_D^{23}$ +11.8° (c 1.0, $CHCl_3$), ^{1}H NMR (400 MHz, $CDCl_3$) δ 4.17 (q, *J* = 7.1 Hz, 2H), 4.06–3.93 (m, 1H), 2.91 (d, *J* = 4.0 Hz, 1H), 2.50 (dd, *J* = 16.4, 3.1 Hz, 1H), 2.39 (dd, *J* = 16.4, 9.0 Hz, 1H), 1.55–1.39 (m, 3H), 1.38–1.21 (m, 20H), 1.15 (q, *J* = 7.1, 6.6 Hz, 2H), 0.86 (d, *J* = 6.6 Hz, 6H). ^{13}C NMR (101 MHz, $CDCl_3$) δ 173.2, 68.1, 60.7, 41.4, 39.1, 36.6, 30.0, 29.8, 29.7, 29.6, 29.6, 28.0, 27.5, 25.5, 22.7, 14.2. A ^{1}H NMR analysis that showed a 02*R*:98*S* mixture for (3*S*)-**19**.

Enzymatic Resolution

Lipase PS (.275 g) was added to a stirred solution of (±)-**19** (5.50 g, 1.92 mmol) and 2,6-di-tert-butyl-4-methylphenol (5 mg) in vinyl acetate (8.8 mL), and stirred at 52-58 °C for 168 h. The resulting mixture was cooled to ambient temperature and filtered through Celite and concentrated under reduced pressure. Column chromatography (MeOH: DCM), yielded (3*R*)-5 (128 mg) as a white solid; $[\alpha]_D^{23}$ +6.4° (c 1.02, $CHCl_3$). After saponification of the acetate product, (3*S*)-**5** (177 mg) was purified to give a white solid; $[\alpha]_D^{23}$ –8.7° (c 1.02, $CHCl_3$). ^{1}H NMR spectra were identical with those of (±)-5.[16c] Conversion to the corresponding Mosher's ester as described above was followed by ^{1}H NMR analysis that showed a 84*R*:15*S* mixture for (3*R*)-**19** and a 11*R*:89*S* mixture for (3*S*)-**19**.

Ethyl (*R*)-15-methyl-3-(((*S*)-3,3,3-trifluoro-2-methoxy-2-phenylpropanoyl) oxy)-Hexadecanoate

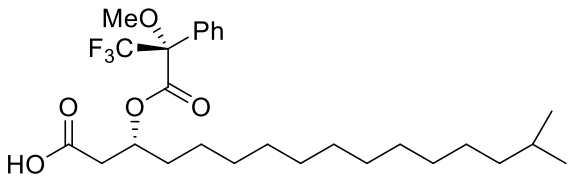

Under a nitrogen atmosphere, (*S*)-(–)-α-Methoxy-α-(trifluoromethyl)phenylacetic acid (Mosher's acid,[45] 23 mg, 0.098 mmol) was dissolved in 2 mL of dry DCM and cooled to 0 °C in an ice bath. Subsequent addition of DCC (24 mg, 0.12 mol) was followed by stirring for 15 min, at which time ethyl (3*R*)-hydroxy-15-methylhexadecanoate, (3*R*)-**19** (29 mg, 0.092 mmol) was added, along with a catalytic amount of DMAP. The reaction was equilibrated to ambient temperature slowly and stirred overnight. Evaporation of solvents *in vacuo* was followed by addition of 15 mL of EtOAc and washing with H_2O 3 X 10 mL and 10 mL of satd brine. The resulting organic layer was dried over $MgSO_4$, filtered, and the solvents removed at reduced pressure. Subsequent purification via column chromatography (1-10% EtOAc:hexanes) yielded ethyl (*R*)-15-methyl-3-(((*S*)-3,3,3-trifluoro-2-methoxy-2-phenylpropanoyl)oxy)hexadecanoate as a clear oil (38 mg, 0.072 mmol, 78 %). ^{1}H NMR (400 MHz, $CDCl_3$) δ 7.55-7.50 (m, 2H), 7.42-7.37 (m, 3H), 5.52-5.45 (p, *J* = 6.4 Hz, 1H), 4.06 (q, *J* = 7.1 Hz, 2H), 3.53 (s, 3H), 2.64 (dd, *J* = 16.0, 7.9 Hz, 1H), 2.55 (dd, *J*= 16.0, 5.0 Hz, 1H) 1.80-1.60 (m, 2H), 1.55-1.47 (sep, *J* = 6.6 Hz, 1H), 1.36-1.12 (m, 23H), 0.86 (d, *J* = 6.6 Hz, 6H).

Ethyl (*S*)-15-methyl-3-(((*S*)-3,3,3-trifluoro-2-methoxy-2-phenylpropanoyl)oxy)-Hexadecanoate

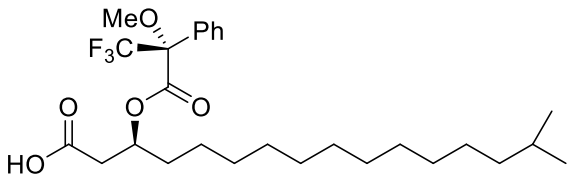

Under a nitrogen atmosphere, (*S*)-(–)-α-Methoxy-α-(trifluoromethyl)phenylacetic acid (Mosher's acid,[45] 23 mg, 0.098 mmol) was dissolved in 2 mL of dry DCM and cooled to 0 °C in an ice bath. Subsequent addition of DCC (23 mg, 0.11 mmol) was followed by stirring for 15 min, at which time ethyl (3*S*)-hydroxy-15-methylhexadecanoate, (3*S*)-**19** ((28 mg, 0.089 mmol) was added, along with a catalytic amount of DMAP. The reaction was equilibrated to ambient temperature slowly and stirred overnight. Evaporation of solvents *in vacuo* was followed by addition of 15 mL of EtOAc and washing with H_2O 3 X 10 mL and 10 mL of satd brine. The resulting organic layer was dried over $MgSO_4$, filtered, and the solvents removed at reduced pressure. Subsequent purification via column chromatography (1-10% EtOAc:hexanes) yielded ethyl (*R*)-15-methyl-3-(((*S*)-3,3,3-trifluoro-2-methoxy-2-phenylpropanoyl)oxy)hexadecanoate as a clear oil (45 mg, 0.084 mmol, 94 %). ^{1}H NMR (400 MHz, $CDCl_3$) δ 7.50-7.55 (m, 2H), 7.37-7.42 (m, 3H), 5.48 (quin, *J* = 6.3 Hz, 1H), 4.12 (q, *J* = 7.1 Hz, 2H), 3.55 (s, 3H), 2.69 (dd, *J* = 16.0, 8.0 Hz, 1H), 2.59 (dd, *J*= 16.0, 4.8 Hz, 1H), 1.70-1.57 (m, 2H), 1.52 (sep, *J* = 6.6 Hz, 1H), 1.36-1.12 (m, 23H), 0.86 (d, *J* = 6.6 Hz, 6H).

3-Hydroxy-15-methylhexadecanoic acid, ((rac)-20)

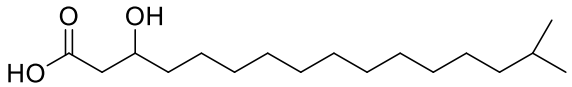

(*rac*)-**20**

Hydroxy ester **19** (2.674 g, 0.0085 mol) was dissolved in 8 mL of MeOH and 16 mL of THF and 1 M aqueous LiOH (9.40 mL, 0.0094 mol) were added. The mixture was stirred overnight at ambient temperature. The reaction was then acidified with 1 M HCl and extracted with EtOAc (3 X 50 mL). The organic layers were washed with 25 mL of brine, dried with $MgSO_4$, filtered, and the solvents were removed at reduced pressure. The crude solid was recrystallized from hexanes to yield 3-hydroxy-15-methylhexadecanoic acid,[37] (3*R*+3*S*)-**20,** as a white solid (2.257 g, 0.0079 mol, 92.7 %), MP, 54-56 °C. ^{1}H NMR (400 MHz, $CDCl_3$) δ 4.09–3.98 (m, 1H), 2.58 (dd, *J* = 16.6, 3.2 Hz, 1H), 2.48 (dd, *J* = 16.6, 8.9 Hz, 1H), 1.59–1.43 (m, 3H), 1.35-1.20 (m, 18H), 1.15 (q, *J* = 6.7 Hz, 2H), 0.86 (d, *J* = 6.6 Hz, 6H). ^{13}C NMR (101 MHz, $CDCl_3$) δ 177.4, 68.1, 41.2, 39.1, 36.6, 30.0, 29.8, 29.7, 29.6, 29.6, 29.5, 28.0, 27.5, 25.5, 22.7.

3(*R*)-Hydroxy-15-methylhexadecanoic acid, ((3*R*)-20)

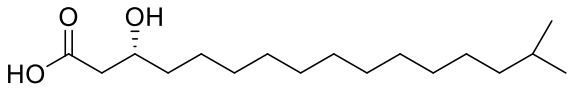

(3*R*)-**20**

Hydroxy ester **(3*R*)-19** (0.818 g, 0.0026 mol) was dissolved in 8 mL of methanol and 16 mL of THF and 1 M aqueous LiOH (2.9 mL, 0.0029 mol) were added. The mixture was stirred overnight at ambient temperature. The reaction was then acidified with 1 M HCl and extracted with EtOAc (3 X 50 mL). The organic layers were washed with 25 mL of brine, dried with $MgSO_4$, filtered, and the solvents were removed at reduced pressure. The crude solid was recrystallized from hexanes to yield (3*R*)-3-hydroxy-15-methylhexadecanoic acid,[37] (3*R*)-**20,** as a white solid

(0.708 g, 0.0024 mol, 92 %), $[\alpha]_D^{23}$ –10.5° (c 1.0, $CHCl_3$), MP, 54-55 °C. ^{1}H NMR (400 MHz, $CDCl_3$) δ 4.09–3.98 (m, 1H), 2.58 (dd, *J* = 16.6, 3.2 Hz, 1H), 2.48 (dd, *J* = 16.6, 8.9 Hz, 1H), 1.59–1.43 (m, 4H), 1.35-1.20 (m, 18H), 1.15 (q, *J* = 6.7 Hz, 2H), 0.86 (d, *J* = 6.6 Hz, 6H). ^{13}C NMR (101 MHz, $CDCl_3$) δ 177.8, 68.1, 41.1, 39.1, 36.6, 30.0, 29.8, 29.7, 29.6, 29.5, 28.0, 27.5, 25.5, 22.7.

3(*S*)-Hydroxy-15-methylhexadecanoic acid, ((3*S*)-20)

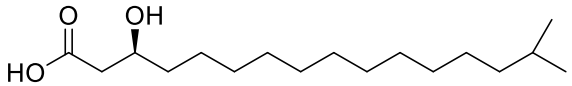

(3*S*)-20

Hydroxy ester **(3*S*)-19** (0.815 g, 0.0026 mol) was dissolved in 8 mL of methanol and 16 mL of THF and 1 M aqueous LiOH (2.9 mL, 0.0029 mol) were added. The mixture was stirred overnight at ambient temperature. The reaction was then acidified with 1 M HCl and extracted with EtOAc (3 X 50 mL). The organic layers were washed with 25 mL of brine, dried with $MgSO_4$, filtered, and the solvents were removed at reduced pressure. The crude solid was recrystallized from hexanes to yield (3*S*)-3-hydroxy-15-methylhexadecanoic acid,[37] (3*S*)-**20,** as a white solid (0.679 g, 0.0024 mol, 92 %), $[\square]_D^{23}$ +14.5° (c 1.0, $CHCl_3$), MP, 54-55 °C. ^{1}H NMR (400 MHz, $CDCl_3$) δ 4.09–3.98 (m, 1H), 2.58 (dd, *J* = 16.6, 3.2 Hz, 1H), 2.48 (dd, *J* = 16.6, 8.9 Hz, 1H), 1.59–1.43 (m, 4H), 1.35-1.20 (m, 18H), 1.15 (q, *J* = 6.7 Hz, 2H), 0.86 (d, *J* = 6.6 Hz, 6H). ^{13}C NMR (101 MHz, $CDCl_3$) δ 177.3, 68.1, 41.0, 39.1, 36.6, 30.0, 29.8, 29.7, 29.6, 29.5, 28.0, 27.5, 25.5, 22.7.

Methyl *O*-(*tert*-butyldiphenylsilyl)-*N*-((3-hydroxy-15-methylhexadecanoyl)glycyl)-L-serinate, ((*rac*)-12)

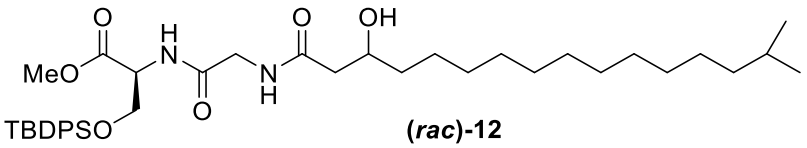

(*rac*)-12

N-Hydroxysuccinimide (116 mg, 1.00 mmol) and dicyclohexylcarbodiimide (DCC, 216 mg, 1.05 mmol) were added to a stirring solution of 3-hydroxy-15-methylhexadecanoic acid (**20**, 250 mg, 0.873 mmol) in 10 mL of dry THF. The solution was stirred for 5 h at ambient temperature, filtered, and the filtrate was concentrated *in vacuo*. The resulting white solid was dissolved in 5 mL of dioxane and this solution was added via cannula to a solution of methyl *N*-(((benzyloxy)carbonyl)glycyl)-*O*-(*tert*-butyldiphenylsilyl)-L-serinate (**14**, 598 mg, 1.09 mmol) and Pd/C (176 mg) in 10 mL of dioxane. The reaction vessel was flushed with H_2 and the mixture was stirred overnight, filtered through Celite, and concentrated under reduced pressure. The crude product was purified via column chromatography (2% MeOH:DCM**)** to yield methyl *O*-(*tert*-butyldiphenylsilyl)-*N*-((3-hydroxy-15-methylhexadecanoyl)glycyl)-L-serinate, (3*R*+3*S*)-L-serine-**12**, as a clear oil (0.478 g, 0.700 mmol, 80.2%). ^{1}H NMR (400 MHz, $CDCl_3$) δ 7.62-7.55 (m, 4H), 7.49–7.34 (m, 6H), two signals [6.86 and 6.99 (d, *J*= 7.0 and 8.1 Hz, 1H)], two signals [6.34 and 6.56 (d, *J*= 5.4 and 5.6 Hz, 1H), 4.67 (dt, *J* = 8.2, 3.0 Hz, 1H), 4.17–4.06 (m, 2H), 4.04–3.82 (m, 3H), 3.82–3.71 (m, 4H), 2.40 (dt, *J* = 14.7, 2.2 Hz, 1H), 2.26 (dd, *J* = 14.5, 9.4 Hz, 1H), 1.57-1.35 (m, 4H), 1.35-1.18 (m, 18H), 1.16 (dd, *J* = 13.6, 7.8 Hz, 2H), 1.03 (s, 9H), 0.86 (d, *J* = 6.6 Hz, 6H). ^{13}C NMR (101 MHz, $CDCl_3$) δ 172.9, 172.8, 170.8, 168.9, 168.7, 135.5, 135.5, 132.9, 132.9, 132.7, 132.6, 130.0, 127.9, 127.9, 68.9, 68.9, 64.2, 54.3, 52.6, 43.1, 43.0, 43.0, 42.8, 39.1, 37.1, 30.0, 29.8, 29.7, 29.6, 29.6, 28.0, 27.5, 26.8, 25.5, 22.7, 19.3. HRMS (AccuTOF): [MH]+ Calc'd for $C_{39}H_{63}N_2O_6Si$ *m/z* 683.4455. Found: *m/z* 683.4470.

Methyl *O*-(*tert*-butyldiphenylsilyl)-*N*-((3R-hydroxy-15-methylhexadecanoyl)glycyl)-L-serinate, ((3*R*)-12)

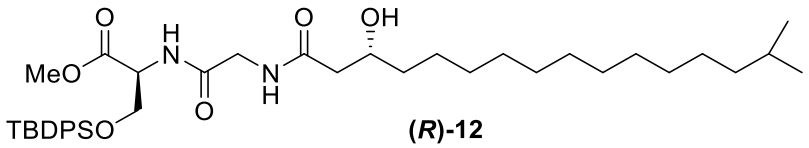

(*R*)-12

N-Hydroxysuccinimide (96 mg, 0.830 mmol) and dicyclohexylcarbodiimide (DCC, 188 mg, 0.913 mmol) were added to a stirring solution of 3-hydroxy-15-methylhexadecanoic acid (3*R*)-**20**, 159 mg, 0.554 mmol) in 10 mL of dry THF. The solution was stirred for 5 h at ambient temperature, filtered, and the filtrate was concentrated *in vacuo*. The resulting white solid was dissolved in 5 mL of dioxane and this solution was added via cannula to a solution of methyl *N*-(((benzyloxy)carbonyl)glycyl)-*O*-(*tert*-butyldiphenylsilyl)-L-serinate (**14**, 349 mg, 0.637 mmol) and Pd/C (122 mg) in 10 mL of dioxane. The reaction vessel was flushed with H_2 and the mixture was stirred overnight, filtered through Celite, and concentrated under reduced pressure. The crude product was purified via column chromatography (2% MeOH:DCM**)** to yield *O*-(*tert*-butyldiphenylsilyl)-*N*-((3R-hydroxy-15-methylhexadecanoyl)glycyl)-L-serinate, (3*R*)-L-serine-**12** as a clear oil (0.279 g, 0.405 mmol, 73.6%) ^{1}H NMR (400 MHz, $CDCl_3$) δ 7.64 – 7.54 (m, 4H), 7.49 – 7.35 (m, 6H), 6.89 (d, *J* = 8.1 Hz, 1H), 6.39 (t, *J* = 5.6 Hz, 1H), 4.67 (dt, *J* = 8.2, 2.9 Hz, 1H), 4.18 – 4.06 (m, 2H), 3.97 (s, 1H), 3.94 – 3.77 (m, 2H), 3.75 (s, 3H), 3.36 (d, *J* = 3.6 Hz, 1H), 2.41 (dd, *J* = 14.6, 2.6 Hz, 1H), 2.27 (dd, *J* = 14.6, 9.4 Hz, 1H), 1.56 – 1.34 (m, 4H), 1.34 – 1.20 (m, 18H), 1.19 – 1.13 (m, 2H), 1.04 (s, 9H), 0.86 (d, *J* = 6.6 Hz, 6H). ^{13}C NMR (101 MHz, $CDCl_3$) δ 172.8, 170.7, 168.6, 135.6, 135.5, 132.9, 132.6, 130.1, 128.0, 127.9, 77.4, 77.1, 76.8, 68.9, 64.3, 54.3, 52.6, 43.1, 42.9, 39.1, 37.2, 30.0, 29.8, 29.7, 29.6, 29.6, 28.0, 27.5, 26.8, 25.5, 22.7, 19.3. HRMS (AccuTOF): [MH]+ Calc'd for $C_{39}H_{63}N_2O_6Si$ *m/z* 683.4455. Found: *m/z* 683.4434.

Methyl *O*-(*tert*-butyldiphenylsilyl)-*N*-((3S-hydroxy-15-methylhexadecanoyl)glycyl)-L-serinate, ((*S*)-12)

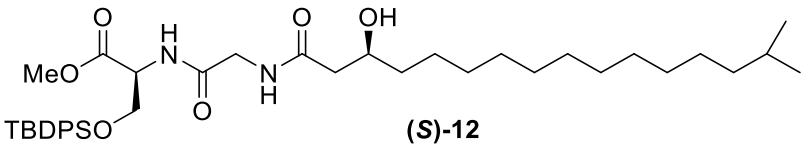

(*S*)-12

N-Hydroxysuccinimide (87 mg, 0.752 mmol) and dicyclohexylcarbodiimide (DCC, 171 mg, 0.827 mmol) were added to a stirring solution of 3-hydroxy-15-methylhexadecanoic acid ((3*S*)-**20**, 144 mg, 0.501 mmol) in 10 mL of dry THF. The solution was stirred for 5 h at ambient temperature, filtered, and the filtrate was concentrated *in vacuo*. The resulting white solid was dissolved in 5 mL of dioxane and this solution was added via cannula to a solution of methyl *N*-(((benzyloxy)carbonyl)glycyl)-*O*-(*tert*-butyldiphenylsilyl)-L-serinate (**14**, 316 mg, 0.576 mmol) and Pd/C (111 mg) in 10 mL of dioxane. The reaction vessel was flushed with H_2 and the mixture was stirred overnight, filtered through Celite, and concentrated under reduced pressure. The crude product was purified via column chromatography (2% MeOH:DCM**)** to yield *O*-(*tert*-butyldiphenylsilyl)-*N*-((3R-hydroxy-15-methylhexadecanoyl)glycyl)-L-serinate, (3*S*)-L-serine-**12** as a clear oil (0.261 g, 0.382 mmol, 76.0%) ^{1}H NMR (400 MHz, $CDCl_3$) δ 7.64 – 7.54 (m, 4H), 7.49 – 7.34 (m, 6H), 6.86 (d, *J* = 7.0 Hz, 1H), 6.34 (d, *J* = 5.4 Hz, 1H), 4.67 (dt, *J* = 8.2, 3.0 Hz, 1H), 4.13 (dd, *J* = 10.4, 2.9 Hz, 1H), 4.03 – 3.81 (m, 4H), 3.74 (s, 3H), 3.53 – 3.44 (m, 1H), 2.40 (dd, *J* = 14.6, 2.6 Hz, 1H), 2.26 (dd, *J* = 14.7, 9.5 Hz, 1H), 1.57 – 1.36 (m, 4H), 1.35 – 1.20 (m, 18H), 1.20 – 1.11 (m, 2H), 1.04 (s, 9H), 0.86 (d, *J* = 6.6 Hz, 6H). ^{13}C NMR (101 MHz, $CDCl_3$) δ 172.8, 170.7, 168.5, 135.6, 133.0, 132.7, 130.1, 127.9, 127.9, 77.4, 77.1, 76.7, 68.9, 64.3, 54.3, 52.6, 43.0, 42.8, 39.1, 37.2, 30.0, 29.8, 29.7, 29.7, 29.6, 28.0, 27.5, 26.8, 25.5, 22.7, 19.3. HRMS (AccuTOF): [MH]+ Calc'd for $C_{39}H_{63}N_2O_6Si$ *m/z* 683.4455. Found: *m/z* 683.4435.

Methyl (3-hydroxy-15-methylhexadecanoyl)glycyl-L-serinate, ((*rac*)-21)

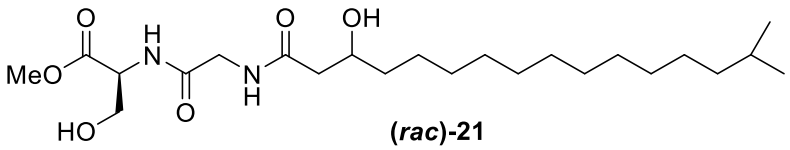

(*rac*)-21

Methyl *O*-(*tert*-butyldiphenylsilyl)-*N*-((3-hydroxy-15-methylhexadecanoyl)glycyl)-L-serinate ((3*R*+3*S*)-L-serine-**12**, 162 mg, 0.237 mmol) was dissolved in 5 mL of dry THF under nitrogen. The solution was cooled to 0°C and was treated with 1 M tetrabutylammonium fluoride (TBAF, 0.26 mL, 0.261 mmol). The reaction was slowly warmed to ambient temperature and stirred for 6 h. The solvent was removed under reduced pressure, and the resulting oil was purified by column chromatography (2.5 % MeOH:DCM) to yield methyl (3-hydroxy-15-methylhexadecanoyl)glycyl-L-serinate, (3*R*+3*S*)-**21**, as a white solid, (101 mg, 0.227 mmol, 95.8 %), MP, 105-107 °C. ^{1}H NMR (400 MHz, $CDCl_3$) δ 7.60 (d, *J* = 7.6 Hz, 1H), 7.20 – 7.11 (m, 1H), 4.67 – 4.58 (m, 1H), 4.12 (dd, *J* = 16.9, 6.2 Hz, 1H), 4.03 – 3.83 (m, 5H), 3.76 (s, 3H), 2.44 (dd, *J* = 14.0, 2.4 Hz, 1H), 2.30 (dd, *J* = 14.1, 9.7 Hz, 1H), 1.60 – 1.05 (m, 23H), 0.86 (d, *J* = 6.6 Hz, 6H). ^{13}C NMR (101 MHz, $CDCl_3$) δ 173.4, 173.3, 171.2, 171.0, 169.6, 77.4, 77.1, 76.7, 69.6, 62.6, 54.9, 52.8, 43.7, 43.2, 39.1, 37.5, 30.0, 29.8, 29.8, 29.7, 29.6, 28.0, 27.5, 25.7, 22.7. HRMS (AccuTOF): [MH]+ Calc'd for $C_{23}H_{45}N_2O_6$ *m/z* 445.3278. Found: *m/z* 445.3307.

Methyl (3(*R*)-hydroxy-15-methylhexadecanoyl)glycyl-L-serinate, ((*R*)-21)

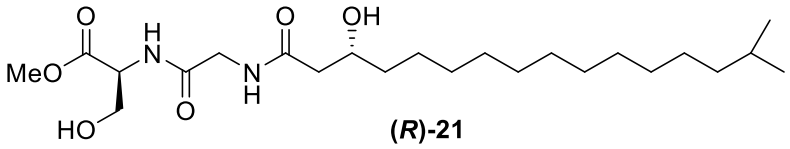

(*R*)-21

Methyl O-(tert-butyldiphenylsilyl)-N-((3R-hydroxy-15-methylhexadecanoyl)glycyl)-L-serinate ((3*R*)-L-serine-**12**, 276 mg, 0.403 mmol) was dissolved in 5 mL of dry THF under nitrogen.

The solution was cooled to 0 °C and was treated with 1 M tetrabutylammonium fluoride (TBAF, 0.44 mL, 0.444 mmol). The reaction was slowly warmed to ambient temperature and stirred for 6 h. The solvent was removed under reduced pressure, and the resulting oil was purified by column chromatography (2.5 % MeOH:DCM) to yield methyl (3*R*-hydroxy-15-methylhexadecanoyl)glycyl-L-serinate, (3*R*)-L-serine-**21**, as a white solid, (129 mg, 0.289 mmol, 71.6 %), MP, 100-104 °C. ^{1}H NMR (500 MHz, $CDCl_3$) δ 7.56 (d, *J* = 7.8 Hz, 1H), 7.00 (t, *J* = 5.9 Hz, 1H), 4.73 – 4.65 (m, 1H), 4.19 (dd, *J* = 16.9, 6.3, 2.1 Hz, 1H), 4.12-4.04 (m, 1H), 4.04 – 3.86 (m, 3H), 3.82 (s, 3H), 2.50 (dt, *J* = 14.1, 2.6 Hz, 1H), 2.40 – 2.30 (m, 1H), 1.63 – 1.44 (m, 4H), 1.44 – 1.23 (m, 18H), 1.19 (q, *J* = 6.8 Hz, 2H), 0.91 (d, *J* = 6.6 Hz, 6H). ^{13}C NMR (126 MHz, $CDCl_3$) δ 173.31, 171.10, 169.40, 77.27, 77.02, 76.76, 69.56, 62.71, 54.85, 52.80, 43.67, 43.30, 39.08, 37.43, 29.97, 29.75, 29.70, 29.63, 29.54, 27.98, 27.44, 25.62, 25.56, 22.67. HRMS (AccuTOF): [MH]+ Calc'd for $C_{23}H_{45}N_2O_6$ *m/z* 445.3278. Found: *m/z* 445.3285.

Methyl (3(*S*)-hydroxy-15-methylhexadecanoyl)glycyl-L-serinate, ((*S*)-21)

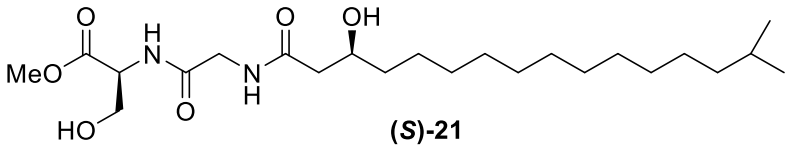

(*S*)-21

Methyl O-(tert-butyldiphenylsilyl)-N-((3S-hydroxy-15-methylhexadecanoyl)glycyl)-L-serinate ((3*S*)-L-serine-**12**, 216 mg, 0.316 mmol) was dissolved in 5 mL of dry THF under nitrogen. The solution was cooled to 0°C and was treated with 1 M tetrabutylammonium fluoride (TBAF, 0.35 mL, 0.347 mmol). The reaction was slowly warmed to ambient temperature and stirred for 6 h. The solvent was removed under reduced pressure, and the resulting oil was purified by column chromatography (2.5 % MeOH:DCM) to yield methyl (3*S*-hydroxy-15-

methylhexadecanoyl)glycyl-L-serinate, (3*S*)-L-serine-**21**, as a white solid, (96 mg, 0.216 mmol, 68.4 %), MP, 109-111 °C. ^{1}H NMR (500 MHz, $CDCl_3$) δ 7.36 (d, *J*= 7.4 Hz, 1H), 6.88-6.78 (m, 1H), 4.65 (dt, *J* = 7.3, 3.4 Hz, 1H), 4.21 – 4.10 (m, 1H), 4.04 (s, 1H), 3.98 – 3.92 (m, 2H), 3.92 – 3.80 (m, 2H), 3.78 (s, 3H), 2.45 (dt, *J* = 13.9, 2.5 Hz, 1H), 2.35 – 2.26 (m, 1H), 1.56 – 1.45 (m, 3H), 1.29 – 1.23 (m, 18H), 1.15 (q, *J* = 6.8 Hz, 2H), 0.86 (d, *J* = 6.6 Hz, 6H). ^{13}C NMR (126 MHz, $CDCl_3$) δ 173.16, 170.90, 169.43, 77.28, 77.02, 76.77, 69.27, 62.83, 62.80, 54.86, 54.81, 52.84, 43.51, 43.26, 39.09, 37.25, 29.97, 29.75, 29.70, 29.63, 29.53, 28.00, 27.45, 25.60, 22.68. HRMS (AccuTOF): [MH]+ Calc'd for $C_{23}H_{45}N_2O_6$ *m/z* 445.3278. Found: *m/z* 445.3242.

(3-Hydroxy-15-methylhexadecanoyl)glycyl-L-serine, ((*rac*)- 1)

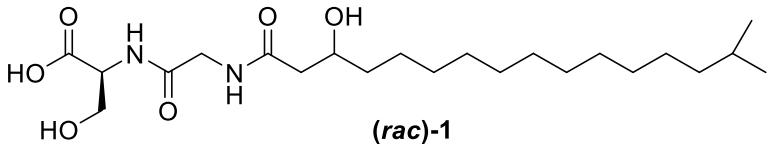

(*rac*)-1

A solution of 0.96 M LiOH (0.49 mL, 0.466 mmol) was added to a solution of methyl (3-hydroxy-15-methylhexadecanoyl)glycyl-L-serinate ((3*R*+3*S*)-L-serine-**21**, 189 mg, 0.424 mmol) in 2 mL of methanol at 0 °C, and 4 mL of tetrahydrofuran was subsequently added. The resulting solution was warmed to ambient temperature and stirred for 2 h. The solution was then neutralized with 10% HCl and diluted with 25 mL of H_2O. The solution was then extracted with EtOAc (3 X 25 mL) and the organic layers were concentrated *in vacuo*. The resulting crude material was recrystallized from hot EtOAc to yield (3-hydroxy-15-methylhexadecanoyl)glycyl-L-serine, (3*R*+3*S*)-L-serine-**1**, as a crystalline solid (177 mL, 0.412 mmol, 97.1 %), MP, 117-120 °C. ^{1}H NMR ^{1}H NMR (400 MHz, Methanol-d_4) δ 4.49 and 4.51 (two s, 1H), 4.11 (d, *J*= 17.3 Hz, 1H), 4.04 – 3.86 (m, 2H), 3.85 – 3.74 (m, 2H), 3.66 (d, *J*= 17.0 Hz, 1H), 3.37 – 3.29 (m, 1H), 2.41 –

2.33 (m, 1H), 2.27 – 2.19 (m, 1H), 1.53 – 1.34 (m, 4H), 1.34 – 1.14 (m, 18H), 1.09 (q, *J* = 7.1, 6.7 Hz, 2H), 0.80 (d, *J* = 6.6 Hz, 6H). ^{13}C NMR (101 MHz, CD_3OD+$CDCl_3$) δ 173.79, 173.58, 172.23, 172.09, 169.65, 169.56, 77.38, 77.06, 76.74, 69.24, 68.90, 62.14, 62.04, 54.69, 54.56, 49.83, 49.62, 49.40, 49.19, 48.97, 48.76, 48.55, 43.48, 43.29, 42.87, 42.77, 38.99, 37.44, 37.17, 29.87, 29.65, 29.60, 29.54, 29.47, 27.89, 27.34, 25.48, 25.43, 22.54. HRMS (AccuTOF): [MH]+ Calc'd for $C_{22}H_{43}N_2O_6$ *m/z* 431.3121. Found: *m/z* 431.3131.

(3(*R*)-Hydroxy-15-methylhexadecanoyl)glycyl-L-serine, ((*R*)-1)

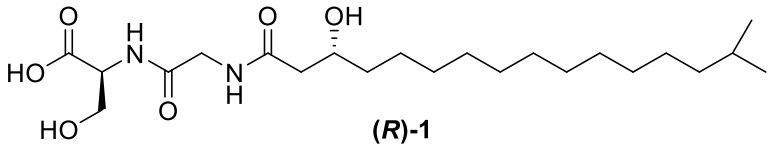

(*R*)-1

A solution of 0.51 M LiOH (0..33 mL, 0.168 mmol) was added to a solution of methyl (3*R*)-hydroxy-15-methylhexadecanoyl)glycyl-L-serinate ((3*R*)-L-serine-**21**, 68 mg, 0.153 mmol) in 2 mL of methanol at 0 °C, and 4 mL of tetrahydrofuran was subsequently added. The resulting solution was warmed to ambient temperature and stirred for 2 h. The solution was then neutralized with 10% HCl and diluted with 25 mL of H_2O. The solution was then extracted with EtOAc (3 X 25 mL) and the organic layers were concentrated *in vacuo*. The resulting crude material was recrystallized from hot EtOAc to yield (3(*R*)-hydroxy-15-methylhexadecanoyl)glycyl-L-serine, (3*R*)-L-serine-**1**, as a crystalline solid (44 mg, 0.102 mmol, 66.7 %), MP, 122-126 °C. ^{1}H NMR (500 MHz, $CDCl_3$) δ 4.53 (s, 1H), 4.15 (d, *J* = 16.8 Hz, 1H), 3.95 (s, 1H), 3.68 (d, *J* = 16.9 Hz, 1H), 3.31 (d, 25.0 Hz, 1H), 2.38 (d, *J* = 13.7 Hz, 1H), 2.24 (t, *J* = 12.1 Hz, 1H), 1.60 – 1.42 (m, 3H), 1.40 – 1.20 (m, 18H), 1.13 – 1.09 (m, 2H), 0.82 (d, 6H). ^{13}C NMR (126 MHz, $CDCl_3$) δ 173.74, 172.42, 169.59, 77.31, 77.06, 77.06, 76.80, 69.32, 62.23, 55.93, 43.54, 42.96, 39.04, 37.47,

29.92, 29.69, 29.65, 29.58, 29.51, 27.94, 27.39, 25.48, 22.65, 22.60. HRMS (AccuTOF): [MH]+ Calc'd for $C_{22}H_{43}N_2O_6$ *m/z* 431.3121. Found: *m/z* 431.3131.

(3(*S*)-Hydroxy-15-methylhexadecanoyl)glycyl-L-serine, ((*S*)-1)

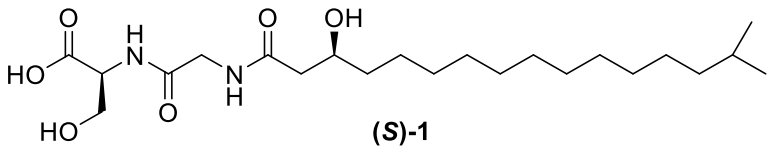

(*S*)-1

A solution of 0.51 M LiOH (0.40 mL, 0.203 mmol) was added to a solution of methyl (3(S)-hydroxy-15-methylhexadecanoyl)glycyl-L-serinate (3*S*)-L-serine-**21**, 82 mg, 0.184 mmol) in 2 mL of methanol at 0 °C, and 4 mL of tetrahydrofuran was subsequently added. The resulting solution was warmed to ambient temperature and stirred for 2 h. The solution was then neutralized with 10% HCl and diluted with 25 mL of H_2O. The solution was then extracted with EtOAc (3 X 25 mL) and the organic layers were concentrated *in vacuo*. The resulting crude material was recrystallized from hot EtOAc to yield (3(*S*)-hydroxy-15-methylhexadecanoyl)glycyl-L-serine, (3*S*)-L-serine-**1**, as a crystalline solid (59 mg, 0.137 mmol, 74.6 %), MP, 109-111 °C. ^{1}H NMR (400 MHz, $CDCl_3$) δ 4.53 (s, 1H), 4.13 (d, *J* = 16.9 Hz, 1H), 3.94 (d, *J* = 11.6 Hz, 2H), 3.82 (d, *J* = 11.6 Hz, 1H), 3.76 – 3.64 (m, 2H), 2.38 (d, *J* = 13.8 Hz, 1H), 2.24 (t, *J* = 12.0 Hz, 1H), 1.21 (s, 17H), 1.11 (s, 2H), 0.82 (d, *J* = 6.7 Hz, 6H). ^{13}C NMR (101 MHz, $CDCl_3$) δ 173.77, 172.35, 169.54, 77.37, 77.06, 76.74, 69.31, 62.20, 54.59, 43.53, 42.91, 39.02, 37.47, 29.90, 29.68, 29.63, 29.56, 29.49, 27.92, 27.38, 25.46, 22.59. HRMS (AccuTOF): [MH]+ Calc'd for $C_{22}H_{43}N_2O_6$ *m/z* 431.3121. Found: *m/z* 431.3131.

6-(Methoxycarbonyl)-2,2,25-trimethyl-8,11-dioxo-3,3-diphenyl-4-oxa-7,10-diaza-3-silahexacosan-13-yl 13-methyltetradecanoate, ((*rac*)-22)

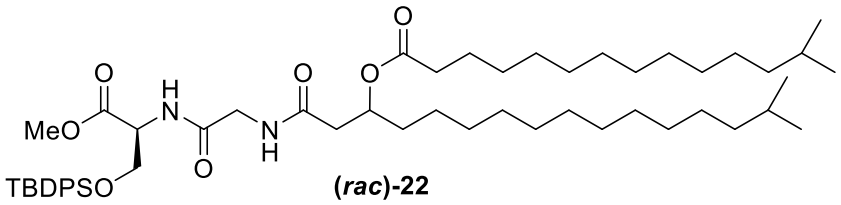

(*rac*)-22

13-Methyltetradecanoic acid (35 mg, 0.156 mmol) was dissolved in 5 mL of dry DCM and stirred at 0 °C. To the solution was then treated with DCC (32 mg, 0.156 mmol), HOBt (21 mg, 0.156 mmol), and a catalytic amount of DMAP. After stirring for 15 min, methyl *O*-(*tert*-butyldiphenylsilyl)-*N*-((3-hydroxy-15-methylhexadecanoyl)glycyl)-L-serinate, ((3*R*+3*S*)-**12**, 98 mg, 0.142 mmol) dissolved in 5 mL of dry DCM was added to the reaction via cannula. The resulting solution was warmed to ambient temperature and stirred overnight. The solvent was removed under reduced pressure and the resulting oil was redissolved in 20 mL of diethyl ether. The resulting precipitate was filtered, and the filtrate washed with satd $NaHCO_3$ (3 X 10 mL). The organic layer was dried, filtered, and solvents evaporated under reduced pressure. Purification via column chromatography (1% MeOH:DCM) yielded 6-(methoxycarbonyl)-2,2,25-trimethyl-8,11-dioxo-3,3-diphenyl-4-oxa-7,10-diaza-3-silahexacosan-13-yl 13-methyltetradecanoate, (3*R*+3*S*)-L-serine-**22**, as a clear oil (124 mg, 0.137 mmol, 96.3%). ^{1}H NMR (400 MHz, $CDCl_3$) δ 7.58 (tt, *J* = 6.8, 1.6 Hz, 4H), 7.49–7.34 (m, 6H), 6.54 (dd, *J* = 8.1, 5.2 Hz, 1H), 6.36 (t, *J*= 4.6 Hz, 1H), 5.16 (quin, *J* = 6.3 Hz, 1H), 4.69-4.62 (m, 1H), 4.12 (dd, *J* = 10.3, 2.9 Hz, 1H), 4.02–3.81 (m, 3H), 3.74 (s, 3H), 2.55–2.42 (m, 2H), 2.29 (t, *J* = 7.5 Hz, 2H), 1.70-1.59 (m, 4H), 1.50 (sep, *J* = 6.6 Hz, 2H), 1.37-1.20 (m, 36H), 1.15 (q, *J* = 7.1, 6.7 Hz, 4H), 1.03 (s, 9H), 0.86 (d, *J* = 6.6 Hz, 12H). ^{13}C NMR (101 MHz, $CDCl_3$) δ 173.41, 170.44, 170.40, 169.95, 168.24, 135.55, 135.51, 132.83, 132.80, 132.64, 130.10, 130.05, 127.96, 127.87, 77.38, 77.06, 76.74, 71.10, 64.15, 54.25, 52.56, 42.88,

41.42, 39.11, 34.55, 34.17, 30.00, 29.77, 29.73, 29.61, 29.56, 29.41, 29.35, 29.20, 28.02, 27.47, 26.77, 25.31, 25.05, 22.71, 19.30. HRMS (AccuTOF): [MH]+ Calc'd for $C_{54}H_{91}N_2O_7Si$ *m/z* 907.6596. Found: *m/z* 907.6557.

(6*S*,13*R*)-6-(Methoxycarbonyl)-2,2,25-trimethyl-8,11-dioxo-3,3-diphenyl-4-oxa-7,10-diaza-3-silahexacosan-13-yl 13-methyltetradecanoate, ((*R*)-22)

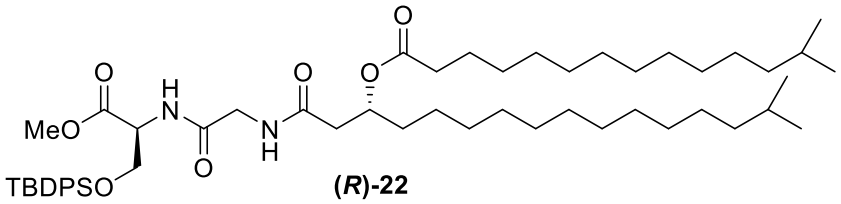

(*R*)-22

13-Methyltetradecanoic acid (77 mg, 0.316 mmol) was dissolved in 5 mL of dry DCM and stirred at 0 °C. To the solution was then treated with DCC (78 mg, 0.380 mmol), HOBt (58 mg, 0.379 mmol), and a catalytic amount of DMAP. After stirring for 15 min, methyl *O*-(*tert*-butyldiphenylsilyl)-*N*-((3*R*-hydroxy-15-methylhexadecanoyl)glycyl)-L-serinate, (3*R*)-L-serine-**12** (178 mg, 0.261 mmol) dissolved in 5 mL of dry DCM was added to the reaction via cannula. The resulting solution was warmed to ambient temperature and stirred overnight. The solvent was removed under reduced pressure and the resulting oil was redissolved in 20 mL of diethyl ether. The resulting precipitate was filtered, and the filtrate washed with satd $NaHCO_3$ (3 X 10 mL). The organic layer was dried, filtered, and solvents evaporated under reduced pressure. Purification via column chromatography (1% MeOH:DCM) yielded **(**6*S*,13*R*)-6-(methoxycarbonyl)-2,2,25-trimethyl-8,11-dioxo-3,3-diphenyl-4-oxa-7,10-diaza-3-silahexacosan-13-yl 13-methyltetradecanoate, (3*R*)-L-serine-**22** as a clear oil (231 mg, 0.255 mmol, 97.7%). ^{1}H NMR (400 MHz, $CDCl_3$) δ 7.58 (t, *J* = 6.6 Hz, 4H), 7.49 – 7.34 (m, 6H), 6.53 (d, *J* = 8.1 Hz, 1H), 6.36 (t, *J*= 4.6 Hz, 1H), 5.16 (d, *J* = 24.6 Hz, 1H), 4.69-4.62 (m, 1H), 4.12 (dd, *J* = 10.3, 2.9 Hz, 1H), 4.00 –

3.82 (m, 3H), 3.74 (s, 3H), 2.55 – 2.43 (m, 2H), 2.29 (t, *J* = 7.5 Hz, 2H), 1.70 – 1.55 (m, 4H), 1.50 (sep, *J* = 6.6 Hz, 2H), 1.25 (s, 36H), 1.15 (q, *J* = 7.1, 6.7 Hz, 4H), 1.03 (s, 9H), 0.86 (d, *J* = 6.6 Hz, 12H). ^{13}C NMR (101 MHz, $CDCl_3$) δ 173.43, 170.42, 169.96, 168.23, 135.56, 135.52, 132.83, 132.65, 130.10, 130.05, 127.96, 127.87, 77.38, 77.06, 76.74, 71.10, 64.15, 54.28, 52.57, 42.87, 41.43, 39.12, 34.55, 34.17, 30.00, 29.78, 29.73, 29.62, 29.57, 29.42, 29.35, 29.21, 28.02, 27.48, 26.78, 25.32, 25.05, 22.71, 19.31, 1.07. HRMS (AccuTOF): [MH]+ Calc'd for $C_{54}H_{91}N_2O_7Si$ *m/z* 907.6596. Found: *m/z* 907.6586.

(6*S*,13*S*)-6-(Methoxycarbonyl)-2,2,25-trimethyl-8,11-dioxo-3,3-diphenyl-4-oxa-7,10-diaza-3-silahexacosan-13-yl 13-methyltetradecanoate, ((*S*)-22)

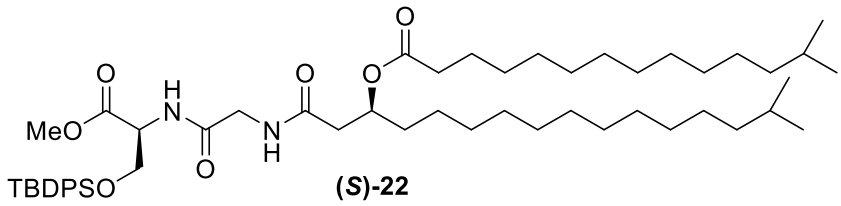

(*S*)-22

13-Methyltetradecanoic acid (84 mg, 0.346 mmol) was dissolved in 5 mL of dry DCM and stirred at 0 °C. The solution was then treated with DCC (85 mg, 0.415 mmol), HOBt (64 mg, 0.418 mmol), and a catalytic amount of DMAP. After stirring for 15 min, methyl *O*-(*tert*-butyldiphenylsilyl)-*N*-((3S-hydroxy-15-methylhexadecanoyl)glycyl)-L-serinate, (3*S*)-L-serine-**12** (189 mg, 0.277 mmol) dissolved in 5 mL of dry DCM was added to the reaction via cannula. The resulting solution was warmed to ambient temperature and stirred overnight. The solvent was removed under reduced pressure and the resulting oil was redissolved in 20 mL of diethyl ether. The resulting precipitate was filtered, and the filtrate washed with satd $NaHCO_3$ (3 X 10 mL). The organic layer was dried, filtered, and solvents evaporated under reduced pressure. Purification via column chromatography (1% MeOH:DCM) yielded **(**6*S*,13*S*)-6-(methoxycarbonyl)-2,2,25-

trimethyl-8,11-dioxo-3,3-diphenyl-4-oxa-7,10-diaza-3-silahexacosan-13-yl 13-methyltetradecanoate, (3*S*)-L-serine-**22** as a clear oil (245 mg, 0.269 mmol, 97.4%). ^{1}H NMR (400 MHz, $CDCl_3$) δ 7.63 – 7.54 (m, 4H), 7.48 – 7.34 (m, 6H), 6.53 (d, *J* = 8.1 Hz, 1H), 6.36 (t, *J*= 4.6 Hz, 1H), 5.16 (d, *J* = 24.6 Hz, 1H), 4.69-4.62 (m, 1H), 4.12 (dd, *J* = 10.3, 2.9 Hz, 1H), 4.04 – 3.79 (m, 2H), 3.73 (s, 3H), 2.57 – 2.41 (m, 2H), 2.28 (t, *J* = 7.5 Hz, 2H), 1.70-1.40 (m, 6H), 1.35-1.10 (m, 40H), 1.03 (s, 9H), 0.86 (d, *J* = 6.6 Hz, 12H). ^{13}C NMR (101 MHz, $CDCl_3$) δ 173.40, 170.46, 169.98, 168.31, 135.53, 135.49, 132.78, 132.62, 130.08, 130.02, 127.93, 127.85, 77.38, 77.06, 76.74, 71.08, 64.13, 54.24, 52.52, 42.89, 41.37, 39.09, 34.53, 34.15, 29.98, 29.76, 29.71, 29.60, 29.55, 29.39, 29.33, 29.19, 28.00, 27.45, 26.75, 26.69, 25.29, 25.03, 22.69, 22.63, 19.27, 1.05. HRMS (AccuTOF): [MH]+ Calc'd for $C_{54}H_{91}N_2O_7Si$ *m/z* 907.6596. Found: *m/z* 907.6583.

1-((2-(((*S*)-3-Hydroxy-1-methoxy-1-oxopropan-2-yl)amino)-2-oxoethyl)amino)-15-methyl-1-oxohexadecan-3-yl 13-methyltetradecanoate, ((*rac*)-23)

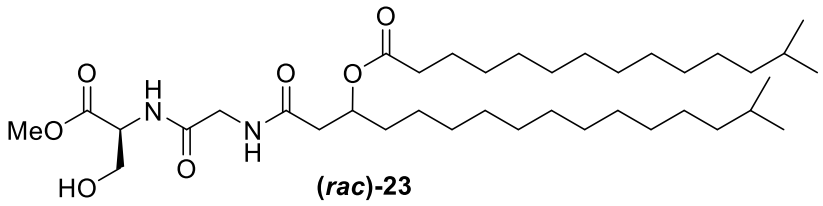

(*rac*)-23

6-(Methoxycarbonyl)-2,2,25-trimethyl-8,11-dioxo-3,3-diphenyl-4-oxa-7,10-diaza-3-silahexacosan-13-yl 13-methyltetradecanoate ((3*R*+3*S*)-L-serine-**22**, 197 mg, 0.217 mmol) was dissolved in 5 mL of dry THF under nitrogen. The solution was cooled to 0 °C and was treated with 1 M TBAF (0.24 mL, 0.24 mmol). The reaction was slowly warmed to ambient temperature and stirred for 6 h. The solvent was removed under reduced pressure, and the resulting oil was purified by column chromatography (2% MeOH:DCM) to yield 1-((2-(((*S*)-3-hydroxy-1-methoxy-1-oxopropan-2-yl)amino)-2-oxoethyl)amino)-15-methyl-1-oxohexadecan-3-yl 13-

methyltetradecanoate, (3*R*+3*S*)-L-serine-**23**, as a clear oil (132 mg, 0.202 mmol, 93.1 %). ^{1}H NMR (400 MHz, $CDCl_3$) δ two signals [7.05 and 7.12 (d, *J*= 7.6 and 7.8 Hz, 1H), 6.74 – 6.64 (m, 1H), 5.26 – 5.11 (m, 1H), 4.65 (h, *J* = 7.7, 3.8 Hz, 1H), 4.08 – 3.87 (m, 4H), 3.78 (d, *J* = 1.9 Hz, 3H), 2.52 – 2.45 (m, 2H), 2.30 (td, *J* = 7.6, 1.7 Hz, 2H), 1.68 – 1.43 (m, 6H), 1.40 – 1.20 (m, 36H), 1.15 (t, *J* = 6.6 Hz, 4H), 0.86 (d, *J* = 6.6 Hz, 12H). ^{13}C NMR (101 MHz, $CDCl_3$) δ 174.45, 174.28, 170.92, 170.80, 170.70, 169.05, 169.01, 77.38, 77.06, 76.74, 71.46, 62.82, 55.05, 52.72, 43.32, 41.91, 41.81, 39.12, 39.08, 34.60, 34.56, 34.50, 30.01, 29.78, 29.74, 29.70, 29.62, 29.57, 29.40, 29.33, 29.22, 29.19, 28.02, 27.48, 25.31, 25.06, 25.01, 22.71. HRMS (AccuTOF): [MH]+ Calc'd for $C_{38}H_{73}N_2O_7$ *m/z* 669.5418. Found: *m/z* 669.5425.

(*R*)-1-((2-(((*S*)-3-Hydroxy-1-methoxy-1-oxopropan-2-yl)amino)-2-oxoethyl)amino)-15-methyl-1-oxohexadecan-3-yl 13-methyltetradecanoate, ((*R*)-23)

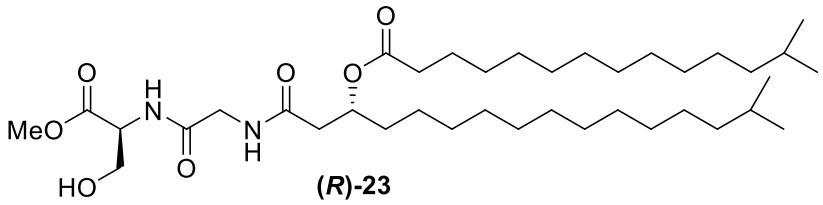

(*R*)-23

(6*S*,13*R*)-6-(Methoxycarbonyl)-2,2,25-trimethyl-8,11-dioxo-3,3-diphenyl-4-oxa-7,10-diaza-3-silahexacosan-13-yl 13-methyltetradecanoate, ((3*R*)-L-serine-**22**, 231 mg, 0.255 mmol) was dissolved in 5 mL of dry THF under nitrogen. The solution was cooled to 0 °C and was treated with 1 M TBAF (0.25 mL, 0.25 mmol). The reaction was slowly warmed to ambient temperature and stirred for 6 h. The solvent was removed under reduced pressure, and the resulting oil was purified by column chromatography (2% MeOH:DCM) to yield ((*R*)-1-((2-(((*S*)-3-hydroxy-1-methoxy-1-oxopropan-2-yl)amino)-2-oxoethyl)amino)-15-methyl-1-oxohexadecan-3-yl 13-

methyltetradecanoate, (3*R*)-L-serine-**23**, as a clear oil (153 mg, 0.229 mmol, 89.9 %) ^{1}H NMR (400 MHz, $CDCl_3$) δ 7.12 (d, *J*= 7.7 Hz, 1H), 6.45 (t, *J* = 5.5 Hz, 1H), 5.25-5.10 (m, 1H), 4.67 (dq, *J* = 7.1, 3.5 Hz, 1H), 4.13-3.87 (m, 4H), 3.79 (s, 3H), 2.49 (d, *J* = 6.1 Hz, 2H), 2.31 (t, *J* = 7.6 Hz, 2H), 1.69 – 1.44 (m, 6H), 1.38-1.20 (m, 36H), 1.15 (q, *J* = 6.7 Hz, 4H), 0.86 (d, *J* = 6.6 Hz, 12H). ^{13}C NMR (101 MHz, $CDCl_3$) δ 174.56, 170.70, 170.65, 168.95, 77.38, 77.06, 76.74, 71.54, 62.99, 55.01, 52.77, 43.43, 42.06, 39.12, 34.62, 30.01, 29.78, 29.74, 29.62, 29.56, 29.38, 29.33, 29.19, 28.03, 27.48, 25.32, 25.06, 25.01, 22.72. HRMS (AccuTOF): [MH]+ Calc'd for $C_{38}H_{73}N_2O_7$ *m/z* 669.5418. Found: *m/z* 669.5389.

(*S*)-1-((2-(((*S*)-3-Hydroxy-1-methoxy-1-oxopropan-2-yl)amino)-2-oxoethyl)amino)-15-methyl-1-oxohexadecan-3-yl 13-methyltetradecanoate, , ((*S*)-23)

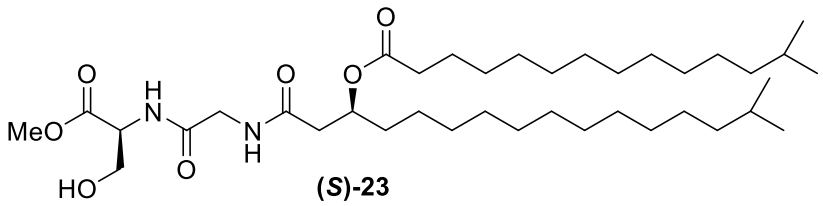

(*S*)-23

(6*S*,13*S*)-6-(Methoxycarbonyl)-2,2,25-trimethyl-8,11-dioxo-3,3-diphenyl-4-oxa-7,10-diaza-3-silahexacosan-13-yl 13-methyltetradecanoate, ((3*S*)-L-serine-**22**, 245 mg, 0.269 mmol) was dissolved in 5 mL of dry THF under nitrogen. The solution was cooled to 0 °C and was treated with 1 M TBAF (0.27 mL, 0.27 mmol). The reaction was slowly warmed to ambient temperature and stirred for 6 h. The solvent was removed under reduced pressure, and the resulting oil was purified by column chromatography (2% MeOH:DCM) to yield ((*S*)-1-((2-(((*S*)-3-hydroxy-1-methoxy-1-oxopropan-2-yl)amino)-2-oxoethyl)amino)-15-methyl-1-oxohexadecan-3-yl 13-methyltetradecanoate, (3*S*)-L-serine-**23,** as a clear oil (164 mg, 0.245 mmol, 90.8 %) ^{1}H NMR (400 MHz, $CDCl_3$) δ 7.05 (d, *J*= 7.6 Hz, 1H), 6.49 (t, *J* = 5.3 Hz, 1H), 5.26-5.10 (m, 1H), 4.70 – 4.61

(m, 1H), 4.13 – 3.88 (m, 4H), 3.79 (s, 3H), 2.49 (d, *J* = 5.9 Hz, 2H), 2.31 (t, *J* = 7.6 Hz, 2H), 1.72 – 1.44 (m, 6H), 1.43 – 1.19 (m, 36H), 1.15 (q, *J* = 6.7 Hz, 4H), 0.86 (d, *J* = 6.6 Hz, 12H). ^{13}C NMR (101 MHz, $CDCl_3$) δ 174.38, 170.79, 170.61, 168.94, 77.38, 77.06, 76.74, 71.54, 62.92, 55.02, 52.76, 43.43, 41.94, 39.12, 34.63, 34.55, 30.01, 29.79, 29.74, 29.62, 29.57, 29.38, 29.34, 29.22, 28.03, 27.48, 25.32, 25.06, 22.72. HRMS (AccuTOF): [MH]+ Calc'd for $C_{38}H_{73}N_2O_7$ *m/z* 669.5418. Found: *m/z* 669.5395.

(15-Methyl-3-((13-methyltetradecanoyl)oxy)hexadecanoyl)glycyl-L-serine, ((*rac*)-2)

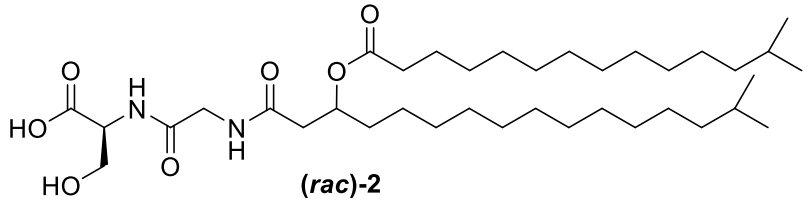

(*rac*)-2

A stirring solution of 1-((2-(3-hydroxy-1-methoxy-1-oxopropan-2-yl)amino)-2-oxoethyl)amino)-15-methyl-1-oxohexadecan-3-yl 13-methyltetradecanoate ((3*R*+3*S*)-L-serine-**23**, 119 mg, 0.178 mmol), in 10 mL of dry DCM, was cooled to 0 °C. Potassium trimethylsilonoate (25 mg, 0.196 mmol) was added, and the reaction was stirred on the ice bath for 1.5 h before being warmed to ambient temperature and stirred for an additional 1.5 hrs. The solvents were evaporated under reduced pressure, and the resulting oil was dissolved in 10 mL of H_2O and acidified with 10% HCl. The resulting precipitate was filtered to yield 15-methyl-3-((13-methyltetradecanoyl)oxy)hexadecanoyl)glycyl-L-serine, (3*R*+3*S*)-L-serine-**2**, as a white sticky solid (105 mg, 0.161 mmol, 90.2%). ^{1}H NMR (500 MHz, $CDCl_3$) δ 5.17 (bs, 1H), 4.27 (bs, 1H), 4.12-3.50 (s, 5H), 1.67 – 1.41 (m, 6H), 1.40-1.20 (m, 36H), 1.12 (t, *J* = 6.6 Hz, 4H), 0.83 (d, *J* = 6.6 Hz, 12H). ^{13}C NMR (126 MHz, $CDCl_3$) δ 174.04, 171.67, 169.92, 77.32, 77.06, 76.81, 71.21, 62.26, 55.95, 42.78, 41.09, 39.07, 34.58, 34.33, 31.91, 29.98, 29.76, 29.70, 29.67, 29.60, 29.52,

29.38, 29.22, 27.96, 27.44, 25.28, 25.07, 22.63. HRMS (+TOF MS): [MNa]+ Calc'd for $C_{37}H_{70}N_2NaO_7$ *m/z* 677.5075. Found: *m/z* 677.5081.

((*R*)-15-methyl-3-((13-methyltetradecanoyl)oxy)hexadecanoyl)glycyl-*L*-serine, ((*R*)-2)

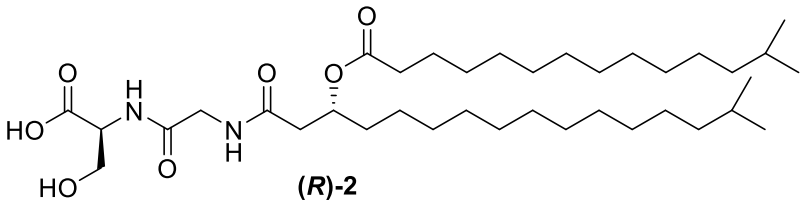

(*R*)-2

A stirring solution of 1(*R)*-1-((2-(((*S*)-3-hydroxy-1-methoxy-1-oxopropan-2-yl)amino)-2-oxoethyl)amino)-15-methyl-1-oxohexadecan-3-yl 13-methyltetradecanoate, ((3*R*)-L-serine-**23,** 25 mg, 0.037 mmol) in 10 mL of dry DCM was cooled to 0 °C. Potassium trimethylsilonoate (5.3 mg, 0.051 mmol) was added, and the reaction was stirred on the ice bath for 1.5 h before being warmed to ambient temperature and stirred for an additional 1.5 hrs. The solvents were evaporated under reduced pressure, and the resulting oil was dissolved in 10 mL of H_2O and acidified with 10% HCl. The resulting precipitate was filtered to yield ((*R*)-15-methyl-3-((13-methyltetradecanoyl)oxy)hexadecanoyl)glycyl-L-serine, (3*R*)-L-serine-**2**, as a white sticky solid (18 mg, 0.028 mmol, 74%). [□] $\frac{23}{D}$ = +12.8$_5$° (c 1.02, $CHCl_3$). ^{1}H NMR (400 MHz, $CDCl_3$) δ 5.15 (bs, 1H), 4.31 (bs, 1H), 4.11 – 3.44 (m, 4H), 2.47 (s, 2H), 2.24 (t, *J* = 7.5 Hz, 2H), 1.68 – 1.35 (m, 6H), 1.35 – 0.99 (m, 36H), 0.81 (d, *J* = 6.6 Hz, 12H). ^{13}C NMR (101 MHz, CD_3OD+ $CDCl_3$) δ 174.08, 173.94, 171.48, 169.54, 77.38, 77.06, 76.74, 71.08, 62.05, 49.39, 49.17, 48.96, 48.74, 48.53, 48.32, 48.10, 42.63, 40.87, 38.89, 34.37, 34.09, 29.78, 29.56, 29.52, 29.48, 29.43, 29.37, 29.26, 29.16, 29.00, 27.78, 27.25, 25.06, 24.87, 22.39. HRMS (+TOF MS): [MNa]+ Calc'd for $C_{37}H_{70}N_2NaO_7$ *m/z* 677.5075. Found: *m/z* 677.5081.

((*S*)-15-methyl-3-((13-methyltetradecanoyl)oxy)hexadecanoyl)glycyl-*L*-serine, ((*S*)-2)

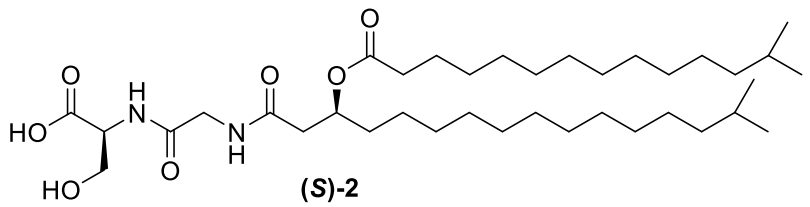

(*S*)-2

A stirring solution of 1(*S*)-1-((2-(((*S*)-3-hydroxy-1-methoxy-1-oxopropan-2-yl)amino)-2-oxoethyl)amino)-15-methyl-1-oxohexadecan-3-yl 13-methyltetradecanoate, ((3*S*)-L-serine-**23,** 25 mg, 0.037 mmol) in 10 mL of dry DCM was cooled to 0 °C. Potassium trimethylsilonoate (5.3 mg, 0.051 mmol) was added, and the reaction was stirred on the ice bath for 1.5 h before being warmed to ambient temperature and stirred for an additional 1.5 hrs. The solvents were evaporated under reduced pressure, and the resulting oil was dissolved in 10 mL of H_2O and acidified with 10% HCl. The resulting precipitate was filtered to yield ((*S*)-15-methyl-3-((13-methyltetradecanoyl)oxy)hexadecanoyl)glycyl-L-serine, (3*S*)-L-serine-**2**, as a white sticky solid (16 mg, 0.024 mmol, 65%). $[\square]_D^{23}$ = +6.3° (c 1.02, $CHCl_3$). ^{1}H NMR (400 MHz, $CDCl_3$) δ 5.16 (t, *J*= 5.6 Hz, 1H), 4.29 (s, 1H), 4.10 – 3.60 (m, 4H), 2.56 – 2.35 (m, 2H), 2.23 (t, *J* = 7.5 Hz, 2H), 1.65 – 1.40 (m, 6H), 1.40 – 0.99 (m, 40H), 0.81 (d, *J* = 6.6 Hz, 12H). ^{13}C NMR (101 MHz, $CDCl_3$) δ 174.03, 173.75, 171.50, 169.73, 77.38, 77.06, 76.74, 71.20, 62.24, 55.60, 50.01, 49.80, 49.58, 49.37, 49.16, 48.94, 48.73, 42.74, 41.11, 39.04, 34.53, 34.33, 29.95, 29.73, 29.70, 29.66, 29.62, 29.55, 29.46, 29.40, 29.33, 29.18, 27.93, 27.41, 25.24, 25.02, 22.60. HRMS (+TOF MS): [MNa]+ Calc'd for $C_{37}H_{70}N_2NaO_7$ *m/z* 677.5075. Found: *m/z* 677.5081.

((11-Bromoundecyl)oxy)(*tert*-butyl)dimethylsilane, (28)

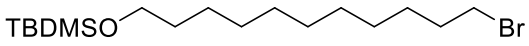

28

A flame-dried 100 mL round bottom flask was charged with 11-bromoundecan-1-ol (2.00 g, 7.96 mmol). The starting material was dissolved in CH_2Cl_2 (50 mL) and cooled on an ice bath. *tert*-Butyldimethylsilyl chloride (1.40 g, 9.15 mmol) was added and stirred for 15 min before the addition of imidazole (0.705 g, 10.4 mmol). The reaction was stirred overnight at room temperature. Upon completion the suspension was gravity filtered and concentrated under reduced pressure. The crude product was purified by column chromatography on silica gel (5% EtOAc:hexane) to yield ((11-bromoundecyl)oxy)(*tert*-butyl)dimethylsilane,[57] **28**, as a clear liquid (2.85 g, 7.78 mmol, 97.7%). ^{1}H NMR (400 MHz, $CDCl_3$) δ 3.60 (t, J = 6.6 Hz, 2H), 3.41 (t, J = 6.9 Hz, 2H), 1.85 (p, J = 7.0 Hz, 2H), 1.51 (t, J = 6.8 Hz, 2H), 1.42 (t, J = 7.4 Hz, 2H), 1.28 (s, 12H), 0.90 (s, 9H), 0.05 (s, 6H). ^{13}C NMR (101 MHz, $CDCl_3$) δ 63.38, 34.09, 32.94, 32.91, 29.63, 29.53, 29.47, 28.82, 28.24, 26.05, 25.85, 18.44, -5.19. ppm HRMS (AccuTOF): [MH]+ Calc'd for $C_{17}H_{37}BrOSi$ *m/z* 365.1875. Found: *m/z* 365.1869.

1-Bromobutane

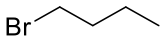

A solution of 48% HBr (2.50 g) was added to a flame dried 25 mL round bottomed flask. Dropwise addition of H_2SO_4 (0.40 mL) was followed by stirring until the flask was cool to the touch. Dropwise addition of butan-1-ol (1.00 g, 13.5 mmol) was followed by treatment with H_2SO_4 (0.35 mL). A reflux condenser was attached and the solution was heated for 3 h. A vacuum distillation apparatus was set up through the top of the original reflux condenser. The product was gently vacuum-distilled into an ice-chilled flask while the vertical condenser was slowly warmed.

The distillate was dried over $CaCO_3$ to yield 1-bromobutane[58] as a clear liquid (1.13 g, 8.25 mmol, 61%). ^{1}H NMR (400 MHz, $CDCl_3$) δ 3.42 (t, *J* = 6.8 Hz, 2H), 1.84 (p, *J* = 6.9 Hz, 2H), 1.48 (hept, *J* = 7.5 Hz, 2H), 0.93 (t, *J* = 7.4 Hz, 3H). ^{13}C NMR (101 MHz, $CDCl_3$) δ 34.83, 33.72, 21.37, 13.23.

<u>*d*$_9$-1-Bromobutane</u>

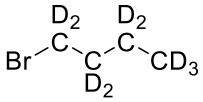

A solution of 48% HBr (2.50 g) was added to a flame-dried 25 mL round bottomed flask. Dropwise addition of H_2SO_4 (0.40 mL) was followed by stirring until the flask was cool to the touch. Dropwise addition of commercially available *d*$_9$-butan-1-ol (1.00 g, 12.0 mmol), was followed by addition of H_2SO_4 (0.35 mL). A reflux condenser was attached and the solution was heated at reflux for 3 h. A vacuum distillation apparatus was set up through the top of the original reflux condenser. The product was gently vacuum distilled into an ice-chilled flask while the vertical condenser was slowly warmed. The distillate was dried over $CaCO_3$ to yield *d*$_9$-1-bromobutane[59] as a clear liquid (0.99 g, 6.78 mmol, 56.4%).

<u>*tert*-Butyldimethyl(pentadecyloxy)silane, (29)</u>

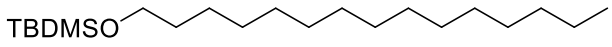

29

Magnesium turnings (33 mg, 1.37 mmol) were added to a 25 mL round bottomed flask that was fitted with a stirbar and the apparatus was flame-dried under a nitrogen atmosphere. After cooling, the Mg turnings were suspended in dry THF (5 mL) and 1-bromobutane (0.13 mL, 1.20 mmol) was rapidly added with vigorously stirring. The reaction was stirred until the flask cooled

to ambient temperature and the flask was subsequently chilled to 0 °C. The Grignard reagent was added to a mixture of ((11-bromoundecyl)oxy)(*tert*-butyl)dimethylsilane (**28**, 0.250 g,0.684 mmol), LiCl (0.88 mg, 0.021 mmol), copper (II) chloride (2.8 mg, 0.021 mmol), and *N*-methyl-2-pyrrolidone (NMP, 0.30 mL, 3.11 mmol) dissolved in THF (5 mL) and held at 0 °C. The mixture was slowly warmed to ambient temperature and stirred for 1 h. The reaction was quenched on ice with 1M HCl (10 mL) before being transferred to a separatory funnel with EtOAc (15 mL) and H_2O (10 mL). The layers were separated and the aqueous layer was extracted once with EtOAc (15 mL). The organic layers were combined and then washed with 1M HCl (10 mL), H_2O (2 X 10 mL), and brine (10 mL). The organic phase was dried with $MgSO_4$, gravity filtered, and solvents removed *in vacuo*. The crude product was purified by column chromatography on silica gel (hexane) to yield *tert*-butyldimethyl(pentadecyloxy)silane, **29**, as a clear liquid (0.218 g,0.636 mmol, 93.0%). ^{1}H NMR (400 MHz, $CDCl_3$) δ 3.60 (t, J = 6.6 Hz, 2H), 1.52 (d, J = 6.8 Hz, 2H), 1.26 (s, 24H), 0.96–0.79 (m, 12H), 0.05 (s, 6H). ^{13}C NMR (101 MHz, $CDCl_3$) δ 63.41, 32.97, 31.99, 29.75, 29.72, 29.51, 29.42, 26.05, 25.87, 22.75, 14.18, -5.19. HRMS (AccuTOF): [MH]+ Calc'd for $C_{21}H_{46}OSi$ *m/z* 343.3396. Found: *m/z* 343.3373.

<u>*tert*-Butyldimethyl((pentadecyl-12,12,13,13,14,14,15,15,15-*d*$_9$)oxy)silane, (37)</u>

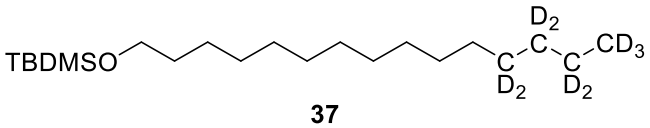

37

Magnesium turnings (133 mg, 5.48 mmol) were added to a 50 mL round bottom flask fitted with a stirbar and the apparatus was flame-dried under a nitrogen atmosphere. After cooling, the Mg turnings were suspended in dry THF (10 mL) and d_9-1-bromobutane (0.52 mL, 4.80 mmol) was rapidly added with vigorously stirring. The reaction was stirred until the flask cooled to

ambient temperature and the temperature was lowered to 0 °C. The Grignard reagent was added to a mixture of ((11-bromoundecyl)oxy)(*tert*-butyl)dimethylsilane (**28**, 1.00 g, 2.74 mmol), LiCl (5.8 mg, 0.14 mmol), copper (II) chloride (9.2 mg, 0.069 mmol), and NMP (1.98 mL, 20.6 mmol) dissolved in THF (10 mL) and the reaction mixture was maintained at 0 °C. The mixture was slowly warmed to ambient temperature and stirred for 1 h. The reaction was quenched on ice with 1M HCl (25 mL) before being transferred to a separatory funnel with EtOAc (50 mL) and H_2O (50 mL). The layers were separated and the aqueous layer was extracted once with EtOAc (50 mL). The organic layers were combined and washed with 1M HCl (25 mL), H_2O (2 X 25 mL), and brine (25 mL). The organic phase was dried with $MgSO_4$, gravity filtered, and solvents removed *in vacuo*. The crude product was purified by column chromatography on silica gel (hexane) to yield *tert*-butyldimethyl((pentadecyl-12,12,13,13,14,14,15,15,15-d_9)oxy)silane, **37**, as a clear liquid (0.949 g, 2.69 mmol, 98.3%). ^{1}H NMR (400 MHz, $CDCl_3$) δ 3.60 (t, J = 6.6 Hz, 2H), 1.51 (t, J = 6.8 Hz, 2H), 1.25 (s, 18H), 0.89 (s, 9H), 0.05 (s, 6H). ^{13}C NMR (101 MHz, $CDCl_3$) δ 63.42, 32.96, 29.76, 29.72, 29.68, 29.52, 29.47, 26.05, 25.87, 18.44, -5.19. HRMS (AccuTOF): [MH]+ Calc'd for $C_{21}H_{37}D_9OSi$ *m/z* 352.3961. Found: *m/z* 352.3949.

Pentadecan-1-ol, (30)

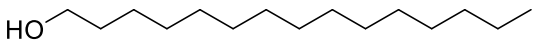

30

tert-Butyldimethyl(pentadecyloxy)silane (**29**, 678 mg, 1.98 mmol) was dissolved in 25 mL of dry THF under nitrogen. The solution was cooled to 0 °C and was treated with 1 M TBAF (4.95 mL, 4.95 mmol). The reaction was slowly warmed to ambient temperature and stirred for 6 h. The solvent was removed under reduced pressure, and the resulting oil was purified by column

chromatography (15% EtOAc:Hexanes) to yield ethyl 3-hydroxyheptadecanoate,[60] **30**, as a white solid (395 mg, 1.73 mmol, 87.4 %), MP 44-46 °C. ^{1}H NMR (400 MHz, $CDCl_3$) δ 3.64 (t, J = 6.6 Hz, 2H), 1.57 (t, J = 7.2, 6.7 Hz, 2H), 1.35–1.23 (m, 25H), 0.88 (t, J = 6.8 Hz, 3H). ^{13}C NMR (101 MHz, $CDCl_3$) δ 63.17, 32.88, 31.98, 29.74, 29.72, 29.66, 29.49, 29.41, 25.80, 22.75, 14.17. HRMS (AccuTOF): [M2H]+ Calc'd for $C_{15}H_{32}O$ *m/z* 457.4985. Found: *m/z* 457.4998.

Pentadecan-12,12,13,13,14,14,15,15,15-*d*$_9$-1-ol, (38)

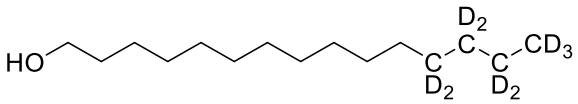

38

tert-Butyldimethyl((pentadecyl-12,12,13,13,14,14,15,15,15-*d*$_9$)oxy)silane (**37**, 961 mg, 2.73 mmol) was dissolved in 25 mL of dry THF under nitrogen. The solution was cooled to 0 °C and was treated with 1 M TBAF (6.83 mL, 6.83 mmol). The reaction was slowly warmed to ambient temperature and stirred for 6 h. The solvent was removed under reduced pressure, and the resulting oil was purified by column chromatography (15% EtOAc:Hexanes) to yield pentadecan-12,12,13,13,14,14,15,15,15-*d*$_9$-1-ol, **38**, as a white solid (643 mg, 2.71 mmol, 99.1 %), MP 42-45 °C. ^{1}H NMR (400 MHz, $CDCl_3$) δ 3.64 (t, J = 6.6 Hz, 2H), 1.57 (p, J = 6.9 Hz, 2H), 1.39–1.22 (m, 19H). ^{13}C NMR (101 MHz, $CDCl_3$) δ 63.18, 32.89, 29.72, 29.67, 29.49, 25.80. HRMS (AccuTOF): [M-OH]+ Calc'd for $C_{15}H_{23}D_9O$ *m/z* 220.2991. Found: *m/z* 220.2975.

Pentadecanal, (31)

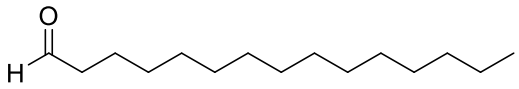

31

4-(Acetyamino)-2,2,6,6-tetramethyl-1-oxo-piperidinium tetrafluoroborate[smith-bobbit] (Bobbit's salt, 3.552 g, 11.84 mmol) was added to pentadecan-1-ol (**30**, 2.351 g, 10.29 mmol) dissolved in 200 mL of dry DCM. An equal mass of silica was slowly added to the stirring mixture. The bright yellow solution stirred at ambient temperature until the color faded, giving a solution with a pale yellow tint. The solution was filtered to remove the silica, and the filtrate was concentrated *in vacuo.* The crude product was purified by column chromatography (5% EtOAc:hexanes) to yield pentadecanal,[61] **31**, as a clear solid, (2.116 g, 9.346 mmol, 90.8%), MP ~25 °C. ^{1}H NMR (400 MHz, $CDCl_3$) δ 9.76 (t, J = 1.9 Hz, 1H), 2.41 (td, J = 7.3, 1.9 Hz, 2H), 1.63 (p, J = 7.3 Hz, 2H), 1.35–1.22 (m, 22H), 0.88 (t, J = 6.7 Hz, 3H). ^{13}C NMR (101 MHz, $CDCl_3$) δ 203.01, 43.98, 31.98, 29.70, 29.63, 29.48, 29.41, 29.23, 22.74, 22.16, 14.17. HRMS (AccuTOF): [M-H]+ Calc'd for $C_{15}H_{30}O$ *m/z* 225.2218. Found: *m/z* 225.2216.

Pentadecanal-12,12,13,13,14,14,15,15,15-*d*$_9$, (39)

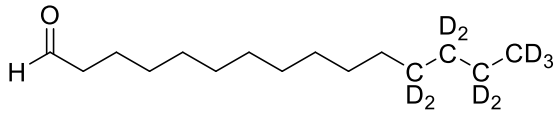

39

4-(Acetyamino)-2,2,6,6-tetramethyl-1-oxo-piperidinium tetrafluoroborate[smith-bobbit] (Bobbit's salt, 829 mg, 2.76 mmol) was added to pentadecan-12,12,13,13,14,14,15,15,15-*d*$_9$-1-ol (**38**, 625 mg, 2.63 mmol) dissolved in 100 mL of dry DCM. An equal mass of silica was slowly added to the stirring mixture. The bright yellow solution stirred at ambient temperature until the

color faded, giving a solution with a pale yellow tint. The solution was filtered to remove the silica, and the filtrate was concentrated *in vacuo.* The crude product was purified by column chromatography (5% EtOAc:hexanes) to yield pentadecanal-12,12,13,13,14,14,15,15,15-d_9, **39**, as a clear solid, (468 mg, 1.99 mmol, 75.6%), MP, ~25 °C. ^{1}H NMR (400 MHz, $CDCl_3$) δ 9.76 (t, J = 2.0 Hz, 1H), 2.41 (td, J = 7.4, 1.9 Hz, 2H), 1.64 (p, J = 7.2 Hz, 2H), 1.32–1.20 (m, 16H). ^{13}C NMR (101 MHz, $CDCl_3$) δ 203.01, 43.98, 29.73, 29.69, 29.64, 29.48, 29.46, 29.41, 29.23, 22.16. HRMS (AccuTOF): [MH]+ Calc'd for $C_{15}H_{21}D_9O$ *m/z* 234.2783. Found: *m/z* 234.2808.

Ethyl 3-oxoheptadecanoate, (32)

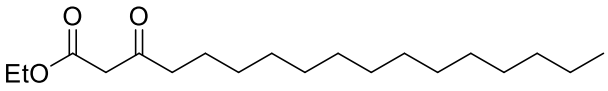

32

Tin (II) chloride dihydrate (52 mg, 0.231 mmol) was suspended in 20 mL of dry DCM. Ethyl diazoacetate (319 mg, 2.43 mmol) was added, dropwise via syringe, and the reaction was stirred for 15 min. Pentadecanal (**31**, 524 mg, 2.31 mmol) was dissolved in 10 mL of DCM and added to the reaction, dropwise, via cannula. The mixture was stirred at ambient temperature for about 6 h, until nitrogen evolution ceased. The reaction mixture was diluted with 100 mL of DCM and washed with a saturated brine solution (2 X 50 mL). The aqueous layers were combined and extracted with DCM (2 X 25 mL). All organic layers were combined, dried with $MgSO_4$, filtered, and solvents evaporated at reduced pressure. The resulting crude product was purified via column chromatography (5% EtOAc:hexanes) to yield ethyl 3-oxoheptadecanoate,[62] **32**, as a clear solid (642 mg, 2.07 mmol, 89.6%), MP 37-39 °C. ^{1}H NMR (400 MHz, $CDCl_3$) δ 4.20 (q, J = 7.1 Hz, 2H), 3.42 (s, 2H), 2.53 (t, J = 7.4 Hz, 2H), 1.59 (p, J = 7.1 Hz, 2H), 1.34–1.22 (m, 25H), 0.88 (t, J = 6.8 Hz, 3H). ^{13}C NMR (101 MHz, $CDCl_3$) δ 203.03, 167.32, 61.38, 49.38, 43.12, 31.98, 29.71,

29.65, 29.50, 29.41, 29.09, 23.54, 22.75, 14.17. HRMS (AccuTOF): [MH]+ Calc'd for $C_{19}H_{36}O_3$ *m/z* 313.2743. Found: *m/z* 313.2724.

Ethyl 3-oxoheptadecanoate-14,14,15,15,16,16,17,17,17-*d*$_9$, (40)

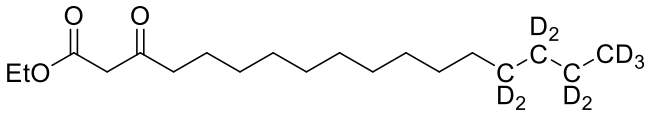

40

Tin (II) chloride dihydrate (46 mg, 0.206 mmol) was suspended in 15 mL of dry DCM. Ethyl diazoacetate (0.275 mL, 2.27 mmol) was added, dropwise via syringe, and the reaction was stirred for 15 min. The pentadecanal-12,12,13,13,14,14,15,15,15-*d*$_9$ (**39**, 486 mg, 2.06 mmol) was dissolved in 10 mL of DCM and added to the reaction, dropwise, via cannula. The mixture was stirred at ambient temperature for about 6 h, until nitrogen evolution ceased. The reaction mixture was diluted with 100 mL of DCM and washed with a saturated brine solution (2 X 50 mL). The aqueous layers were combined and extracted with DCM (2 X 25 mL). All organic layers were combined, dried with $MgSO_4$, filtered, and solvents evaporated at reduced pressure. The resulting crude product was purified via column chromatography (5% EtOAc:hexanes) to yield ethyl 3-oxoheptadecanoate-14,14,15,15,16,16,17,17,17-*d*$_9$, **40**, as a clear solid (534 mg, 1.66 mmol, 80.6%), MP 36-38 °C. ^{1}H NMR (400 MHz, $CDCl_3$) δ 4.19 (q, J = 7.1 Hz, 2H), 3.42 (s, 2H), 2.52 (t, J = 7.4 Hz, 2H), 1.59 (t, J = 7.2 Hz, 2H), 1.29–1.24 (m, 19H). ^{13}C NMR (101 MHz, $CDCl_3$) δ 203.05, 167.32, 61.38, 49.38, 43.12, 29.73, 29.70, 29.65, 29.50, 29.46, 29.41, 29.09, 23.54, 14.16. HRMS (AccuTOF): [MH]+ Calc'd for $C_{19}H_{27}D_9O_3$ *m/z* 322.3308. Found: *m/z* 322.3324.

Ethyl 3-hydroxy-heptadecanoate, (33)

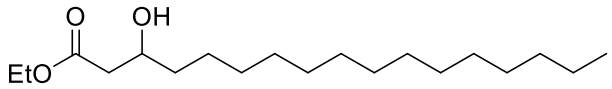

33

A solution of ethyl 3-oxoheptadecanoate (**32**, 620 mg, 1.98 mmol) in 2 mL of ethanol and 18 mL of THF was cooled to 0 °C on an ice bath. Sodium borohydride (60 mg, 1.59 mmol) was added and the resulting slurry was stirred vigorously for 1 h. The reaction was quenched by the slow addition of 10 mL of a 10 % aq. citric acid solution. Subsequent neutralization with satd. K_2CO_3 solution was followed by extraction with EtOAc (3 X 20 mL). The organic layers were washed with 10 mL of satd. brine solution, dried with $MgSO_4$, filtered, and the solvents were removed at reduced pressure. The crude product was purified by column chromatography (10% EtOAc:Hexanes) to yield ethyl 3-hydroxy-heptadecanoate, 33, as a white solid (455 mg, 1.45 mmol, 77.6 % brsm) MP 41-43 °C. ^{1}H NMR (400 MHz, $CDCl_3$) δ 4.17 (q, J = 7.1 Hz, 2H), 3.99 (tt, J = 7.9, 3.9 Hz, 1H), 2.90 (d, J = 4.0 Hz, 1H), 2.50 (dd, J = 16.4, 3.1 Hz, 1H), 2.39 (dd, J = 16.4, 9.0 Hz, 1H), 1.43 (dd, J = 8.5, 4.3 Hz, 2H), 1.38–1.19 (m, 27H), 0.88 (t, J = 6.6 Hz, 3H). ^{13}C NMR (101 MHz, $CDCl_3$) δ 173.19, 68.11, 60.71, 41.35, 36.59, 31.99, 29.74, 29.71, 29.64, 29.59, 29.42, 25.54, 22.75, 14.25, 14.18. HRMS (AccuTOF): [MH]+ Calc'd for $C_{19}H_{38}O_3$ *m/z* 315.2899. Found: *m/z* 315.2899.

Ethyl 3-hydroxyheptadecanoate-14,14,15,15,16,16,17,17,17-*d*$_9$, (41)

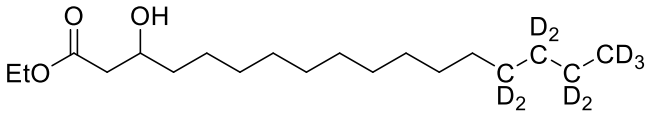

41

A solution of ethyl 3-oxoheptadecanoate-14,14,15,15,16,16,17,17,17-*d*$_9$ (**40**, 515 mg, 1.60 mmol) in 2 mL of ethanol and 18 mL of THF was cooled to 0 °C on an ice bath. Sodium borohydride (48 mg, 1.28 mmol) was added and the resulting slurry was stirred vigorously for 1 h. The reaction was quenched by the slow addition of 10 mL of a 10 % aq. citric acid solution. Subsequent neutralization with satd. K_2CO_3 solution was followed by extraction with EtOAc (3 X 20 mL). The organic layers were washed with 10 mL of satd. brine solution, dried with $MgSO_4$, filtered, and the solvents were removed at reduced pressure. The crude product was purified by column chromatography (10% EtOAc:Hexanes) to yield ethyl 3-hydroxyheptadecanoate-14,14,15,15,16,16,17,17,17-*d*$_9$, **41**, as a white solid (392 mg, 1.21 mmol, 79.7 % brsm) MP 38-40 °C. ^{1}H NMR (400 MHz, $CDCl_3$) δ 4.17 (q, J = 7.2 Hz, 2H), 4.00 (ddt, J = 12.0, 7.3, 4.0 Hz, 1H), 2.90 (d, J = 4.0 Hz, 1H), 2.50 (dd, J = 16.4, 3.2 Hz, 1H), 2.39 (dd, J = 16.4, 9.0 Hz, 1H), 1.47–1.39 (m, 2H), 1.39–1.12 (m, 21H). ^{13}C NMR (101 MHz, $CDCl_3$) δ 173.19, 68.11, 60.72, 41.35, 36.59, 29.75, 29.71, 29.64, 29.59, 29.47, 25.54, 14.25. HRMS (AccuTOF): [MH]+ Calc'd for $C_{19}H_{29}D_9O_3$ *m/z* 324.3464. Found: *m/z* 324.2442.

3-Hydroxy heptadecanoic acid, (34)

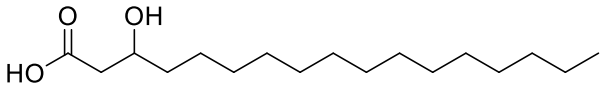

34

Hydroxy ester **33** (440 mg, 1.40 mmol) was dissolved in 2 mL of MeOH and 4 mL of THF and 1 M aqueous LiOH (1.68 mL, 1.61 mmol) were added. The mixture was stirred overnight at ambient temperature. The reaction was then acidified with 1 M HCl and extracted with EtOAc (3 X 15 mL). The organic layers were washed with 10 mL of brine, dried with $MgSO_4$, filtered, and the solvents were removed at reduced pressure. The crude solid was recrystallized from hexanes to yield 3-hydroxy-heptadecanoic acid, **34,** as a white solid (335 mg, 1.17 mmol, 83.6%), MP 86-88 °C. ^{1}H NMR (400 MHz, $CDCl_3$) δ 4.04 (tt, J = 8.1, 3.8 Hz, 1H), 2.59 (dd, J = 16.6, 3.2 Hz, 1H), 2.48 (dd, J = 16.6, 8.9 Hz, 1H), 1.55–1.43 (m, 3H), 1.40–1.15 (m, 24H), 0.88 (t, J = 6.7 Hz, 3H). ^{13}C NMR (101 MHz, $CDCl_3$) δ 175.72, 68.07, 40.73, 36.62, 31.98, 29.75, 29.71, 29.63, 29.60, 29.52, 29.42, 25.48, 22.75, 14.18. HRMS (AccuTOF): [MH]+ Calc'd for $C_{17}H_{34}O_3$ *m/z* 287.2586. Found: *m/z* 287.2605.

3-Hydroxyheptadecanoic-14,14,15,15,16,16,17,17,17-*d*$_9$ acid, (42)

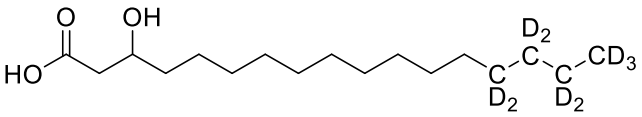

42

Ethyl 3-hydroxyheptadecanoate-14,14,15,15,16,16,17,17,17-*d*$_9$, **41** (390 mg, 1.21 mmol) was dissolved in 2 mL of MeOH and 4 mL of THF and 1 M aqueous LiOH (1.45 mL, 1.39 mmol) were added. The mixture was stirred overnight at ambient temperature. The reaction was then acidified with 1 M HCl and extracted with EtOAc (3 X 15 mL). The organic layers were washed

with 10 mL of brine, dried with $MgSO_4$, filtered, and the solvents were removed at reduced pressure. The crude solid was recrystallized from hexanes to yield 3-hydroxyheptadecanoic-14,14,15,15,16,16,17,17,17-d_9 acid, **42,** as a white solid (318 mg, 1.08 mmol, 89.3%), MP 79-81 °C. ^{1}H NMR (400 MHz, $CDCl_3$) δ 4.03 (s, 1H), 2.58 (dd, J = 16.6, 3.2 Hz, 1H), 2.48 (dd, J = 16.6, 8.9 Hz, 1H), 1.58–1.40 (m, 3H), 1.25 (s, 18H). ^{13}C NMR (101 MHz, $CDCl_3$) δ 175.79, 68.06, 40.76, 36.63, 29.71, 29.63, 29.60, 29.53, 29.47, 25.49. HRMS (-TOF MS): [M-H]- Calc'd for $C_{17}H_{25}D_9O_3$ *m/z* 294.2995. Found: *m/z* 294.2982.

Methyl-*O*-(*tert*-butyldiphenylsilyl)-*N*-((3-hydroxy-heptadecanoyl)glycyl)-L-serinate, (35)

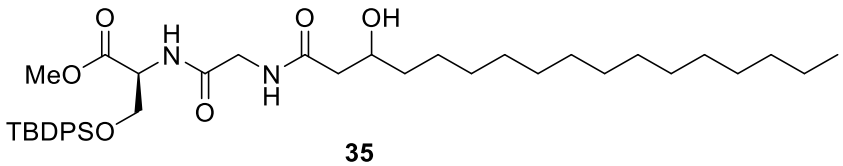

35

N-Hydroxy succinimide (185 mg, 1.61 mmol) and *N*-(3-dimethylaminopropyl)-*N*′-ethylcarbodiimide hydrochloride (308 mg, 1.61 mmol) were added to a stirring solution of 3-hydroxyheptadecanoic acid (**34**, 401 mg, 1.40 mmol) in 25 mL of dry DCM. The solution was stirred for 5 h at ambient temperature, filtered, and the filtrate was concentrated *in vacuo*. The resulting white solid was dissolved in 25 mL of methanol and this solution was added via cannula to a solution of methyl *N*-(((benzyloxy)carbonyl)glycyl)-*O*-(*tert*-butyldiphenylsilyl)-L-serinate (**14**, 960 mg, 1.75 mmol) and Pd/C (298 mg) in 50 mL of methanol. The reaction vessel was flushed with H_2 and the mixture was stirred overnight, filtered through Celite, and concentrated under reduced pressure. The crude product was purified via column chromatography (2% MeOH:DCM**)** to yield methyl *O*-(*tert*-butyldiphenylsilyl)-*N*-((3-hydroxy-heptadecanoyl)glycyl)-L-serinate, **35**, as a clear oil (641 mg, 0.938 mmol, 67.0%). ^{1}H NMR (400 MHz, $CDCl_3$) δ 7.58 (t, J = 7.0 Hz, 4H), 7.50–7.33 (m, 6H), 6.88 (dd, J = 28.7, 8.2 Hz, 1H), 6.39 (dt, J = 42.3, 5.5 Hz, 1H),

4.67 (dt, J = 7.7, 2.5 Hz, 1H), 4.19–3.76 (m, 5H), 3.75 (s, 3H), 3.43 (dd, J = 38.5, 3.6 Hz, 1H), 2.41 (dt, J = 14.6, 2.2 Hz, 1H), 2.27 (dd, J = 13.9, 9.4 Hz, 1H), 1.52–1.35 (m, 3H), 1.33–1.22 (m, 24H), 1.04 (s, 9H), 0.88 (t, J = 6.6 Hz, 3H). ^{13}C NMR (101 MHz, $CDCl_3$) δ 172.80, 172.75, 170.73, 168.71, 168.71, 168.53, 135.56, 135.52, 132.98, 132.93, 132.69, 132.64, 130.08, 127.97, 127.94, 127.90, 127.87, 68.93, 64.31, 64.27, 54.34, 52.63, 43.06, 43.02, 42.93, 42.81, 37.19, 37.15, 31.98, 29.75, 29.72, 29.64, 29.57, 29.42, 26.80, 25.49, 22.75, 19.33, 14.17. HRMS (AccuTOF): [MH]+ Calc'd for $C_{39}H_{62}N_2O_6Si$ *m/z* 683.4455. Found: *m/z* 683.4432.

Methyl *O*-(*tert*-butyldiphenylsilyl)-*N*-((3-hydroxyheptadecanoyl-14,14,15,15,16,16,17,17,17-*d*$_9$)glycyl)-L-serinate, (43)

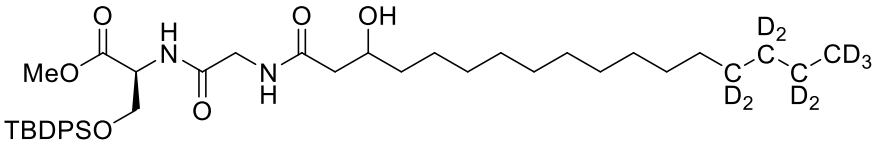

43

N-Hydroxy succinimide (130 mg, 1.13 mmol) and *N*-(3-dimethylaminopropyl)-*N*′-ethylcarbodiimide hydrochloride (216 mg, 1.13 mmol) were added to a stirring solution of 3-hydroxyheptadecanoic-14,14,15,15,16,16,17,17,17-*d*$_9$ acid (**42**, 303 mg, 1.03 mmol) in 10 mL of dry THF. The solution was stirred for 5 h at ambient temperature, filtered, and the filtrate was concentrated *in vacuo*. The resulting white solid was dissolved in 25 mL of methanol and this solution was added via cannula to a solution of methyl *N*-(((benzyloxy)carbonyl)glycyl)-*O*-(*tert*-butyldiphenylsilyl)-L-serinate (**14**, 563 mg, 1.03 mmol) and Pd/C (273 mg) in 50 mL of methanol. The reaction vessel was flushed with H_2 and the mixture was stirred overnight, filtered through Celite, and concentrated under reduced pressure. The crude product was purified via column chromatography (2% MeOH:DCM**)** to yield methyl *O*-(*tert*-butyldiphenylsilyl)-*N*-((3-

hydroxyheptadecanoyl-14,14,15,15,16,16,17,17,17-d_9)glycyl)-L-serinate, **43**, as a clear oil (555 mg, 0.802 mmol, 78.2%). ^{1}H NMR (400 MHz, $CDCl_3$) δ 7.59 (tt, J = 8.1, 1.6 Hz, 4H), 7.49–7.33 (m, 6H), 6.86 (dd, J = 26.2, 8.2 Hz, 1H), 6.34 (dt, J = 41.6, 5.4 Hz, 1H), 4.67 (dtd, J = 7.6, 2.9, 1.2 Hz, 1H), 4.19–3.78 (m, 5H), 3.75 (s, 3H), 3.41 (dd, J = 35.9, 3.6 Hz, 1H), 2.40 (dt, J = 14.6, 2.5 Hz, 1H), 2.26 (ddd, J = 14.6, 9.5, 2.1 Hz, 1H), 1.53–1.34 (m, 3H), 1.32–1.22 (m, 17H), 1.04 (s, 9H). ^{13}C NMR (101 MHz, $CDCl_3$) δ 172.78, 172.73, 170.70, 168.66, 168.49, 135.57, 135.52, 132.98, 132.93, 132.70, 132.64, 130.09, 127.96, 127.93, 127.90, 127.87, 68.92, 64.31, 64.26, 54.34, 52.61, 43.05, 43.02, 42.94, 42.82, 37.19, 37.14, 29.72, 29.65, 29.57, 29.47, 26.80, 25.49, 19.33. HRMS (AccuTOF): [MH]+ Calc'd for $C_{39}H_{53}D_9N_2O_6$ *m/z* 692.5020. Found: *m/z* 692.5007.

Methyl (3-hydroxyheptadecanoyl)glycyl-*L*-serinate

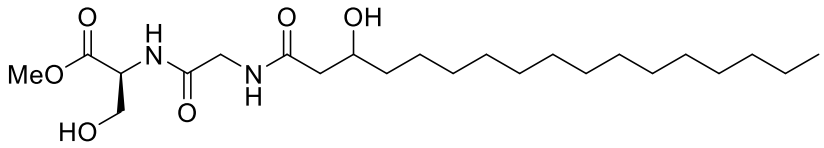

Methyl *O*-(*tert*-butyldiphenylsilyl)-*N*-((3-hydroxy-heptadecanoyl)glycyl)-L-serinate (**35**, 124 mg, 0.182 mmol) was dissolved in 10 mL of dry THF under nitrogen. The solution was cooled to 0°C and was treated with 1 M tetrabutylammonium fluoride (TBAF, 0.20 mL, 0.200 mmol). The reaction was slowly warmed to ambient temperature and stirred for 6 h. The solvent was removed under reduced pressure, and the resulting oil was purified by column chromatography (2.5 % MeOH:DCM) to yield methyl (3-hydroxyheptadecanoyl)glycyl-*L*-serinate as a white solid, (65 mg, 0.146 mmol, 80.5 %), MP, 104-111 °C. ^{1}H NMR (400 MHz, $CDCl_3$) δ 7.36 (d, J = 7.8 Hz, 1H), 6.71 (d, J = 5.5 Hz, 1H), 4.66 (dt, J = 7.3, 3.4 Hz, 1H), 4.22–3.80 (m, 6H), 3.79 (s, 3H), 3.55 (d, J = 23.0 Hz, 1H), 2.46 (dt, J = 13.9, 2.8 Hz, 1H), 2.36–2.24 (m, 1H), 1.52–1.36 (m, 3H), 1.32–1.24 (m, 24H), 0.88 (t, J = 6.6 Hz, 3H). ^{13}C NMR (101 MHz, $CDCl_3$) δ 173.30, 173.10,

171.07, 170.89, 169.39, 169.18, 69.59, 69.31, 62.92, 54.87, 54.83, 52.89, 43.69, 43.50, 43.46, 43.32, 37.48, 37.27, 31.98, 29.75, 29.72, 29.65, 29.55, 29.42, 25.61, 25.54, 22.75, 14.17. HRMS (AccuTOF): [MH]+ Calc'd for $C_{23}H_{44}N_2O_6$ *m/z* 445.3278. Found: *m/z* 444.3278.

Methyl (3-hydroxyheptadecanoyl-14,14,15,15,16,16,17,17,17-*d*$_9$)glycyl-*L*-serinate

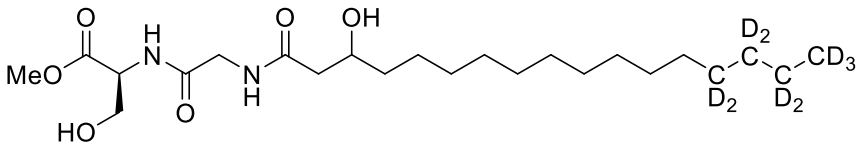

Methyl *O*-(*tert*-butyldiphenylsilyl)-*N*-((3-hydroxyheptadecanoyl-14,14,15,15,16,16,17,17,17-*d*$_9$)glycyl)-L-serinate, (**43**, 192 mg, 0.277 mmol) was dissolved in 10 mL of dry THF under nitrogen. The solution was cooled to 0°C and was treated with 1 M tetrabutylammonium fluoride (TBAF, 0.30 mL, 0.304 mmol). The reaction was slowly warmed to ambient temperature and stirred for 6 h. The solvent was removed under reduced pressure, and the resulting oil was purified by column chromatography (2.5 % MeOH:DCM) to yield methyl (3-hydroxyheptadecanoyl-14,14,15,15,16,16,17,17,17-*d*$_9$)glycyl-*L*-serinate as a white solid, (107 mg, 0.236 mmol, 85.1 %), MP, 95-102 °C. ^{1}H NMR (400 MHz, $CDCl_3$) δ 7.47 (dd, J = 30.8, 7.7 Hz, 1H), 6.93 (d, J = 6.2 Hz, 1H), 4.65 (dt, J = 7.4, 3.5 Hz, 1H), 4.23–3.78 (m, 6H), 3.78 (s, 3H), 2.45 (dt, J = 14.0, 2.4 Hz, 1H), 2.36–2.25 (m, 1H), 1.54–1.37 (m, 3H), 1.33–1.23 (m, 17H). ^{13}C NMR (101 MHz, $CDCl_3$) δ 173.36, 173.21, 171.17, 170.97, 169.54, 169.39, 69.62, 69.30, 62.76, 54.92, 54.87, 52.86, 43.72, 43.57, 43.35, 43.26, 37.49, 37.28, 29.76, 29.73, 29.67, 29.58, 29.47, 25.65, 25.59. HRMS (AccuTOF): [MH]+ Calc'd for $C_{23}H_{35}D_9N_2O_6$ *m/z* 454.3843. Found: *m/z* 454.3814.

(3-Hydroxyheptadecanoyl-14,14,15,15,16,16,17,17,17-*d*$_9$)glycyl-L-serine, (26)

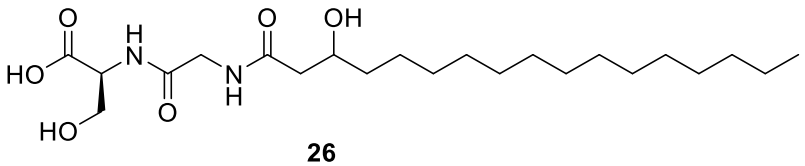

26

A solution of 1 M LiOH (0.12 mL, 0.12 mmol) was added to a solution of methyl (3-hydroxyheptadecanoyl)glycyl-L-serinate (47 mg, 0.11 mmol) in 2 mL of methanol at 0 °C, and 4 mL of THF was subsequently added. The resulting solution was warmed to ambient temperature and stirred for 2 h. The solution was then neutralized with 10% HCl and diluted with 25 mL of H_2O. The solution was then extracted with EtOAc (3 X 25 mL) and the organic layers were concentrated *in vacuo*. The resulting crude material was recrystallized from hot EtOAc to yield (3-hydroxyheptadecanoyl-14,14,15,15,16,16,17,17,17-*d*$_9$)glycyl-L-serine, **26**, as a crystalline solid (38 mg, 0.088 mmol, 84 %), MP, 119-122 °C. ^{1}H NMR (400 MHz, $CDCl_3$) δ 4.64–4.40 (m, 1H), 4.14–3.69 (m, 5H), 2.43–2.33 (m, 1H), 2.30–2.20 (m, 1H), 1.52–1.20 (m, 26H), 0.83 (t, J = 6.7 Hz, 3H). ^{13}C NMR (101 MHz, DMSO) δ 171.95, 171.25, 168.89, 67.48, 61.38, 54.54, 51.82, 43.63, 41.83, 36.86, 31.27, 29.08, 29.03, 28.98, 28.68, 25.10, 22.07, 13.93. HRMS (-TOF MS): [M-H]- Calc'd for $C_{22}H_{42}N_2O_6$ *m/z* 429.2965. Found: *m/z* 429.2989.

(3-Hydroxyheptadecanoyl-14,14,15,15,16,16,17,17,17-*d*$_9$)glycyl-L-serine, (24)

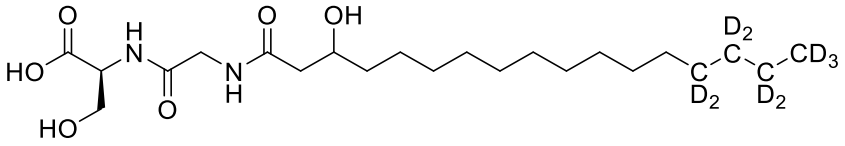

24

A solution of 1 M LiOH (0.28 mL, 0.28 mmol) was added to a solution of methyl (3-hydroxyheptadecanoyl-14,14,15,15,16,16,17,17,17-*d*$_9$)glycyl-L-serinate (117 mg, 0.258 mmol) in 2 mL of methanol at 0 °C, and 4 mL of THF was subsequently added. The resulting solution was

warmed to ambient temperature and stirred for 2 h. The solution was then neutralized with 10% HCl and diluted with 25 mL of H_2O. The solution was then extracted with EtOAc (3 X 25 mL) and the organic layers were concentrated *in vacuo*. The resulting crude material was recrystallized from hot EtOAc to yield ((3-hydroxyheptadecanoyl-14,14,15,15,16,16,17,17,17-d_9)glycyl-L-serine, **24**, as a crystalline solid (83 mg, 0.19 mmol, 73 %), MP, 118-122 °C. ^{1}H NMR (400 MHz, $CDCl_3$) δ 4.50 (dt, J = 11.0, 3.4 Hz, 1H), 4.17–3.65 (m, 5H), 2.37 (ddd, J = 13.6, 7.9, 2.8 Hz, 1H), 2.29–2.19 (m, 1H), 1.49–1.16 (m, 20H). ^{13}C NMR (101 MHz, DMSO) δ 171.78, 171.22, 168.96, 67.47, 61.31, 54.51, 51.83, 43.60, 41.75, 36.84, 29.08, 29.04, 28.99, 28.74, 25.10. HRMS (AccuTOF): [MH]+ Calc'd for $C_{22}H_{33}D_9N_2O_6$ *m/z* 440.3686. Found: *m/z* 440.3689.

(6*S*)-6-(Methoxycarbonyl)-2,2-dimethyl-8,11-dioxo-3,3-diphenyl-4-oxa-7,10-diaza-3-silaheptacosan-13-yl 13-methyltetradecanoate, (36)

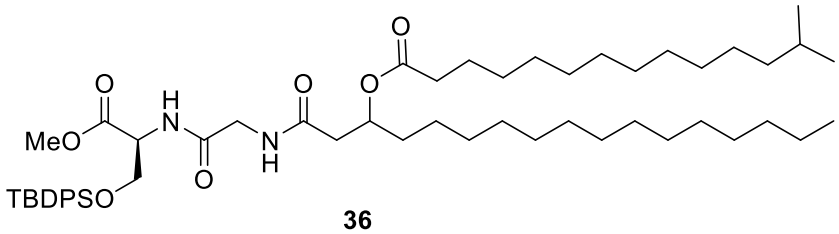

36

13-Methyltetradecanoic acid (82 mg, 0.338 mmol) was dissolved in 15 mL of dry DCM and stirred at 0 °C. To the solution was then treated with DCC (87 mg, 0.423 mmol) and a catalytic amount of DMAP. After stirring for 15 min, methyl (3-hydroxy-haptadecanoyl)glycyl-L-serine (**35**, 231 mg, 0.338 mmol) dissolved in 5 mL of dry DCM was added to the reaction via cannula. The resulting solution was warmed to ambient temperature and stirred overnight. The solvent was removed under reduced pressure and the resulting oil was redissolved in 20 mL of diethyl ether. The resulting precipitate was filtered, and the filtrate washed with satd $NaHCO_3$ (3 X 10 mL). The organic layer was dried, filtered, and solvents evaporated under reduced pressure. Purification via

column chromatography (1% MeOH:DCM) yielded (6*S*)-6-(methoxycarbonyl)-2,2-dimethyl-8,11-dioxo-3,3-diphenyl-4-oxa-7,10-diaza-3-silaheptacosan-13-yl 13-methyltetradecanoate**,** **36**, as a clear wax (123 mg, 0.136 mmol, 63.4% brsm). ^{1}H NMR (400 MHz, $CDCl_3$) δ 7.58 (t, J = 7.1 Hz, 4H), 7.46–7.37 (m, 6H), 6.54 (t, J = 6.7 Hz, 1H), 6.37 (d, J = 4.9 Hz, 1H), 5.16 (p, J = 6.3 Hz, 1H), 4.66 (d, J = 7.8 Hz, 1H), 4.14–3.82 (m, 5H), 3.74 (s, 3H), 2.55–2.42 (m, 2H), 2.29 (t, J = 7.5 Hz, 2H), 1.50 (hept, J = 6.6 Hz, 1H), 1.31–1.24 (m, 42H), 1.15–1.10 (m, 4H), 1.03 (s, 9H), 0.89–0.84 (m, 9H). ^{13}C NMR (101 MHz, $CDCl_3$) δ 173.45, 170.47, 169.98, 168.26, 135.56, 135.52, 132.82, 132.64, 130.11, 130.06, 127.97, 127.88, 71.12, 64.15, 54.28, 52.58, 49.26, 42.88, 41.43, 39.12, 34.56, 34.18, 34.00, 31.98, 30.01, 29.75, 29.62, 29.57, 29.42, 29.36, 29.21, 28.03, 27.48, 26.78, 25.67, 25.32, 25.05, 24.99, 22.75, 22.72, 14.17. HRMS (AccuTOF): [MH]+ Calc'd for $C_{54}H_{90}N_2O_7Si$ *m/z* 907.6596. Found: *m/z* 907.6570.

(6*S*)-6-(Methoxycarbonyl)-2,2-dimethyl-8,11-dioxo-3,3-diphenyl-4-oxa-7,10-diaza-3-silaheptacosan-13-yl-24,24,25,25,26,26,27,27,27-*d*$_9$ 13-methyltetradecanoate, (44)

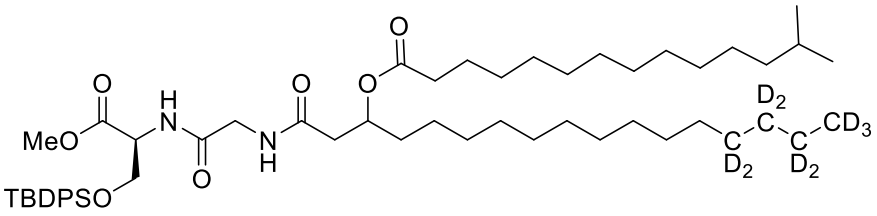

44

13-Methyltetradecanoic acid (130 mg, 0.535 mmol) was dissolved in 15 mL of dry DCM and stirred at 0 °C. To the solution was then treated with DCC (110 mg, 0.535 mmol) and a catalytic amount of DMAP. After stirring for 15 min, methyl (3-hydroxyheptadecanoyl-14,14,15,15,16,16,17,17,17-*d*$_9$)glycyl-*L*-serine (**43**, 322 mg, 0.465 mmol) dissolved in 5 mL of dry DCM was added to the reaction via cannula. The resulting solution was warmed to ambient temperature and stirred overnight. The solvent was removed under reduced pressure and the

resulting oil was redissolved in 20 mL of diethyl ether. The resulting precipitate was filtered, and the filtrate washed with satd $NaHCO_3$ (3 X 10 mL). The organic layer was dried, filtered, and solvents evaporated under reduced pressure. Purification via column chromatography (1% MeOH:DCM) yielded (6*S*)-6-(methoxycarbonyl)-2,2-dimethyl-8,11-dioxo-3,3-diphenyl-4-oxa-7,10-diaza-3-silaheptacosan-13-yl-24,24,25,25,26,26,27,27,27-d_9 13-methyltetradecanoate**, 44**, as a clear wax (216 mg, 0.236 mmol, 79.6% brsm). ^{1}H NMR (400 MHz, $CDCl_3$) δ 7.63–7.55 (m, 4H), 7.48–7.36 (m, 6H), 6.52 (d, J = 6.8 Hz, 1H), 6.33 (d, J = 5.0 Hz, 1H), 5.20–5.13 (m, 1H), 4.66 (dd, J = 7.6, 3.4 Hz, 1H), 4.13 (dd, J = 10.3, 2.9 Hz, 1H), 4.01–3.81 (m, 3H), 3.75 (s, 3H), 2.54–2.44 (m, 2H), 2.29 (t, J = 7.5 Hz, 2H), 1.51 (hept, J = 13.2, 6.6 Hz, 1H), 1.39–1.16 (m, 38H), 1.15 (q, J = 6.7 Hz, 2H), 1.03 (s, 9H), 0.86 (d, J = 6.6 Hz, 6H). ^{13}C NMR (101 MHz, $CDCl_3$) δ 173.42, 170.44, 170.40, 169.95, 168.21, 135.56, 135.52, 132.83, 132.65, 130.11, 130.06, 127.97, 127.88, 71.10, 64.15, 54.28, 54.26, 52.57, 42.88, 41.43, 39.12, 34.56, 34.18, 30.01, 29.72, 29.62, 29.57, 29.47, 29.42, 29.36, 29.21, 28.03, 27.48, 26.78, 25.32, 25.06, 22.72, 19.31. HRMS (AccuTOF): [MH]+ Calc'd for $C_{54}H_{81}D_9N_2O_7Si$ *m/z* 916.7160. Found: *m/z* 916.7154.

1-((2-(((*S*)-3-Hydroxy-1-methoxy-1-oxopropan-2-yl)amino)-2-oxoethyl)amino)-1-oxoheptadecan-3-yl 13-methyltetradecanoate

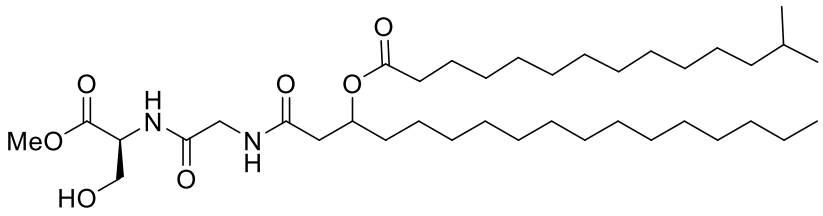

(6*S*)-6-(Methoxycarbonyl)-2,2-dimethyl-8,11-dioxo-3,3-diphenyl-4-oxa-7,10-diaza-3-silaheptacosan-13-yl 13-methyltetradecanoate (**36**, 123 mg, 0.136 mmol) was dissolved in 5 mL of dry THF under nitrogen. The solution was cooled to 0 °C and was treated with 1 M TBAF (0.15

mL, 0.15 mmol). The reaction was slowly warmed to ambient temperature and stirred for 1 h. The solvent was removed under reduced pressure, and the resulting oil was purified by column chromatography (5% MeOH:DCM) to yield 1-((2-(((*S*)-3-hydroxy-1-methoxy-1-oxopropan-2-yl)amino)-2-oxoethyl)amino)-1-oxoheptadecan-3-yl 13-methyltetradecanoate as a white solid (69 mg, 0.103 mmol, 76.1 % brsm) MP 84-92 °C. ^{1}H NMR (400 MHz, $CDCl_3$) δ 7.06 (dd, J = 46.7, 7.5 Hz, 1H), 6.44 (s, 1H), 5.24–5.12 (m, 1H), 4.66 (t, J = 3.4 Hz, 1H), 4.11–3.89 (m, 4H), 3.79 (s, 3H), 3.20 (d, J = 68.5 Hz, 1H), 2.49 (dd, J = 6.0, 3.2 Hz, 2H), 2.31 (td, J = 7.6, 2.1 Hz, 2H), 1.51 (hept, J = 6.6 Hz, 1H), 1.38–1.20 (m, 40H), 1.15 (q, J = 6.8 Hz, 2H), 0.93–0.79 (m, 9H). 13C NMR (101 MHz, $CDCl_3$) δ 174.55, 174.39, 170.78, 170.71, 170.66, 170.60, 168.97, 168.93, 71.53, 62.96, 55.02, 52.76, 43.43, 42.04, 41.95, 39.12, 34.62, 34.55, 31.99, 30.01, 29.76, 29.71, 29.62, 29.57, 29.42, 29.38, 29.33, 29.21, 28.03, 27.48, 25.32, 25.06, 25.00, 22.76, 22.72, 14.17. HRMS (-TOF MS): [M-H]- Calc'd for $C_{38}H_{72}N_2O_7$ *m/z* 667.5261. Found: *m/z* 667.5243.

1-((2-(((*S*)-3-Hydroxy-1-methoxy-1-oxopropan-2-yl)amino)-2-oxoethyl)amino)-1-oxoheptadecan-3-yl-14,14,15,15,16,16,17,17,17-*d*$_9$ 13-methyltetradecanoate

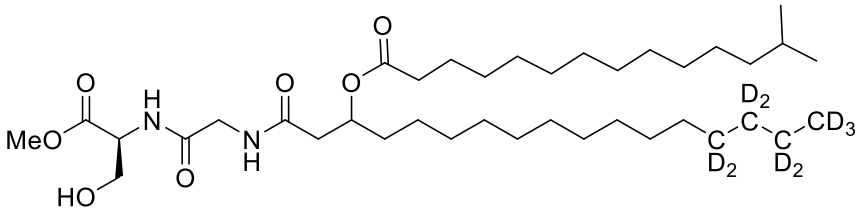

(6*S*)-6-(Methoxycarbonyl)-2,2-dimethyl-8,11-dioxo-3,3-diphenyl-4-oxa-7,10-diaza-3-silaheptacosan-13-yl-24,24,25,25,26,26,27,27,27-*d*$_9$ 13-methyltetradecanoate (**44**, 192 mg, 0.277 mmol) was dissolved in 5 mL of dry THF under nitrogen. The solution was cooled to 0 °C and was treated with 1 M TBAF (0.30 mL, 0.15 mmol). The reaction was slowly warmed to ambient temperature and stirred for 1 h. The solvent was removed under reduced pressure, and the resulting

oil was purified by column chromatography (5% MeOH:DCM) to yield 1-((2-(((*S*)-3-hydroxy-1-methoxy-1-oxopropan-2-yl)amino)-2-oxoethyl)amino)-1-oxoheptadecan-3-yl-14,14,15,15,16,16,17,17,17-d_9 13-methyltetradecanoate as a white solid (107 mg, 0.236 mmol, 85.1 % brsm) MP 82-88 °C. ^{1}H NMR (400 MHz, $CDCl_3$) δ 7.10 (dd, J = 43.2, 7.8 Hz, 1H), 6.48 (d, J = 4.2 Hz, 1H), 5.18 (dt, J = 19.0, 6.4 Hz, 1H), 4.66 (t, J = 3.4 Hz, 1H), 4.14–3.89 (m, 4H), 3.79 (s, 3H), 3.27 (d, J = 65.9 Hz, 1H), 2.49 (dd, J = 6.1, 3.1 Hz, 2H), 2.31 (td, J = 7.6, 2.3 Hz, 2H), 1.50 (t, J = 7.0 Hz, 1H), 1.41–1.18 (m, 34H), 1.15 (q, J = 6.4 Hz, 2H), 0.86 (d, J = 6.6 Hz, 6H). ^{13}C NMR (101 MHz, $CDCl_3$) δ 174.56, 174.39, 170.79, 170.73, 170.67, 170.61, 168.98, 168.93, 71.53, 62.96, 62.92, 55.02, 52.76, 43.44, 43.40, 42.05, 41.94, 39.12, 34.62, 34.55, 30.01, 29.78, 29.73, 29.62, 29.57, 29.48, 29.38, 29.33, 29.22, 29.19, 28.03, 27.48, 25.32, 25.06, 25.00, 22.71. HRMS (AccuTOF): [MH]+ Calc'd for $C_{38}H_{63}D_9N_2O_7$ *m/z* 678.5983. Found: *m/z* 678.5992.

(3-((13-Methyltetradecanoyl)oxy)heptadecanoyl)glycyl-L-serine, (27)

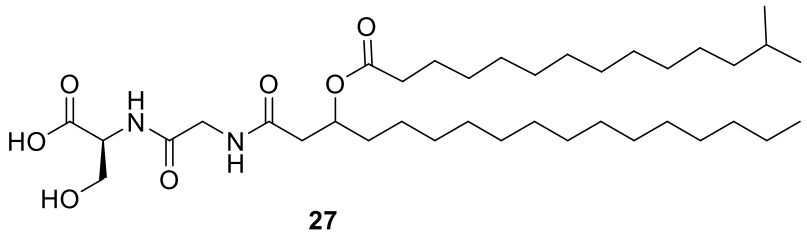

27

A stirring solution of 1-((2-(((*S*)-3-hydroxy-1-methoxy-1-oxopropan-2-yl)amino)-2-oxoethyl)amino)-1-oxoheptadecan-3-yl 13-methyltetradecanoate (48 mg, 0.078 mmol), in 3 mL of dry DMF, was cooled to 0 °C. Potassium trimethylsilonoate (11 mg, 0.083 mmol) was added, and the reaction was stirred on the ice bath for 1.5 h before being warmed to ambient temperature and stirred for an additional 1.5 h. The solution was diluted with 10 mL of 10 mL of H_2O and acidified with 10% HCl. The resulting cloudy precipitate was extracted with ethyl acetate (3 X 15mL). The organic layer was dried, filtered, and solvents evaporated under reduced pressure. The

resulting solid was purified by column chromatography (10% MeOH:DCM) to yield (3-((13-methyltetradecanoyl)oxy)heptadecanoyl)glycyl-L-serine, **27**, as a white sticky solid (33 mg, 0.050 mmol, 65 % brsm). ^{1}H NMR (500 MHz, $CDCl_3$) δ 7.07 (d, J = 8.4 Hz,0.5H), 6.77 (d, J = 8.2 Hz,0.5H), 5.17–5.07 (m, 1H), 4.26 (s, 1H), 4.11–3.60 (m, 4H), 3.36–3.30 (m, 1H), 2.47 (s, 2H), 2.23 (s, 2H), 1.67–1.41 (m, 6H), 1.21 (s, 41H), 0.82 (t, J = 7.0 Hz, 9H). ^{13}C NMR spectrum could not be obtained due to liposome formation. HRMS (-TOF MS): [M-H]- Calc'd for $C_{37}H_{70}N_2O_7$ *m/z* 653.5105. Found: *m/z* 653.5077.

(3-((13-Methyltetradecanoyl)oxy)heptadecanoyl-14,14,15,15,16,16,17,17,17-*d*$_9$)glycyl-L-serine, (25)

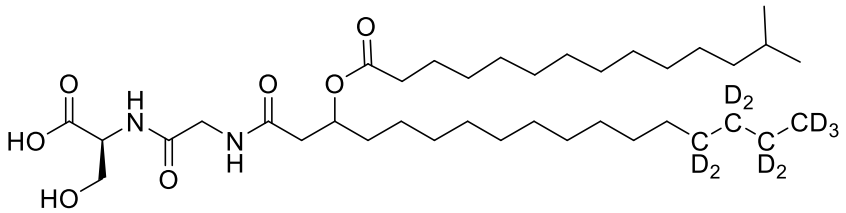

25

A stirring solution of 1-((2-(((*S*)-3-hydroxy-1-methoxy-1-oxopropan-2-yl)amino)-2-oxoethyl)amino)-1-oxoheptadecan-3-yl-14,14,15,15,16,16,17,17,17-*d*$_9$ 13-methyltetradecanoate (98 mg, 0.144 mmol), in 3 mL of dry DMF, was cooled to 0 °C. Potassium trimethylsilonoate (18 mg, 0.144 mmol) was added, and the reaction was stirred on the ice bath for 1.5 h before being warmed to ambient temperature and stirred for an additional 1.5 h. The solution was diluted with 10 mL of 10 mL of H_2O and acidified with 10% HCl. The resulting cloudy precipitate was extracted with ethyl acetate (3 X 15mL). The organic layer was dried, filtered, and solvents evaporated under reduced pressure. The resulting solid was purified by column chromatography (10% MeOH:DCM) to yield (3-((13-methyltetradecanoyl)oxy)heptadecanoyl-14,14,15,15,16,16,17,17,17-*d*$_9$)glycyl-L-serine, **25**, as a white sticky solid (55 mg, 0.083 mmol,

58% brsm). ^{1}H NMR (400 MHz, $CDCl_3$) δ 7.09 (d, J = 8.1 Hz,0.5H), 6.78 (d, J = 8.4 Hz,0.5H), 5.24–5.08 (m, 1H), 4.30 (s, 1H), 4.14–3.55 (m, 4H), 3.43–3.28 (m, 1H), 2.52 (s, 2H), 2.25 (t, J = 7.4 Hz, 2H), 1.57 (d, J = 13.1 Hz, 4H), 1.51–1.44 (m, 1H), 1.42–1.15 (m, 30H), 1.12 (q, J = 6.8 Hz, 2H), 0.83 (d, J = 6.6 Hz, 6H). ^{13}C NMR spectrum could not be obtained due to liposome formation. HRMS (-TOF MS): [M-H]- Calc'd for $C_{37}H_{61}D_9N_2O_7$ *m/z* 662.5670. Found: *m/z* 662.5640.

1.4 NMR Spectra

0.85
0.87
1.12
1.14
1.16
1.17
1.20
1.26
1.32
1.34
1.37
1.47
1.48
1.50
1.51
1.53
1.55
1.57
1.58
1.60
3.63
3.64
3.66
7.26 CDCl3
6.06
3.20
11.99
4.11
3.10
CH3
CH3
HO
0.5
1.0
1.5
2.0
2.5
3.0
3.5
4.0
4.5
5.0
5.5
6.0
6.5
7.0
7.5
ppm

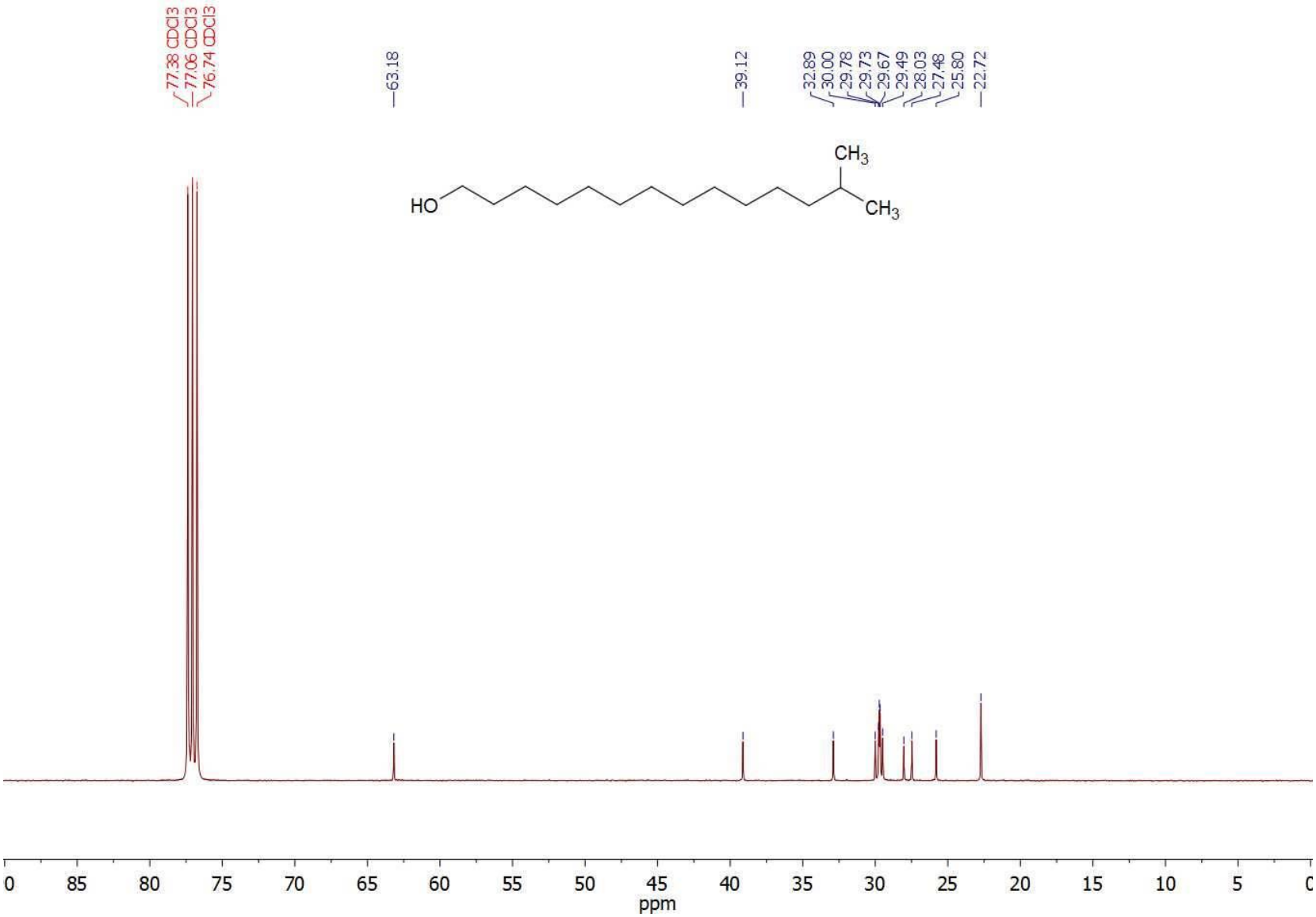
77.38 CDCl3
77.06 CDCl3
76.74 CDCl3
63.18
39.12
32.89
30.00
29.78
29.73
29.67
29.49
28.03
27.48
25.80
22.72
HO
CH3
CH3
0
85
80
75
70
65
60
55
50
45
40
35
30
25
20
15
10
5
ppm

9.77
9.76
9.76
7.26 CDCl3
2.43
2.43
2.42
2.41
2.40
2.39
1.66
1.64
1.63
1.61
1.59
1.57
1.56
1.55
1.53
1.51
1.50
1.48
1.46
1.34
1.30
1.25
1.17
1.15
1.14
1.12
0.87
0.85
CH3
CH3
O
H
6.00
2.06
16.14
1.08
2.11
1.92
0.89
ppm

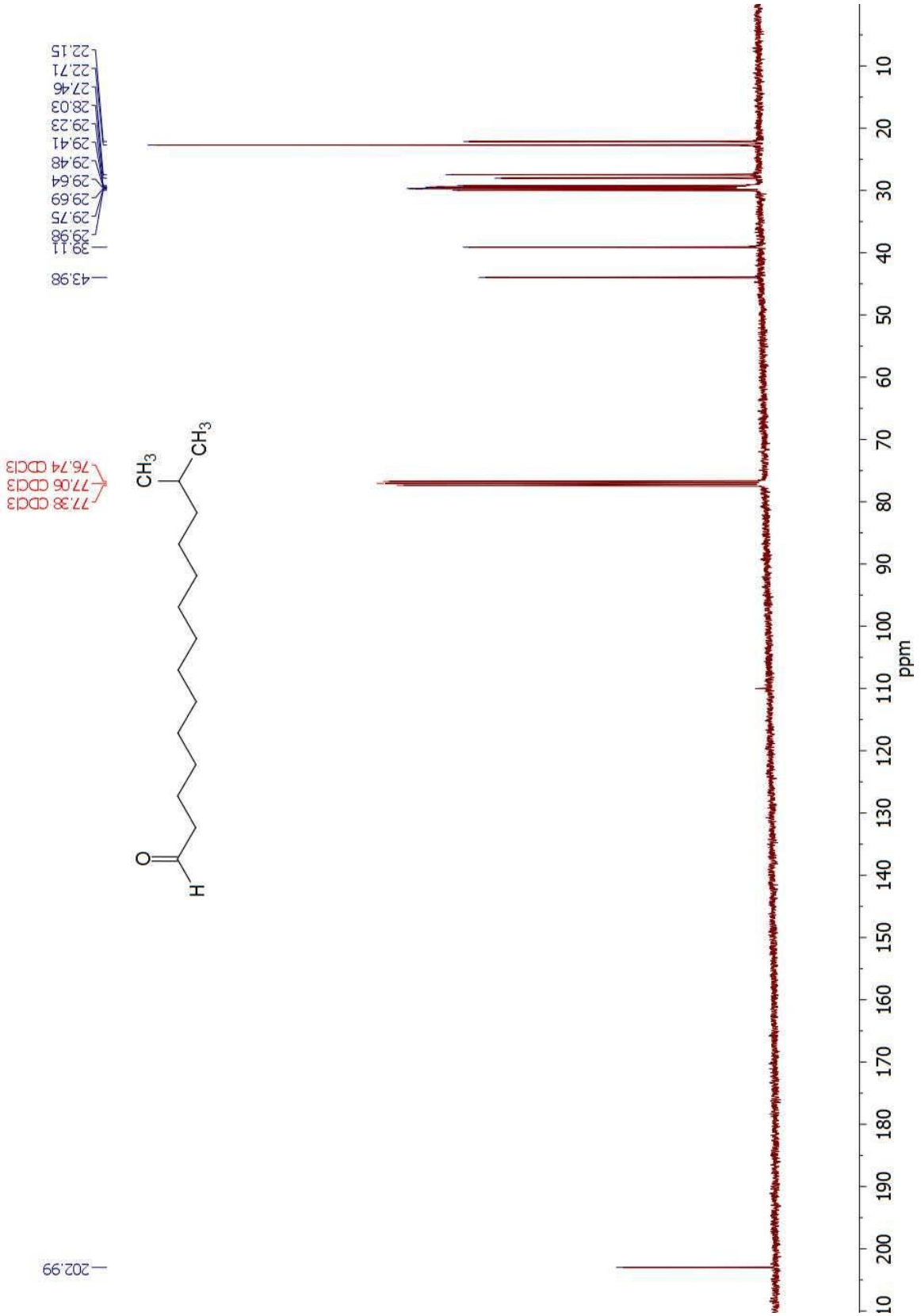
202.99
43.98
39.11
29.98
29.75
29.69
29.64
29.48
29.41
29.23
28.03
27.46
22.71
22.15
77.38 CDCl3
77.06 CDCl3
76.74 CDCl3
CH3
CH3
O
H
ppm

7.26 CDCl3
0.85
0.87
1.12
1.14
1.16
1.17
1.26
1.31
1.32
1.35
1.46
1.48
1.50
1.51
1.53
1.55
1.56
1.60
1.61
1.63
1.65
1.67
2.33
2.35
2.37
CH3
CH3
O
HO
6.10
2.30
16.80
1.07
2.20
2.05
ppm

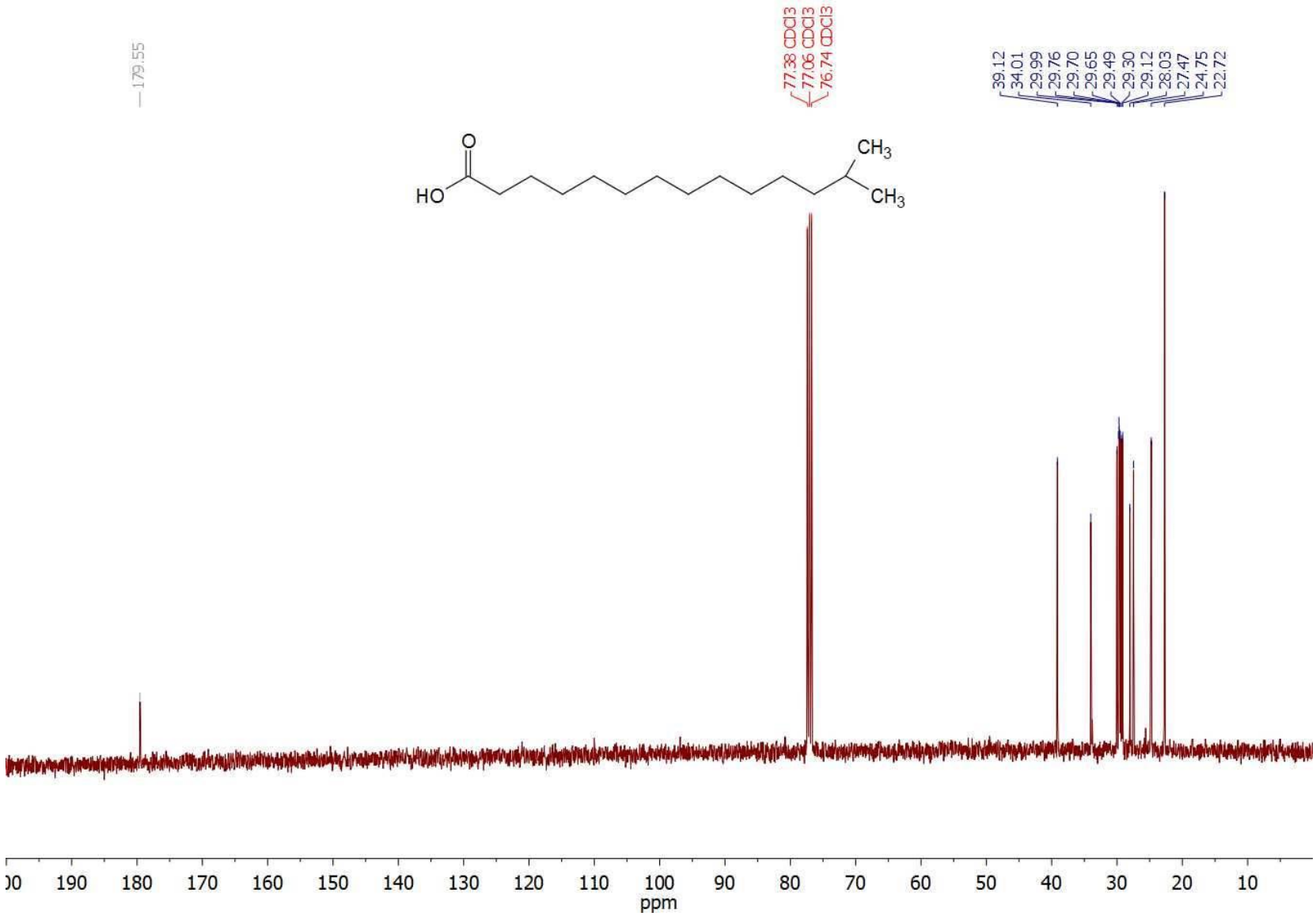
179.55
77.38 CDCl3
77.06 CDCl3
76.74 CDCl3
39.12
34.01
29.99
29.76
29.70
29.65
29.49
29.30
29.12
28.03
27.47
24.75
22.72
HO
O
CH3
CH3
190
180
170
160
150
140
130
120
110
100
90
80
70
60
50
40
30
20
10
ppm

7.26 CDCl3
4.22
4.20
4.19
4.17
3.42
2.54
2.53
2.51
1.61
1.59
1.57
1.54
1.53
1.51
1.50
1.48
1.46
1.30
1.28
1.25
1.17
1.15
1.14
1.12
0.87
0.85
H3C
CH3
O
O
O
H3C
6.36
2.43
20.45
4.36
1.95
1.91
2.00
ppm

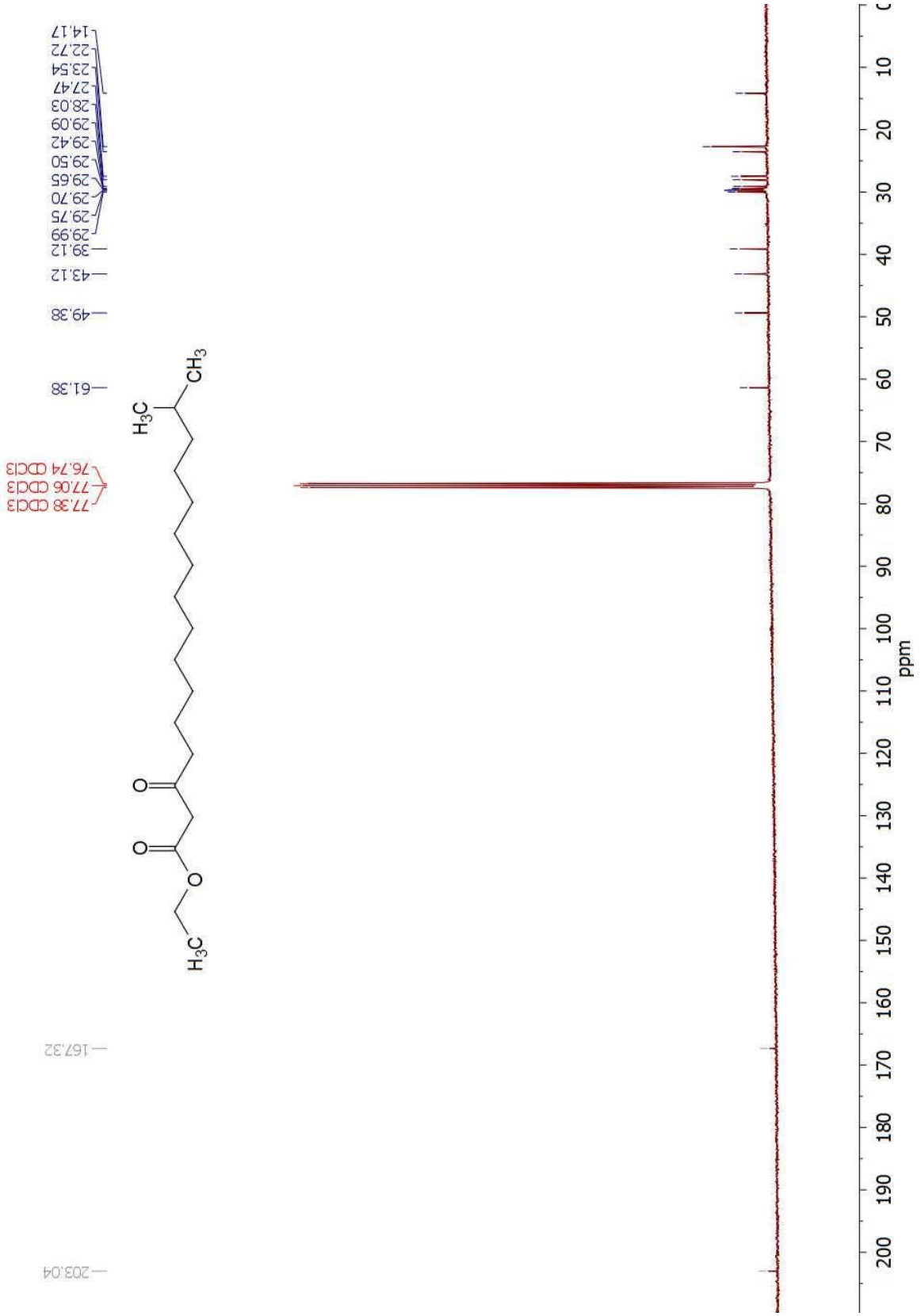
14.17
22.72
23.54
27.47
28.03
29.09
29.42
29.50
29.65
29.70
29.75
29.99
39.12
43.12
49.38
61.38
76.74 CDCl3
77.06 CDCl3
77.38 CDCl3
167.32
203.04
H3C
CH3
O
O
O
H3C
ppm

7.26 CDCl3
0.87
1.14
1.15
1.17
1.26
1.27
1.29
1.41
1.42
1.43
1.44
1.50
1.51
1.53
1.57
2.36
2.38
2.40
2.42
2.48
2.48
2.52
2.52
2.90
2.91
3.97
3.98
3.99
4.00
4.01
4.02
4.15
4.16
4.18
4.20
H3C
CH3
HO
O
O
H3C
5.99
2.11
20.08
4.58
1.02
1.01
0.93
1.02
2.00
ppm

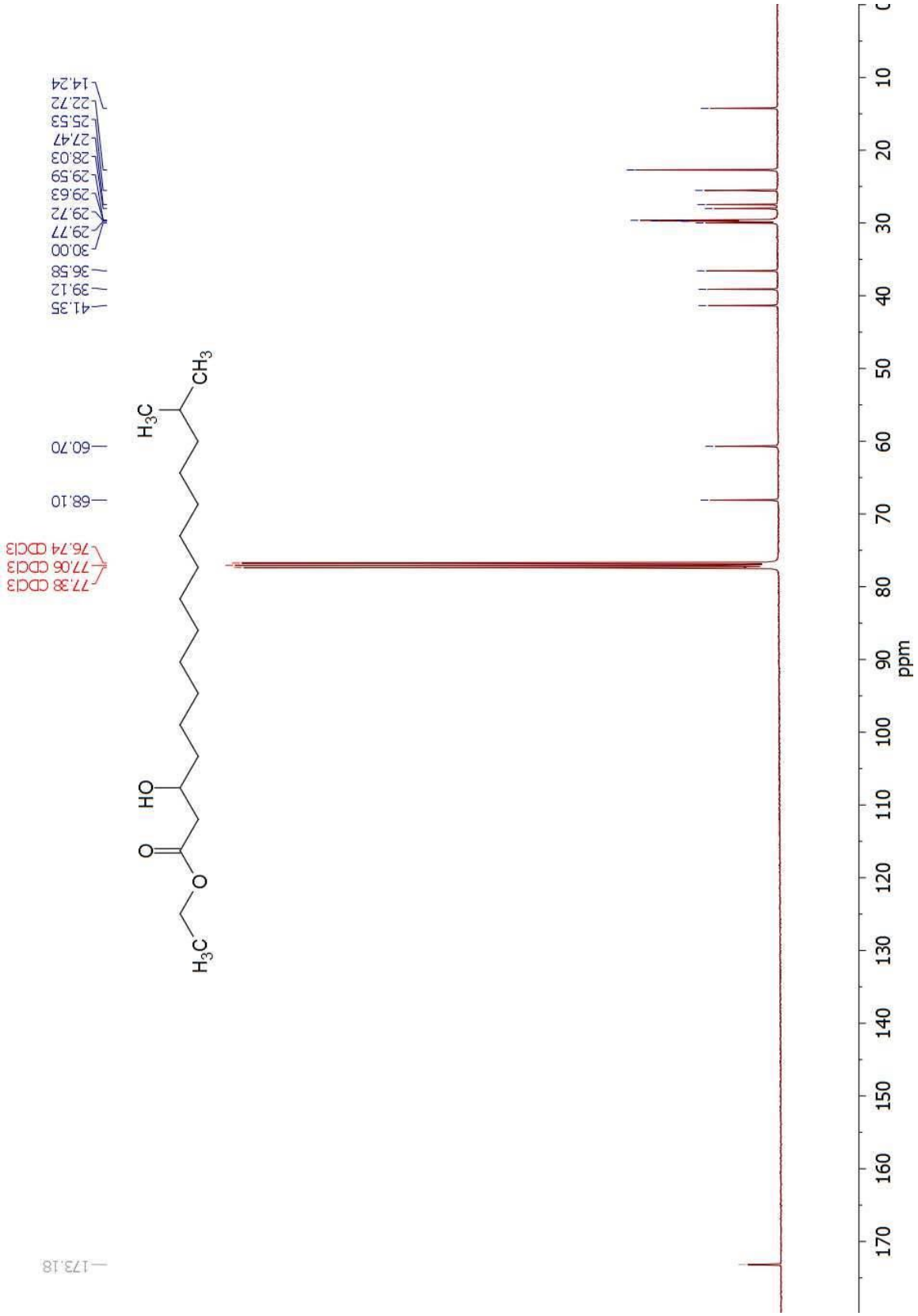
14.24
22.72
25.53
27.47
28.03
29.59
29.63
29.72
29.77
30.00
36.58
39.12
41.35
60.70
68.10
76.74 CDCl3
77.06 CDCl3
77.38 CDCl3
173.18
H3C
CH3
HO
O
O
H3C
10
20
30
40
50
60
70
80
90
100
110
120
130
140
150
160
170
ppm

7.26 CDCl3
1.57 HDO
0.87
1.14
1.15
1.17
1.24
1.25
1.26
1.27
1.29
1.30
1.32
1.41
1.42
1.43
1.44
1.50
1.51
1.53
2.36
2.38
2.40
2.42
2.48
2.48
2.52
2.53
2.90
2.91
3.96
3.97
3.98
3.99
4.00
4.01
4.02
4.03
4.15
4.16
4.18
4.20
HO
O
O
H3C
H3C
CH3
6.02
2.18
20.71
2.36
2.13
1.03
1.04
0.95
1.03
2.00
ppm

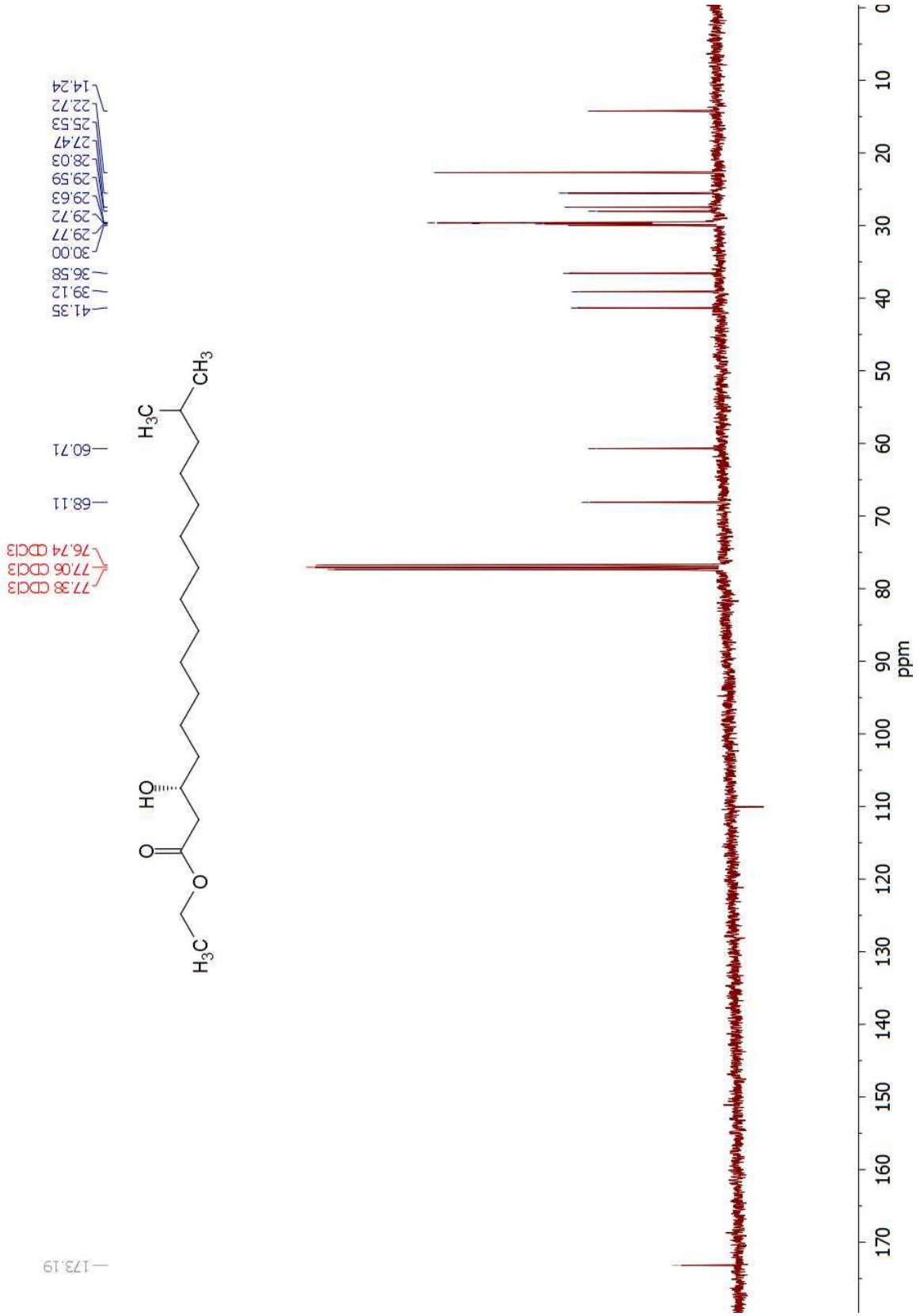
14.24
22.72
25.53
27.47
28.03
29.59
29.63
29.72
29.77
30.00
36.58
39.12
41.35
60.71
68.11
76.74 CDCl3
77.06 CDCl3
77.38 CDCl3
173.19
HO
O
O
H3C
CH3
ppm

0.86
0.87
1.12
1.14
1.16
1.18
1.19
1.21
1.25
1.29
1.31
1.33
1.34
1.36
1.47
1.48
1.50
1.52
1.53
1.55
1.56
1.63
1.65
1.66
1.68
1.70
1.72
1.74
1.76
2.53
2.54
2.57
2.58
2.61
2.63
2.65
2.67
3.53
3.53
4.03
4.05
4.07
4.08
4.09
4.11
4.13
4.15
5.45
5.47
5.48
5.50
5.52
7.26 CDCl3
7.38
7.39
7.40
7.41
7.52
7.53
7.54
CH3
O
F
F
F
O
O
O
O
CH3
CH3
H3C
6.00
23.52
1.36
2.14
1.99
2.97
1.94
0.04
0.01
0.99
3.02
1.99
0.5
1.0
1.5
2.0
2.5
3.0
3.5
4.0
4.5
5.0
5.5
6.0
6.5
7.0
7.5
ppm

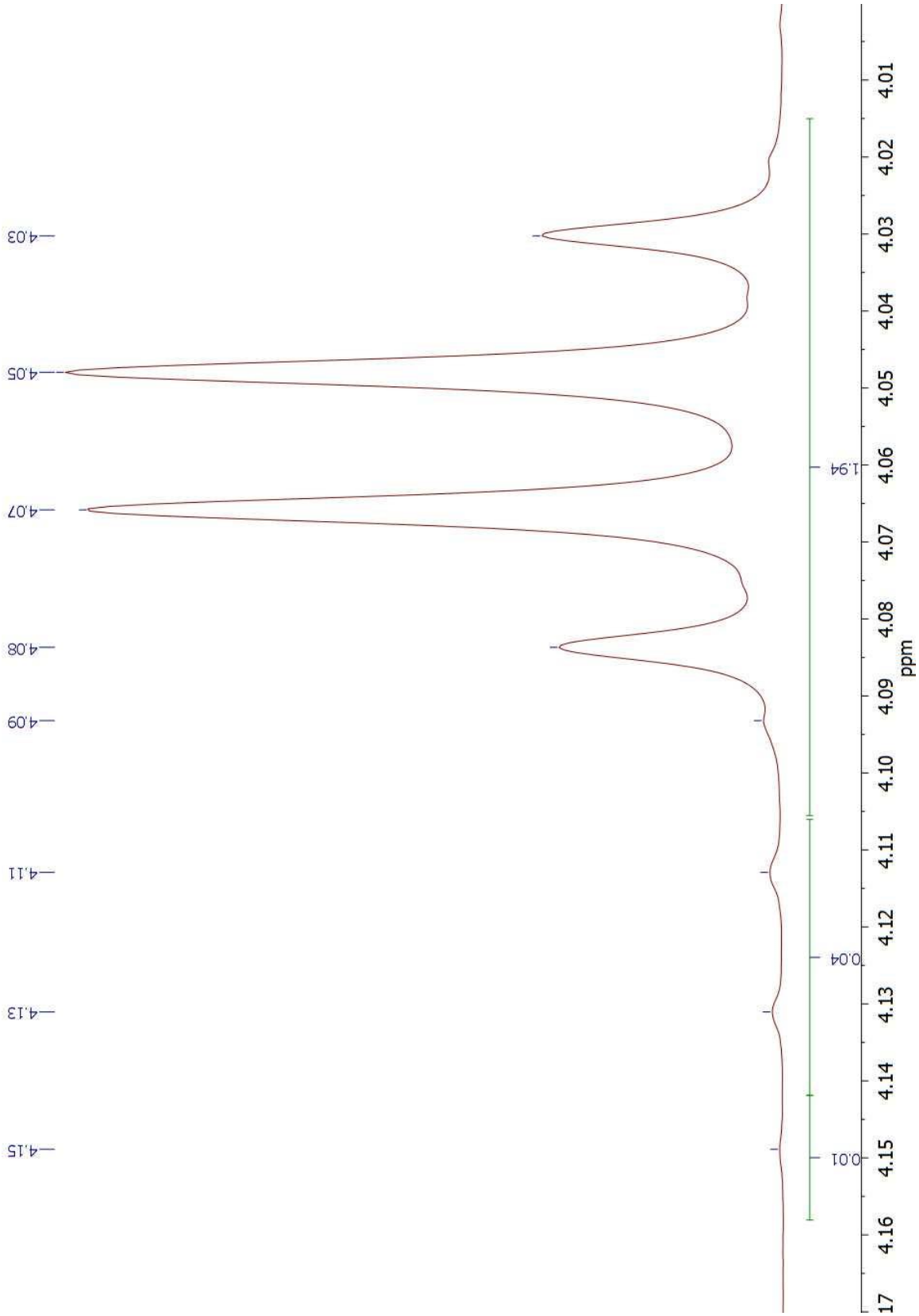
4.03
4.05
4.07
4.08
4.09
4.11
4.13
4.15
1.94
0.04
0.01
4.01
4.02
4.03
4.04
4.05
4.06
4.07
4.08
4.09
4.10
4.11
4.12
4.13
4.14
4.15
4.16
17
ppm

7.26 CDCl3
0.87
1.14
1.15
1.17
1.26
1.27
1.29
1.41
1.42
1.43
1.44
1.48
1.50
1.51
1.53
1.55
1.58 HDO
2.40
2.42
2.48
2.48
2.52
2.53
2.91
2.92
3.97
3.98
3.99
4.00
4.01
4.02
4.03
4.15
4.16
4.18
4.20
5.94
2.19
20.79
4.77
1.02
1.08
0.93
1.04
2.00
ppm

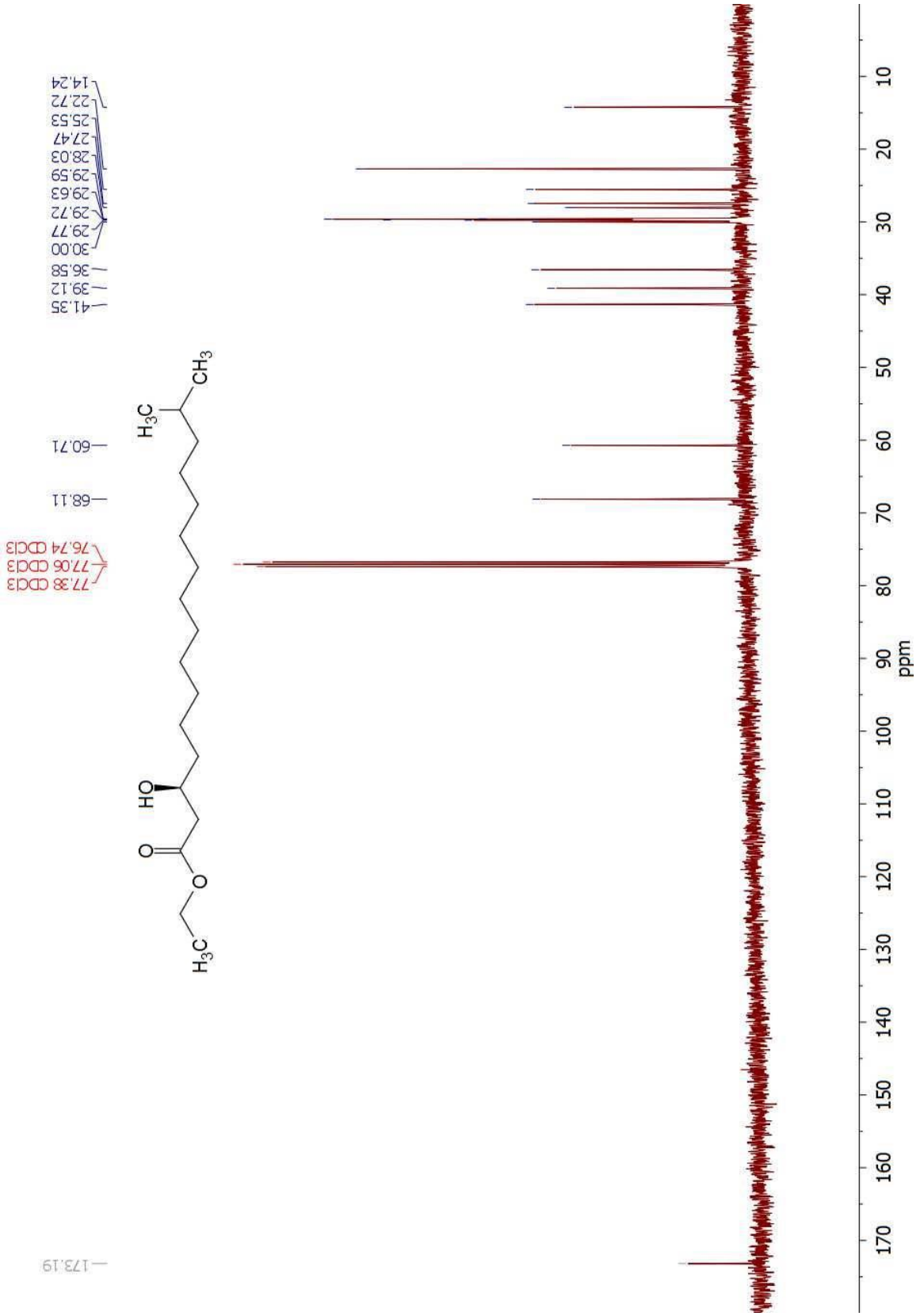
14.24
22.72
25.53
27.47
28.03
29.59
29.63
29.72
29.77
30.00
36.58
39.12
41.35
60.71
68.11
76.74 CDCl3
77.06 CDCl3
77.38 CDCl3
173.19
H3C
CH3
HO
O
O
H3C
10
20
30
40
50
60
70
80
90
100
110
120
130
140
150
160
170
ppm

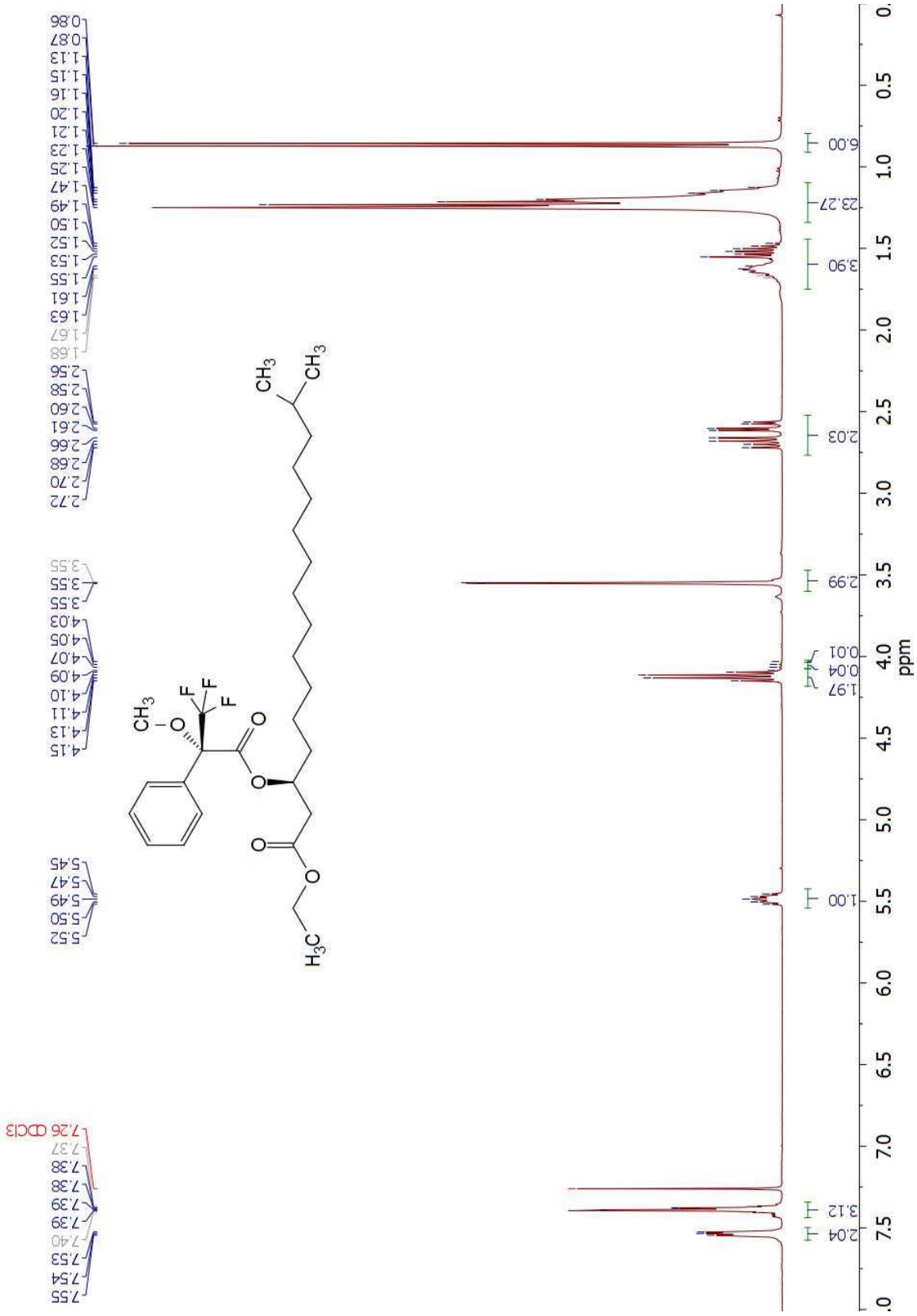
CH3
CH3
F
F
F
CH3
O
O
O
O
O
H3C
ppm
6.00
23.27
3.90
2.03
2.99
1.97
0.04
0.01
1.00
3.12
2.04
7.26 CDCl3

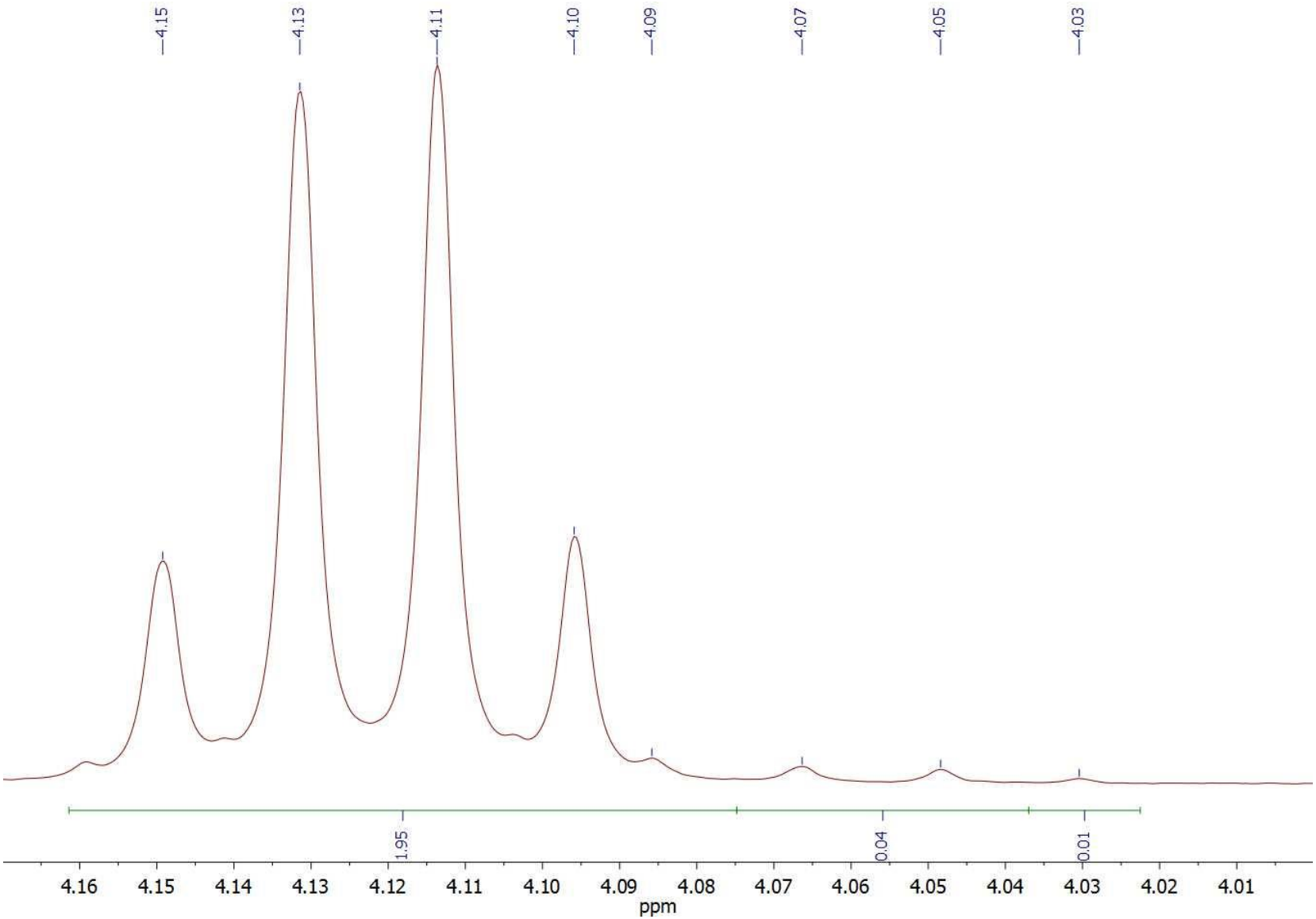
4.15
4.13
4.11
4.10
4.09
4.07
4.05
4.03
1.95
0.04
0.01
4.16
4.15
4.14
4.13
4.12
4.11
4.10
4.09
4.08
4.07
4.06
4.05
4.04
4.03
4.02
4.01
ppm

7.26 CDCl3
0.85
0.86
1.12
1.13
1.15
1.17
1.25
1.43
1.46
1.48
1.49
1.51
1.52
1.54
1.56
1.58
2.42
2.44
2.46
2.48
2.53
2.54
2.57
2.58
4.00
4.01
4.02
4.03
4.04
4.05
4.06
CH3
CH3
OH
O
HO
5.81
2.02
16.84
3.95
0.98
1.00
1.00
ppm

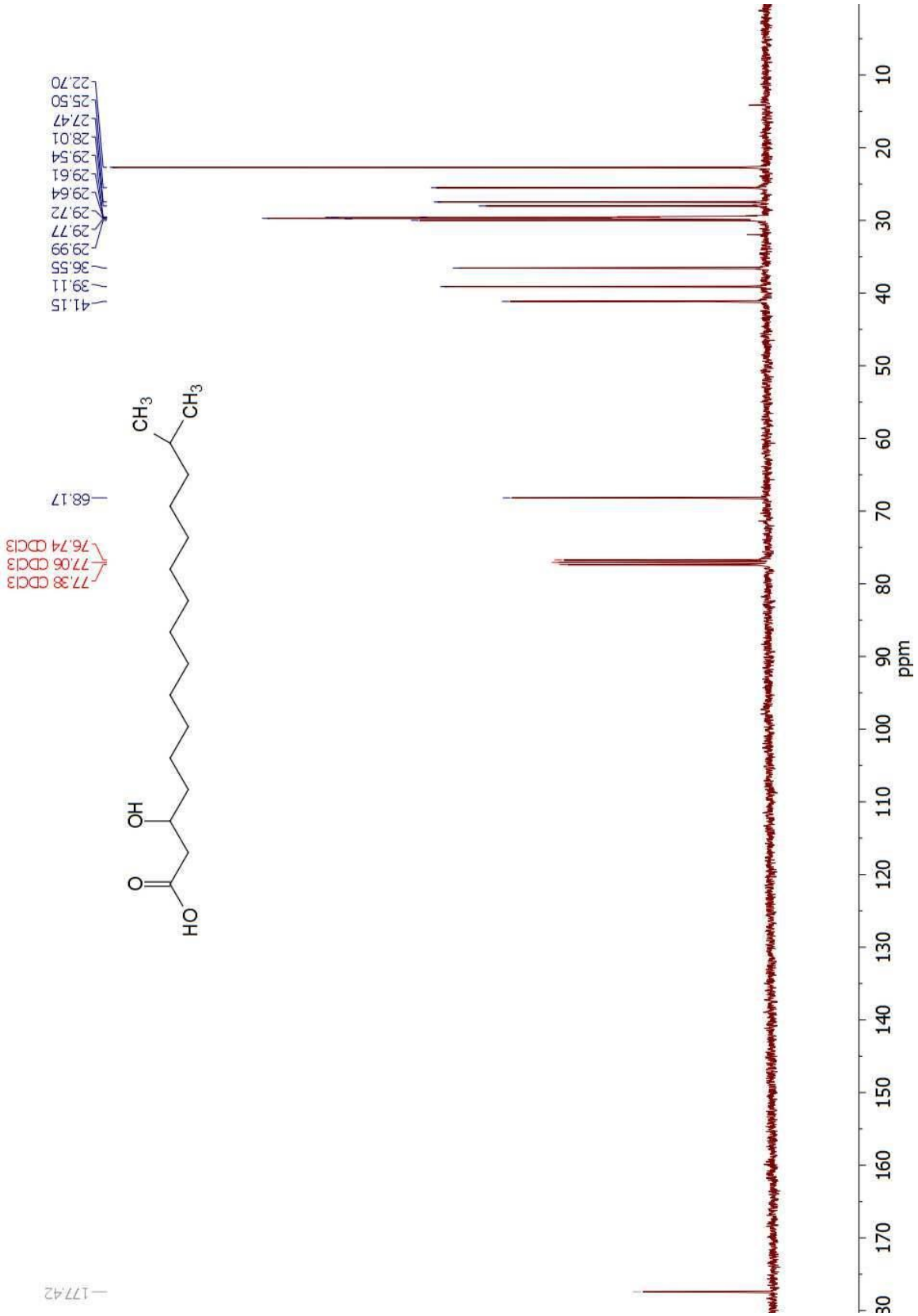
177.42
77.38 CDCl3
77.06 CDCl3
76.74 CDCl3
68.17
41.15
39.11
36.55
29.99
29.77
29.72
29.64
29.61
29.54
28.01
27.47
25.50
22.70
CH3
CH3
OH
O
HO
ppm

7.26 CDCl3
0.85
0.87
1.12
1.14
1.16
1.17
1.26
1.44
1.45
1.47
1.48
1.50
1.51
1.53
1.55
1.56
1.58
2.44
2.46
2.48
2.50
2.55
2.56
2.59
2.60
4.00
4.01
4.02
4.03
4.04
4.05
4.06
CH3
CH3
OH
O
HO
5.99
2.16
18.29
4.76
0.99
1.05
1.00
ppm

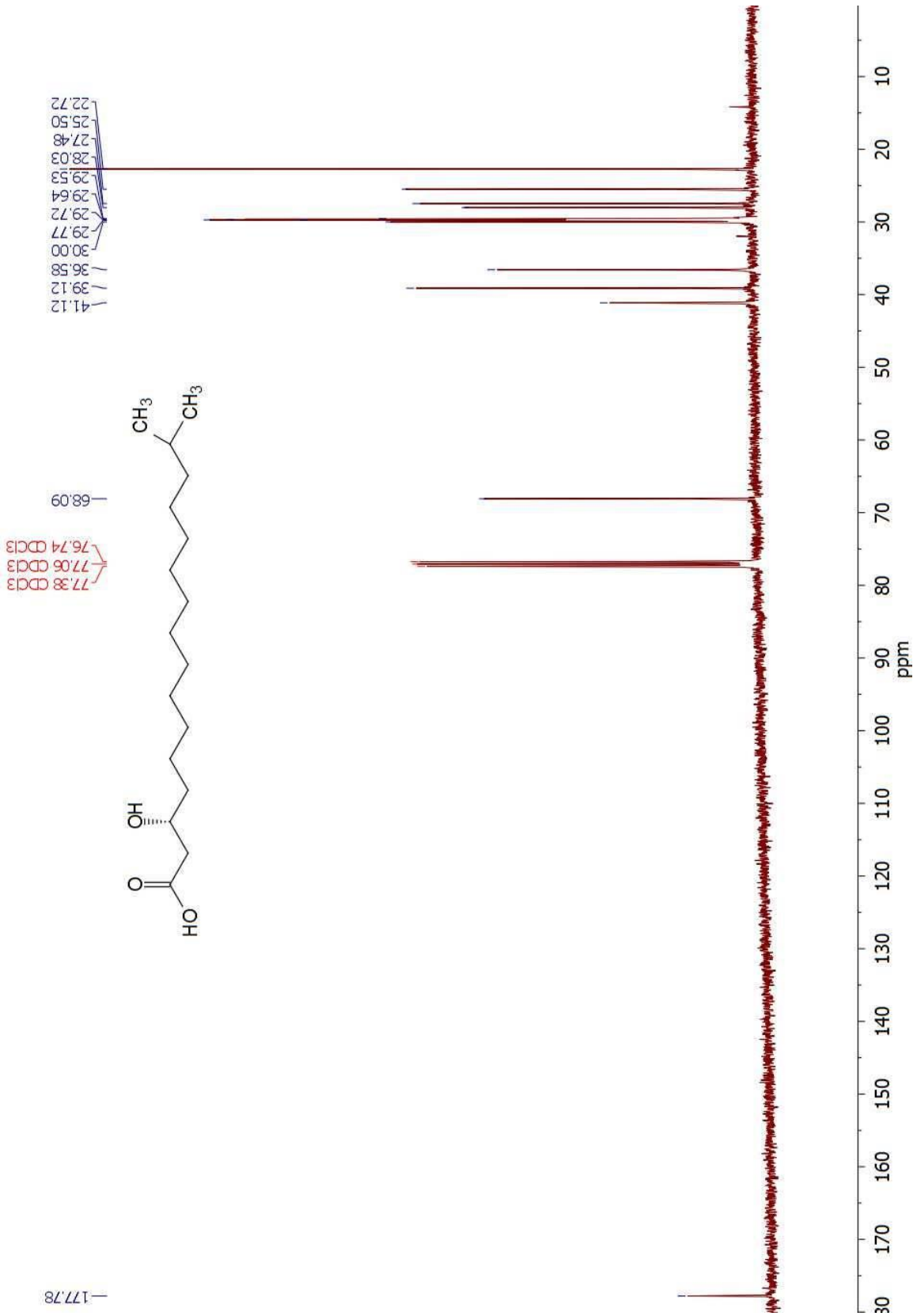
177.78
77.38 CDCl3
77.06 CDCl3
76.74 CDCl3
68.09
41.12
39.12
36.58
30.00
29.77
29.72
29.64
29.53
28.03
27.48
25.50
22.72
CH3
CH3
OH
O
HO
ppm

7.26 CDCl3
0.87
0.88
1.12
1.14
1.16
1.17
1.26
1.44
1.45
1.46
1.47
1.48
1.50
1.51
1.53
1.55
1.56
2.44
2.47
2.49
2.51
2.55
2.56
2.60
2.60
4.00
4.01
4.02
4.03
4.04
4.05
4.06
CH3
CH3
OH
O
HO
1.00
0.98
1.02
1.97
16.77
3.94
5.76
ppm

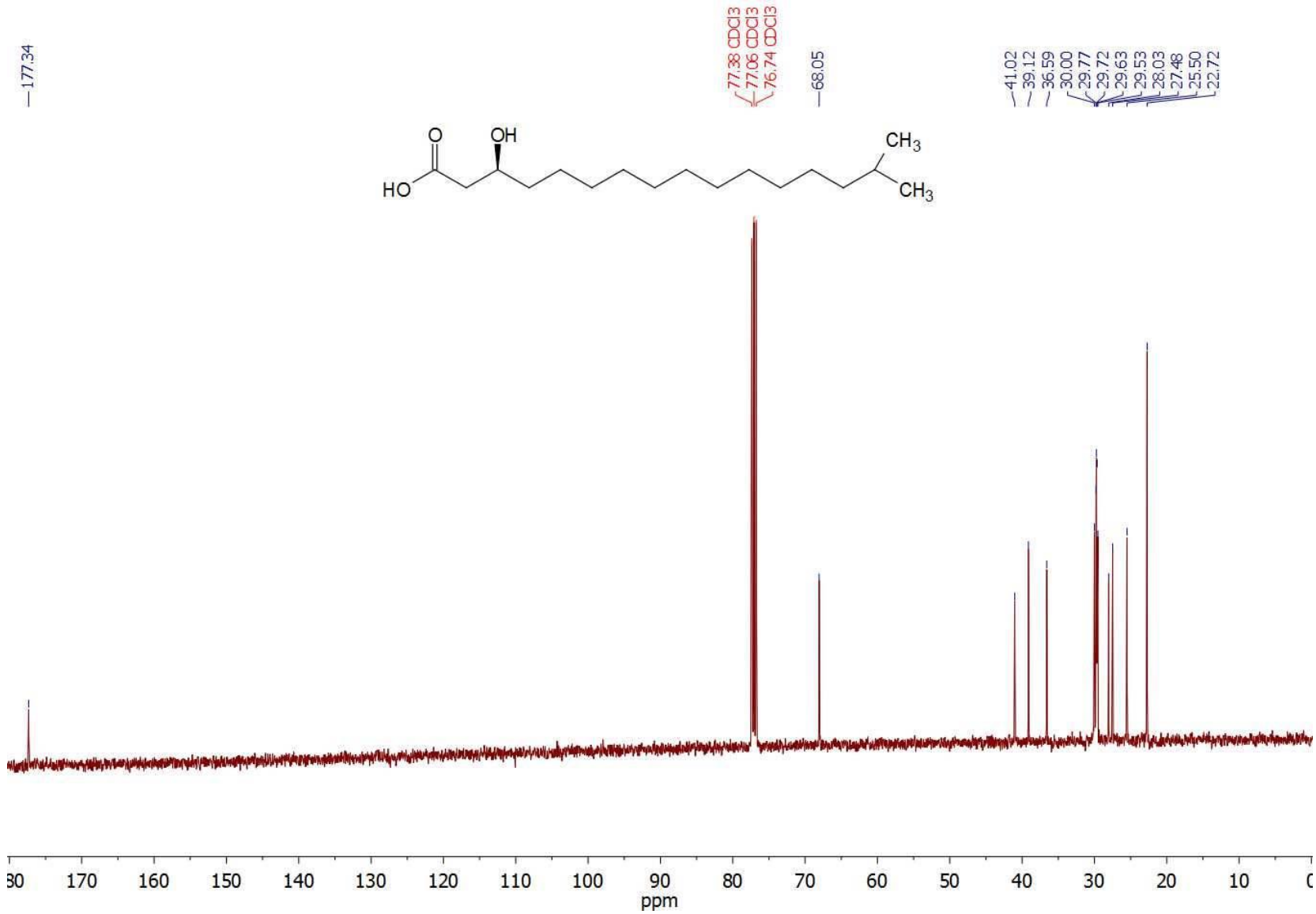
177.34
77.38 CDCl3
77.06 CDCl3
76.74 CDCl3
68.05
41.02
39.12
36.59
30.00
29.77
29.72
29.63
29.53
28.03
27.48
25.50
22.72
O
OH
HO
CH3
CH3
ppm

7.26 CDCl3
4.14
4.13
4.12
2.85
2.82
2.81
2.78
2.77
2.73
2.71
2.69
2.67
1.61
1.60
1.59
1.58
1.57
1.56
1.55
1.53
1.53
1.51
1.50
1.50
1.48
1.47
1.45
1.38
1.26
1.17
1.15
1.14
1.12
0.87
0.85
CH3
CH3
OH
O
O
N
O
O
1.01
7.20
5.00
18.00
2.16
6.00
ppm
0.5
1.0
1.5
2.0
2.5
3.0
3.5
4.0
4.5
5.0
5.5
6.0
6.5
7.0
7.5

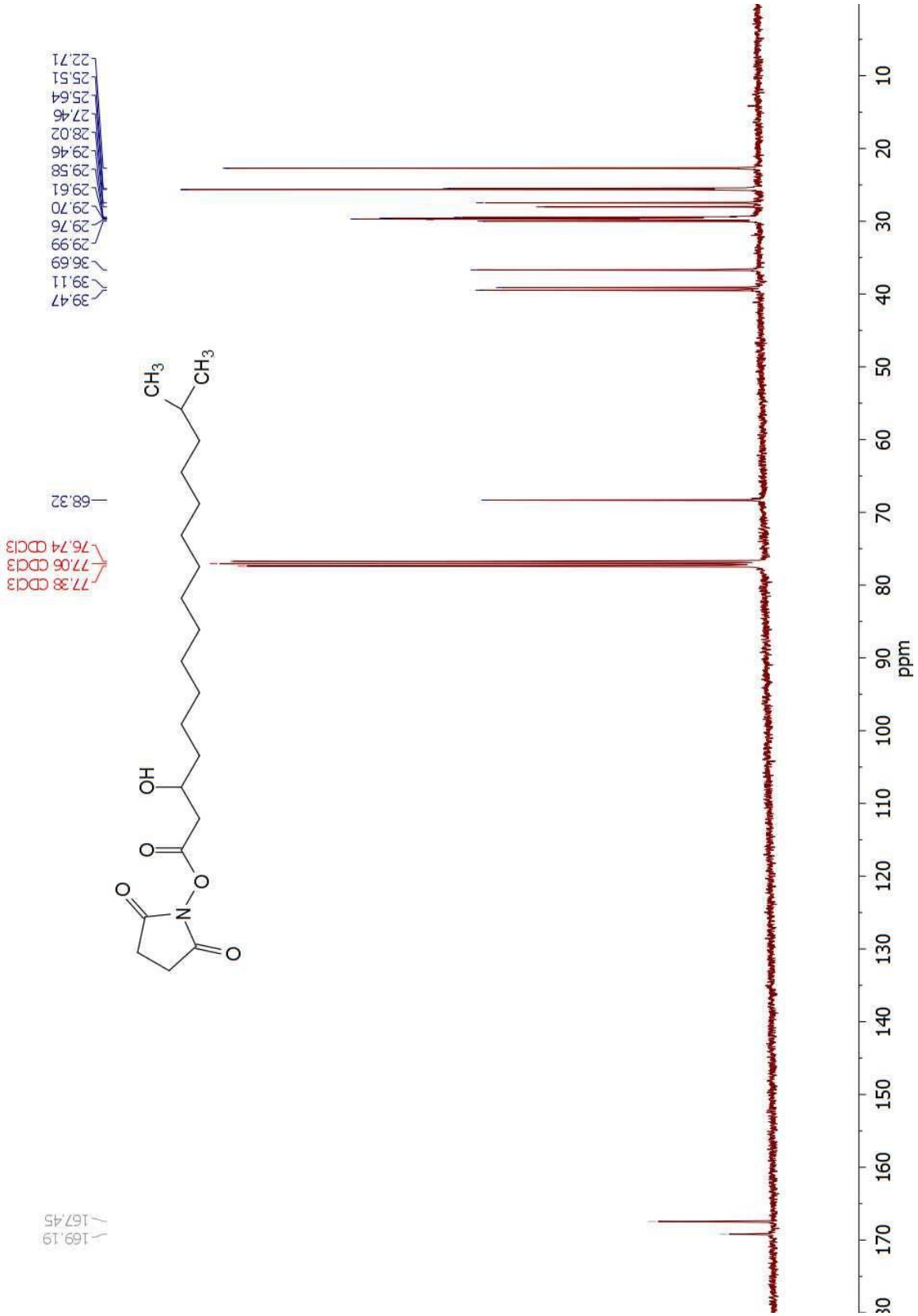
22.71
25.51
25.64
27.46
28.02
29.46
29.58
29.61
29.70
29.76
29.99
36.69
39.11
39.47
68.32
76.74 CDCl3
77.06 CDCl3
77.38 CDCl3
167.45
169.19
CH3
CH3
OH
O
O
N
O
O
ppm

7.26 CDCl3
0.85
0.87
1.12
1.14
1.16
1.17
1.26
1.45
1.47
1.47
1.48
1.50
1.51
1.52
1.53
1.54
1.55
1.56
1.58
1.59
1.60
1.61
1.62
1.64
2.67
2.69
2.71
2.73
2.78
2.78
2.81
2.82
2.86
4.11
4.11
4.12
4.13
4.14
4.15
4.16
4.17
CH3
CH3
OH
O
O
N
O
O
6.00
2.34
18.45
5.71
6.28
1.00
ppm

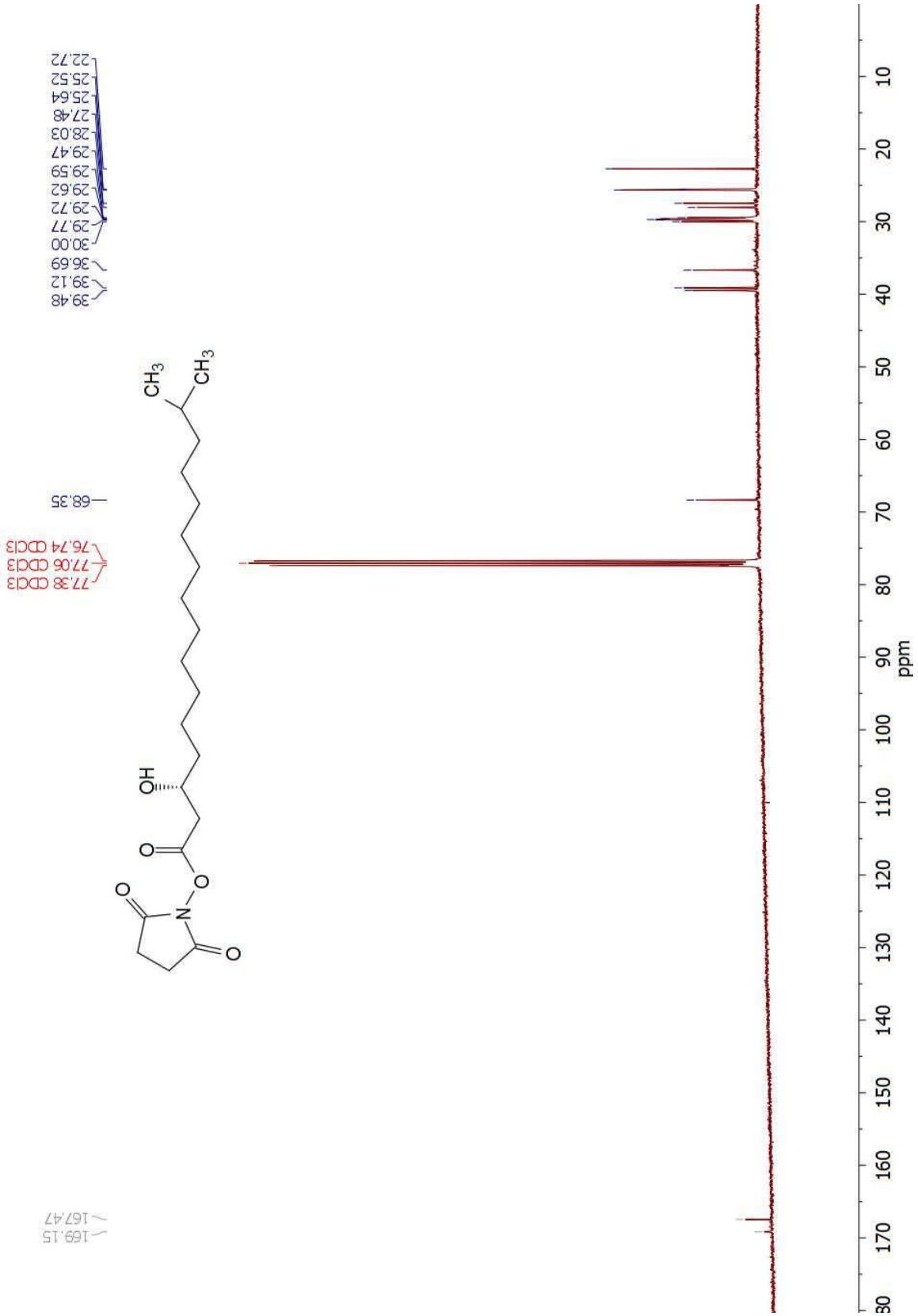
22.72
25.52
25.64
27.48
28.03
29.47
29.59
29.62
29.72
29.77
30.00
36.69
39.12
39.48
68.35
76.74 CDCl3
77.06 CDCl3
77.38 CDCl3
169.15
167.47
CH3
CH3
OH
O
O
N
O
O
ppm

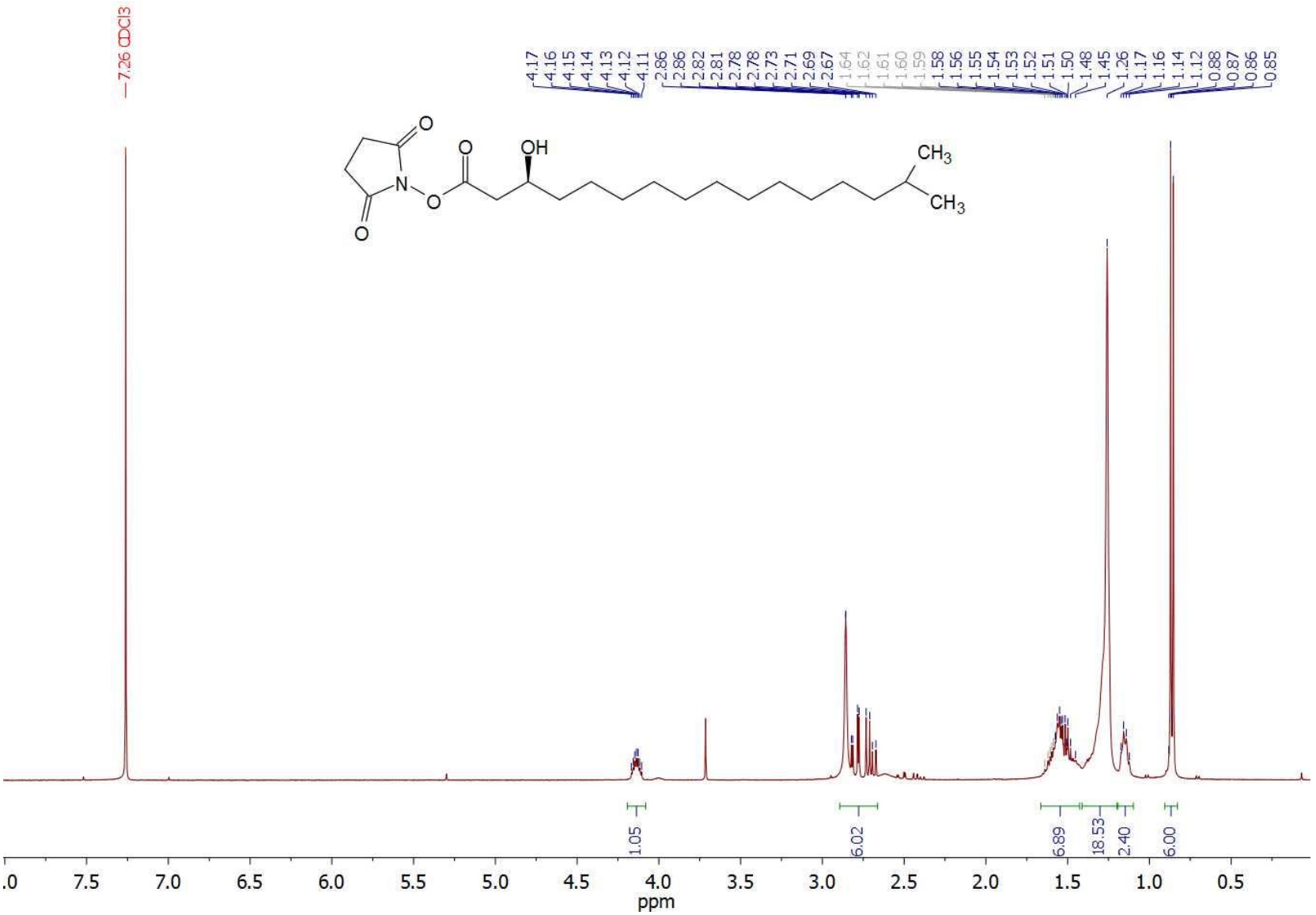
7.26 CDCl3
4.17
4.16
4.15
4.14
4.13
4.12
4.11
2.86
2.86
2.82
2.81
2.78
2.78
2.73
2.71
2.69
2.67
1.64
1.62
1.61
1.60
1.59
1.58
1.56
1.55
1.54
1.53
1.52
1.51
1.50
1.48
1.45
1.26
1.17
1.16
1.14
1.12
0.88
0.87
0.86
0.85
O
O
OH
CH3
N
O
CH3
O
1.05
6.02
6.89
18.53
2.40
6.00
.0
7.5
7.0
6.5
6.0
5.5
5.0
4.5
4.0
3.5
3.0
2.5
2.0
1.5
1.0
0.5
ppm

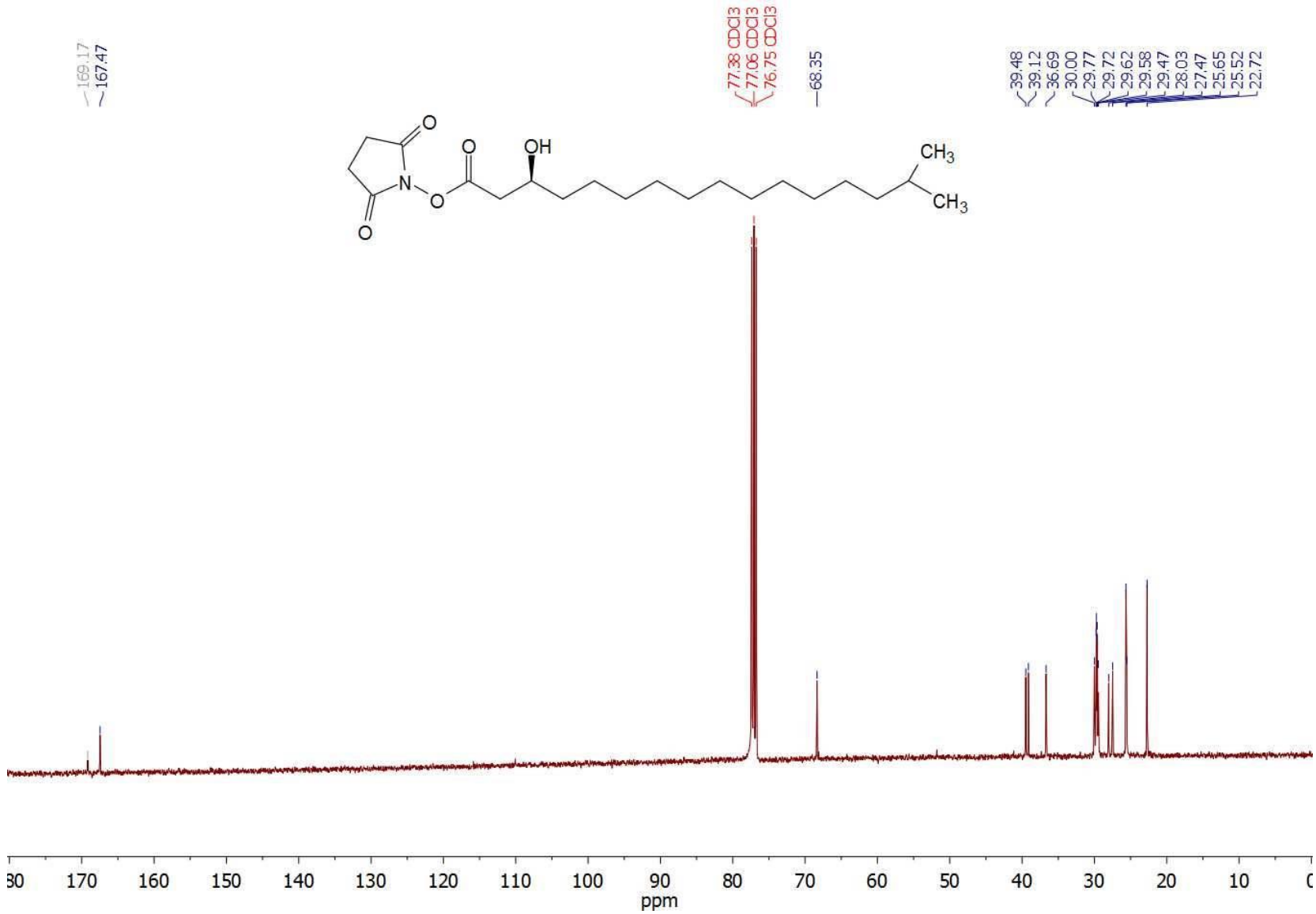
169.17
167.47
77.38 CDCl3
77.06 CDCl3
76.75 CDCl3
68.35
39.48
39.12
36.69
30.00
29.77
29.72
29.62
29.58
29.47
28.03
27.47
25.65
25.52
22.72
O
O
N
O
O
OH
CH3
CH3
ppm

4.84 HDO
4.15
4.14
4.13
4.04
4.03
4.02
4.00
3.99
3.95
3.94
3.92
3.91
3.85
3.32 MeOD
3.31 MeOD
3.31 MeOD
3.31 MeOD
3.30 MeOD
3.00
2.21
0.99
NH2
HO
O
O
H3C
0.0
0.5
1.0
1.5
2.0
2.5
3.0
3.5
4.0
4.5
ppm

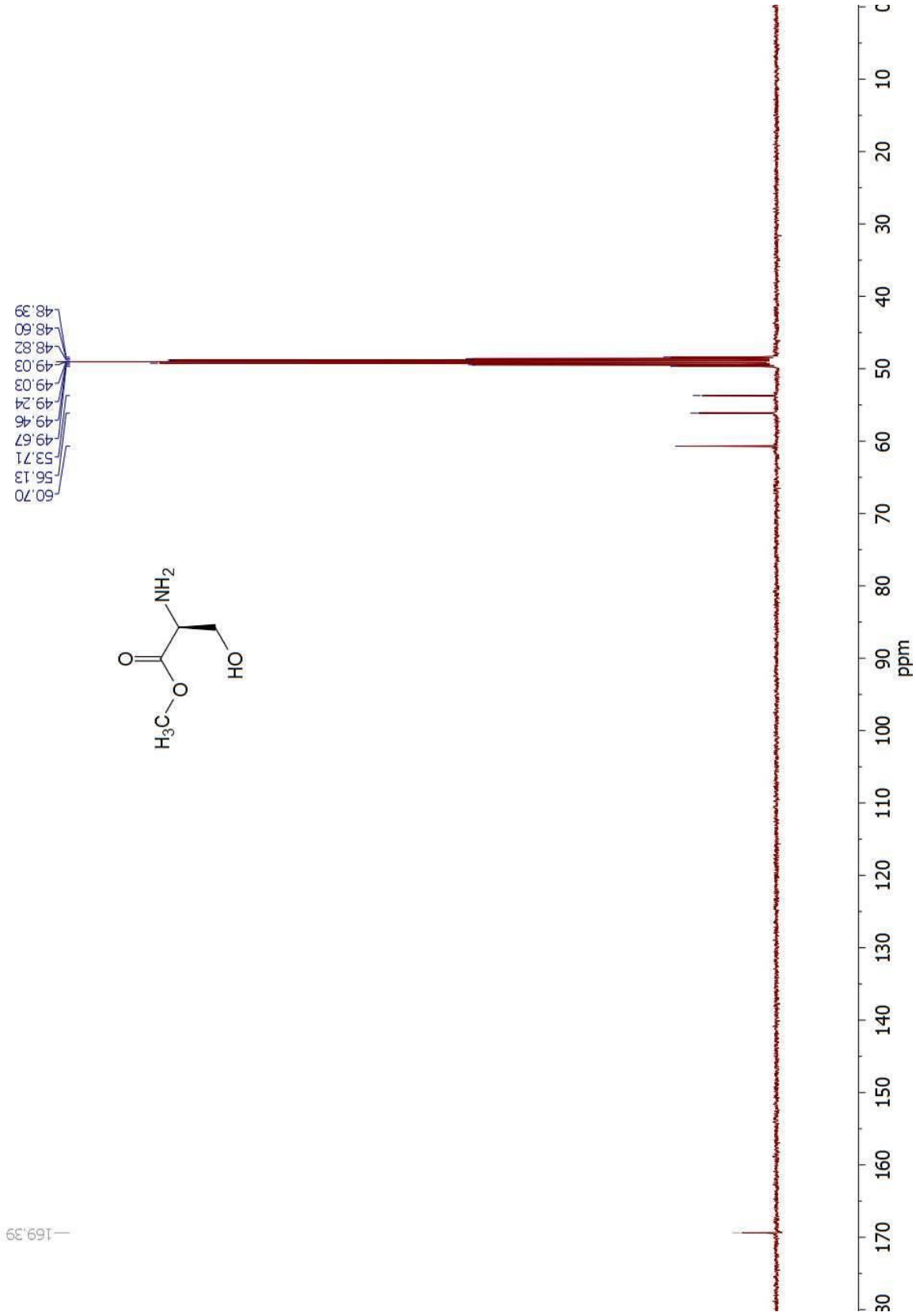
169.39
60.70
56.13
53.71
49.67
49.46
49.24
49.03
49.03
48.82
48.60
48.39
NH2
O
O
H3C
HO
ppm

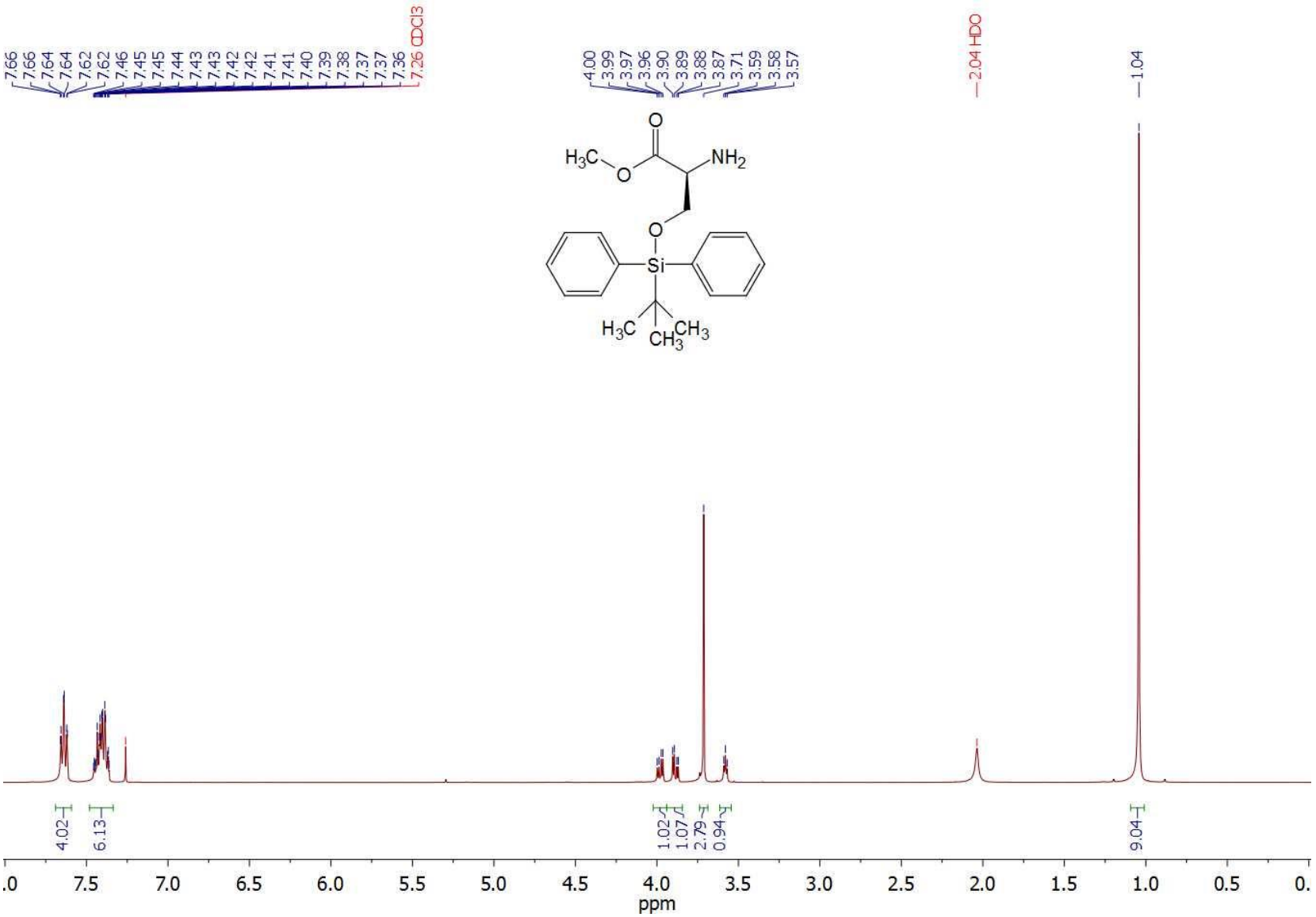
7.66
7.66
7.64
7.64
7.62
7.62
7.46
7.45
7.45
7.44
7.43
7.43
7.42
7.42
7.41
7.41
7.40
7.39
7.38
7.37
7.37
7.36
7.26 CDCl3
4.00
3.99
3.97
3.96
3.90
3.89
3.88
3.87
3.71
3.59
3.58
3.57
2.04 HDO
1.04
O
H3C
O
NH2
O
Si
H3C
CH3
CH3
4.02
6.13
1.02
1.07
2.79
0.94
9.04
.0
7.5
7.0
6.5
6.0
5.5
5.0
4.5
4.0
3.5
3.0
2.5
2.0
1.5
1.0
0.5
0.
ppm

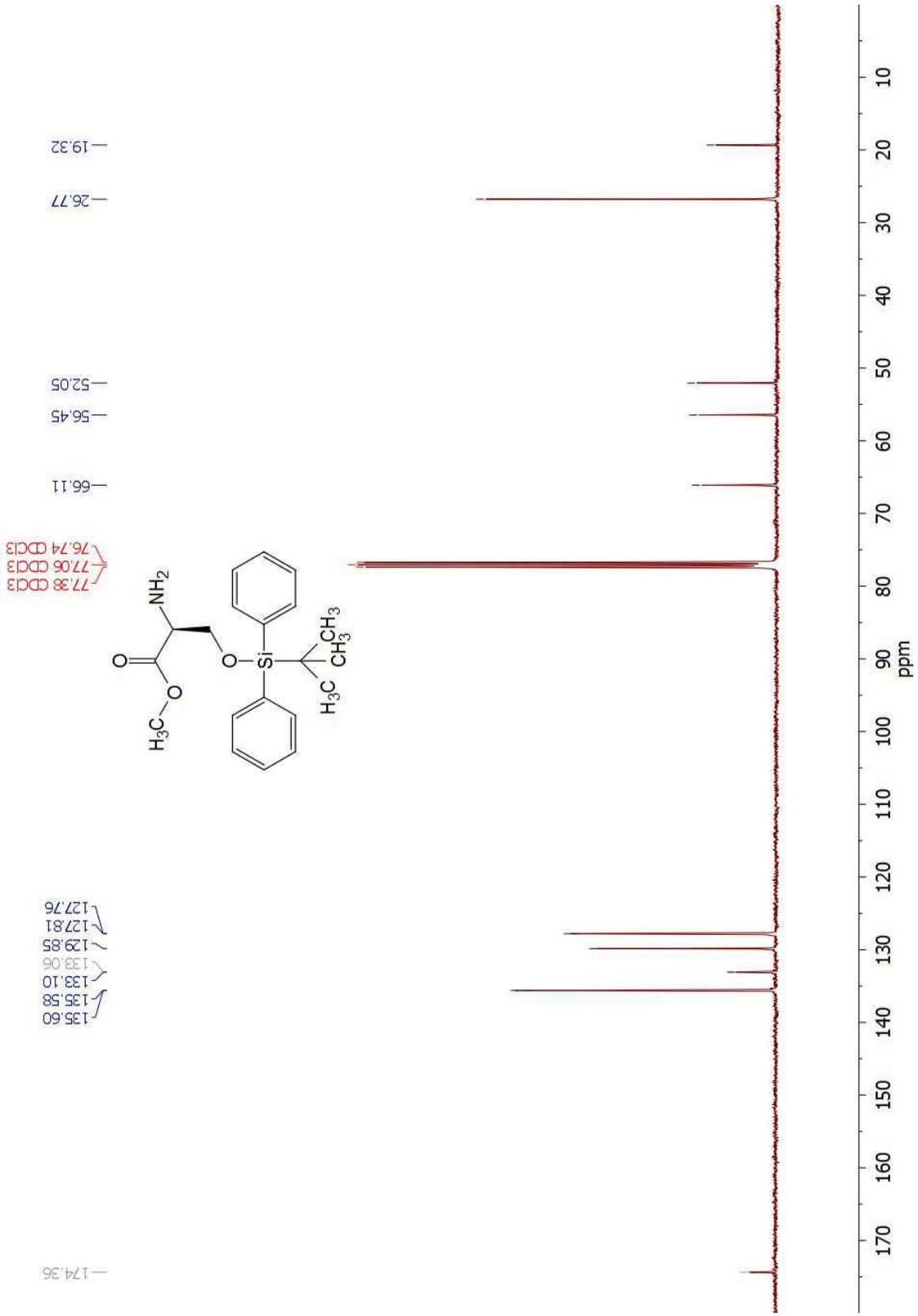
19.32
26.77
52.05
56.45
66.11
76.74 CDCl3
77.06 CDCl3
77.38 CDCl3
127.76
127.81
129.85
133.06
133.10
135.58
135.60
174.36
NH2
O
O
O
Si
H3C
CH3
CH3
H3C
10
20
30
40
50
60
70
80
90
100
110
120
130
140
150
160
170
ppm


7.38
7.37
7.35
7.34
7.32
7.32
7.31
7.30
7.30
7.29
7.28
7.27
7.27
5.10
4.85 HDO
3.84
3.66
3.32 MeOD
3.31 MeOD
3.31 MeOD
3.31 MeOD
3.30 MeOD
5.00
2.04
1.94
0.54
ppm

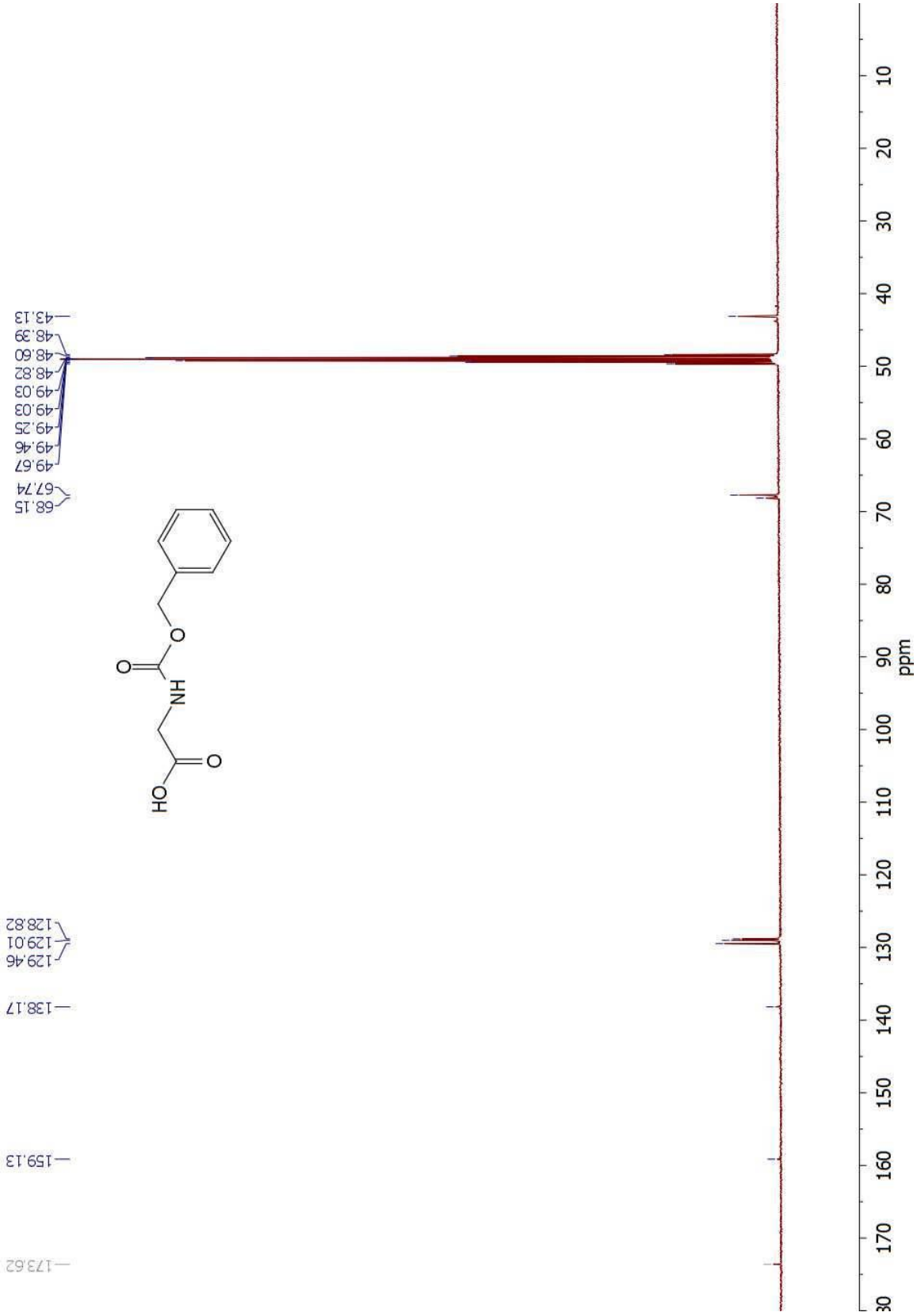
43.13
48.39
48.60
48.82
49.03
49.03
49.25
49.46
49.67
67.74
68.15
128.82
129.01
129.46
138.17
159.13
173.62
HO
O
O
NH
O
ppm

1.03
1.75 HDO
3.74
3.80
3.81
3.84
3.85
3.88
3.89
3.91
3.92
3.95
3.97
4.12
4.12
4.14
4.15
4.66
4.67
4.68
4.69
4.69
4.70
5.07
5.11
5.12
5.15
5.36
6.76
6.78
7.26 CDCl3
7.29
7.30
7.31
7.32
7.32
7.33
7.34
7.35
7.37
7.39
7.39
7.40
7.42
7.42
7.43
7.43
7.44
7.45
7.45
7.46
7.57
7.59
7.61
NH
NH
O
O
O
O
O
O
Si
H3C
CH3
CH3
9.00
3.09
3.04
1.02
1.00
2.03
0.96
0.98
11.17
4.09
ppm

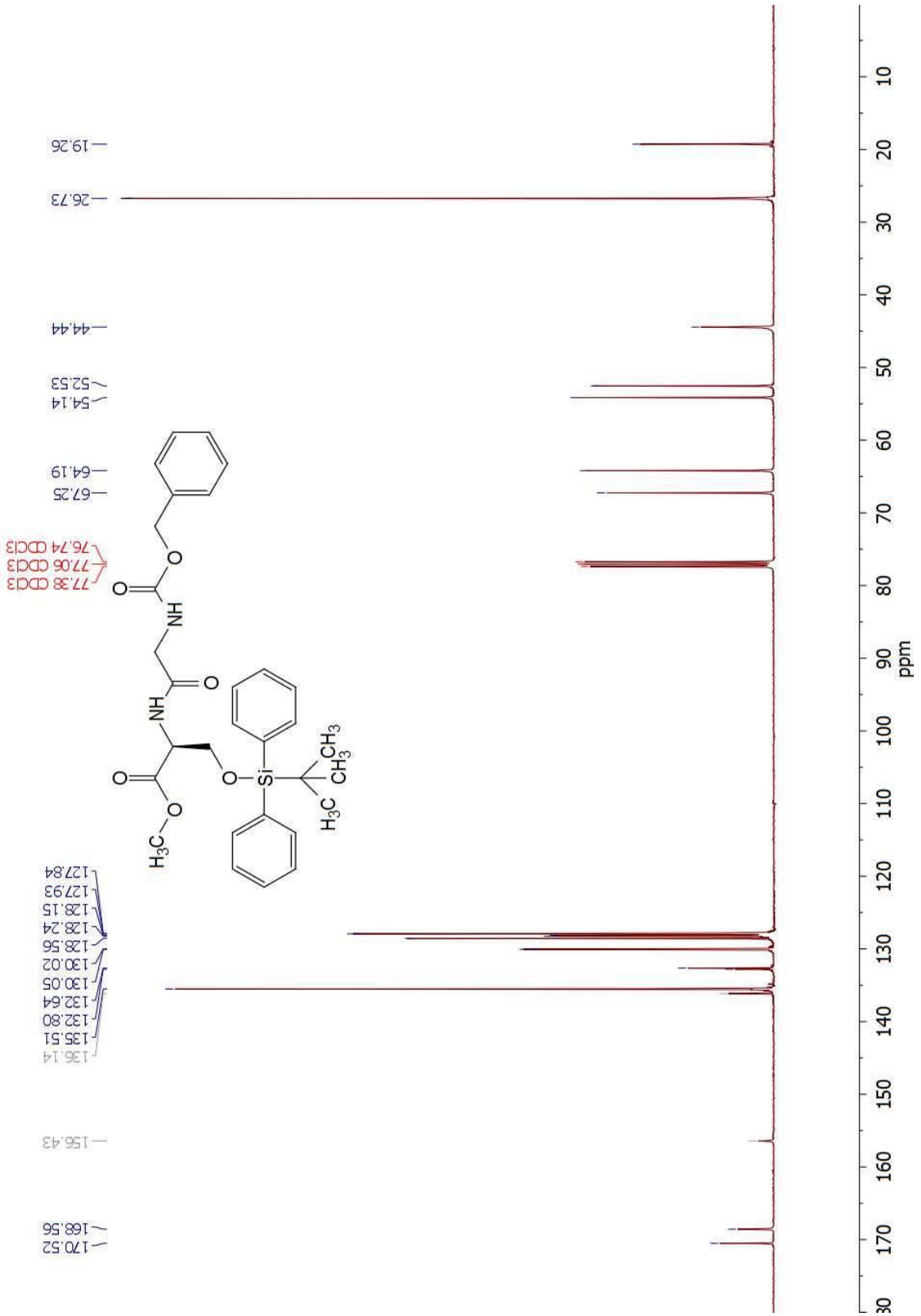
19.26
26.73
44.44
52.53
54.14
64.19
67.25
76.74 CDCl3
77.06 CDCl3
77.38 CDCl3
127.84
127.93
128.15
128.24
128.56
130.02
130.05
132.64
132.80
135.51
136.14
156.43
168.56
170.52
ppm

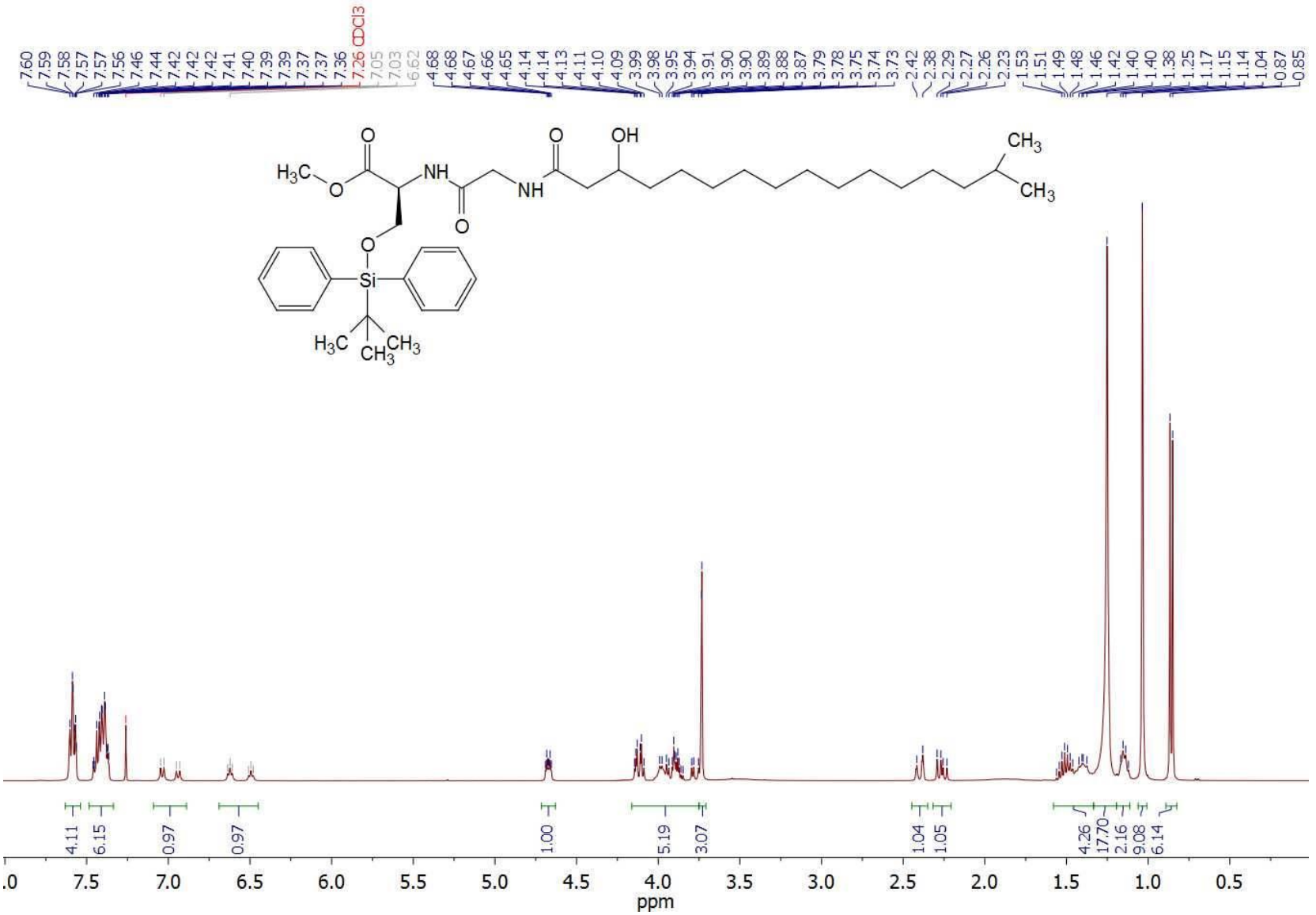
7.60 7.59 7.58 7.57 7.57 7.56 7.46 7.44 7.42 7.42 7.42 7.41 7.40 7.39 7.39 7.37 7.37 7.36 7.26 CDCl3 7.05 7.03 6.62
4.68 4.68 4.67 4.66 4.65 4.14 4.14 4.13 4.11 4.10 4.09 3.99 3.98 3.95 3.94 3.91 3.90 3.90 3.89 3.88 3.87 3.79 3.78 3.75 3.74 3.73
2.42 2.38 2.29 2.27 2.26 2.23
1.53 1.51 1.49 1.48 1.46 1.42 1.40 1.40 1.38 1.25 1.17 1.15 1.14 1.04 0.87 0.85
H3C O O NH NH O OH CH3 CH3
O O
Si
H3C CH3 CH3
4.11 6.15 0.97 0.97 1.00 5.19 3.07 1.04 1.05 4.26 17.70 2.16 9.08 6.14
.0 7.5 7.0 6.5 6.0 5.5 5.0 4.5 4.0 3.5 3.0 2.5 2.0 1.5 1.0 0.5
ppm

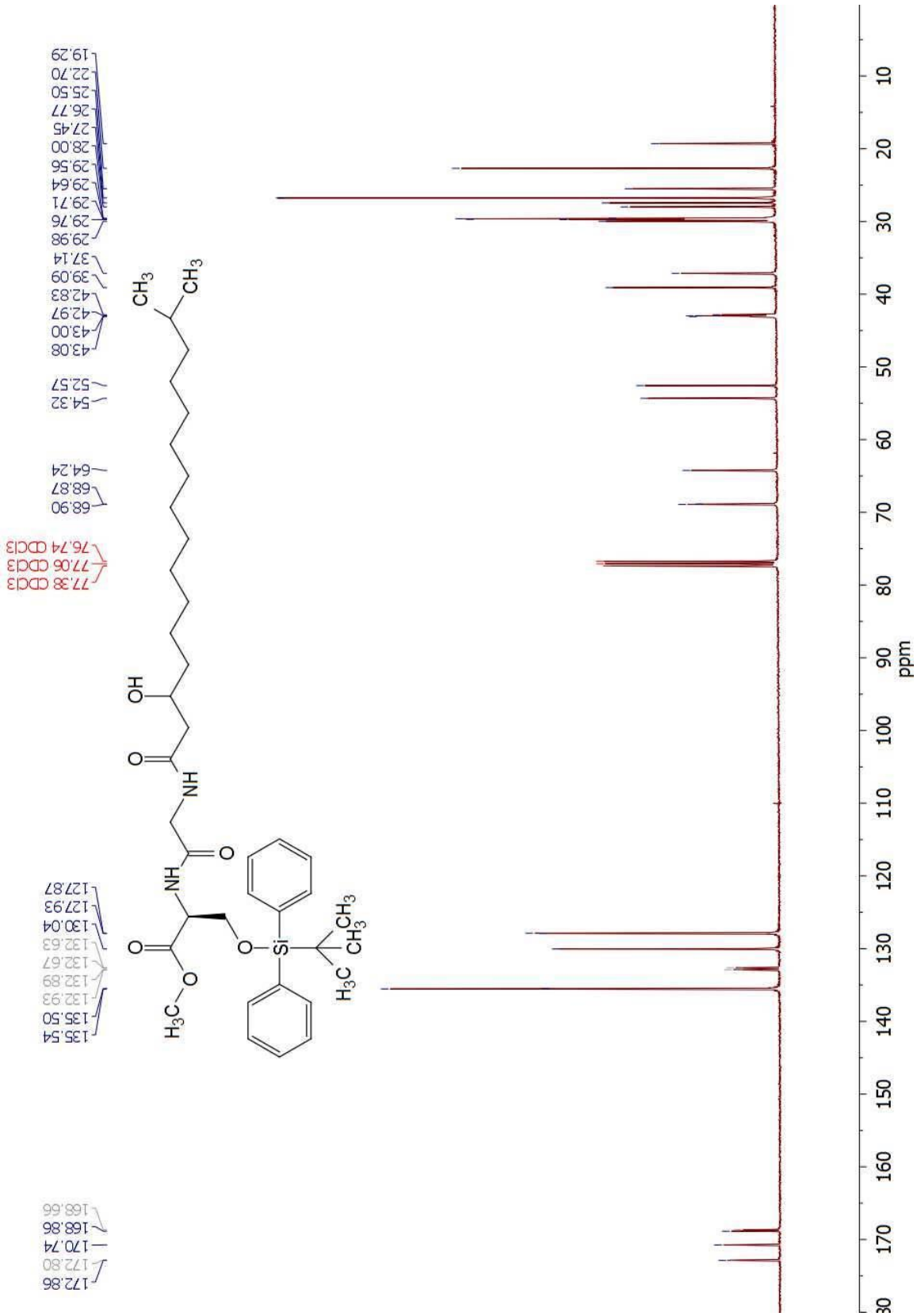
19.29
22.70
25.50
26.77
27.45
28.00
29.56
29.64
29.71
29.76
29.98
37.14
39.09
42.83
42.97
43.00
43.08
52.57
54.32
64.24
68.87
68.90
76.74 CDCl3
77.06 CDCl3
77.38 CDCl3
127.87
127.93
130.04
132.63
132.67
132.89
132.93
135.50
135.54
168.66
168.86
170.74
172.80
172.86
CH3
CH3
OH
O
NH
O
NH
O
O
O
H3C
Si
H3C
CH3
CH3
10
20
30
40
50
60
70
80
90
100
110
120
130
140
150
160
170
180
ppm

0.85
0.87
1.04
1.12
1.14
1.16
1.25
1.38
1.39
1.48
1.50
1.51
1.53
1.55
1.59 HDO
2.24
2.26
2.27
2.30
2.39
2.39
2.42
2.43
3.35
3.36
3.75
3.79
3.80
3.88
3.89
3.91
3.92
3.98
4.09
4.10
4.12
4.12
4.13
4.14
4.15
4.65
4.66
4.67
4.67
4.68
4.69
6.37
6.39
6.40
6.88
6.90
7.26
7.26 CDCl3
7.38
7.38
7.40
7.41
7.42
7.43
7.44
7.45
7.46
7.57
7.57
7.59
7.60
7.61
CH3
CH3
OH
O
NH
NH
O
O
O
H3C
O
Si
H3C
CH3
CH3
6.05
9.03
2.06
18.18
4.35
1.06
1.08
0.86
3.21
2.00
0.98
1.98
1.04
0.98
1.00
6.24
4.08
0.5
1.0
1.5
2.0
2.5
3.0
3.5
4.0
4.5
5.0
5.5
6.0
6.5
7.0
7.5
.0
ppm

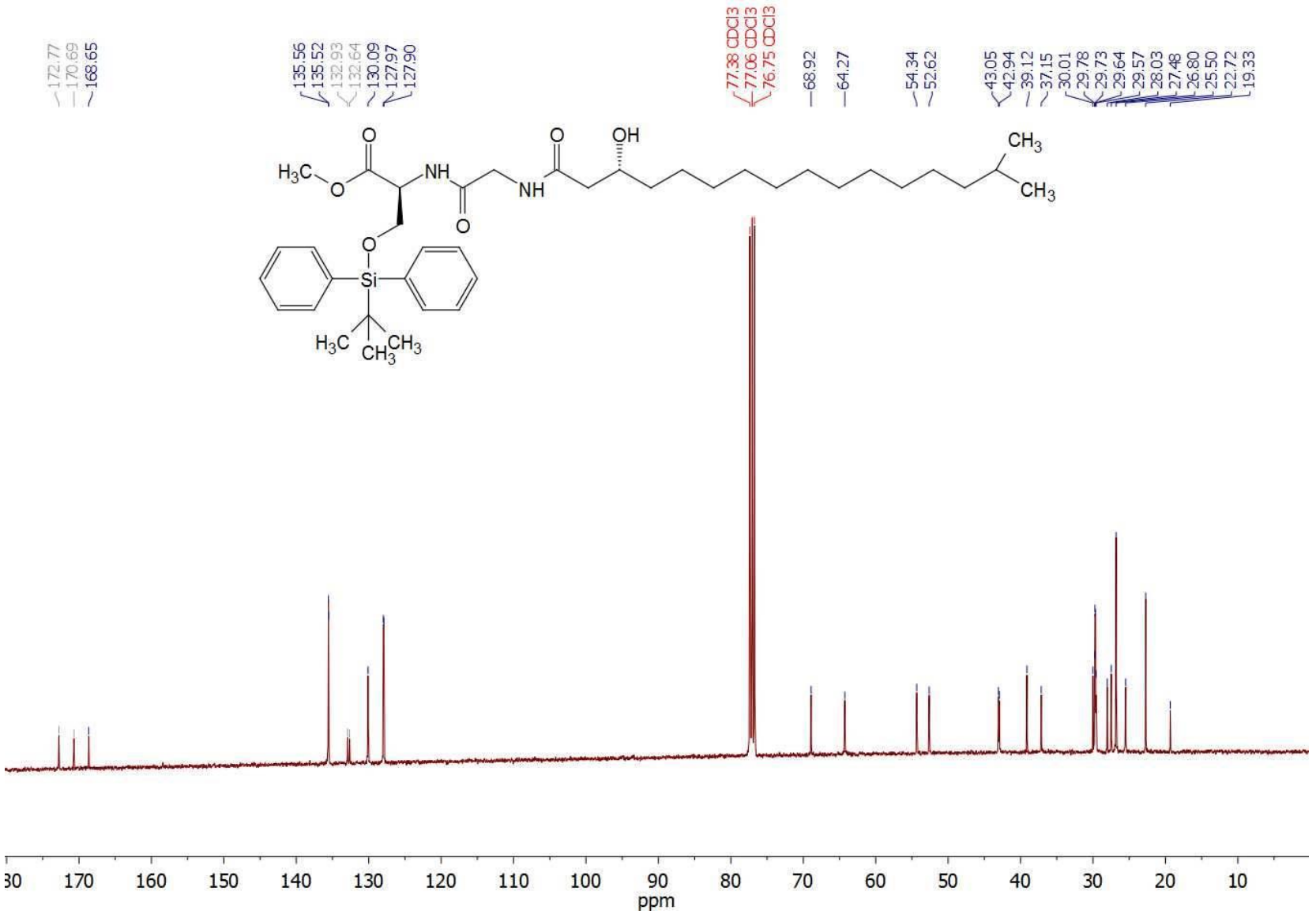
172.77
170.69
168.65
135.56
135.52
132.93
132.64
130.09
127.97
127.90
77.38 CDCl3
77.06 CDCl3
76.75 CDCl3
68.92
64.27
54.34
52.62
43.05
42.94
39.12
37.15
30.01
29.78
29.73
29.64
29.57
28.03
27.48
26.80
25.50
22.72
19.33
H3C
O
O
NH
O
NH
O
OH
CH3
CH3
O
Si
H3C
CH3
CH3
30
170
160
150
140
130
120
110
100
90
80
70
60
50
40
30
20
10
ppm

0.85
0.87
1.04
1.12
1.15
1.16
1.17
1.25
1.40
1.43
1.48
1.50
1.51
1.53
1.55
1.67 HDO
2.23
2.25
2.27
2.29
2.38
2.38
2.41
2.42
3.48
3.49
3.49
3.74
3.83
3.84
3.87
3.89
3.89
3.91
3.92
3.94
3.96
3.98
4.00
4.11
4.12
4.14
4.14
4.66
4.66
4.67
4.68
4.68
6.33
6.35
6.85
6.87
7.26 CDCl3
7.37
7.37
7.39
7.40
7.40
7.40
7.41
7.43
7.43
7.44
7.45
7.46
7.46
7.56
7.57
7.59
7.61
CH3
CH3
OH
O
NH
NH
O
O
O
H3C
O
O
Si
CH3
CH3
H3C
6.12
9.06
2.61
19.92
4.74
1.11
1.08
0.92
3.03
4.02
1.07
1.01
0.95
0.97
6.16
4.10
0.
0.5
1.0
1.5
2.0
2.5
3.0
3.5
4.0
4.5
5.0
5.5
6.0
6.5
7.0
7.5
.0
ppm

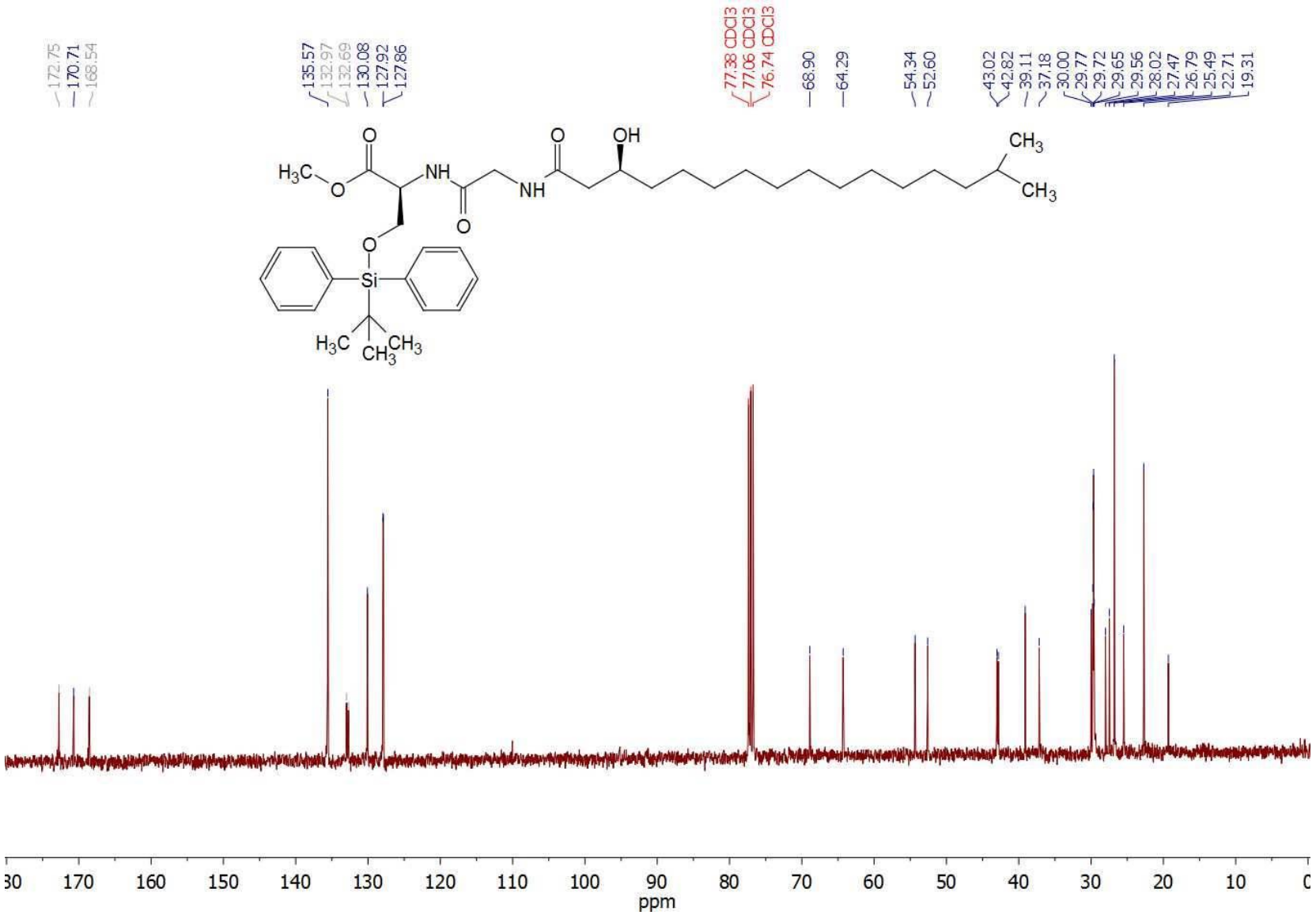
172.75
170.71
168.54
135.57
132.97
132.69
130.08
127.92
127.86
77.38 CDCl3
77.06 CDCl3
76.74 CDCl3
68.90
64.29
54.34
52.60
43.02
42.82
39.11
37.18
30.00
29.77
29.72
29.65
29.56
28.02
27.47
26.79
25.49
22.71
19.31
H3C
O
O
NH
O
NH
O
OH
CH3
CH3
O
Si
H3C
CH3
CH3
ppm

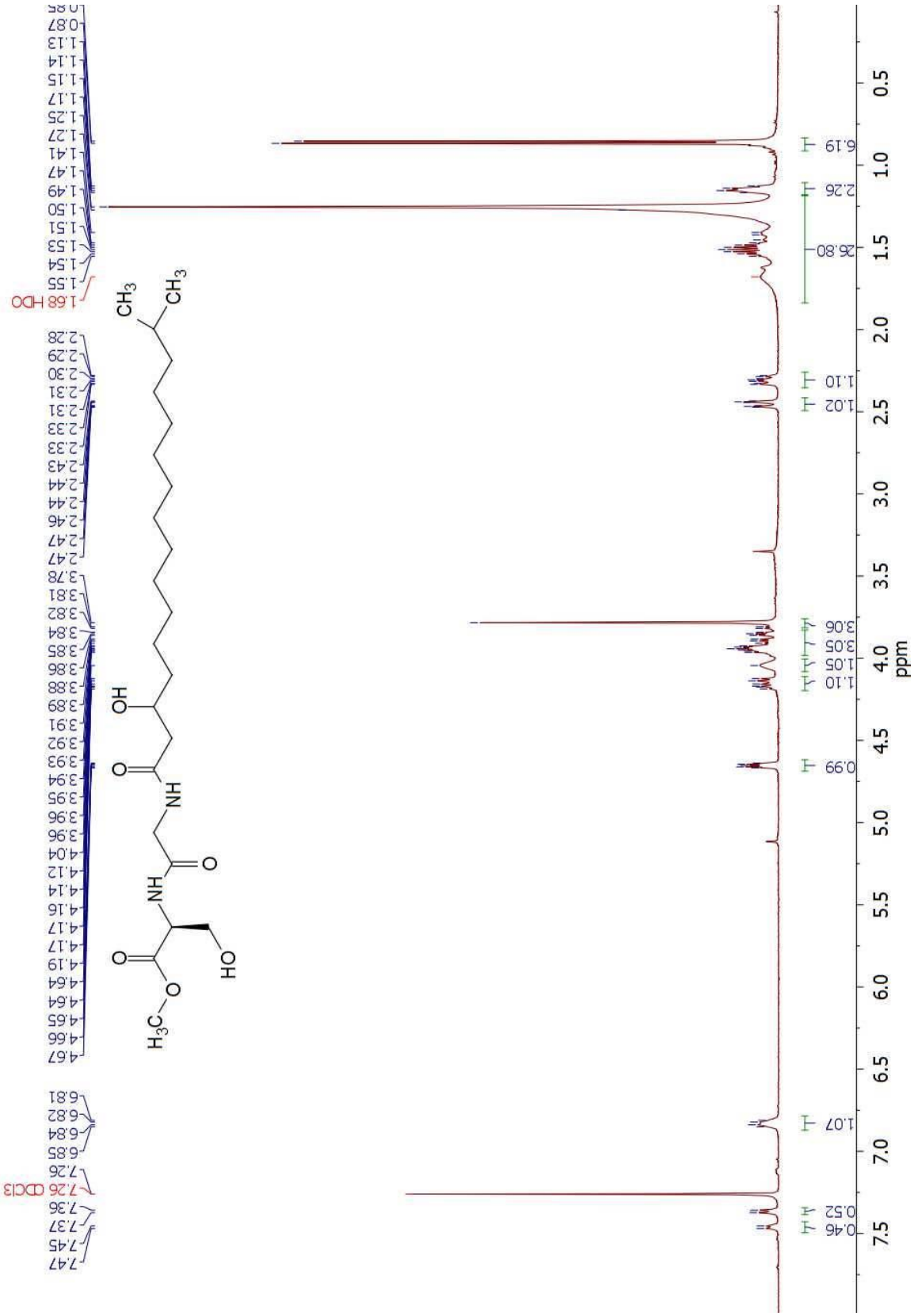
CH3
CH3
OH
O
NH
O
NH
O
O
O
H3C
OH
ppm

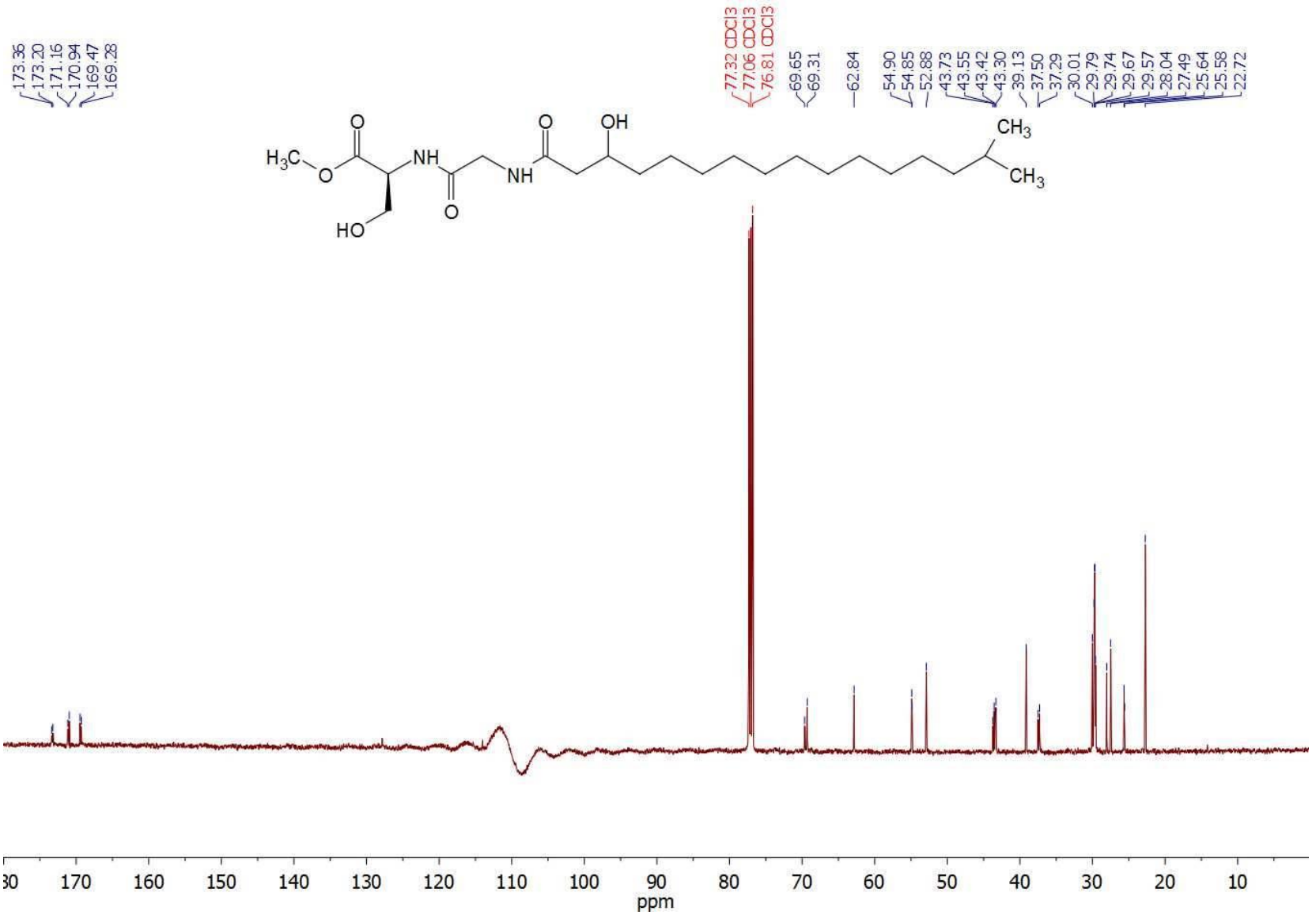
173.36
173.20
171.16
170.94
169.47
169.28
77.32 CDCl3
77.06 CDCl3
76.81 CDCl3
69.65
69.31
62.84
54.90
54.85
52.88
43.73
43.55
43.42
43.30
39.13
37.50
37.29
30.01
29.79
29.74
29.67
29.57
28.04
27.49
25.64
25.58
22.72
H3C
O
NH
NH
OH
CH3
CH3
HO
ppm

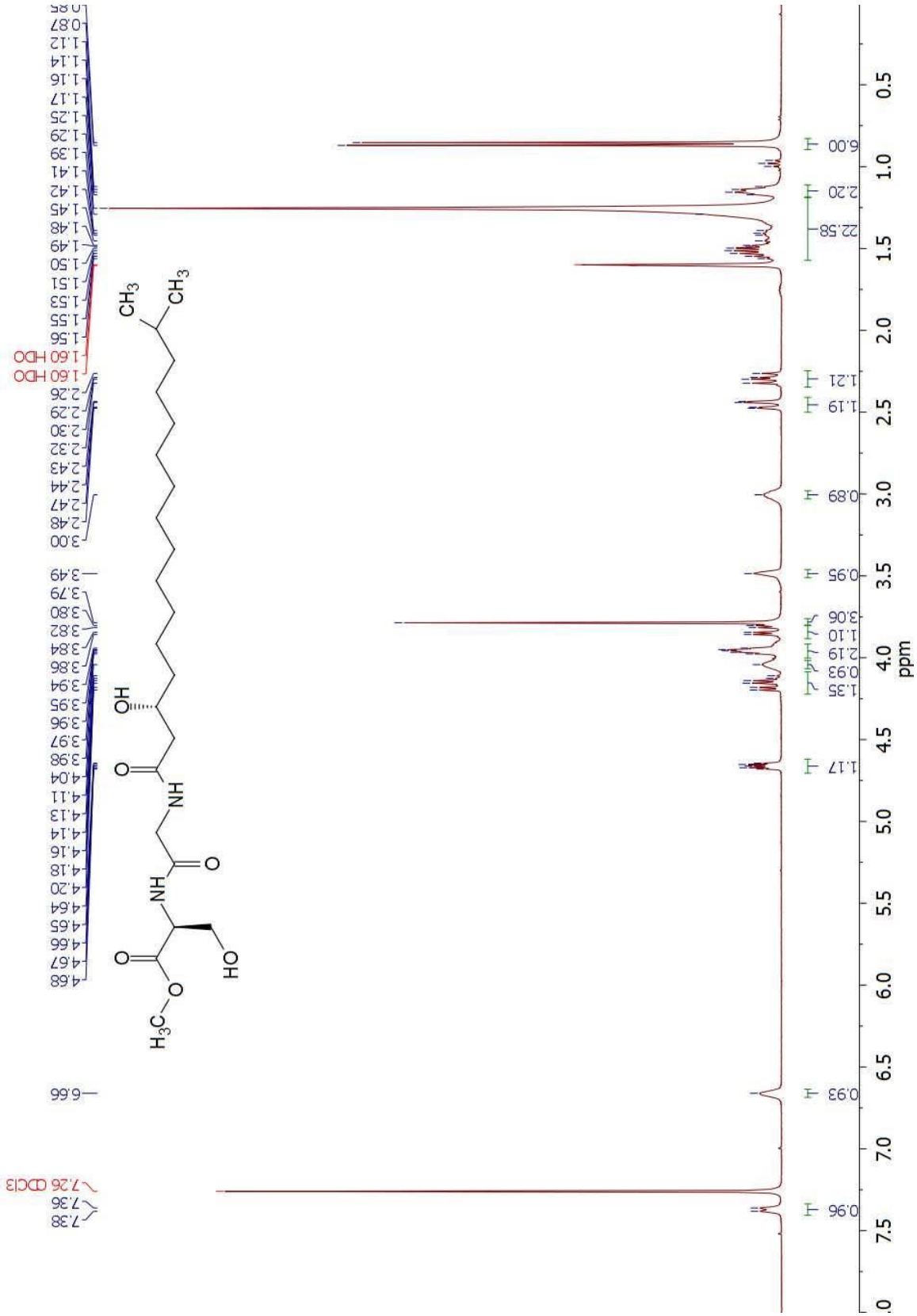
CH3
CH3
OH
O
NH
NH
O
O
O
O
H3C
OH
ppm

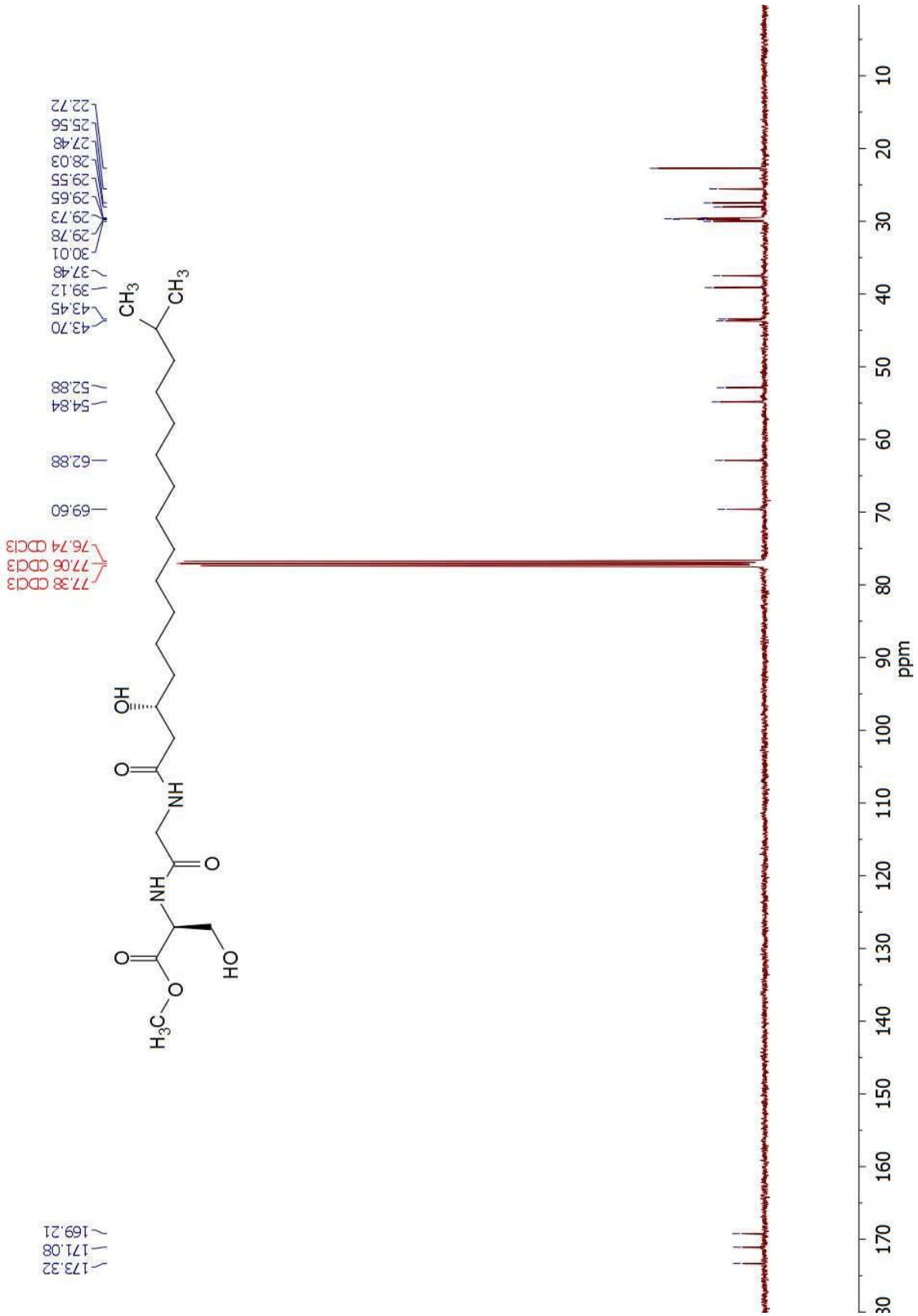
22.72
25.56
27.48
28.03
29.55
29.65
29.73
29.78
30.01
37.48
39.12
43.45
43.70
52.88
54.84
62.88
69.60
76.74 CDCl3
77.06 CDCl3
77.38 CDCl3
173.32
171.08
169.21
CH3
CH3
OH
O
NH
NH
O
O
O
H3C
OH
ppm

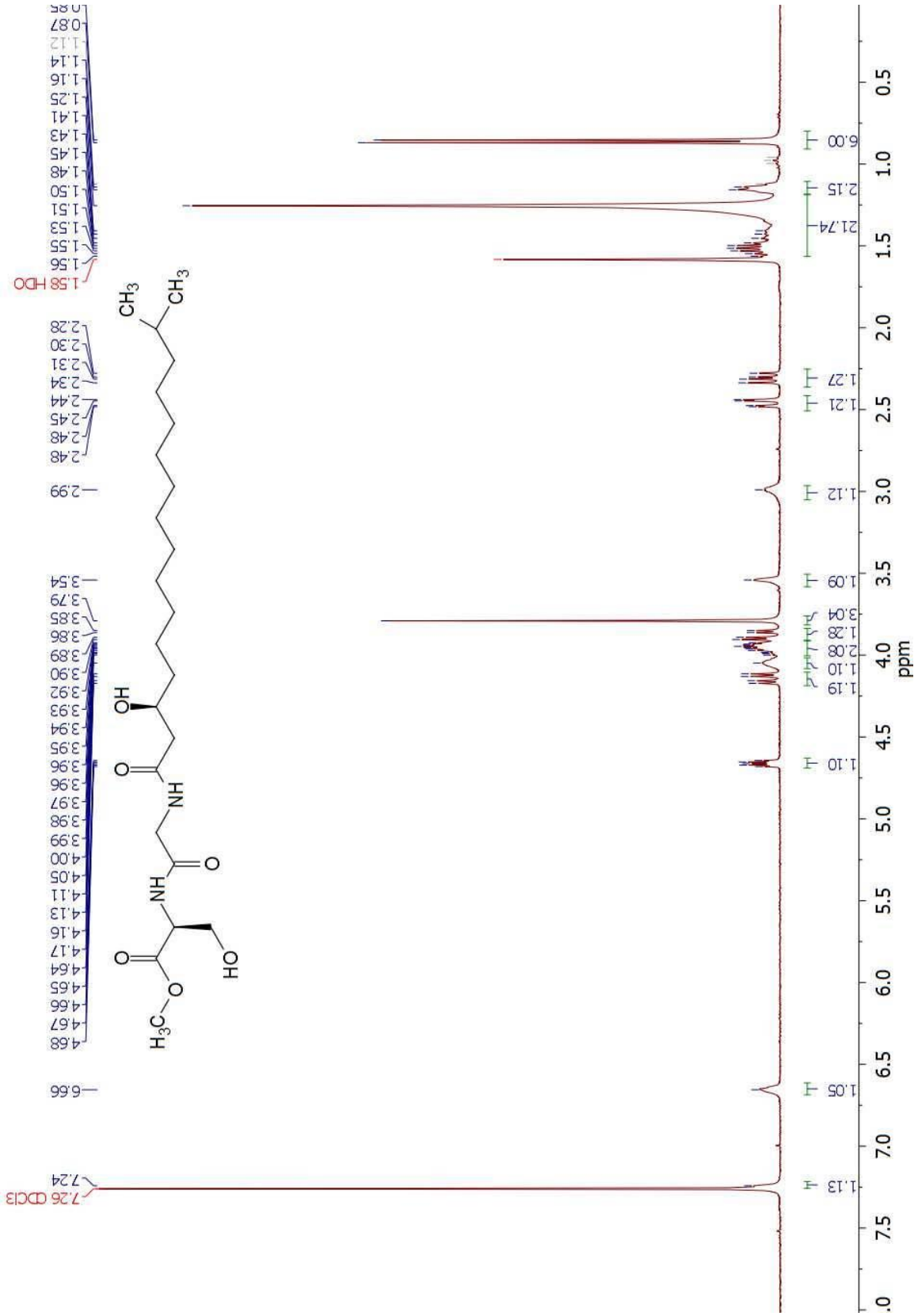
CH3
CH3
OH
O
NH
NH
O
O
O
O
H3C
OH
ppm

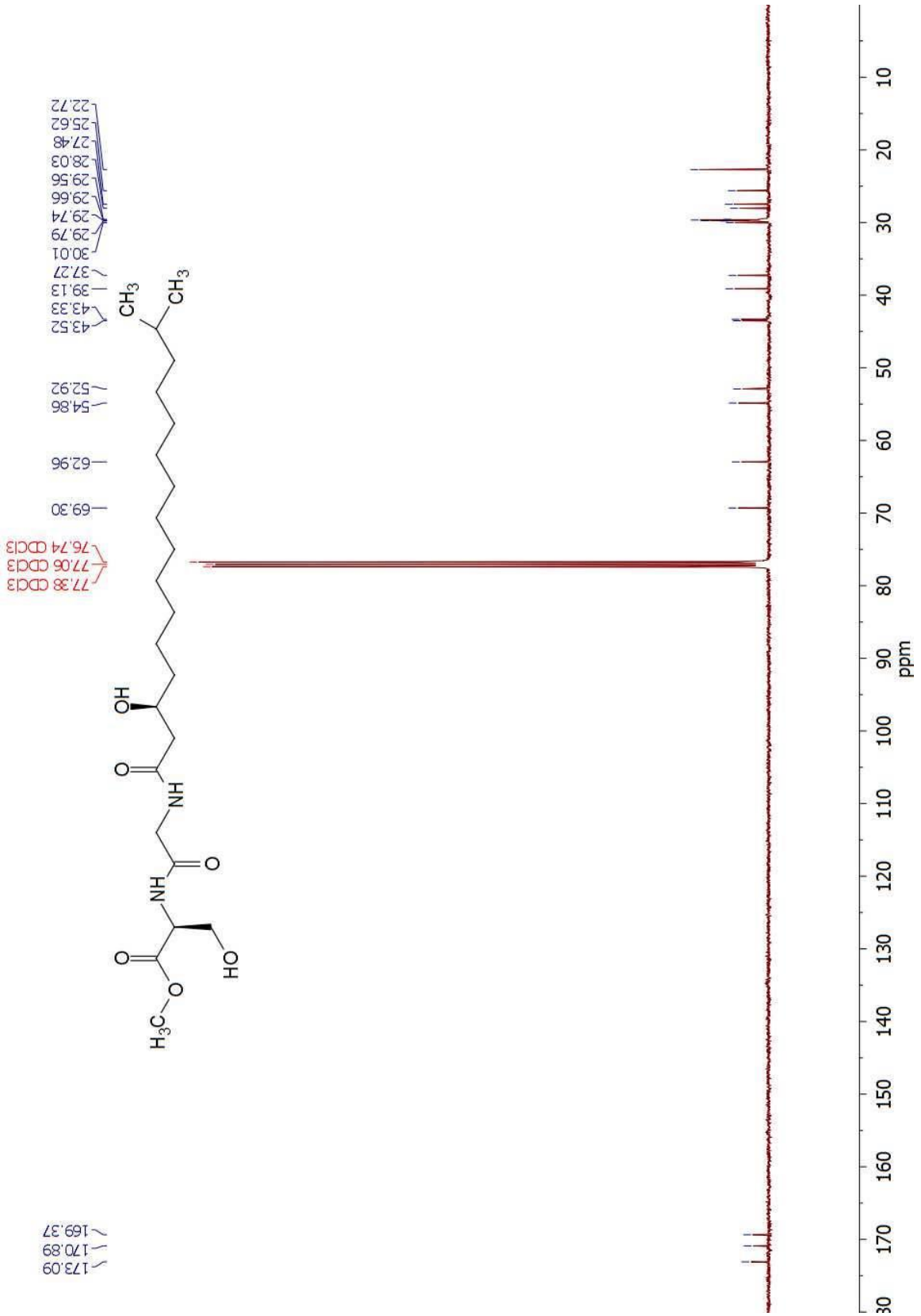
22.72
25.62
27.48
28.03
29.56
29.66
29.74
29.79
30.01
37.27
39.13
43.33
43.52
52.92
54.86
62.96
69.30
76.74 CDCl3
77.06 CDCl3
77.38 CDCl3
169.37
170.89
173.09
CH3
CH3
OH
O
NH
O
NH
O
O
O
H3C
OH
ppm

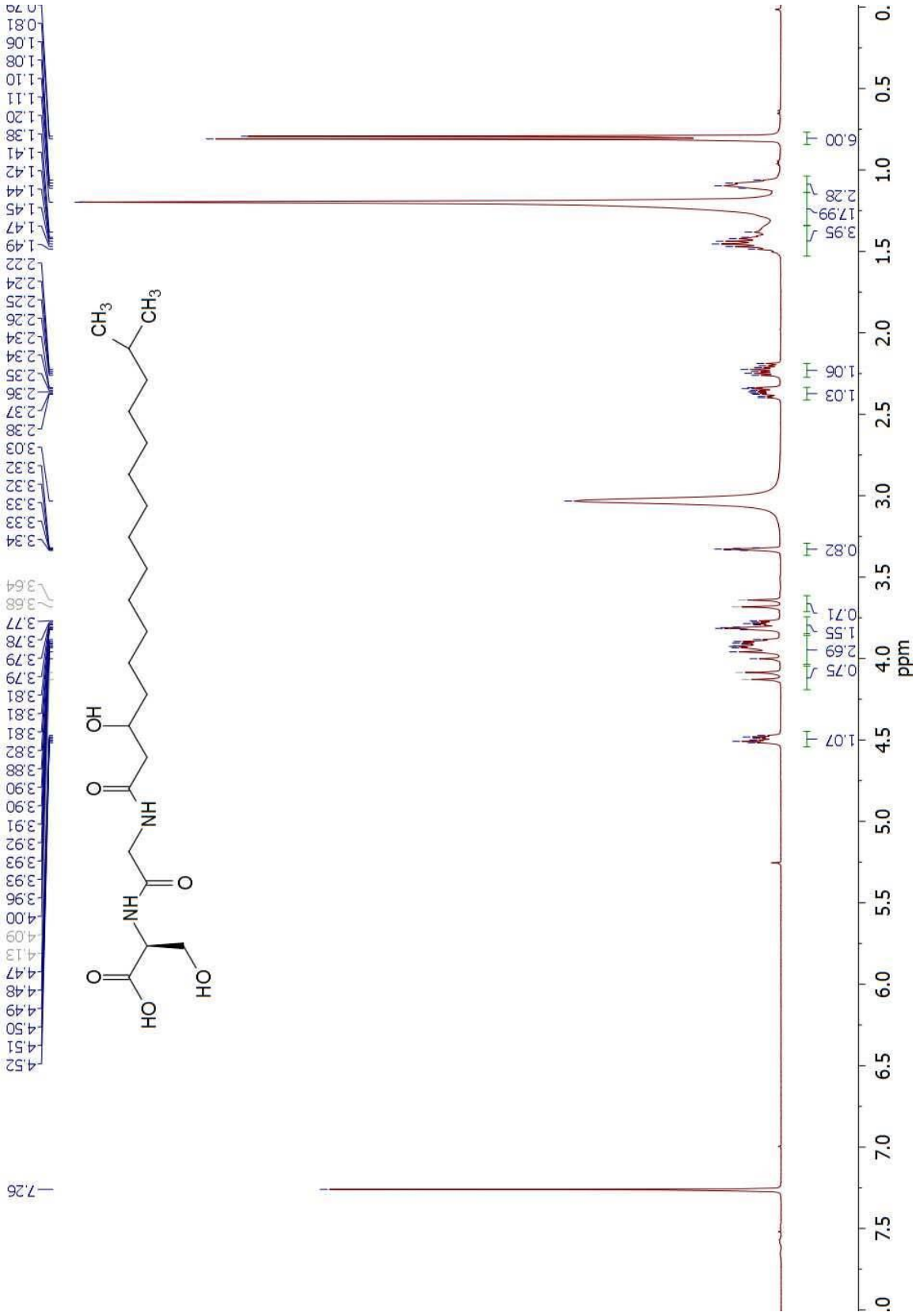
CH3
CH3
OH
O
NH
O
NH
O
O
HO
HO
ppm

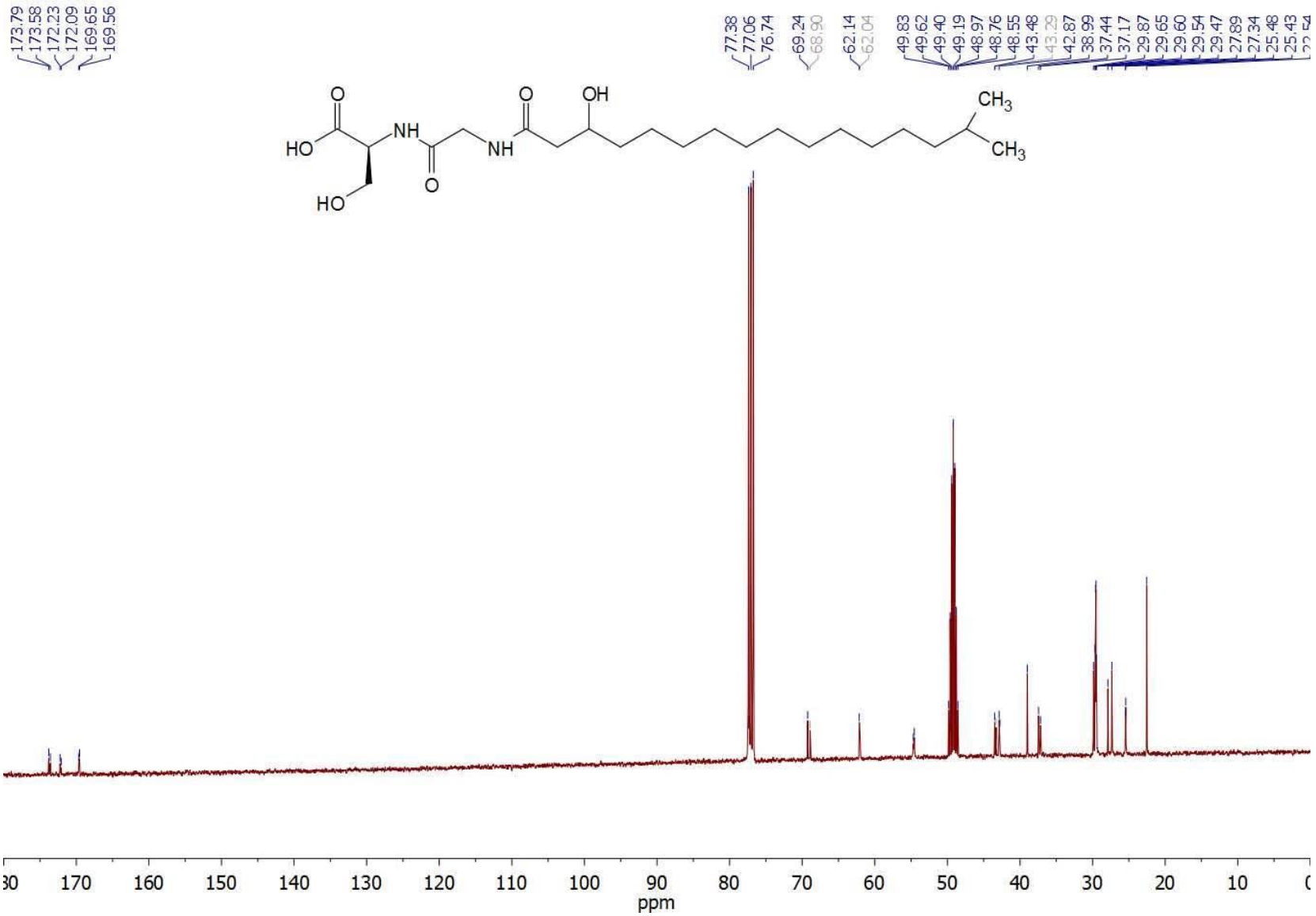
173.79
173.58
172.23
172.09
169.65
169.56
77.38
77.06
76.74
69.24
68.90
62.14
62.04
49.83
49.62
49.40
49.19
48.97
48.76
48.55
43.48
43.29
42.87
38.99
37.44
37.17
29.87
29.65
29.60
29.54
29.47
27.89
27.34
25.48
25.43
HO
O
NH
O
NH
O
OH
HO
CH3
CH3
ppm

7.26 CDCl3
3.48 CDCl3
CH3
CH3
OH
O
NH
O
NH
O
O
HO
HO
6.21
2.17
18.50
4.20
1.12
1.12
0.90
5.97
1.10
ppm

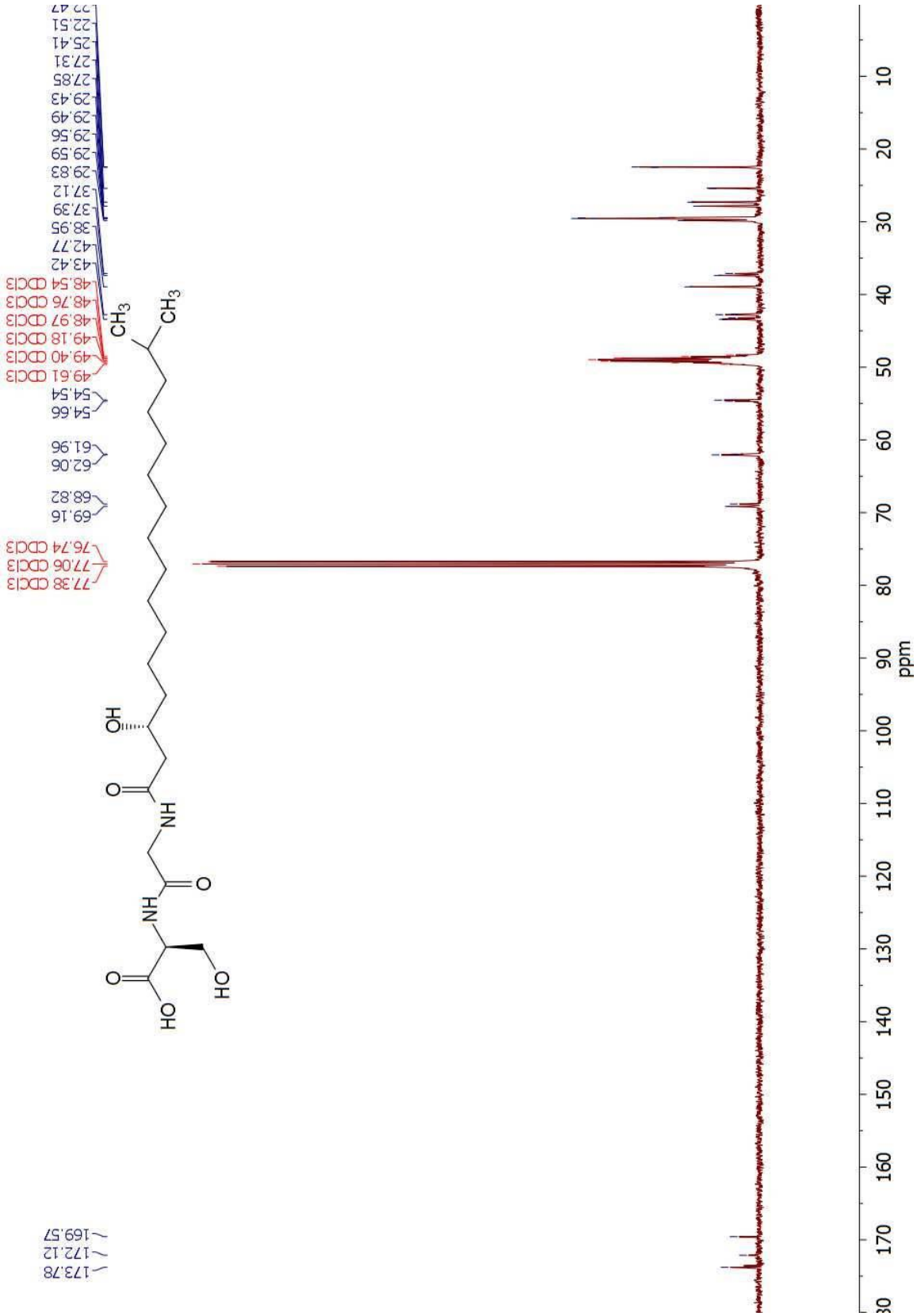
22.47
22.51
25.41
27.31
27.85
29.43
29.49
29.56
29.59
29.83
37.12
37.39
38.95
42.77
43.42
48.54 CDCl3
48.76 CDCl3
48.97 CDCl3
49.18 CDCl3
49.40 CDCl3
49.61 CDCl3
54.54
54.66
61.96
62.06
68.82
69.16
76.74 CDCl3
77.06 CDCl3
77.38 CDCl3
169.57
172.12
173.78
CH3
CH3
OH
O
NH
O
NH
O
HO
O
HO
10
20
30
40
50
60
70
80
90
100
110
120
130
140
150
160
170
ppm

7.26 CDCl3
2.50 HDO
6.11
2.14
17.77
3.98
1.26
2.02
5.38
1.00
ppm

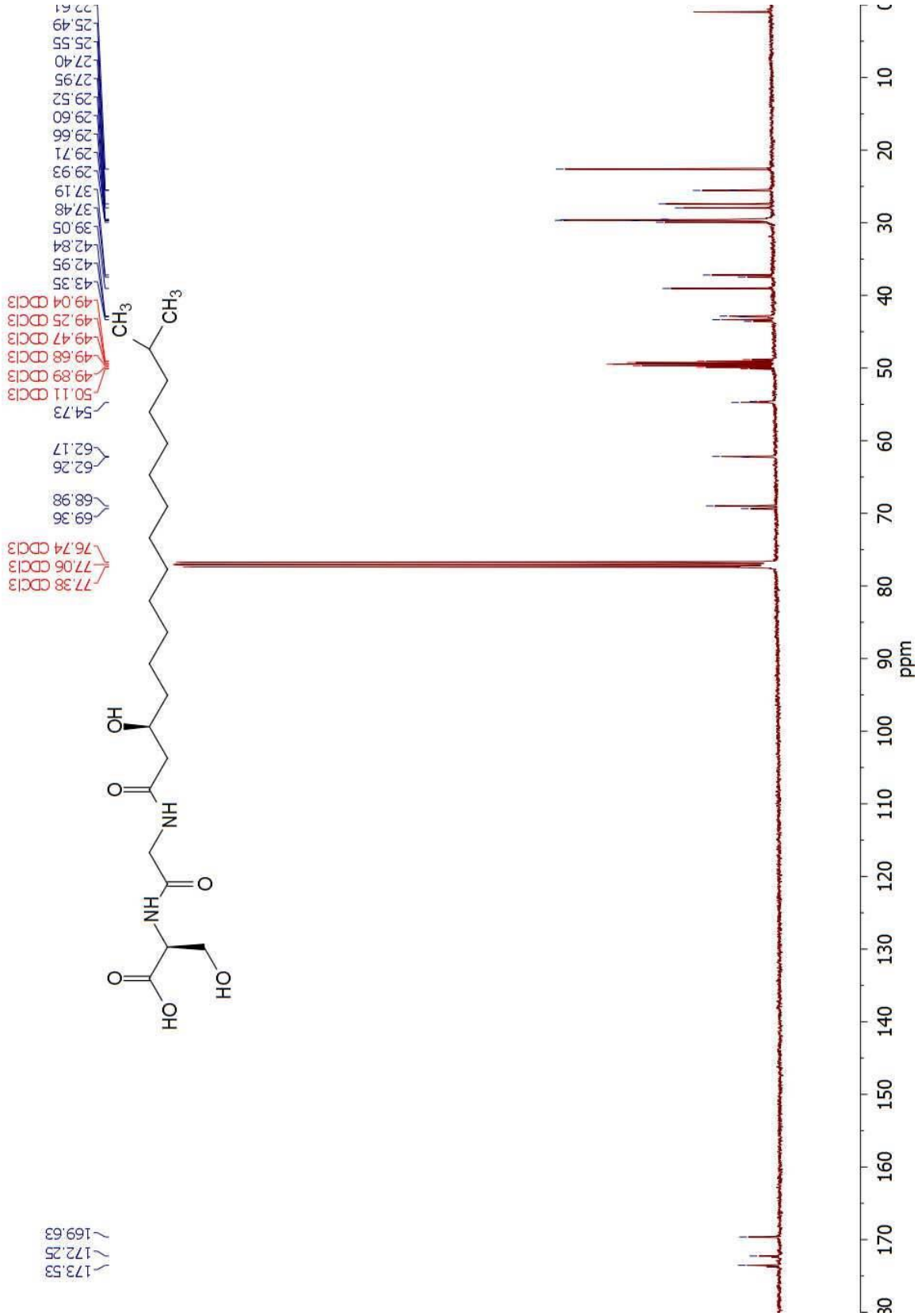
22.61
25.49
25.55
27.40
27.95
29.52
29.60
29.66
29.71
29.93
37.19
37.48
39.05
42.84
42.95
43.35
49.04 CDCl3
49.25 CDCl3
49.47 CDCl3
49.68 CDCl3
49.89 CDCl3
50.11 CDCl3
54.73
62.17
62.26
68.98
69.36
76.74 CDCl3
77.06 CDCl3
77.38 CDCl3
169.63
172.25
173.53
CH3
CH3
OH
O
NH
O
NH
O
HO
O
OH
ppm

CH3
CH3
CH3
O
O
NH
O
NH
O
O
O
O
Si
H3C
CH3
CH3
ppm

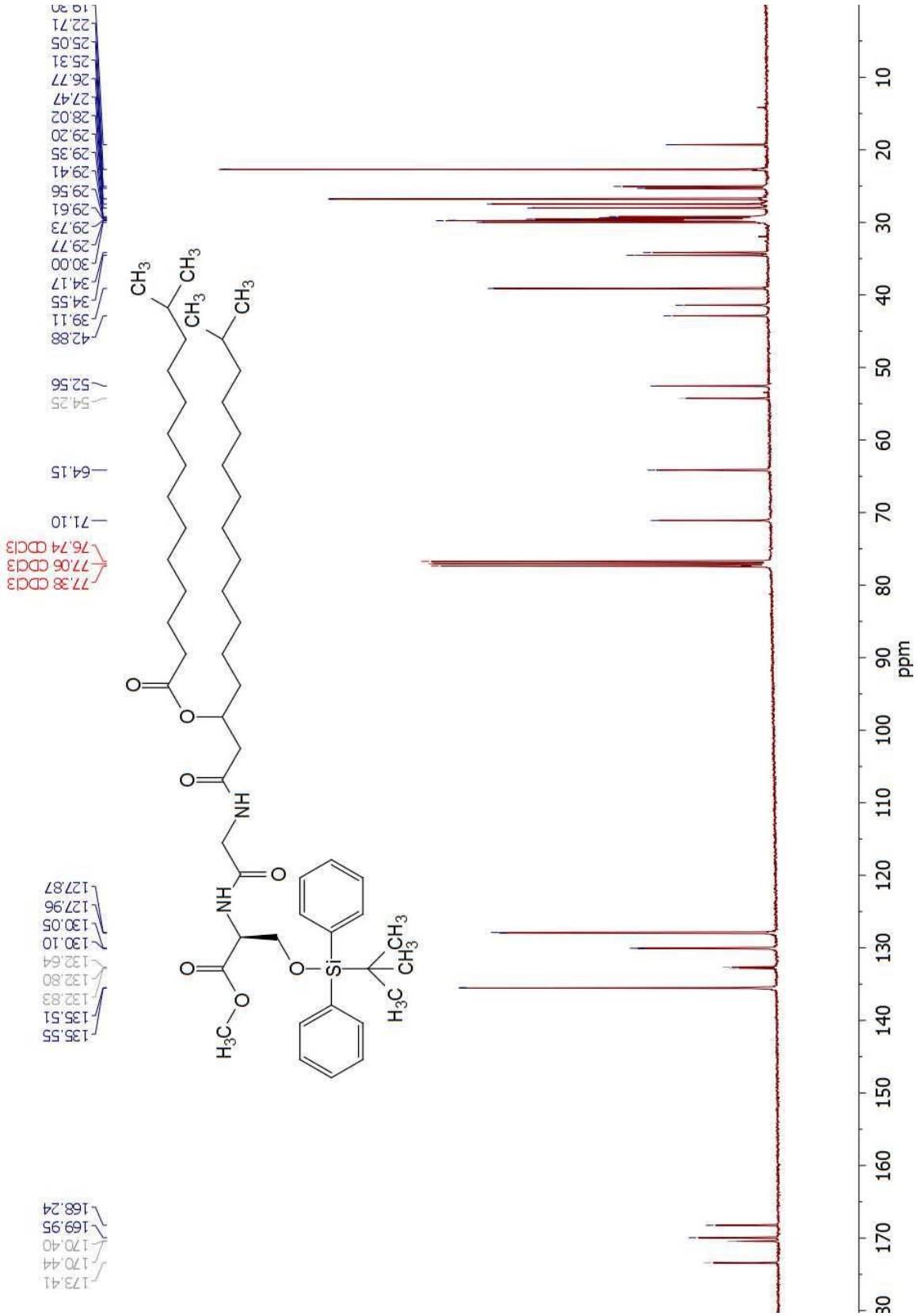
19.30
22.71
25.05
25.31
26.77
27.47
28.02
29.20
29.35
29.41
29.56
29.61
29.73
29.77
30.00
34.17
34.55
39.11
42.88
52.56
54.25
64.15
71.10
76.74 CDCl3
77.06 CDCl3
77.38 CDCl3
127.87
127.96
130.05
130.10
132.64
132.80
132.83
135.51
135.55
168.24
169.95
170.40
170.44
173.41
CH3
CH3
CH3
CH3
O
O
O
NH
NH
O
O
O
O
Si
H3C
CH3
CH3
H3C
ppm
10
20
30
40
50
60
70
80
90
100
110
120
130
140
150
160
170
180

0.07
0.85
0.87
1.03
1.12
1.14
1.15
1.17
1.25
1.46
1.48
1.50
1.51
1.53
1.55
1.56
1.58
1.59
1.61
1.63
2.27
2.29
2.30
2.45
2.47
2.49
2.50
3.74
3.84
3.85
3.88
3.88
3.89
3.90
3.91
3.94
3.95
3.98
3.99
4.11
4.12
4.13
4.14
4.64
4.65
4.65
4.66
4.67
4.67
5.15
5.16
5.18
6.34
6.36
6.37
6.52
6.54
7.26 CDCl3
7.37
7.38
7.39
7.39
7.41
7.41
7.43
7.44
7.46
7.57
7.58
7.60
CH3
CH3
CH3
CH3
O
O
O
NH
NH
O
O
O
O
H3C
Si
H3C
CH3
CH3
12.00
8.99
4.16
36.00
2.15
5.87
2.06
2.06
2.97
3.08
1.07
0.97
1.04
0.99
0.97
5.92
3.93
0.
0.5
1.0
1.5
2.0
2.5
3.0
3.5
4.0
4.5
5.0
5.5
6.0
6.5
7.0
7.5
.0
ppm

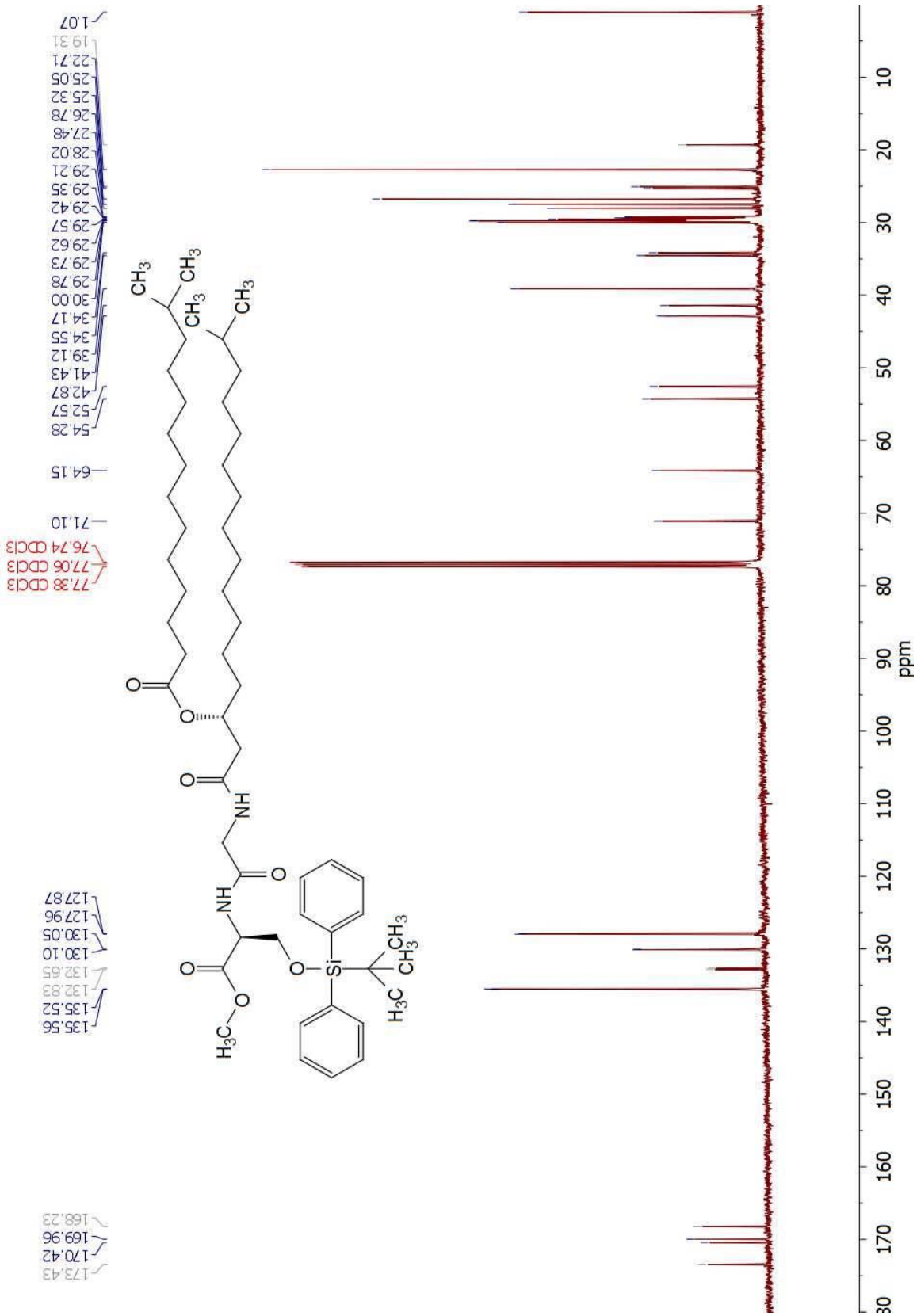
14.07
19.31
22.71
25.05
25.32
26.78
27.48
28.02
29.21
29.35
29.42
29.57
29.62
29.73
29.78
30.00
34.17
34.55
39.12
41.43
42.87
52.57
54.28
64.15
71.10
76.74 CDCl3
77.06 CDCl3
77.38 CDCl3
127.87
127.96
130.05
130.10
132.65
132.83
135.52
135.56
168.23
169.96
170.42
173.43
CH3
CH3
CH3
CH3
O
O
O
NH
NH
O
O
O
O
Si
H3C
CH3
CH3
H3C
ppm

CH3
CH3
CH3
O
O
NH
O
NH
O
O
O
Si
H3C
CH3
CH3
ppm

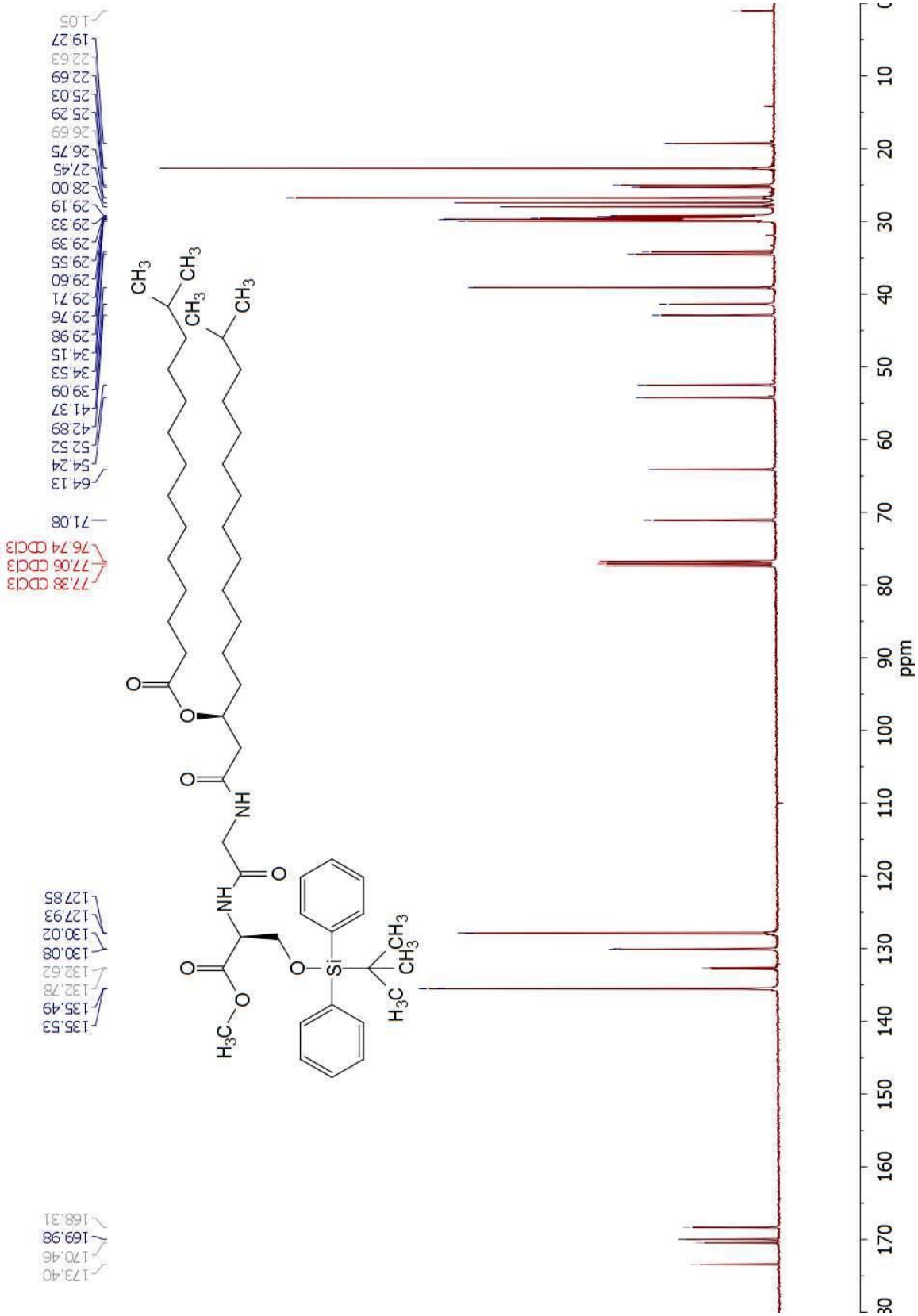
1.05
19.27
22.63
22.69
25.03
25.29
26.69
26.75
27.45
28.00
29.19
29.33
29.39
29.55
29.60
29.71
29.76
29.98
34.15
34.53
39.09
41.37
42.89
52.52
54.24
64.13
71.08
76.74 CDCl3
77.06 CDCl3
77.38 CDCl3
127.85
127.93
130.02
130.08
132.62
132.78
135.49
135.53
173.40
170.46
169.98
168.31
CH3
CH3
CH3
CH3
O
O
O
NH
NH
O
O
O
O
Si
H3C
CH3
CH3
H3C
ppm

CH3
CH3
CH3
CH3
O
O
NH
O
NH
O
O
O
H3C
HO
0.87
1.12
1.13
1.15
1.17
1.25
1.26
1.28
1.30
1.46
1.48
1.49
1.51
1.53
1.54
1.57
1.59
1.61
2.28
2.28
2.30
2.32
2.32
2.48
2.49
3.77
3.78
3.90
3.92
3.93
3.95
3.98
3.99
4.00
4.01
4.03
4.05
4.63
4.63
4.64
4.65
4.66
4.67
5.13
5.15
5.16
5.18
5.19
5.21
5.22
5.24
6.66
6.67
6.69
6.70
6.71
7.23
7.25
7.26 CDCl3
7.30
7.32
0.51
1.09
0.96
1.03
0.98
4.06
2.98
1.93
2.07
3.95
2.08
34.96
4.10
11.70
ppm

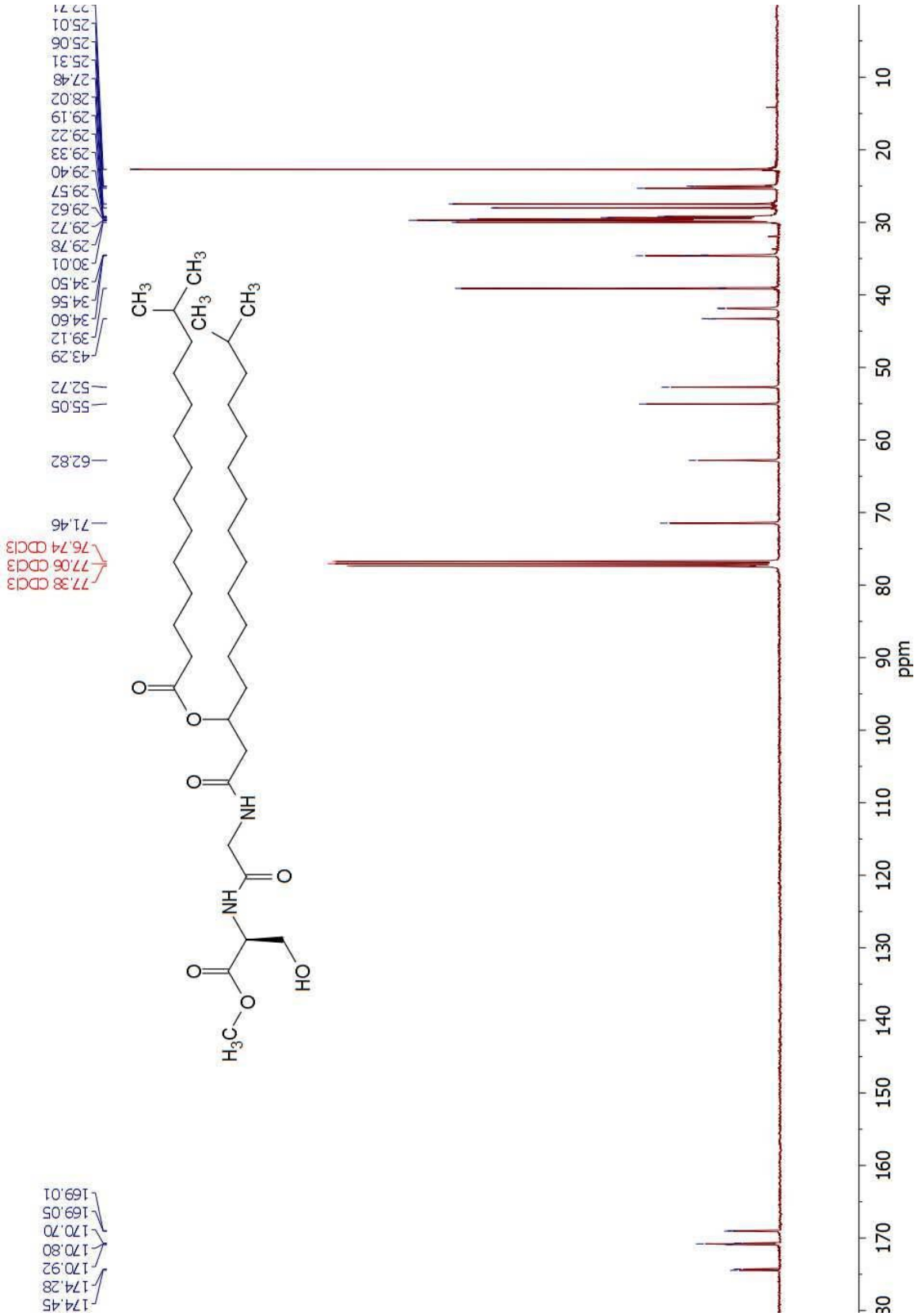
22.71
25.01
25.06
25.31
27.48
28.02
29.19
29.22
29.33
29.40
29.57
29.62
29.72
29.78
30.01
34.50
34.56
34.60
39.12
43.29
52.72
55.05
62.82
71.46
76.74 CDCl3
77.06 CDCl3
77.38 CDCl3
169.01
169.05
170.70
170.80
170.92
174.28
174.45
CH3
CH3
CH3
O
O
NH
O
NH
O
O
O
HO
H3C
ppm

7.26 CDCl3
7.13
7.11
6.46
6.45
6.44
5.22
5.21
5.19
5.18
4.69
4.68
4.67
4.66
4.65
4.11
4.09
4.07
4.05
4.01
4.00
3.98
3.95
3.94
3.91
3.90
3.79
3.30
3.28
3.26
2.49
2.48
2.33
2.31
2.30
1.60
1.53
1.51
1.50
1.25
1.17
1.16
1.14
1.12
0.87
0.85
CH3
CH3
CH3
CH3
O
O
O
NH
NH
O
O
O
O
H3C
HO
12.00
4.07
34.87
10.16
2.08
1.97
0.97
2.91
2.27
2.15
1.09
1.16
1.02
0.97
ppm

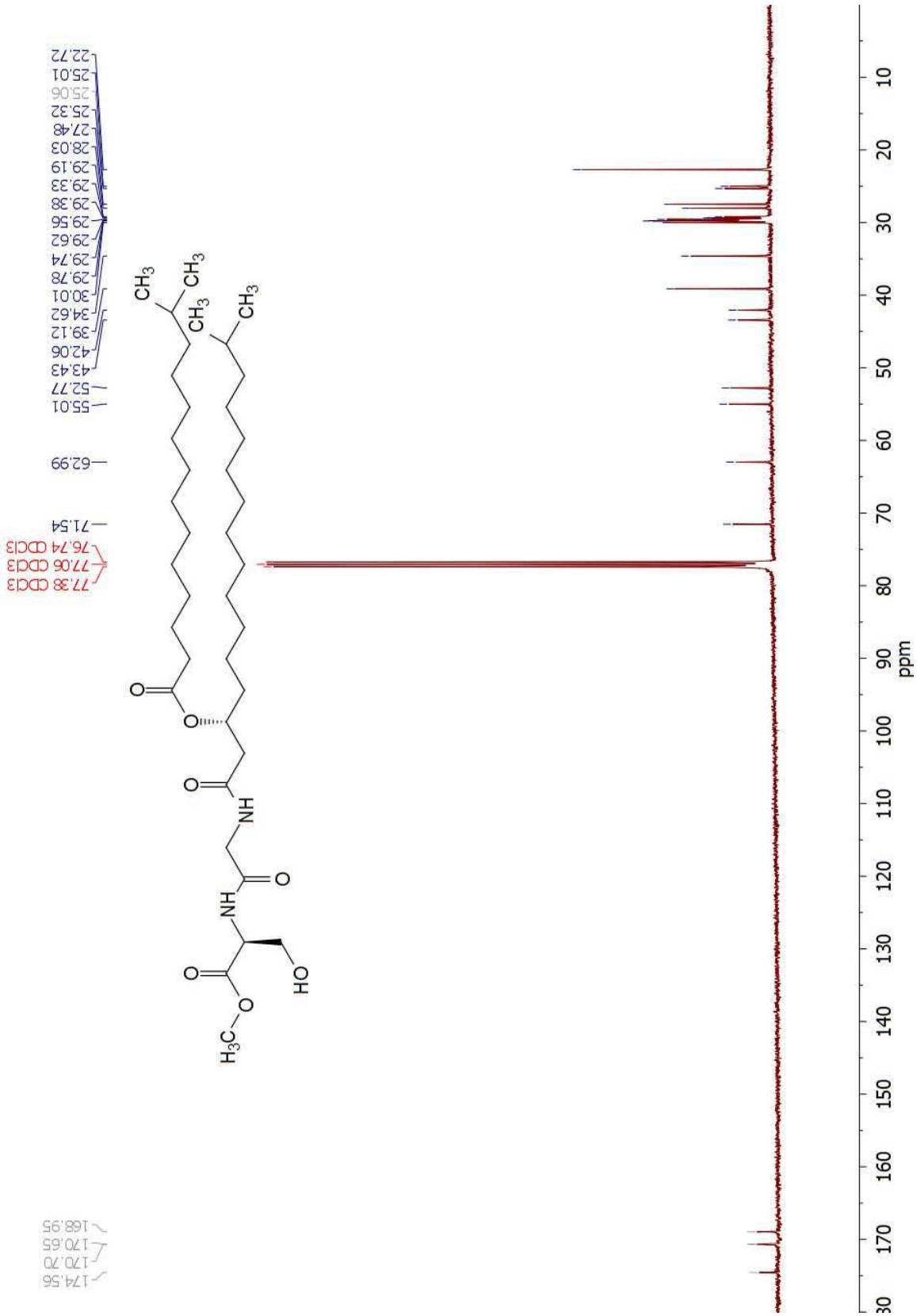
22.72
25.01
25.06
25.32
27.48
28.03
29.19
29.33
29.38
29.56
29.62
29.74
29.78
30.01
34.62
39.12
42.06
43.43
52.77
55.01
62.99
71.54
76.74 CDCl3
77.06 CDCl3
77.38 CDCl3
174.56
170.70
170.65
168.95
CH3
CH3
CH3
CH3
O
O
O
NH
NH
O
O
O
O
H3C
HO
ppm

7.26 CDCl3
7.06
7.04
6.50
6.49
6.48
5.19
5.18
5.16
5.16
5.14
4.68
4.67
4.66
4.65
4.64
4.63
4.06
4.04
4.00
3.98
3.97
3.95
3.92
3.79
3.78
3.21
2.50
2.49
2.33
2.31
2.29
1.62
1.60
1.58
1.56
1.53
1.51
1.50
1.48
1.46
1.25
1.17
1.15
1.14
1.12
0.87
0.85
CH3
CH3
CH3
CH3
O
O
NH
O
NH
O
O
O
O
H3C
HO
11.25
4.11
35.58
9.87
1.98
1.97
0.95
3.00
4.45
1.01
1.16
0.92
1.02
ppm

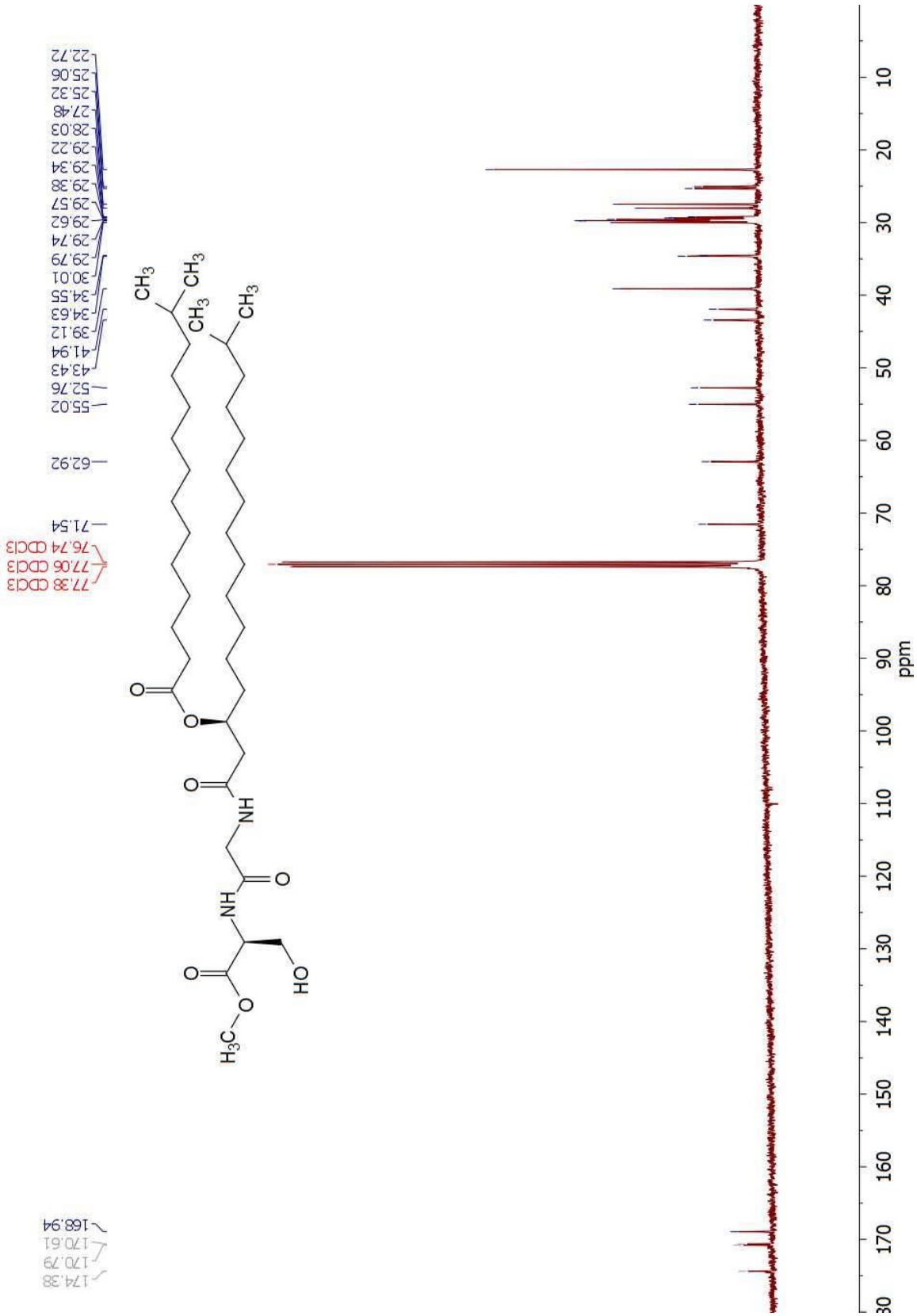
22.72
25.06
25.32
27.48
28.03
29.22
29.34
29.38
29.57
29.62
29.74
29.79
30.01
34.55
34.63
39.12
41.94
43.43
52.76
55.02
62.92
71.54
76.74 CDCl3
77.06 CDCl3
77.38 CDCl3
168.94
170.61
170.79
174.38
CH3
CH3
CH3
CH3
O
O
O
NH
O
NH
O
O
O
H3C
HO
ppm

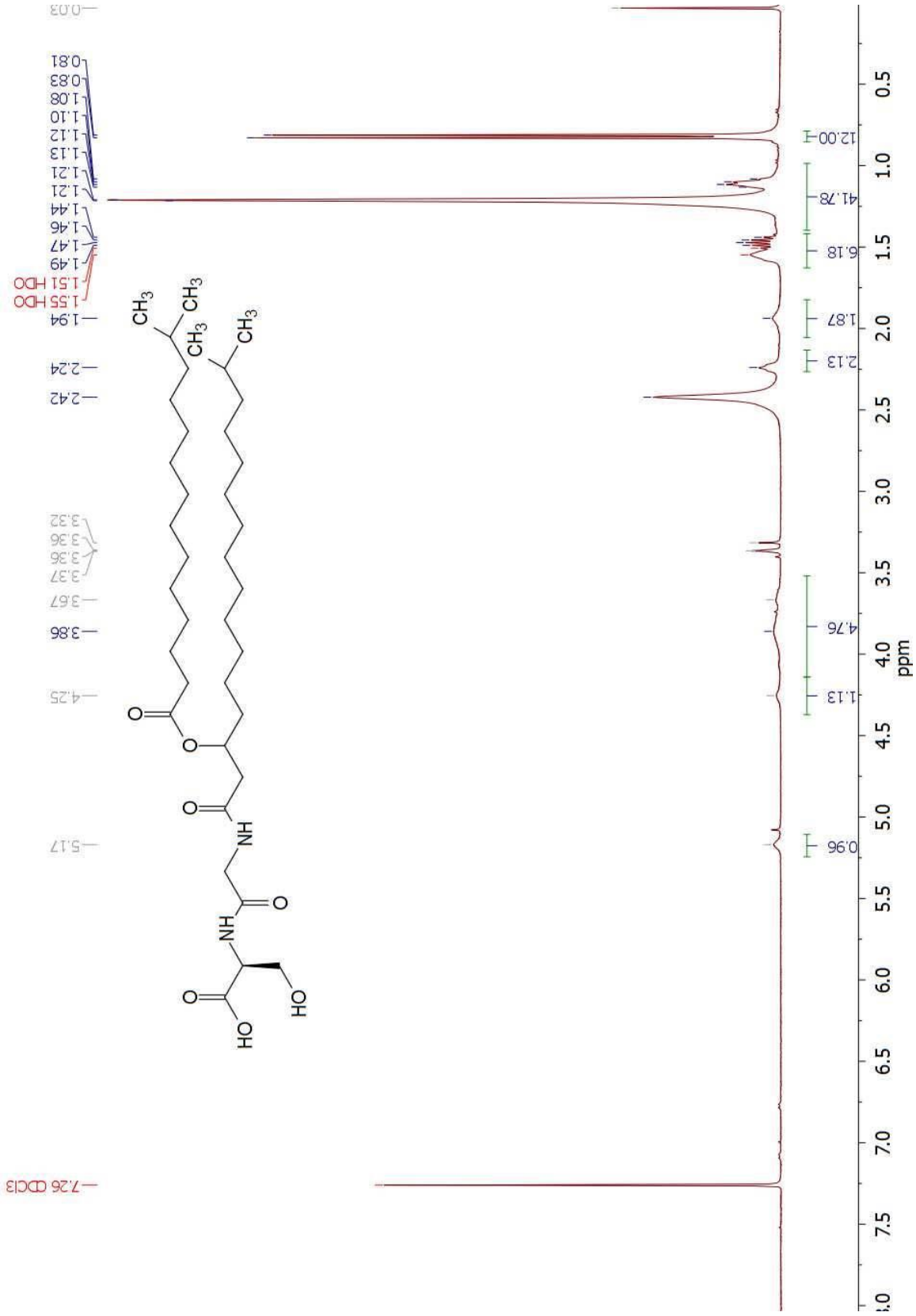
7.26 CDCl3
5.17
4.25
3.86
3.67
3.37
3.36
3.36
3.32
2.42
2.24
1.94
1.55 HDO
1.51 HDO
1.49
1.47
1.46
1.44
1.21
1.21
1.13
1.12
1.10
1.08
0.83
0.81
0.03
CH3
CH3
CH3
O
O
O
NH
NH
O
O
HO
HO
12.00
41.78
6.18
1.87
2.13
4.76
1.13
0.96
ppm

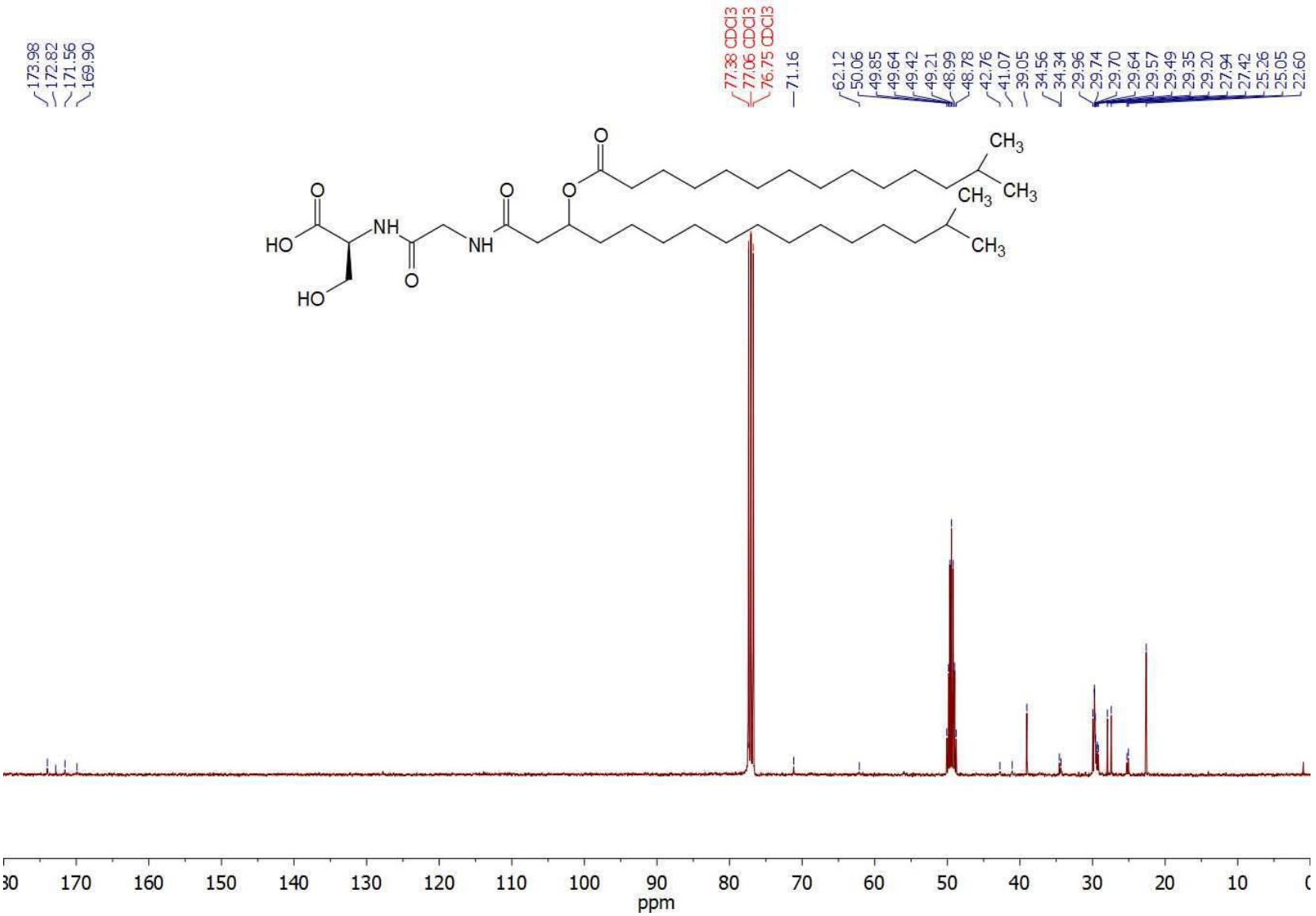
173.98
172.82
171.56
169.90
77.38 CDCl3
77.06 CDCl3
76.75 CDCl3
71.16
62.12
50.06
49.85
49.64
49.42
49.21
48.99
48.78
42.76
41.07
39.05
34.56
34.34
29.96
29.74
29.70
29.64
29.57
29.49
29.35
29.20
27.94
27.42
25.26
25.05
22.60
HO
O
NH
O
NH
O
O
O
CH3
CH3
CH3
CH3
HO
170
160
150
140
130
120
110
100
90
80
70
60
50
40
30
20
10
ppm

0.02
0.80
0.82
1.07
1.09
1.11
1.12
1.20
1.41
1.43
1.45
1.46
1.48
1.50
1.51
1.54
2.22
2.24
2.25
2.47
2.90
3.71
3.85
4.31
5.13
5.15
5.16
7.26 CDCl3
12.00
39.82
6.61
2.05
1.97
4.03
0.73
0.82
ppm
CH3
CH3
CH3
O
O
O
NH
NH
O
O
HO
HO

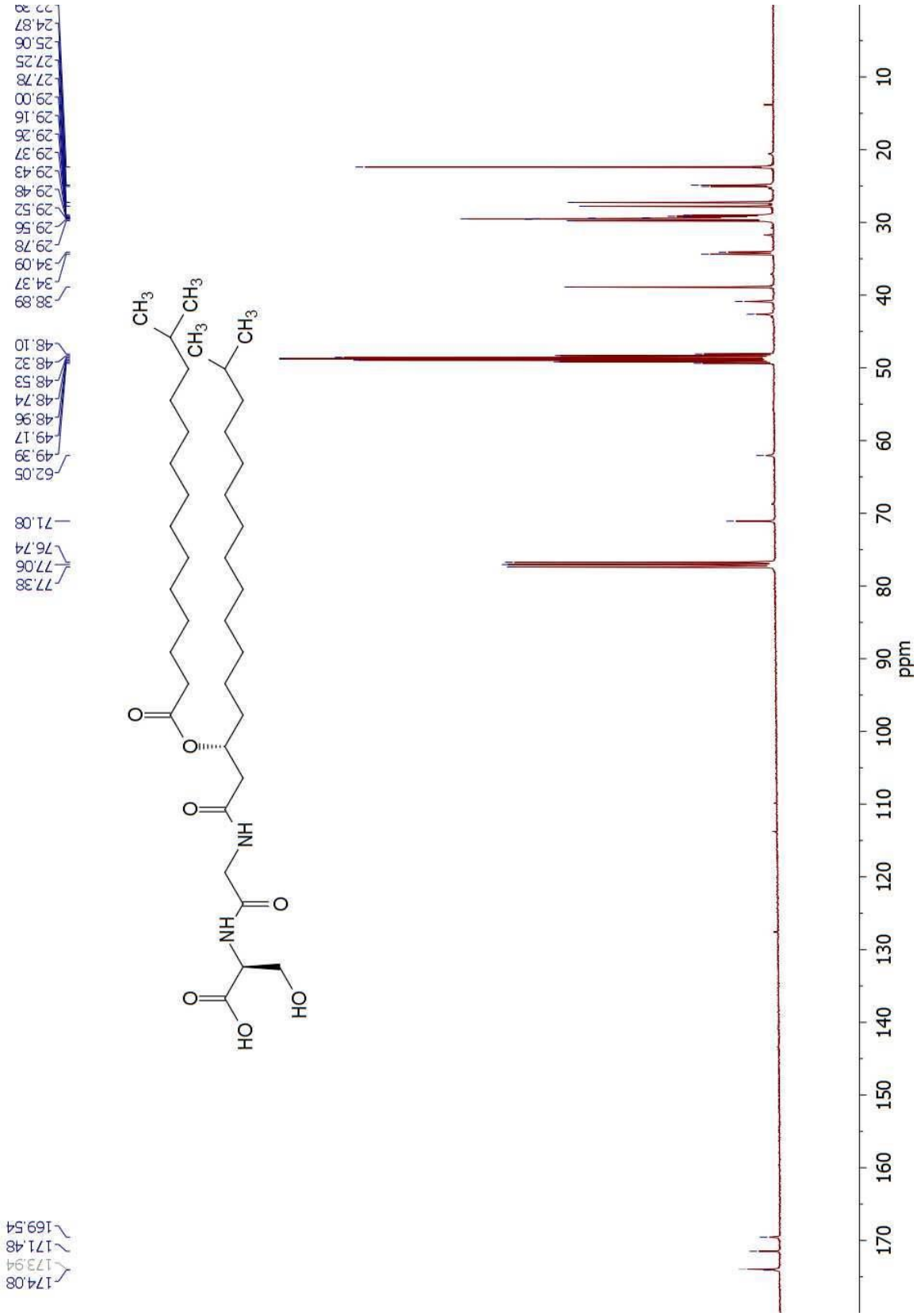
174.08
173.94
171.48
169.54
77.38
77.06
76.74
71.08
62.05
49.39
49.17
48.96
48.74
48.53
48.32
48.10
38.89
34.37
34.09
29.78
29.56
29.52
29.48
29.43
29.37
29.26
29.16
29.00
27.78
27.25
25.06
24.87
CH3
CH3
CH3
O
O
O
NH
NH
O
O
HO
OH
10
20
30
40
50
60
70
80
90
ppm
100
110
120
130
140
150
160
170

7.26 CDCl3
5.16
4.29
3.89
3.84
3.79
3.70
2.84
2.48
2.46
2.44
2.25
2.23
2.21
1.54
1.50
1.48
1.46
1.45
1.43
1.26
1.23
1.20
1.11
1.09
1.07
0.82
0.80
CH3
CH3
CH3
O
O
O
NH
NH
O
O
HO
HO
12.00
39.23
6.07
2.05
1.87
4.25
1.04
0.97
ppm

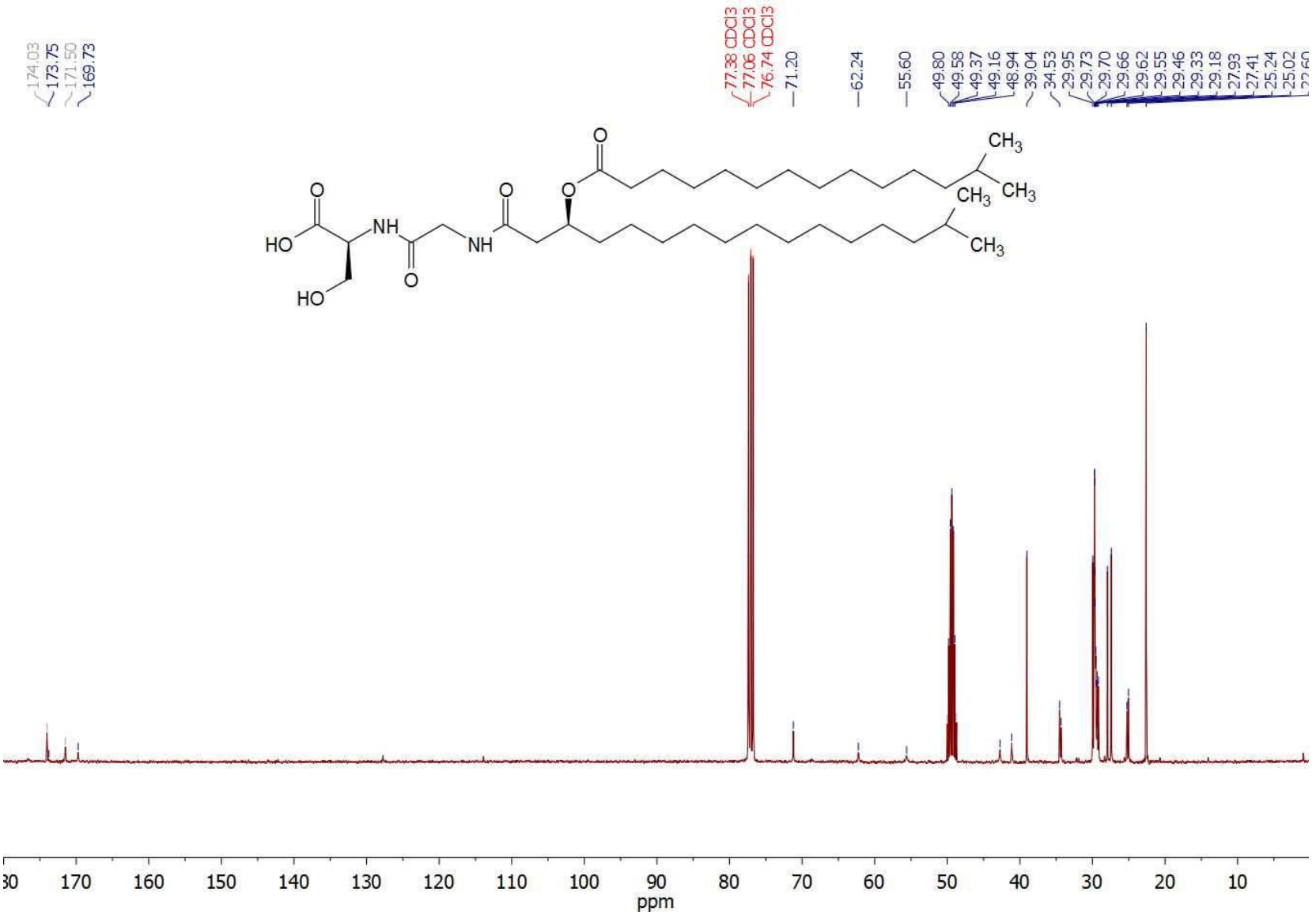
174.03
173.75
171.50
169.73
77.38 CDCl3
77.06 CDCl3
76.74 CDCl3
71.20
62.24
55.60
49.80
49.58
49.37
49.16
48.94
39.04
34.53
29.95
29.73
29.70
29.66
29.62
29.55
29.46
29.33
29.18
27.93
27.41
25.24
25.02
HO
NH
NH
O
O
O
O
O
HO
CH3
CH3
CH3
CH3
170
160
150
140
130
120
110
100
90
80
70
60
50
40
30
20
10
ppm

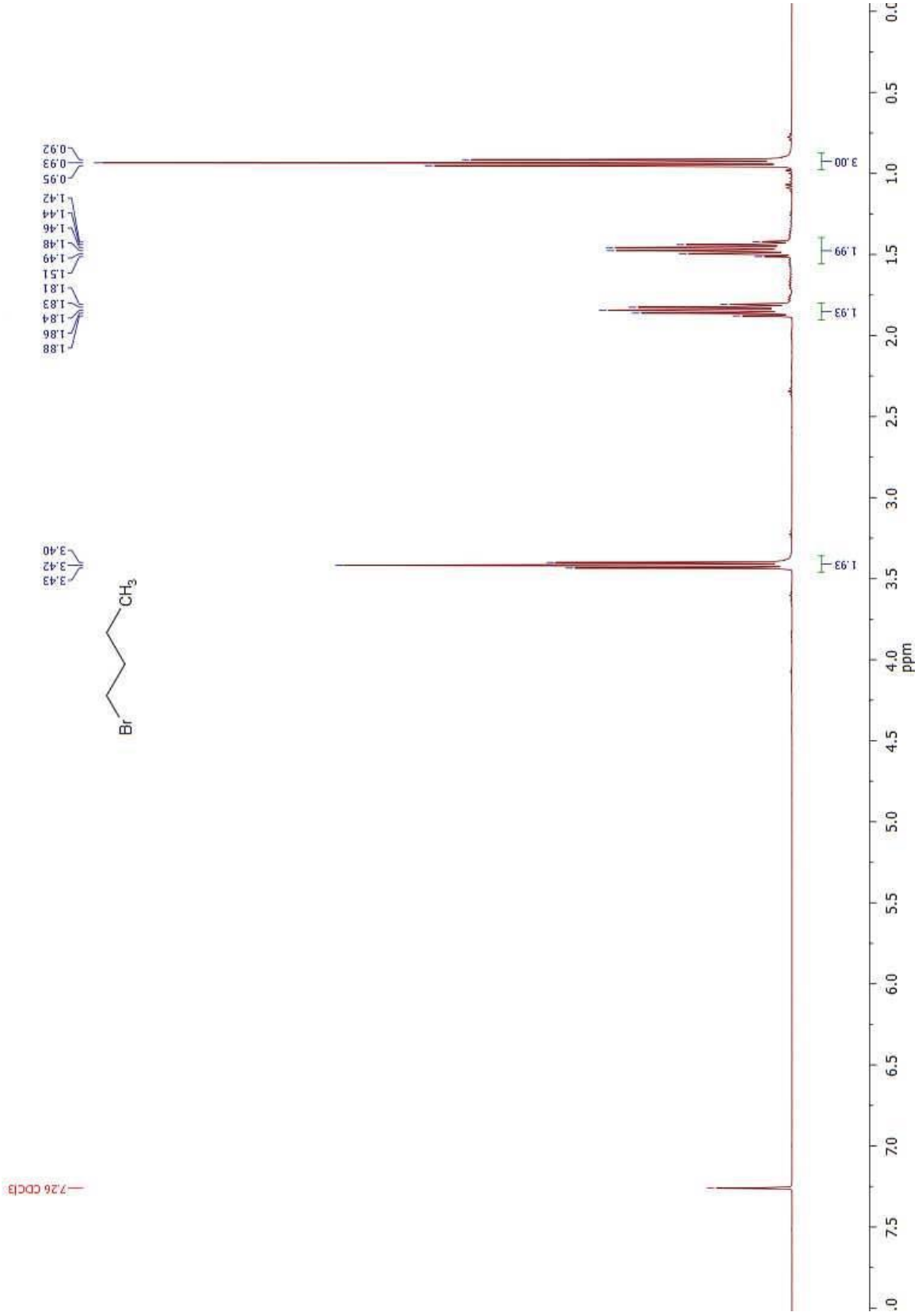
7.26 CDCl3
3.43
3.42
3.40
1.88
1.86
1.84
1.83
1.81
1.51
1.49
1.48
1.46
1.44
1.42
0.95
0.93
0.92
3.00
1.99
1.93
1.93
Br
CH3
ppm

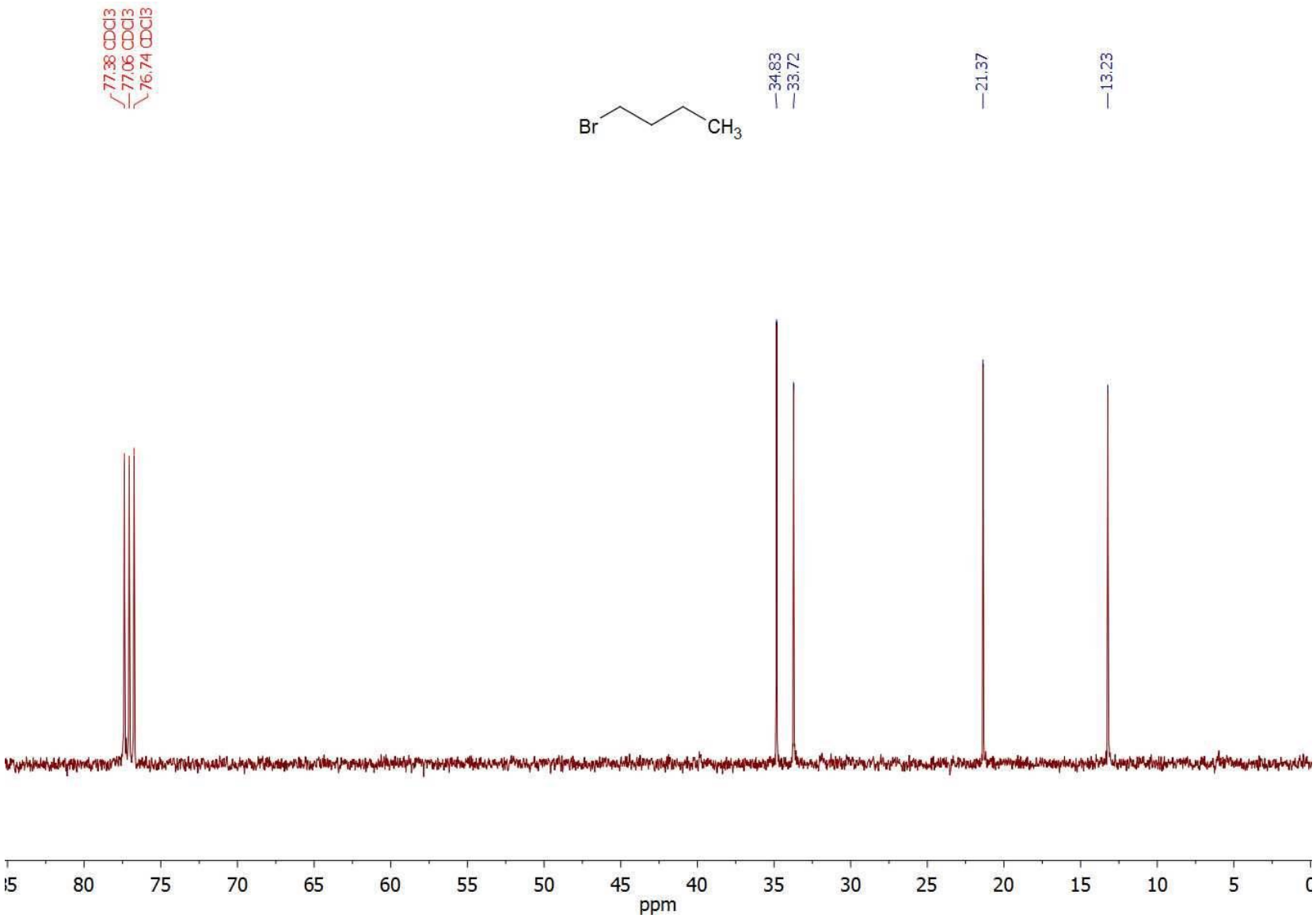
77.38 CDCl3
77.06 CDCl3
76.74 CDCl3
34.83
33.72
21.37
13.23
Br
CH3
80
75
70
65
60
55
50
45
40
35
30
25
20
15
10
5
ppm

7.26 CDCl3
0.05
0.90
1.28
1.40
1.42
1.44
1.47
1.49
1.51
1.52
1.54
1.82
1.83
1.85
1.87
1.89
3.39
3.41
3.42
3.58
3.60
3.61
Br
O
Si
CH3
H3C
H3C
CH3
H3C
5.97
9.08
12.10
1.98
2.05
1.96
1.97
2.00
ppm

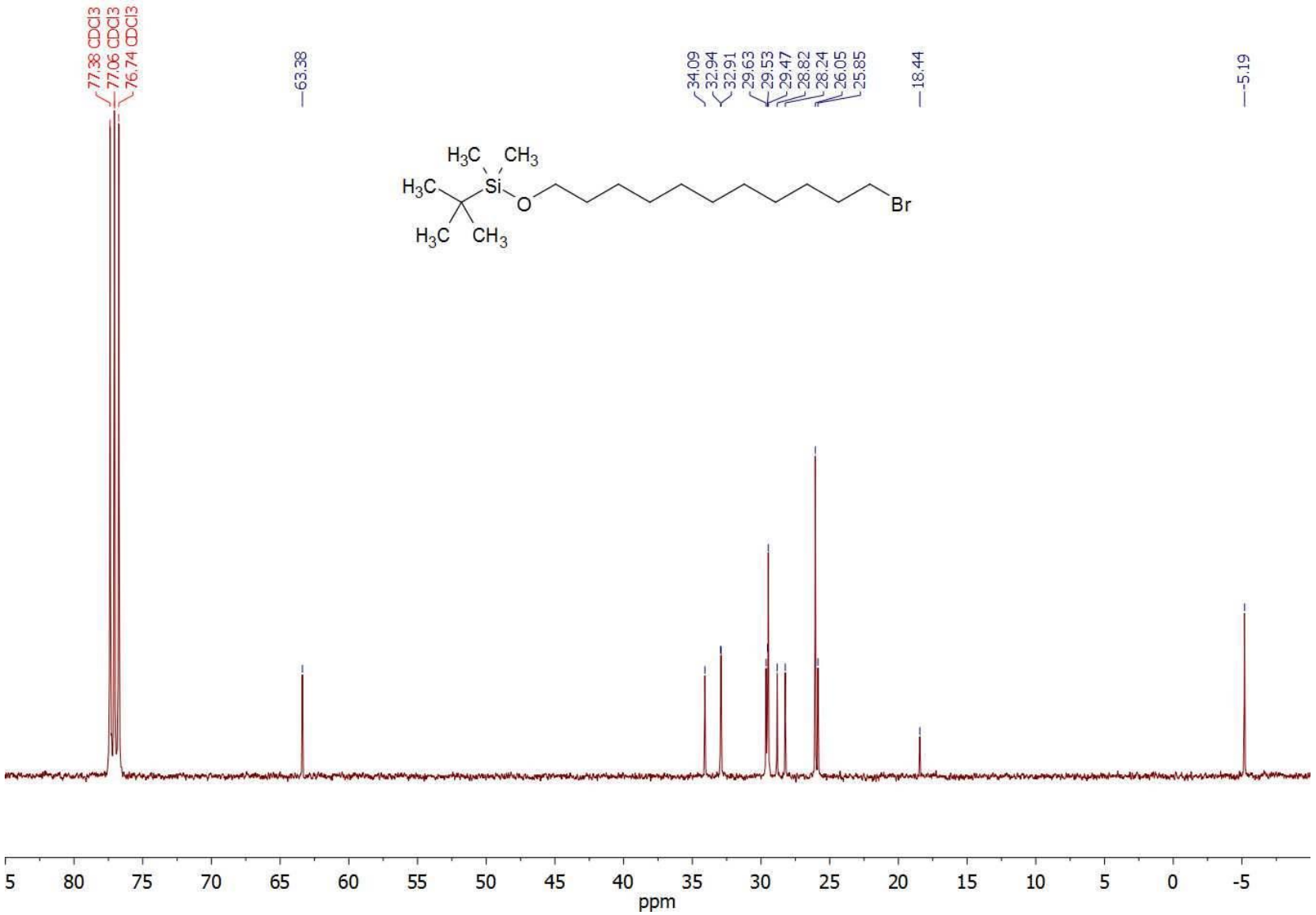
77.38 CDCl3
77.06 CDCl3
76.74 CDCl3
63.38
34.09
32.94
32.91
29.63
29.53
29.47
28.82
28.24
26.05
25.85
18.44
-5.19
H3C
CH3
Si
O
Br
ppm

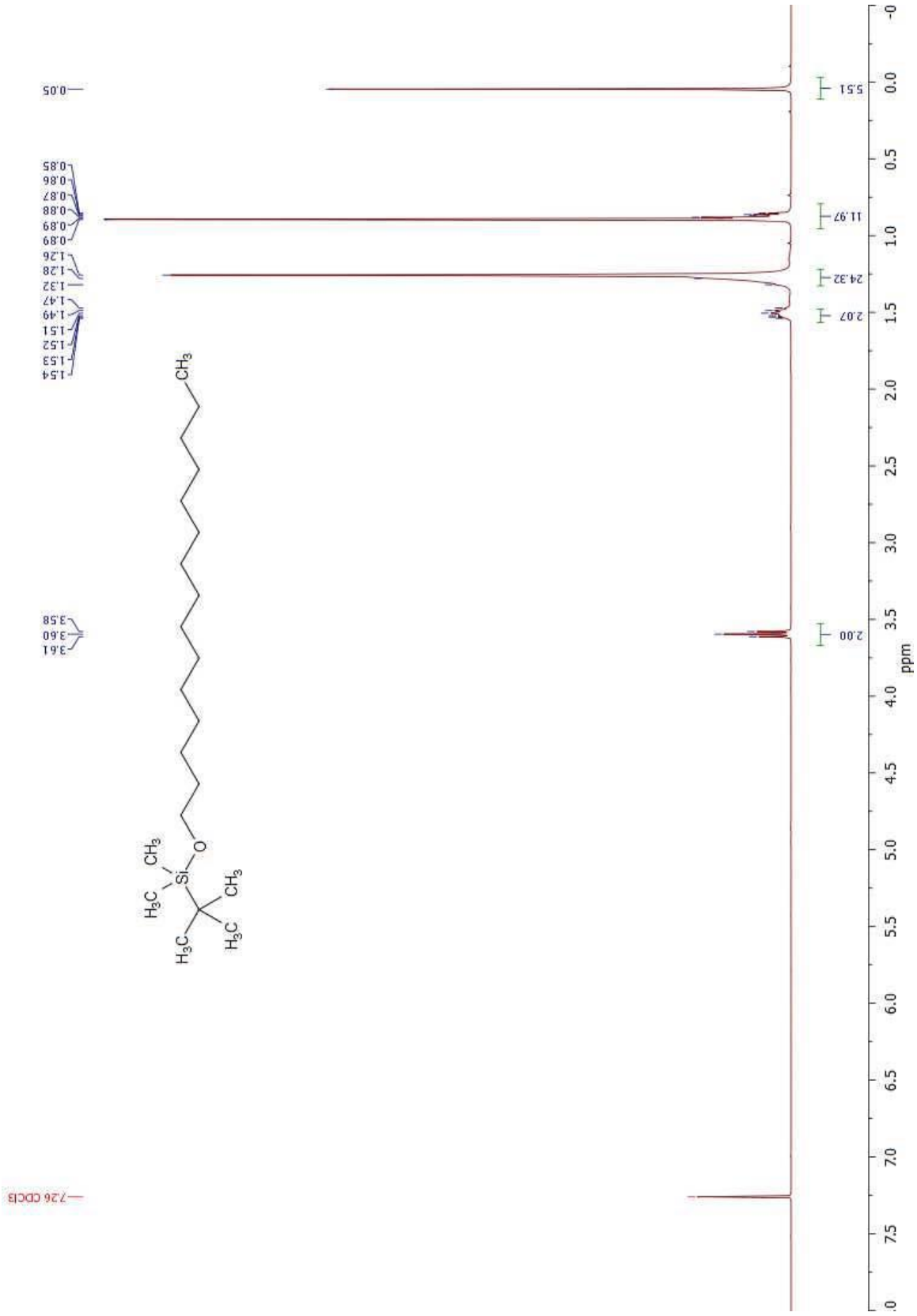
0.05
0.85
0.86
0.87
0.88
0.89
0.89
1.26
1.28
1.32
1.47
1.49
1.51
1.52
1.53
1.54
3.58
3.60
3.61
7.26 CDCl3
5.51
11.97
24.32
2.07
2.00
ppm
CH3
H3C
Si
O
CH3
H3C
CH3

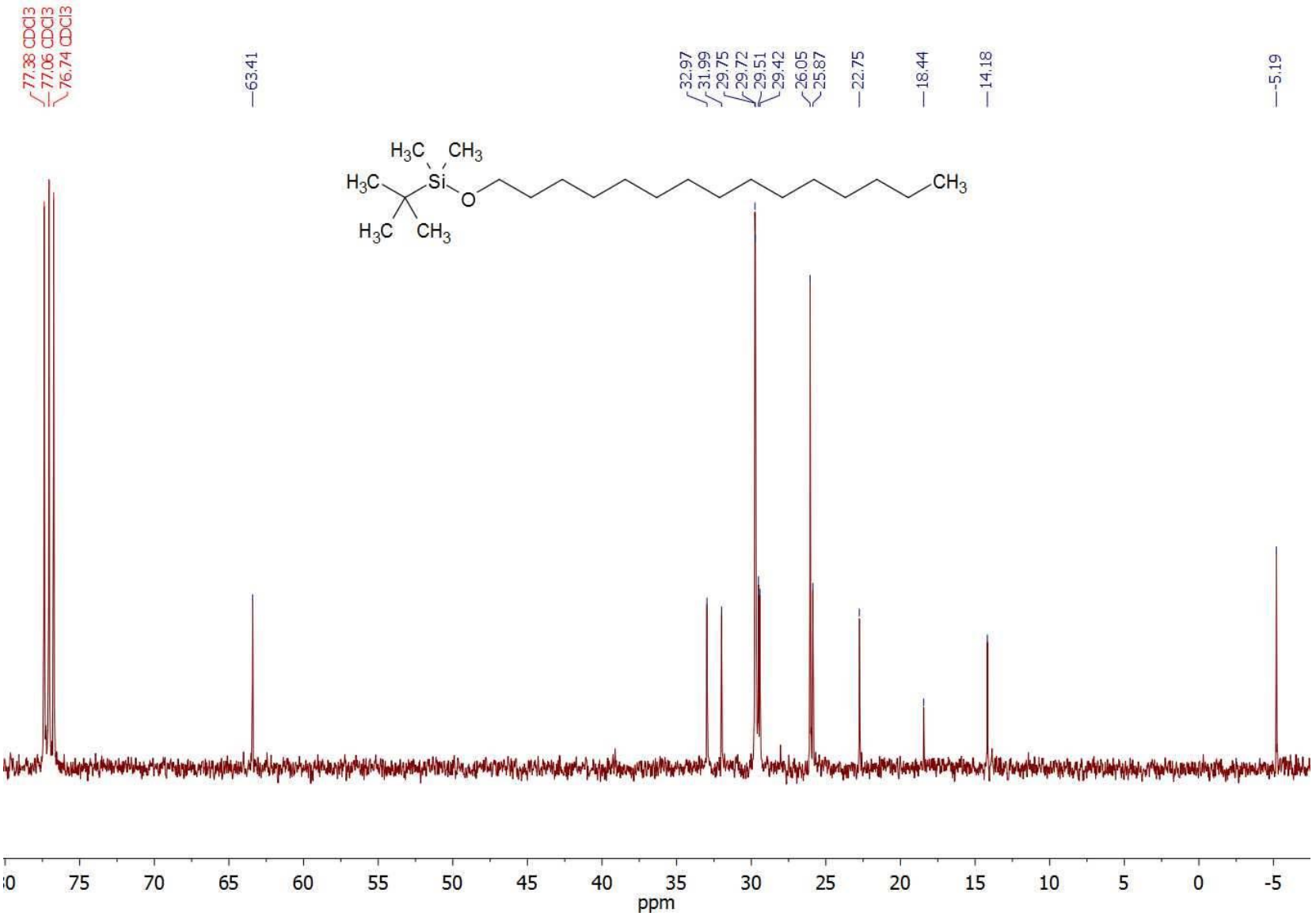
77.38 CDCl3
77.06 CDCl3
76.74 CDCl3
63.41
32.97
31.99
29.75
29.72
29.51
29.42
26.05
25.87
22.75
18.44
14.18
-5.19
H3C
CH3
H3C
Si
O
CH3
H3C
CH3
ppm

7.26 CDCl3
3.61
3.60
3.58
1.55 HDO
1.52
1.51
1.49
1.28
1.25
0.89
0.05
6.00
9.07
18.04
2.02
2.04
ppm
0.0
0.5
1.0
1.5
2.0
2.5
3.0
3.5
4.0
4.5
5.0
5.5
6.0
6.5
7.0
7.5
D
D
D
D
D
D
D
D
D
H3C
CH3
Si
O
H3C
CH3
H3C

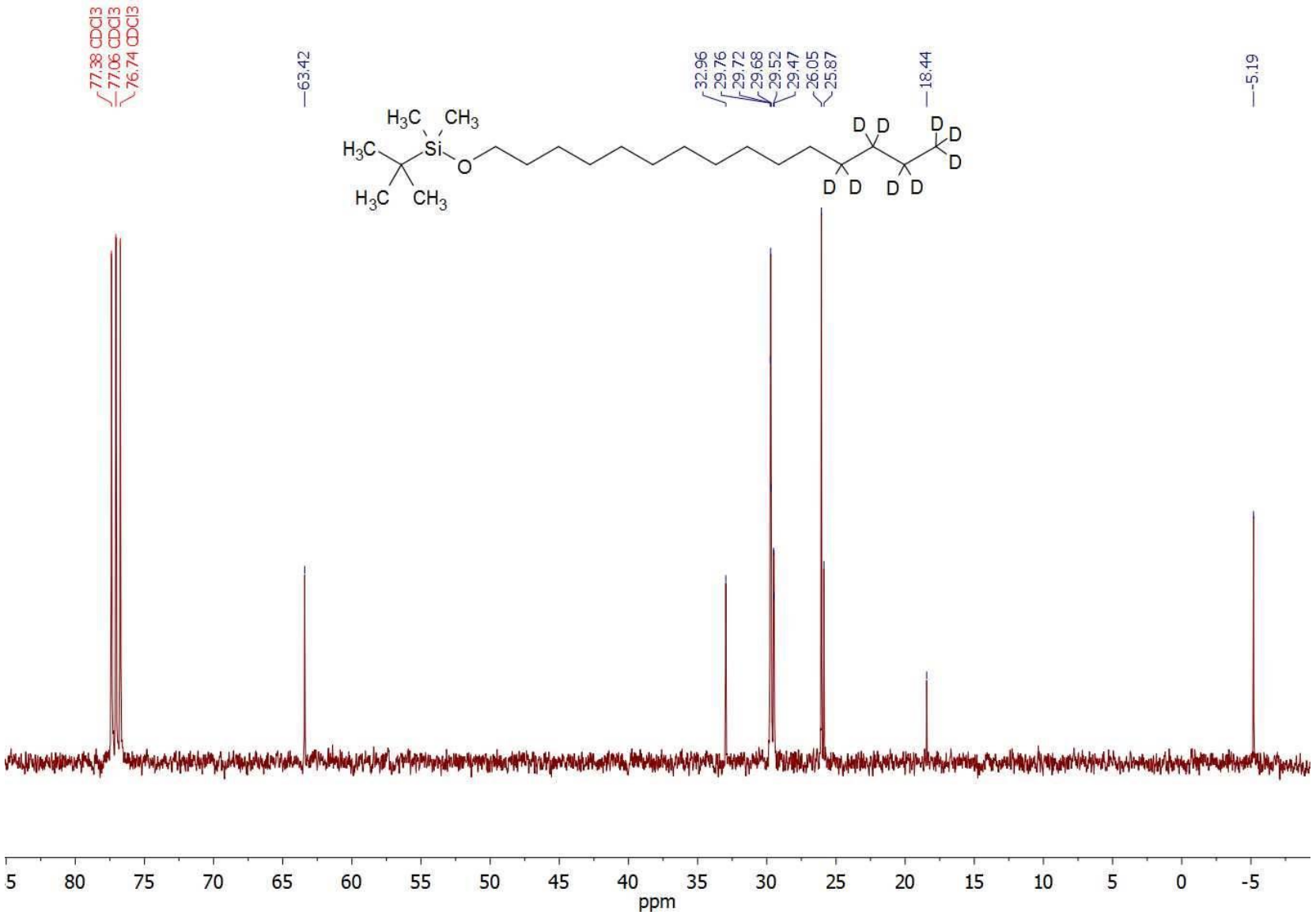
77.38 CDCl3
77.06 CDCl3
76.74 CDCl3
63.42
32.96
29.76
29.72
29.68
29.52
29.47
26.05
25.87
18.44
-5.19
H3C
CH3
H3C
Si
O
H3C
CH3
D
D
D
D
D
D
D
D
D
D
5
80
75
70
65
60
55
50
45
40
35
30
25
20
15
10
5
0
-5
ppm

7.26 CDCl3
3.66
3.64
3.62
1.60
1.58
1.57
1.56
1.55
1.53
1.37
1.34
1.32
1.30
1.26
0.90
0.88
0.86
HO
CH3
2.00
25.08
2.29
3.09
ppm

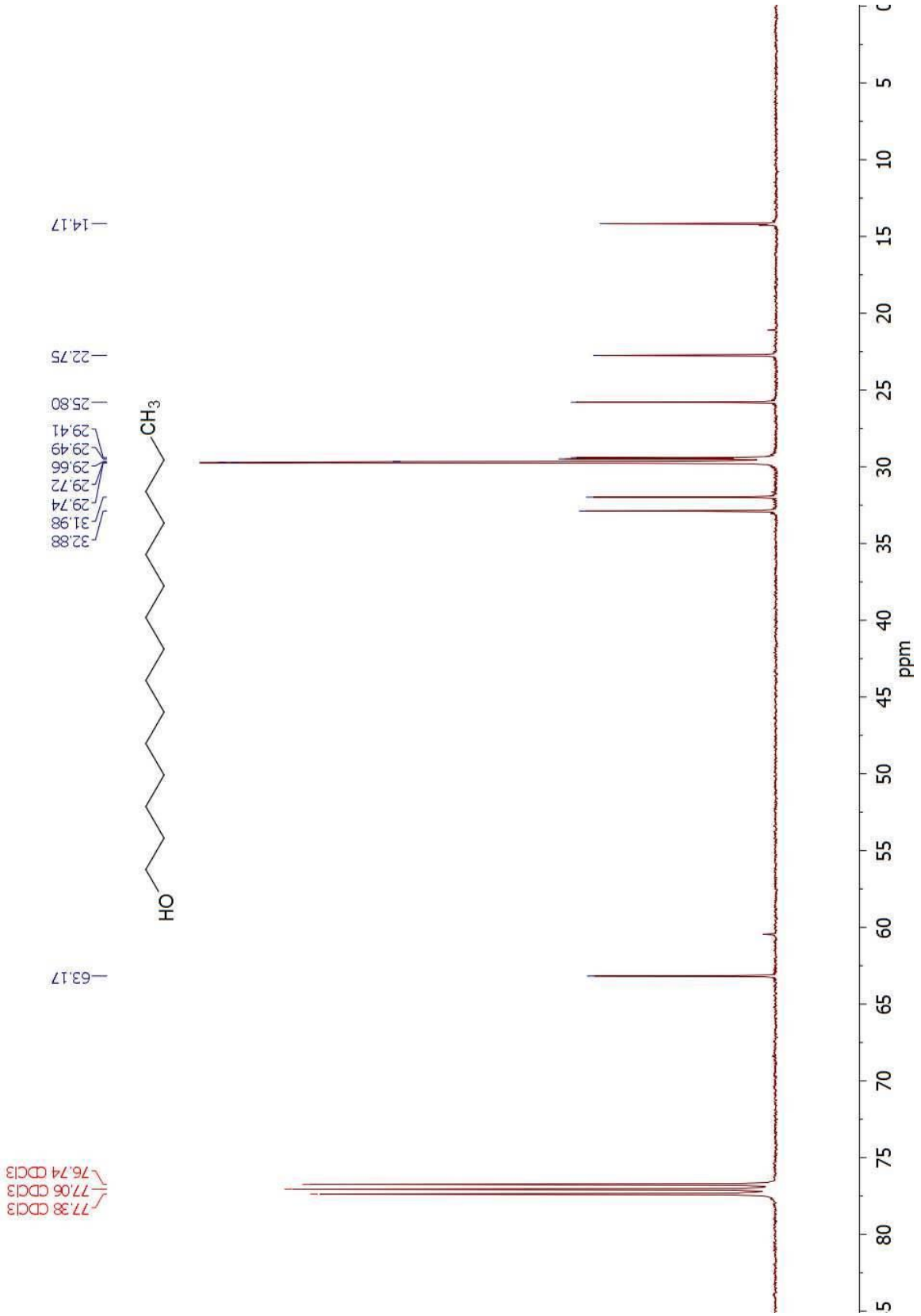
77.38 CDCl3
77.06 CDCl3
76.74 CDCl3
63.17
32.88
31.98
29.74
29.72
29.66
29.49
29.41
25.80
22.75
14.17
HO
CH3
ppm

7.26 CDCl3
5.30
3.66
3.64
3.62
1.60
1.58
1.57
1.55
1.53
1.36
1.34
1.33
1.32
1.28
1.25
19.11
2.16
2.00
HO
D
D
D
D
D
D
D
D
ppm

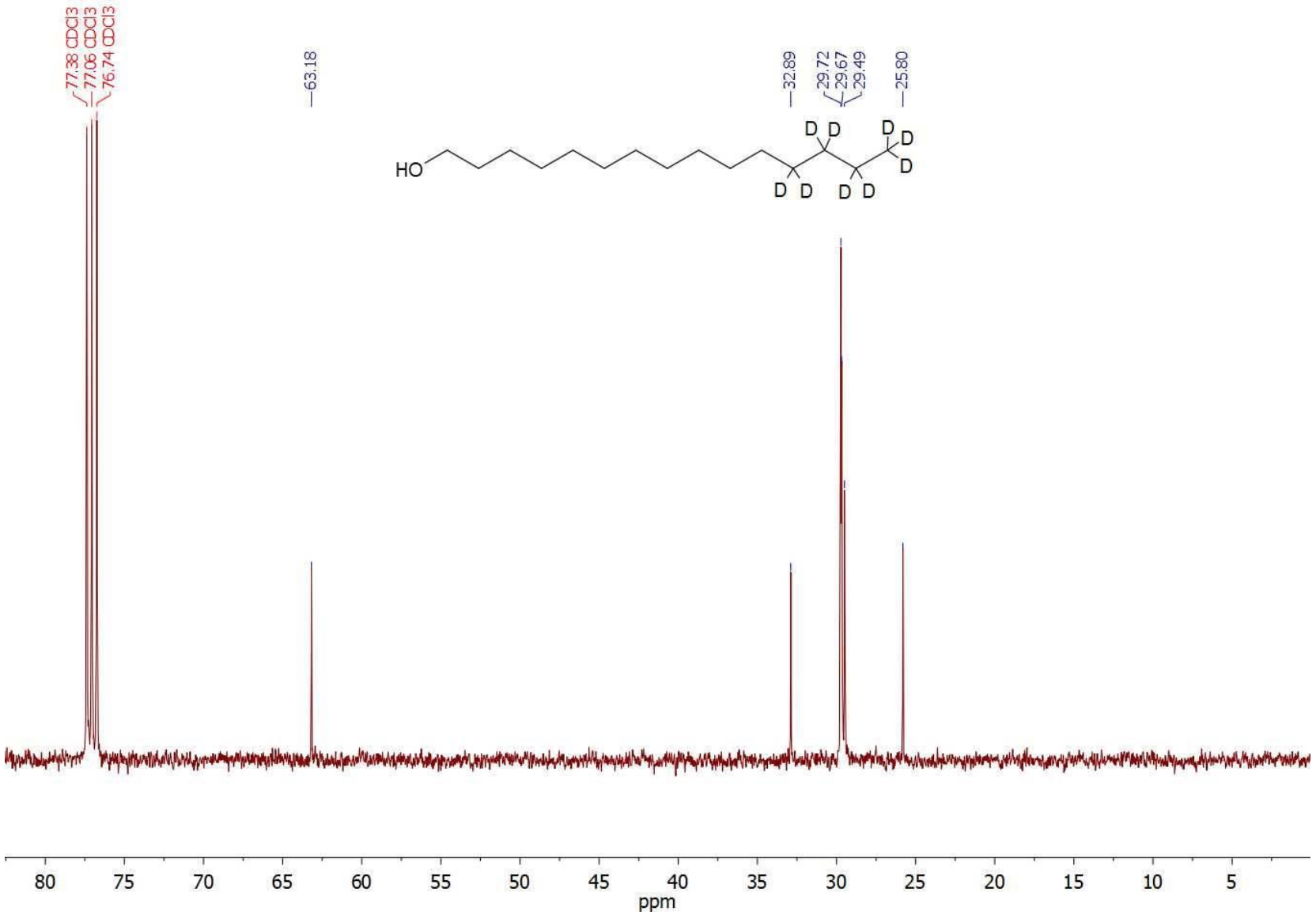
77.38 CDCl3
77.06 CDCl3
76.74 CDCl3
63.18
32.89
29.72
29.67
29.49
25.80
HO
D D
D D
D D
D D
D
ppm
80
75
70
65
60
55
50
45
40
35
30
25
20
15
10
5

9.77
9.76
9.76
7.26 CDCl3
2.44
2.43
2.42
2.41
2.40
2.39
1.66
1.64
1.63
1.61
1.59
1.55
1.34
1.30
1.26
0.90
0.88
0.86
CH3
O
0.95
2.00
21.99
2.01
2.98
ppm

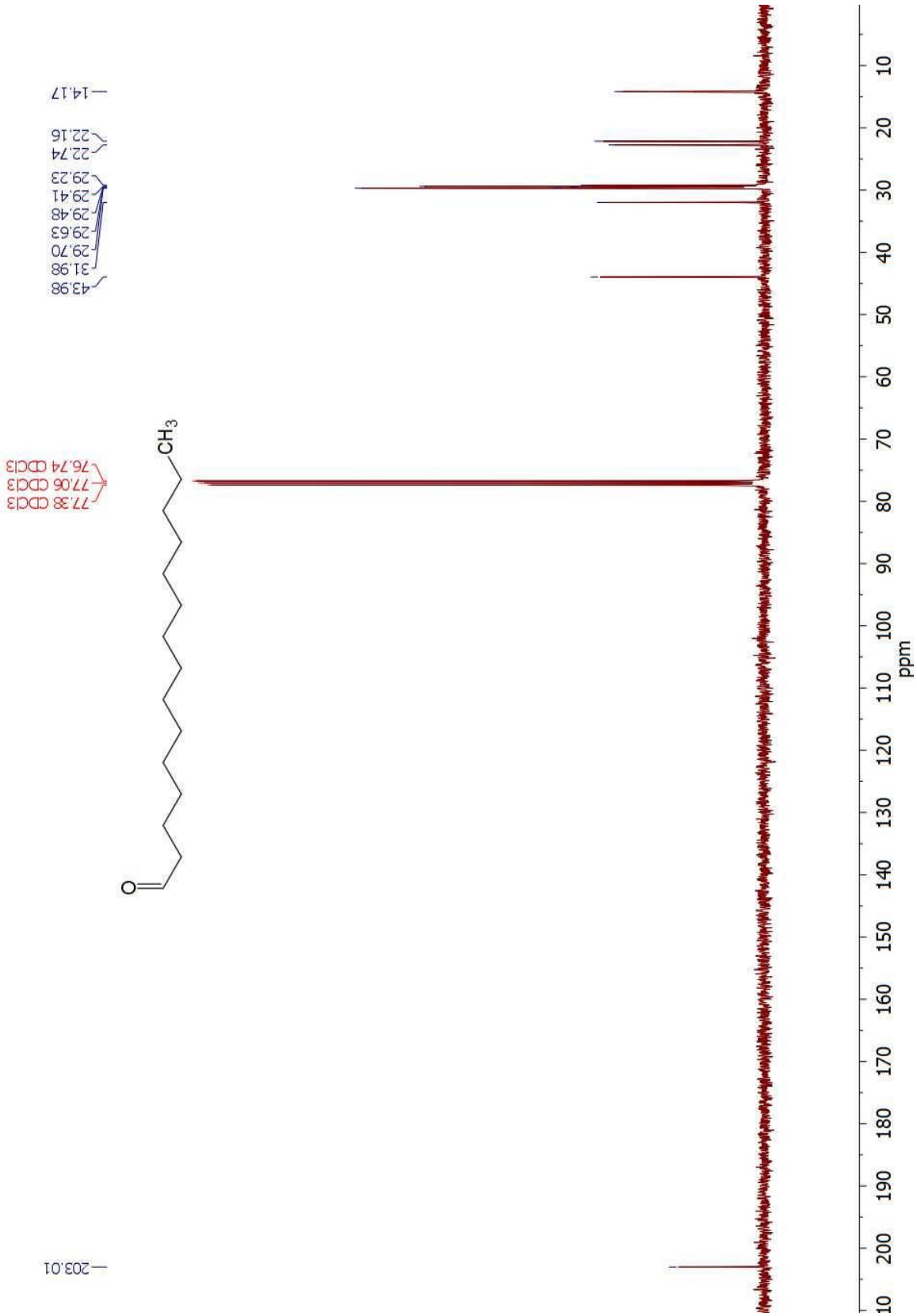
203.01
77.38 CDCl3
77.06 CDCl3
76.74 CDCl3
43.98
31.98
29.70
29.63
29.48
29.41
29.23
22.74
22.16
14.17
CH3
O
ppm

9.77
9.76
9.76
7.26 CDCl3
2.44
2.43
2.42
2.41
2.40
2.39
1.66
1.64
1.63
1.61
1.59
1.57 HDO
1.34
1.30
1.25
D
D
D
D
D
D
D
D
O
1.00
16.33
2.07
2.07
ppm

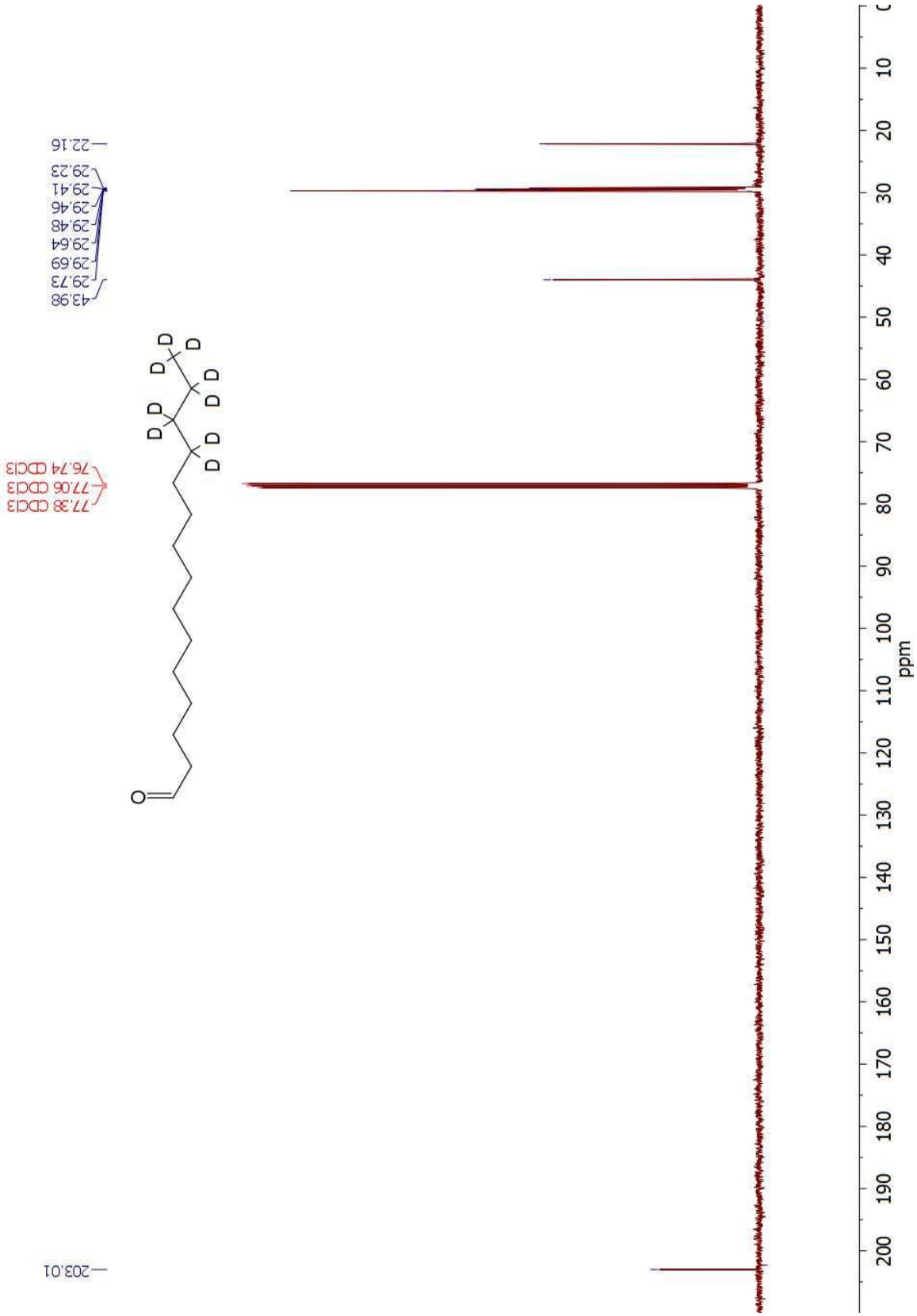
203.01
77.38 CDCl3
77.06 CDCl3
76.74 CDCl3
43.98
29.73
29.69
29.64
29.48
29.46
29.41
29.23
22.16
O
D
ppm

7.26 CDCl3
4.22
4.21
4.19
4.17
3.42
2.54
2.53
2.51
1.61
1.59
1.57
1.55
1.53 HDO
1.33
1.32
1.31
1.30
1.29
1.28
1.26
1.25
0.90
0.88
0.86
3.11
25.16
2.07
2.00
1.87
2.09
ppm

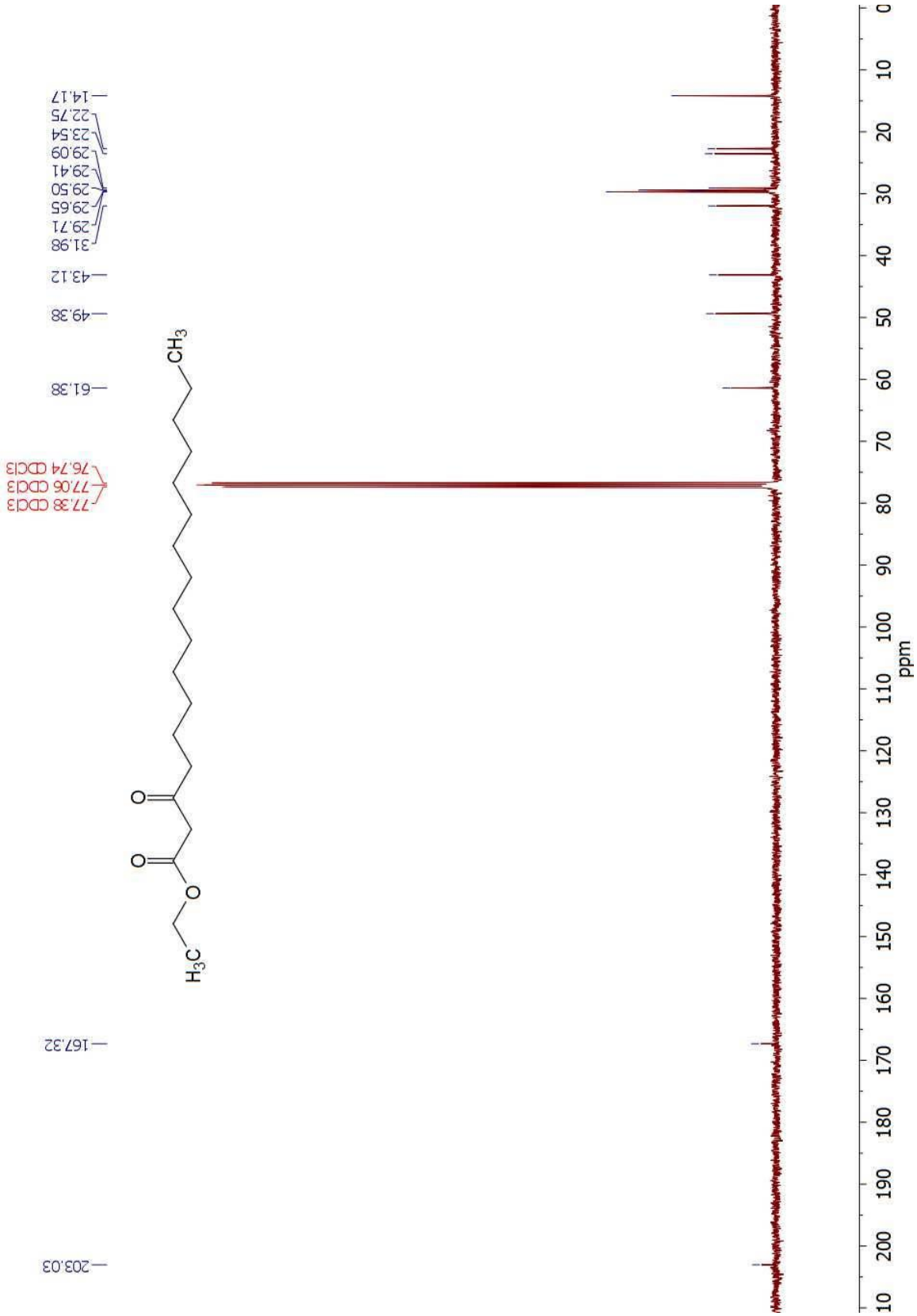
203.03
167.32
77.38 CDCl3
77.06 CDCl3
76.74 CDCl3
61.38
49.38
43.12
31.98
29.71
29.65
29.50
29.41
29.09
23.54
22.75
14.17
CH3
O
O
O
H3C
ppm

7.26 CDCl3
5.30
4.22
4.20
4.19
4.17
3.42
2.54
2.52
2.51
1.61
1.59
1.57
1.55 HDO
1.32
1.31
1.30
1.29
1.28
1.26
1.25
18.92
2.09
1.92
1.85
2.10
ppm

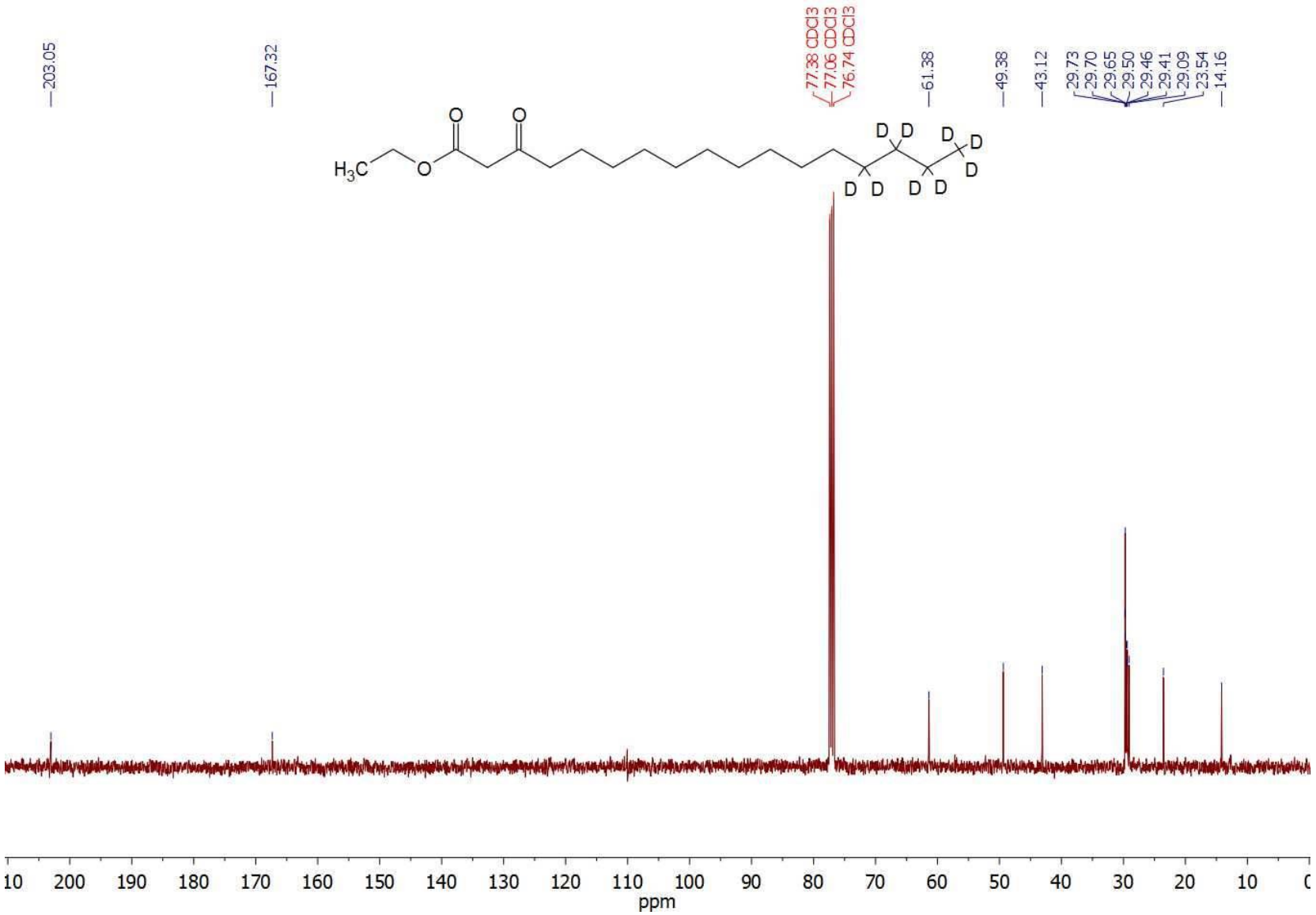
203.05
167.32
77.38 CDCl3
77.06 CDCl3
76.74 CDCl3
61.38
49.38
43.12
29.73
29.70
29.65
29.50
29.46
29.41
29.09
23.54
14.16
H3C
O
O
O
D
D
D
D
D
D
D
D
D
D
ppm

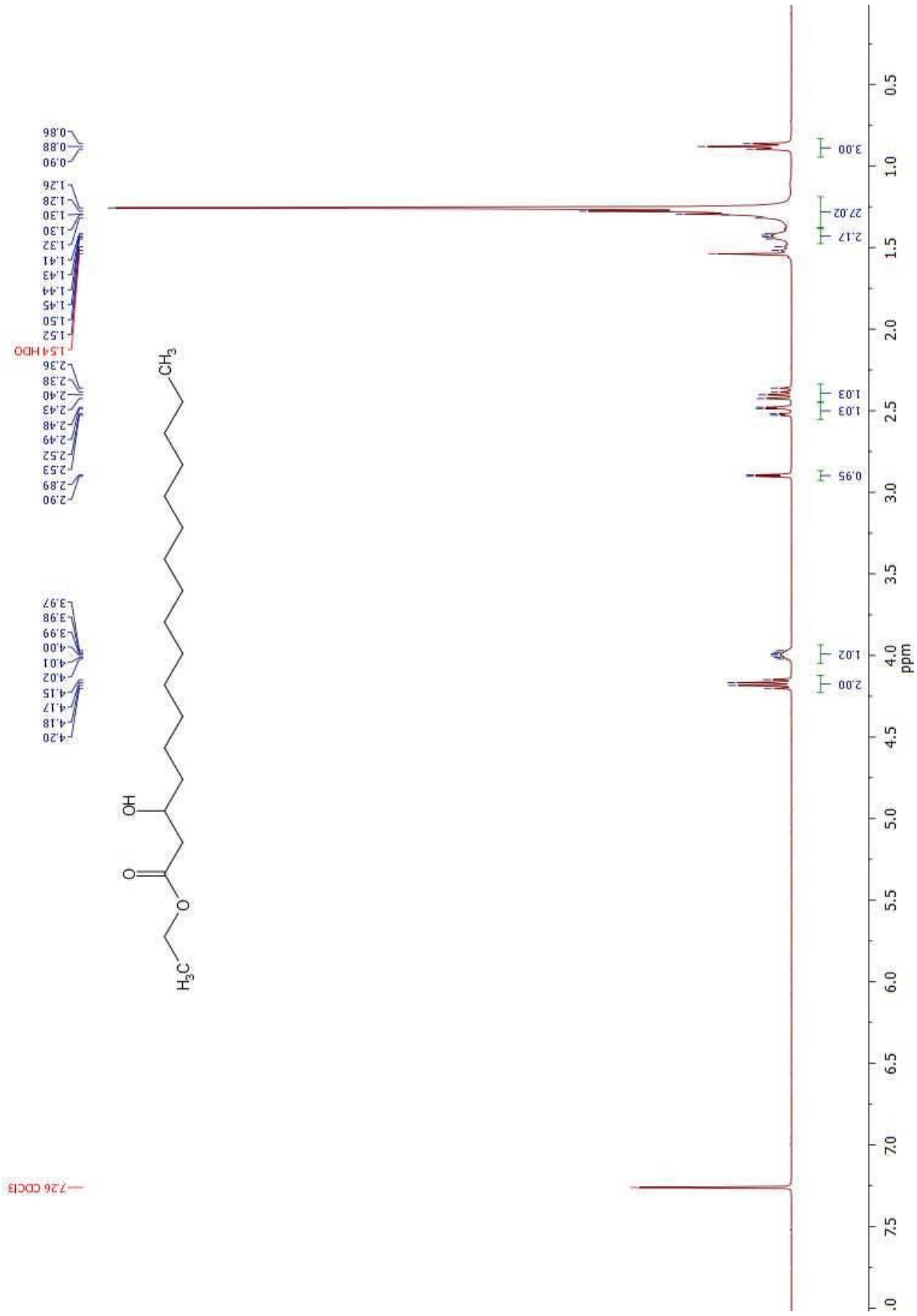
0.86
0.88
0.90
1.26
1.28
1.30
1.30
1.32
1.41
1.43
1.44
1.45
1.50
1.52
1.54 HDO
2.36
2.38
2.40
2.43
2.48
2.49
2.52
2.53
2.89
2.90
3.97
3.98
3.99
4.00
4.01
4.02
4.15
4.17
4.18
4.20
7.26 CDCl3
3.00
27.02
2.17
1.03
1.03
0.95
1.02
2.00
ppm
OH
O
O
H3C
CH3

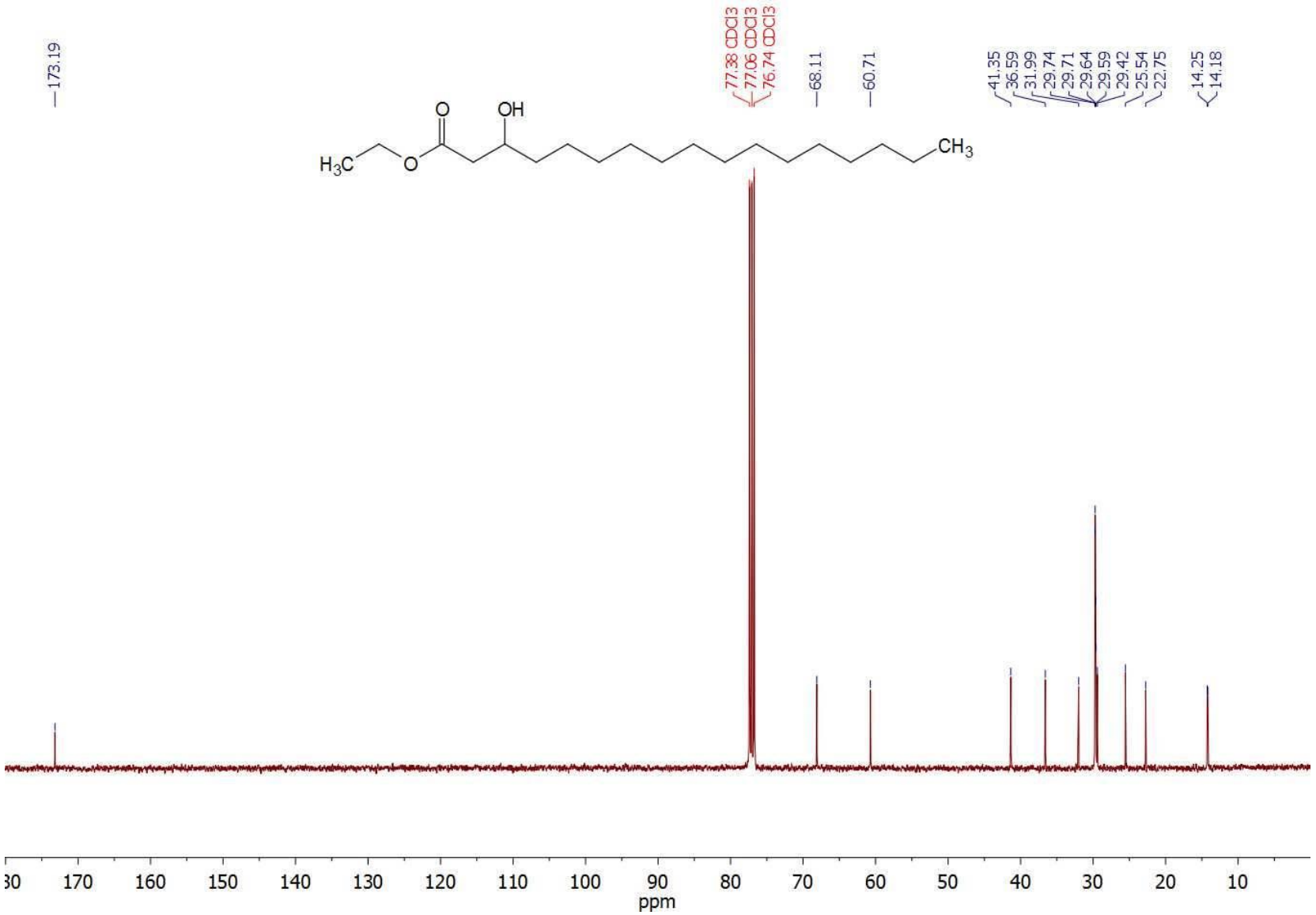
173.19
77.38 CDCl3
77.06 CDCl3
76.74 CDCl3
68.11
60.71
41.35
36.59
31.99
29.74
29.71
29.64
29.59
29.42
25.54
22.75
14.25
14.18
O
OH
H3C
O
CH3
ppm

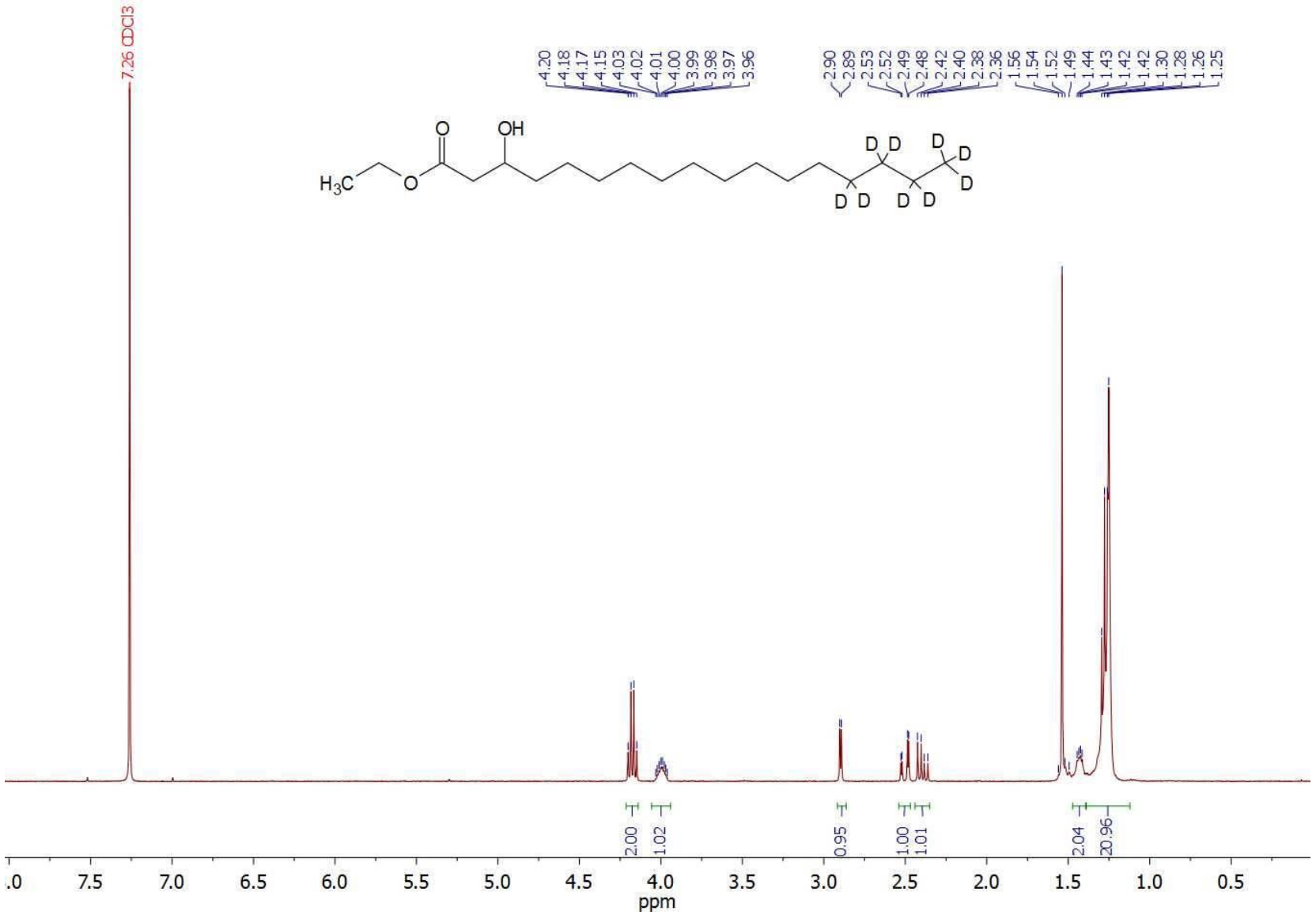
7.26 CDCl3
4.20
4.18
4.17
4.15
4.03
4.02
4.01
4.00
3.99
3.98
3.97
3.96
2.90
2.89
2.53
2.52
2.49
2.48
2.42
2.40
2.38
2.36
1.56
1.54
1.52
1.49
1.44
1.43
1.42
1.42
1.30
1.28
1.26
1.25
O
OH
H3C
O
D D
D
D
D D
D D
D
2.00
1.02
0.95
1.00
1.01
2.04
20.96
.0
7.5
7.0
6.5
6.0
5.5
5.0
4.5
4.0
3.5
3.0
2.5
2.0
1.5
1.0
0.5
ppm

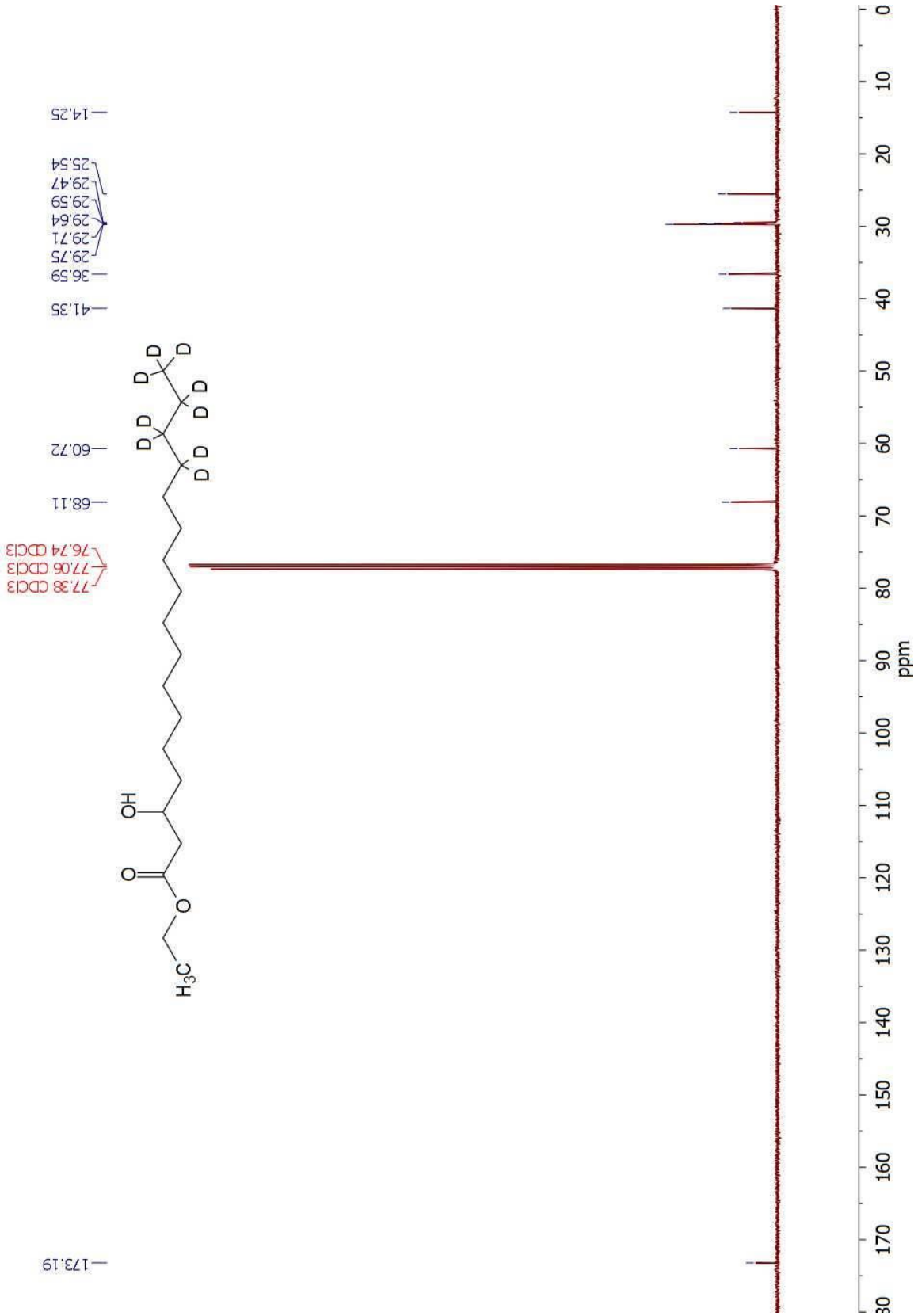
173.19
77.38 CDCl3
77.06 CDCl3
76.74 CDCl3
68.11
60.72
41.35
36.59
29.75
29.71
29.64
29.59
29.47
25.54
14.25
OH
O
O
H3C
D
D
D
D
D
D
D
D
D
ppm

7.26 CDCl3
0.86
0.88
0.90
1.26
1.28
1.45
1.46
1.48
1.49
1.50
1.52
1.55
1.56
1.57
2.45
2.47
2.49
2.51
2.56
2.57
2.60
2.61
4.01
4.01
4.03
4.04
4.05
4.06
4.07
CH3
OH
O
HO
0.96
1.01
1.05
3.20
23.94
3.00
ppm

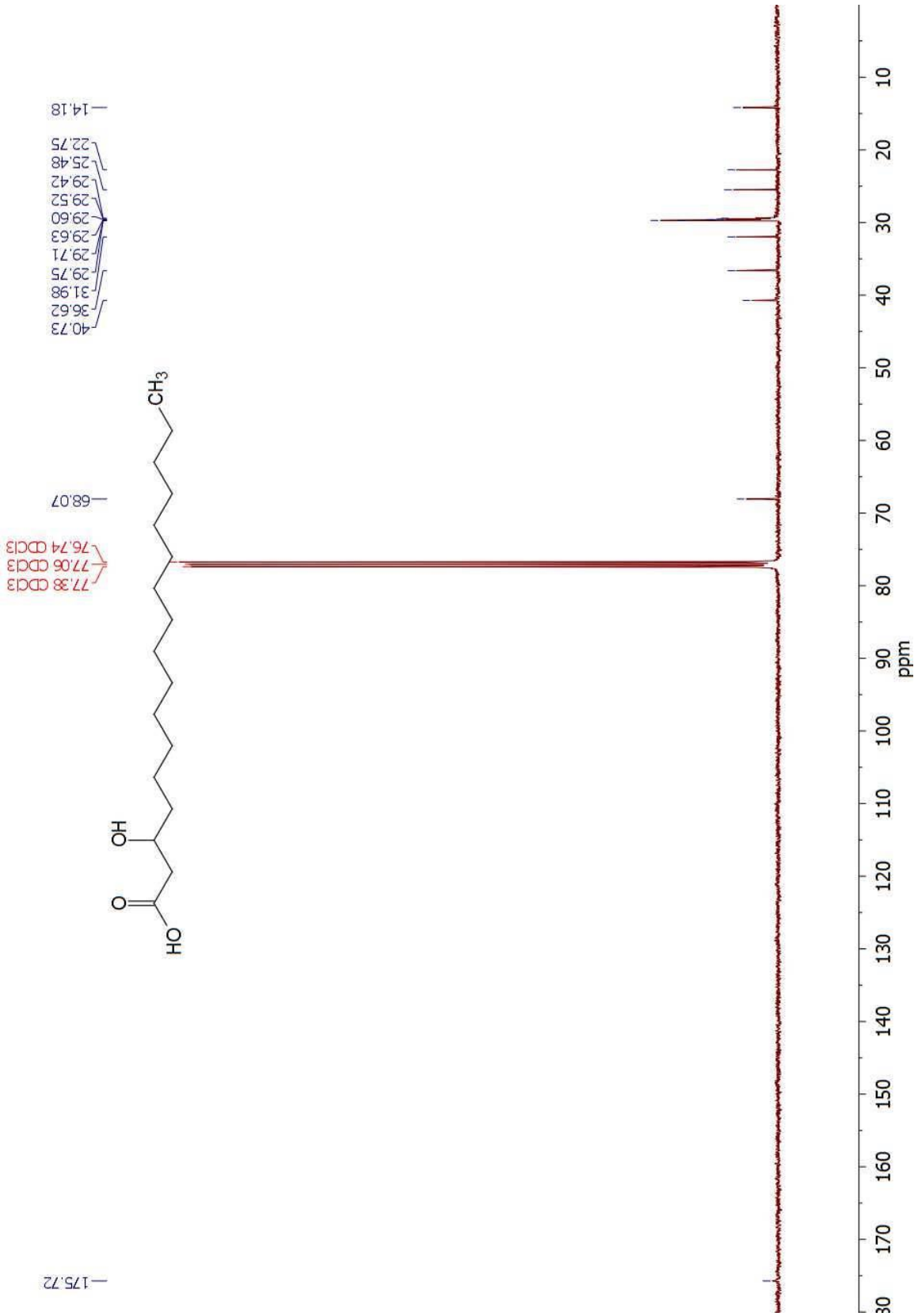
175.72
68.07
77.38 CDCl3
77.06 CDCl3
76.74 CDCl3
40.73
36.62
31.98
29.75
29.71
29.63
29.60
29.52
29.42
25.48
22.75
14.18
CH3
OH
O
HO
ppm

7.26 CDCl3
4.03
2.61
2.60
2.57
2.56
2.51
2.49
2.47
2.45
1.59
1.57
1.56
1.54
1.50
1.49
1.48
1.46
1.46
1.45
1.38
1.35
1.25
1.21
1.19
0.99
1.01
1.08
3.18
18.04
ppm
OH
O
HO
D
D
D
D
D
D
D
D

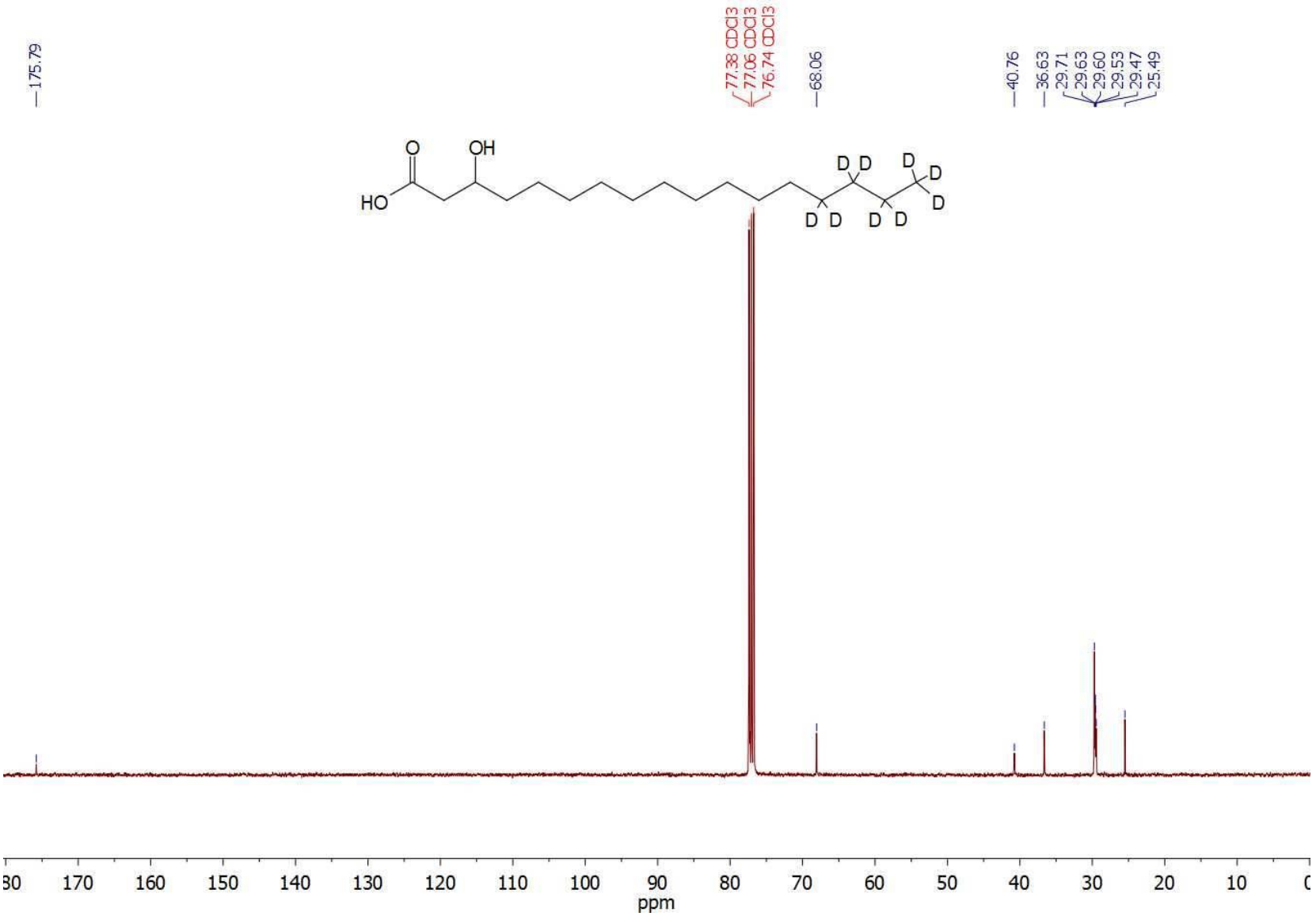
175.79
77.38 CDCl3
77.06 CDCl3
76.74 CDCl3
68.06
40.76
36.63
29.71
29.63
29.60
29.53
29.47
25.49
O
OH
HO
D D
D
D
D
D D
D D
ppm

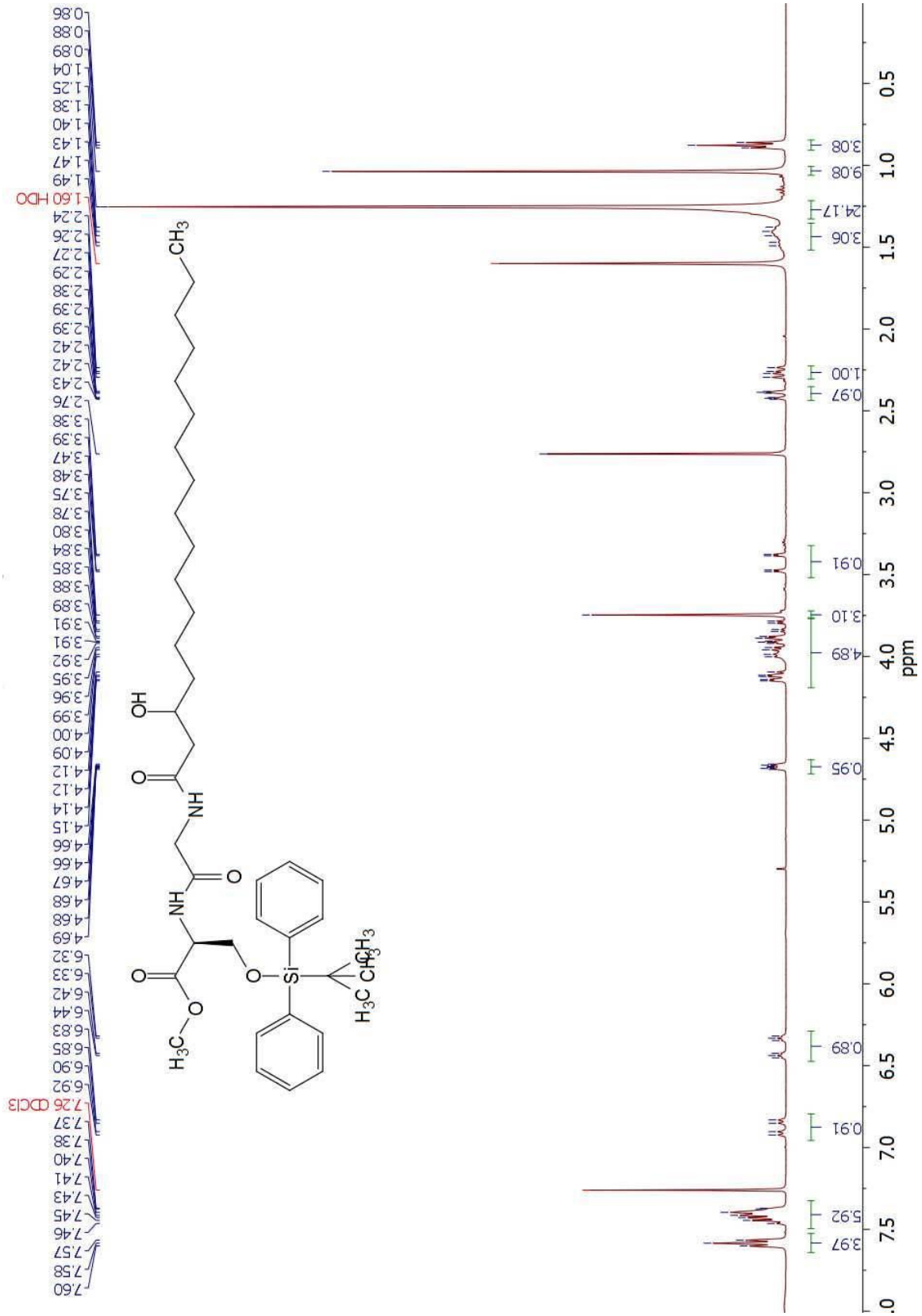
0.86
0.88
0.89
1.04
1.25
1.38
1.40
1.43
1.47
1.49
1.60 HDO
2.24
2.26
2.27
2.29
2.38
2.39
2.39
2.42
2.42
2.43
2.76
3.38
3.39
3.47
3.48
3.75
3.78
3.80
3.84
3.85
3.88
3.89
3.91
3.91
3.92
3.95
3.96
3.99
4.00
4.09
4.12
4.12
4.14
4.15
4.66
4.66
4.67
4.68
4.68
4.69
6.32
6.33
6.42
6.44
6.83
6.85
6.90
6.92
7.26 CDCl3
7.37
7.38
7.40
7.41
7.43
7.45
7.46
7.57
7.58
7.60
CH3
OH
O
NH
NH
O
O
O
O
Si
H3C
H3C CH3
CH3
3.08
9.08
24.17
3.06
1.00
0.97
0.91
3.10
4.89
0.95
0.89
0.91
5.92
3.97
0.
0.5
1.0
1.5
2.0
2.5
3.0
3.5
4.0
4.5
5.0
5.5
6.0
6.5
7.0
7.5
ppm

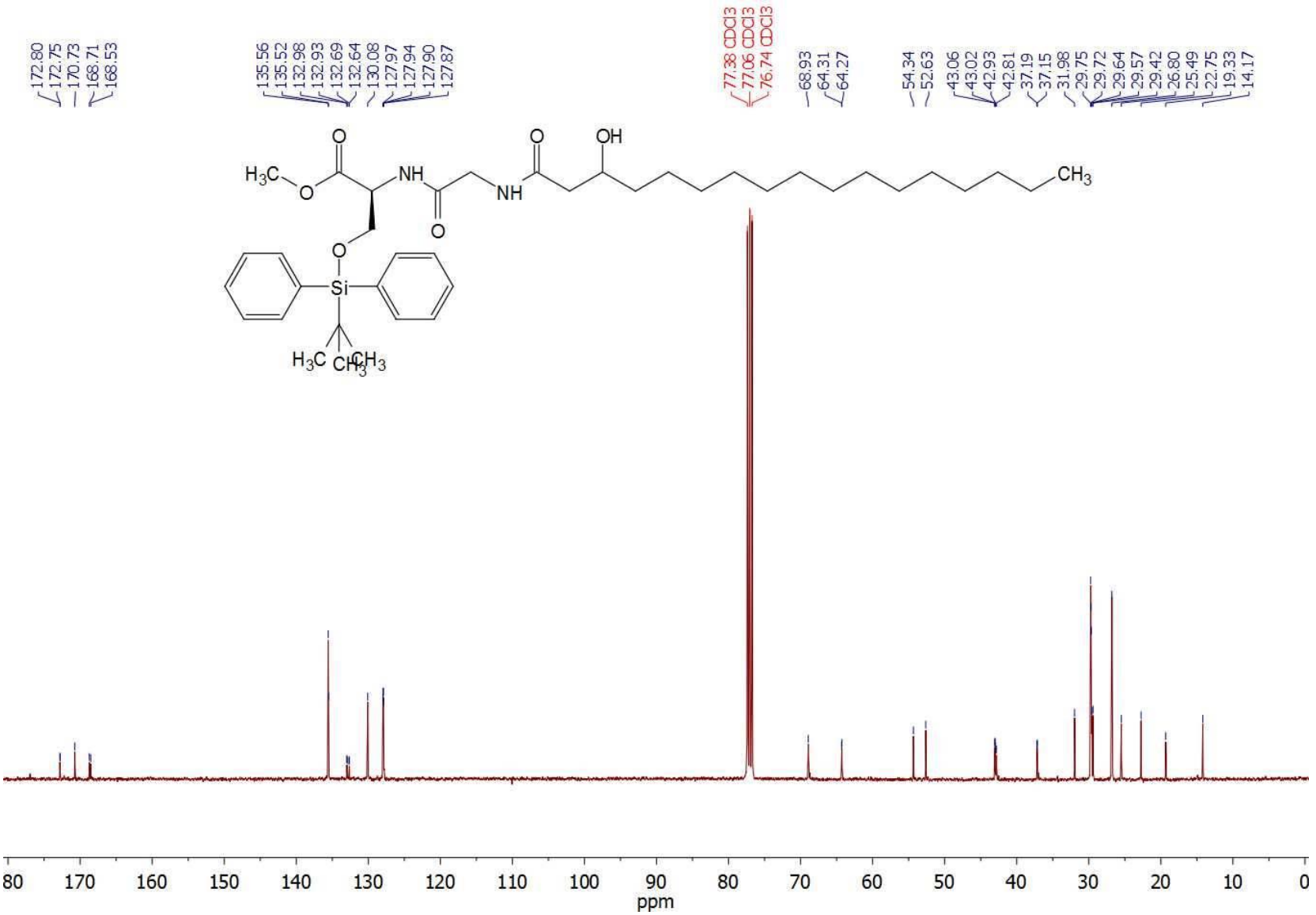
172.80
172.75
170.73
168.71
168.53
135.56
135.52
132.98
132.93
132.69
132.64
130.08
127.97
127.94
127.90
127.87
77.38 CDCl3
77.06 CDCl3
76.74 CDCl3
68.93
64.31
64.27
54.34
52.63
43.06
43.02
42.93
42.81
37.19
37.15
31.98
29.75
29.72
29.64
29.57
29.42
26.80
25.49
22.75
19.33
14.17
H3C
O
NH
O
NH
O
OH
CH3
O
Si
H3C
CH3
CH3
80
170
160
150
140
130
120
110
100
90
80
70
60
50
40
30
20
10
0
ppm

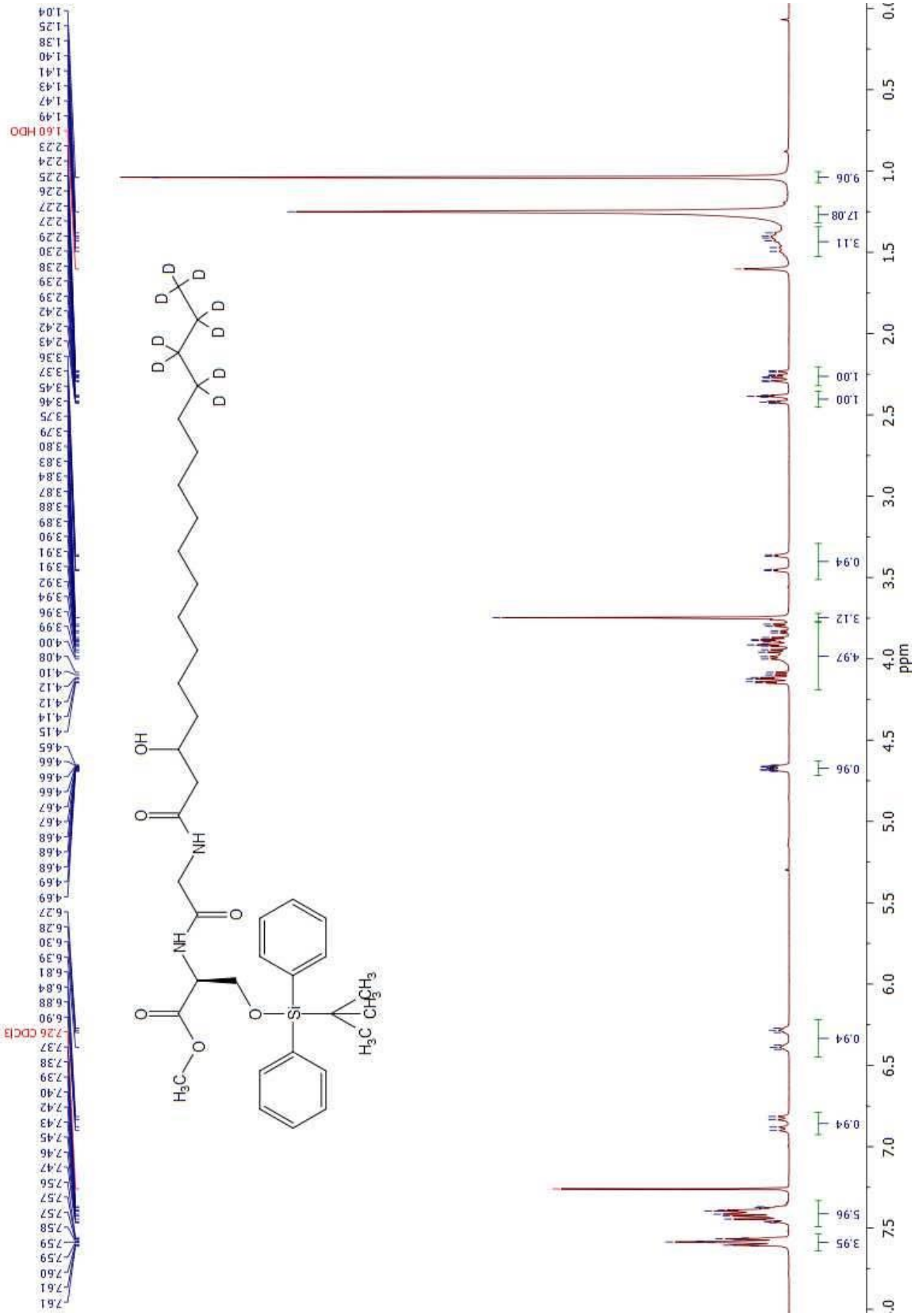
OH
O
NH
NH
O
O
O
H3C
O
Si
H3C
CH3
CH3
D
D
D
D
D
D
D
D
D
D
ppm

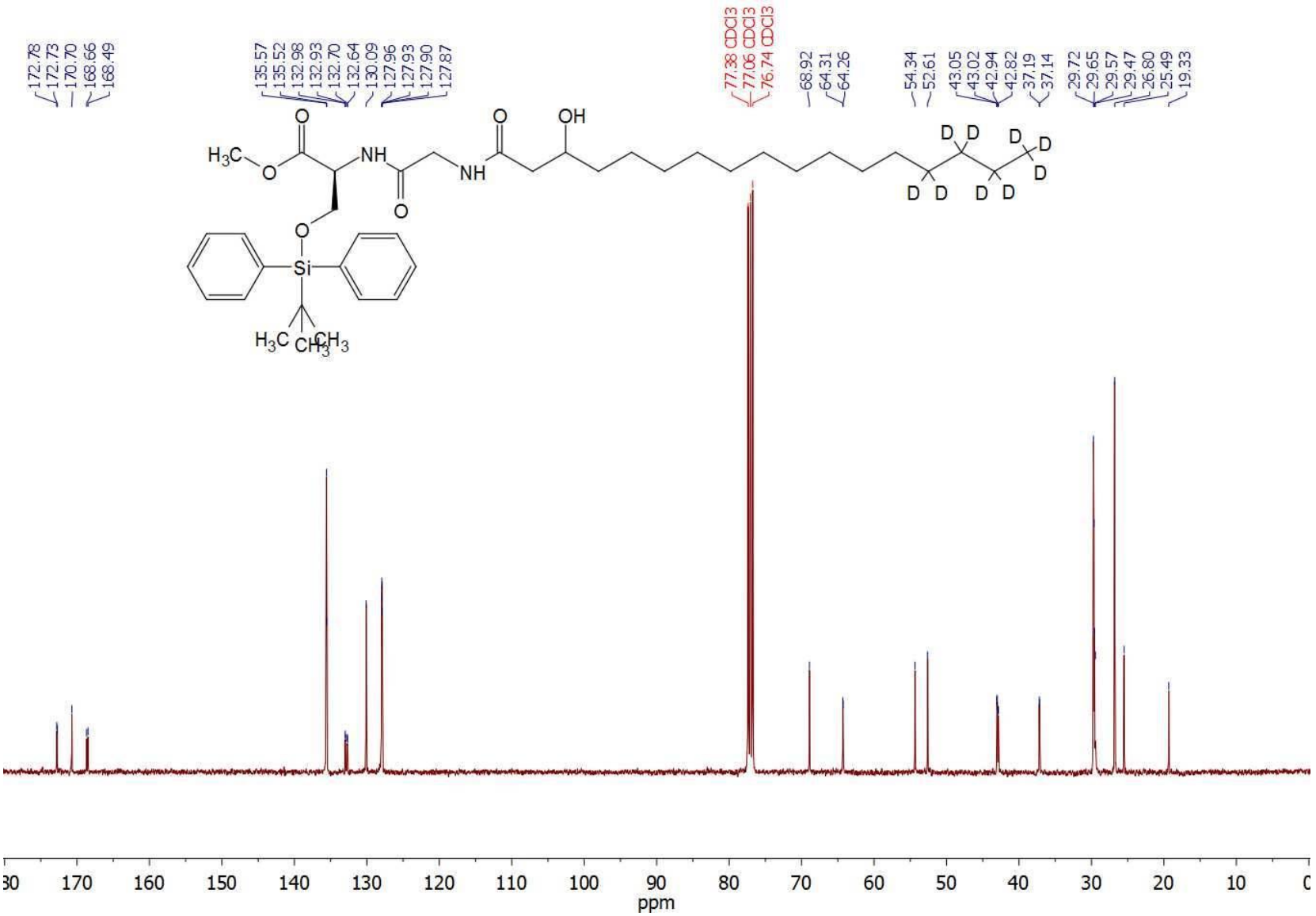
172.78
172.73
170.70
168.66
168.49
135.57
135.52
132.98
132.93
132.70
132.64
130.09
127.96
127.93
127.90
127.87
77.38 CDCl3
77.06 CDCl3
76.74 CDCl3
68.92
64.31
64.26
54.34
52.61
43.05
43.02
42.94
42.82
37.19
37.14
29.72
29.65
29.57
29.47
26.80
25.49
19.33
O
H3C
O
NH
O
NH
O
OH
O
Si
H3C
CH3
CH3
D
D
D
D
D
D
D
D
D
D
170
160
150
140
130
120
110
100
90
80
70
60
50
40
30
20
10
ppm

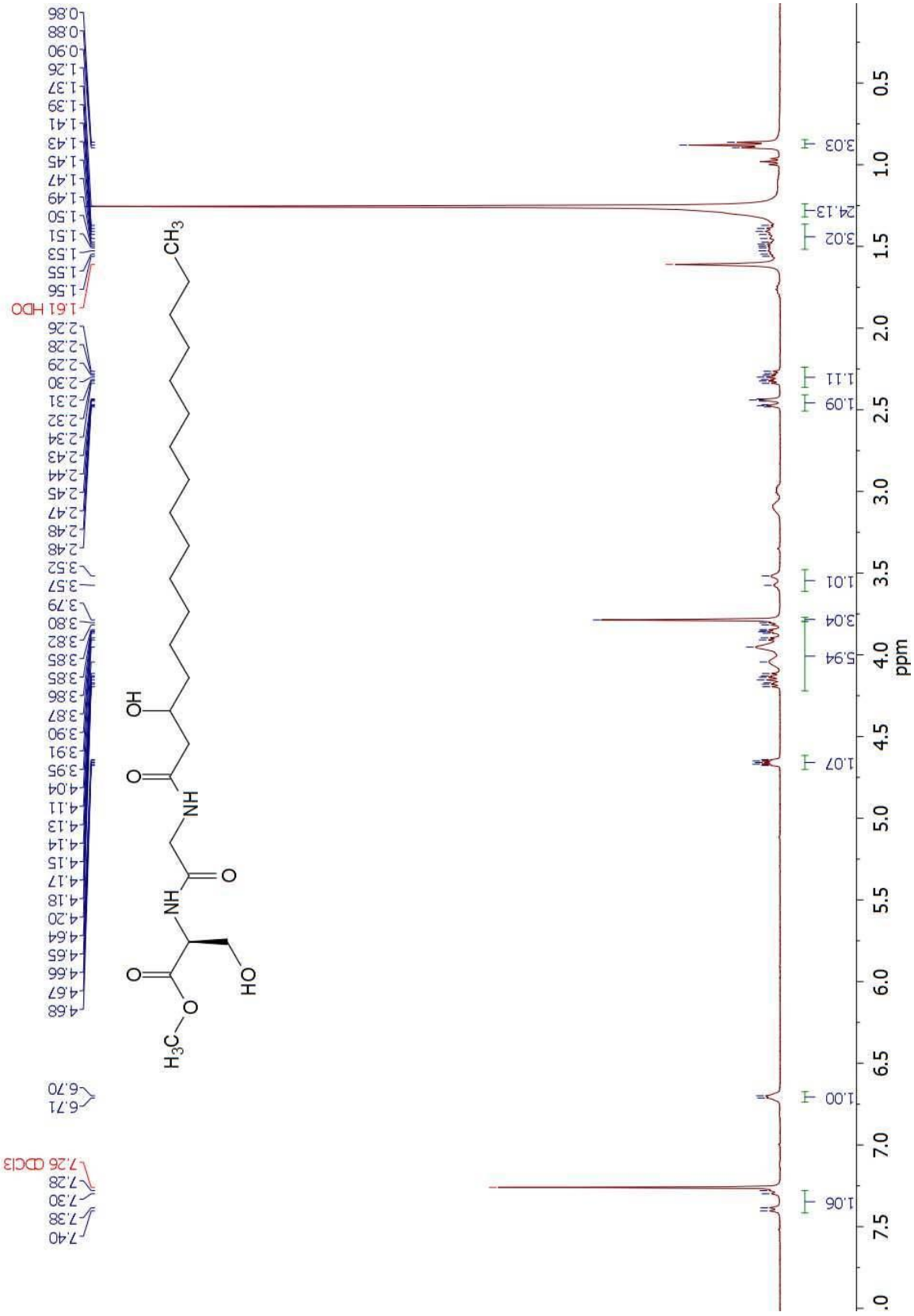
0.86
0.88
0.90
1.26
1.37
1.39
1.41
1.43
1.45
1.47
1.49
1.50
1.51
1.53
1.55
1.56
1.61 HDO
2.26
2.28
2.29
2.30
2.31
2.32
2.34
2.43
2.44
2.45
2.47
2.48
2.48
3.52
3.57
3.79
3.80
3.82
3.85
3.85
3.86
3.87
3.90
3.91
3.95
4.04
4.11
4.13
4.14
4.15
4.17
4.18
4.20
4.64
4.65
4.66
4.67
4.68
6.70
6.71
7.26 CDCl3
7.28
7.30
7.38
7.40
CH3
OH
O
NH
NH
O
O
O
H3C
OH
1.06
1.00
1.07
5.94
3.04
1.01
3.52
1.09
1.11
3.02
24.13
3.03
0.5
1.0
1.5
2.0
2.5
3.0
3.5
4.0
4.5
5.0
5.5
6.0
6.5
7.0
7.5
.0
ppm

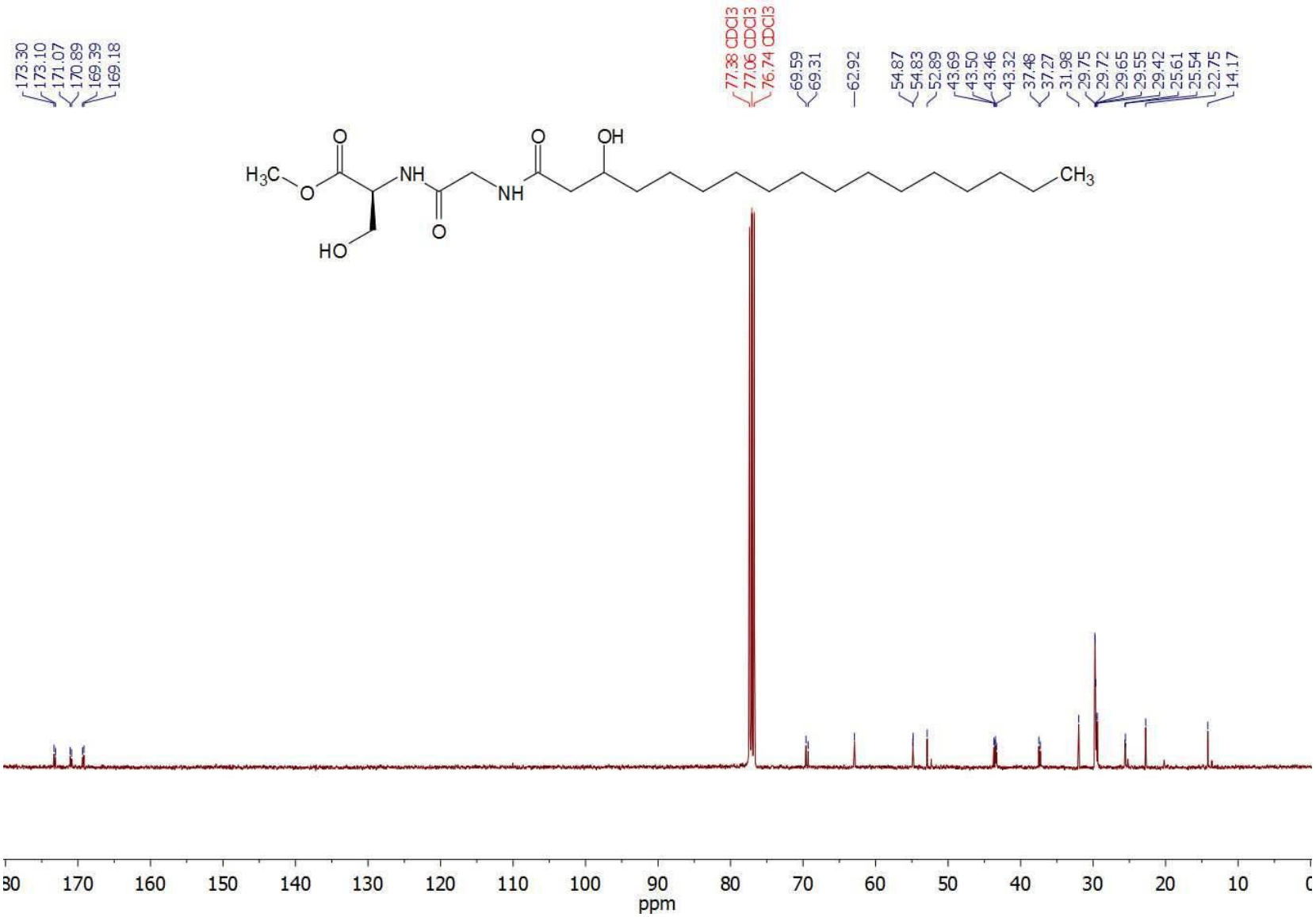
173.30
173.10
171.07
170.89
169.39
169.18
77.38 CDCl3
77.06 CDCl3
76.74 CDCl3
69.59
69.31
62.92
54.87
54.83
52.89
43.69
43.50
43.46
43.32
37.48
37.27
31.98
29.75
29.72
29.65
29.55
29.42
25.61
25.54
22.75
14.17
H3C
O
O
NH
O
NH
O
OH
CH3
HO
ppm

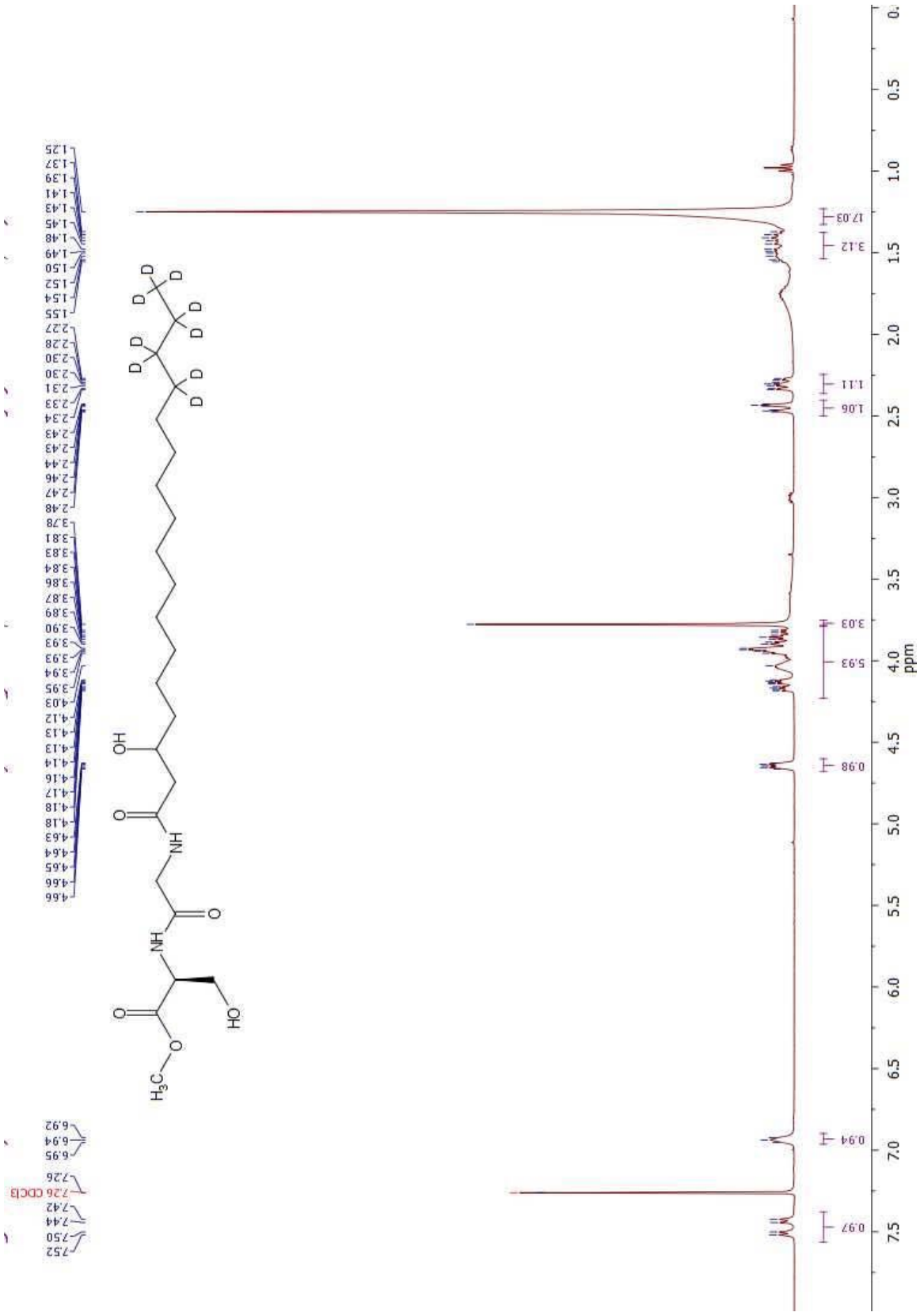
ppm
17.03
3.12
1.11
1.06
3.03
5.93
0.98
0.94
0.97
CDCl3
OH
NH
NH
O
O
O
O
HO
H3C
D

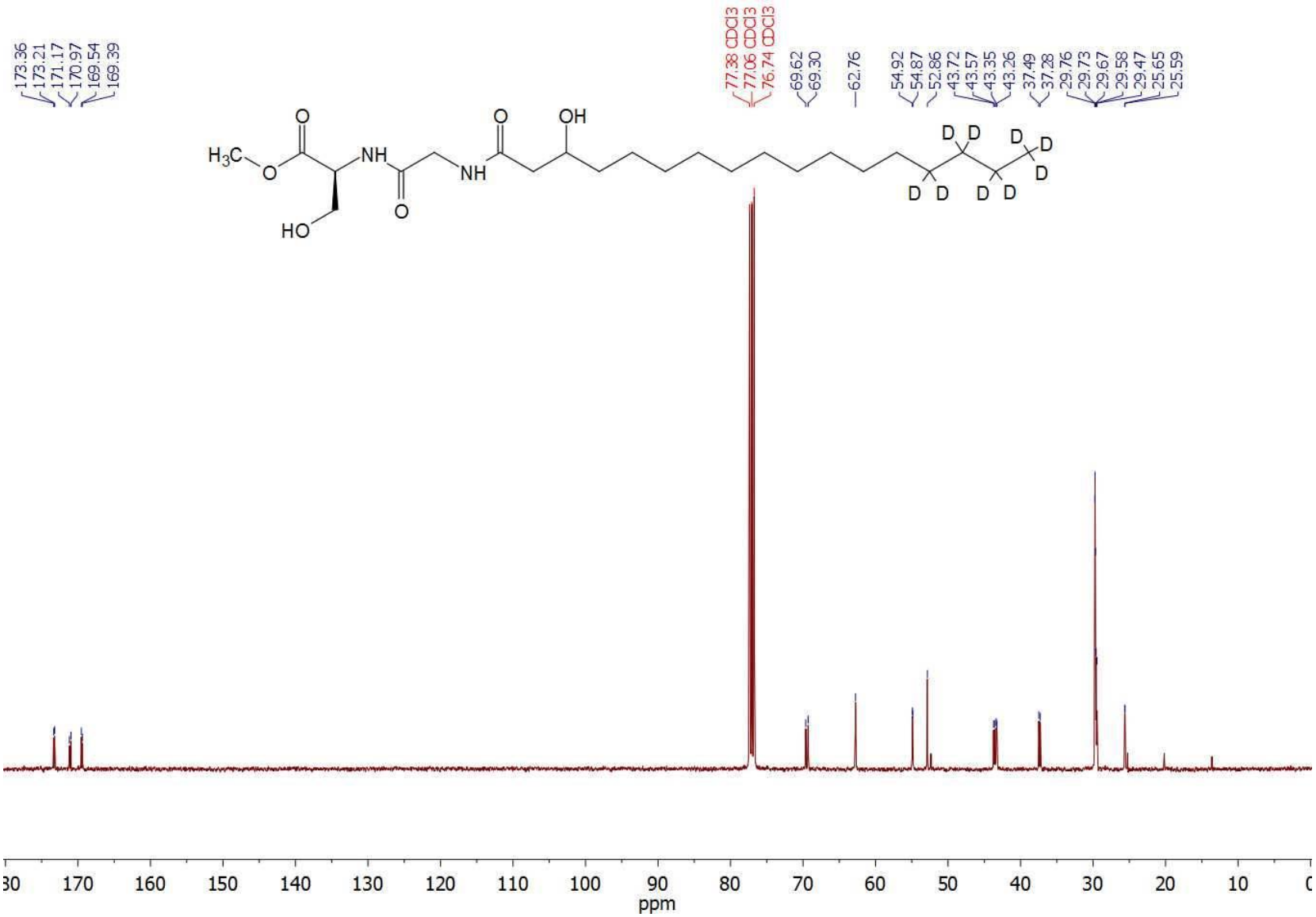
173.36
173.21
171.17
170.97
169.54
169.39
77.38 CDCl3
77.06 CDCl3
76.74 CDCl3
69.62
69.30
62.76
54.92
54.87
52.86
43.72
43.57
43.35
43.26
37.49
37.28
29.76
29.73
29.67
29.58
29.47
25.65
25.59
H3C
O
NH
NH
OH
HO
D
ppm

7.26 CDCl3
0.81
0.83
0.84
1.20
1.38
1.39
1.42
1.44
1.46
1.49
1.57
2.22
2.24
2.25
2.27
2.29
2.36
2.37
2.38
2.39
2.41
2.42
3.65
3.66
3.69
3.70
3.72
3.77
3.78
3.79
3.80
3.82
3.90
3.91
3.94
3.97
4.01
4.09
4.13
4.46
4.49
4.52
4.53
4.54
4.55
4.56
4.57
3.14
25.90
1.19
1.18
5.00
0.83
ppm

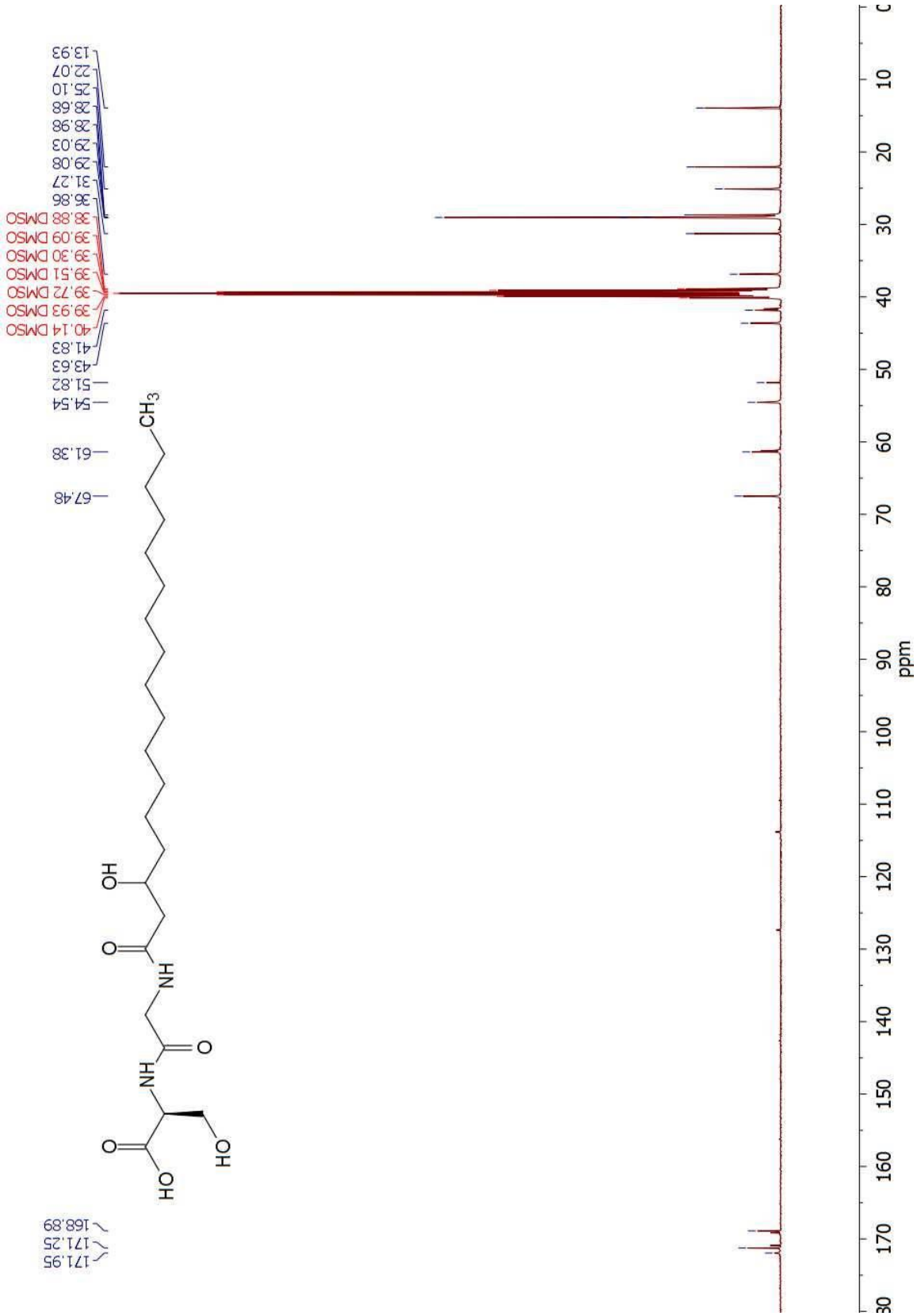
13.93
22.07
25.10
28.68
28.98
29.03
29.08
31.27
36.86
38.88 DMSO
39.09 DMSO
39.30 DMSO
39.51 DMSO
39.72 DMSO
39.93 DMSO
40.14 DMSO
41.83
43.63
51.82
54.54
61.38
67.48
171.95
171.25
168.89
CH3
OH
O
NH
NH
O
O
HO
OH
ppm

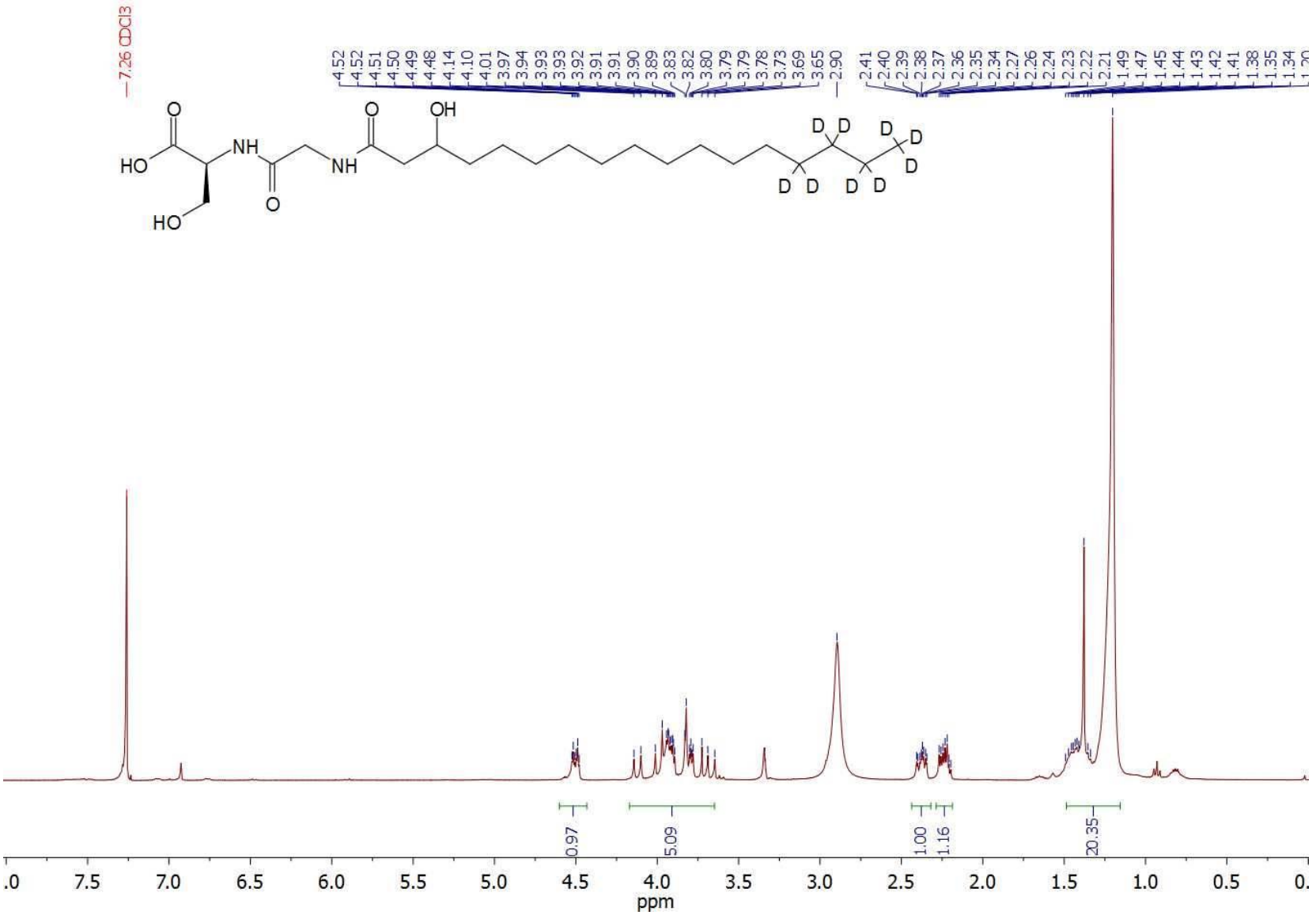
7.26 CDCl3
4.52
4.52
4.51
4.50
4.49
4.48
4.14
4.10
4.01
3.97
3.94
3.93
3.93
3.92
3.91
3.91
3.90
3.89
3.83
3.82
3.80
3.79
3.79
3.78
3.73
3.69
3.65
2.90
2.41
2.40
2.39
2.38
2.37
2.36
2.35
2.34
2.27
2.26
2.24
2.23
2.22
2.21
1.49
1.47
1.45
1.44
1.43
1.42
1.41
1.38
1.35
1.34
HO
O
NH
O
NH
O
OH
HO
D
D
D
D
D
D
D
D
D
D
0.97
5.09
1.00
1.16
20.35
.0
7.5
7.0
6.5
6.0
5.5
5.0
4.5
4.0
3.5
3.0
2.5
2.0
1.5
1.0
0.5
0.
ppm

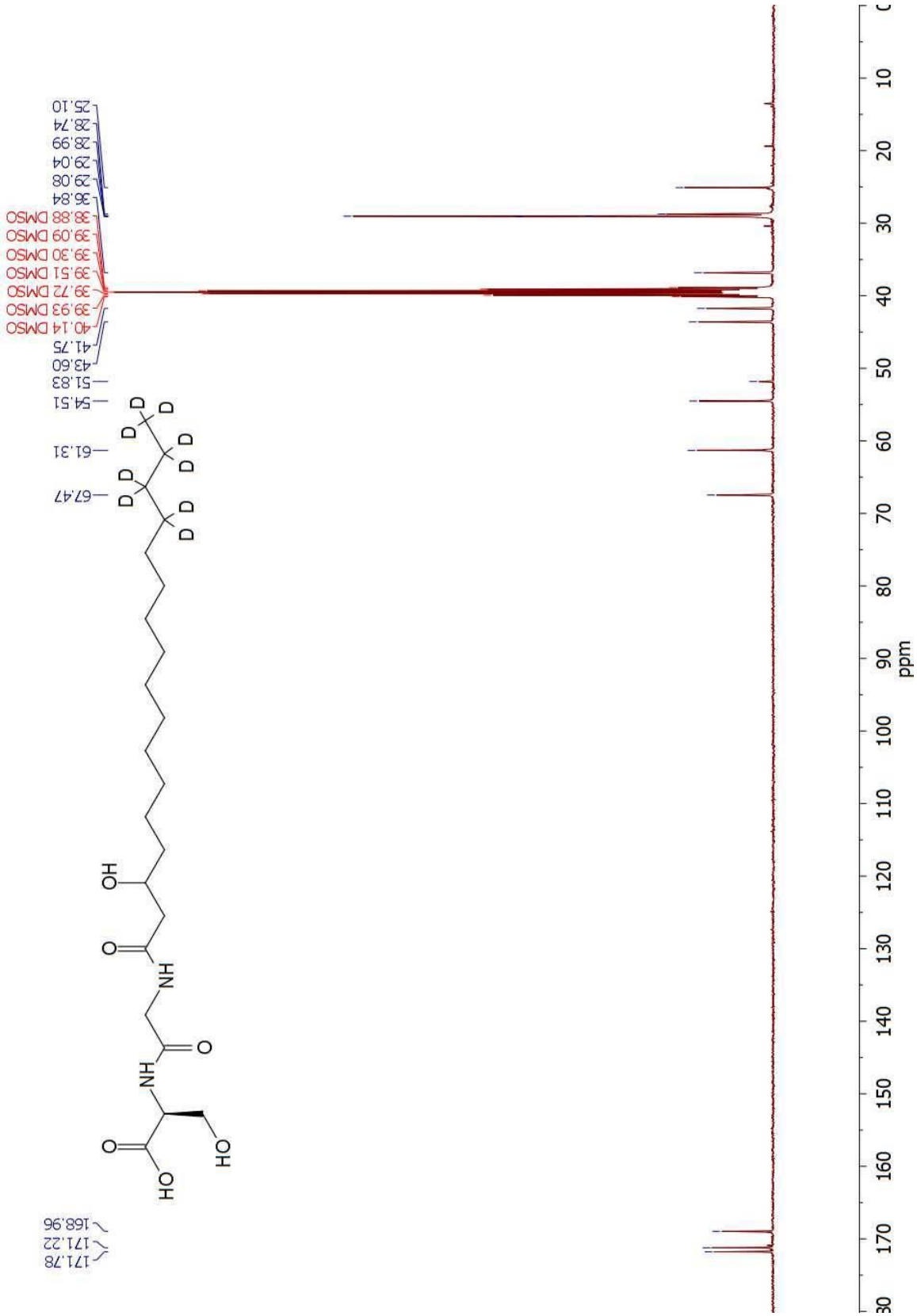
171.78
171.22
168.96
OH
HO
O
NH
O
NH
O
OH
HO
D
67.47
61.31
54.51
51.83
43.60
41.75
40.14 DMSO
39.93 DMSO
39.72 DMSO
39.51 DMSO
39.30 DMSO
39.09 DMSO
38.88 DMSO
36.84
29.08
29.04
28.99
28.74
25.10
ppm

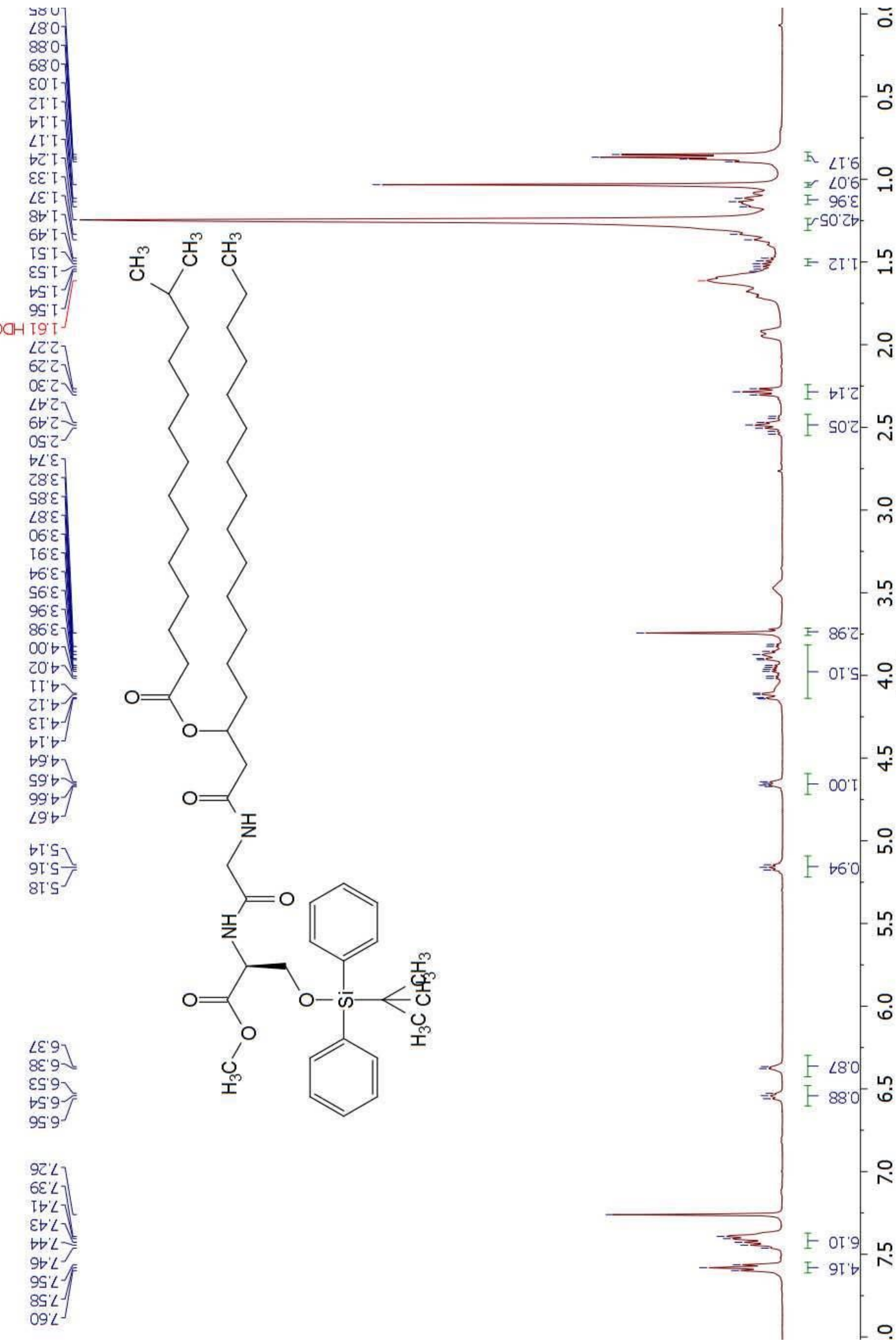
ppm
1.61 HDO

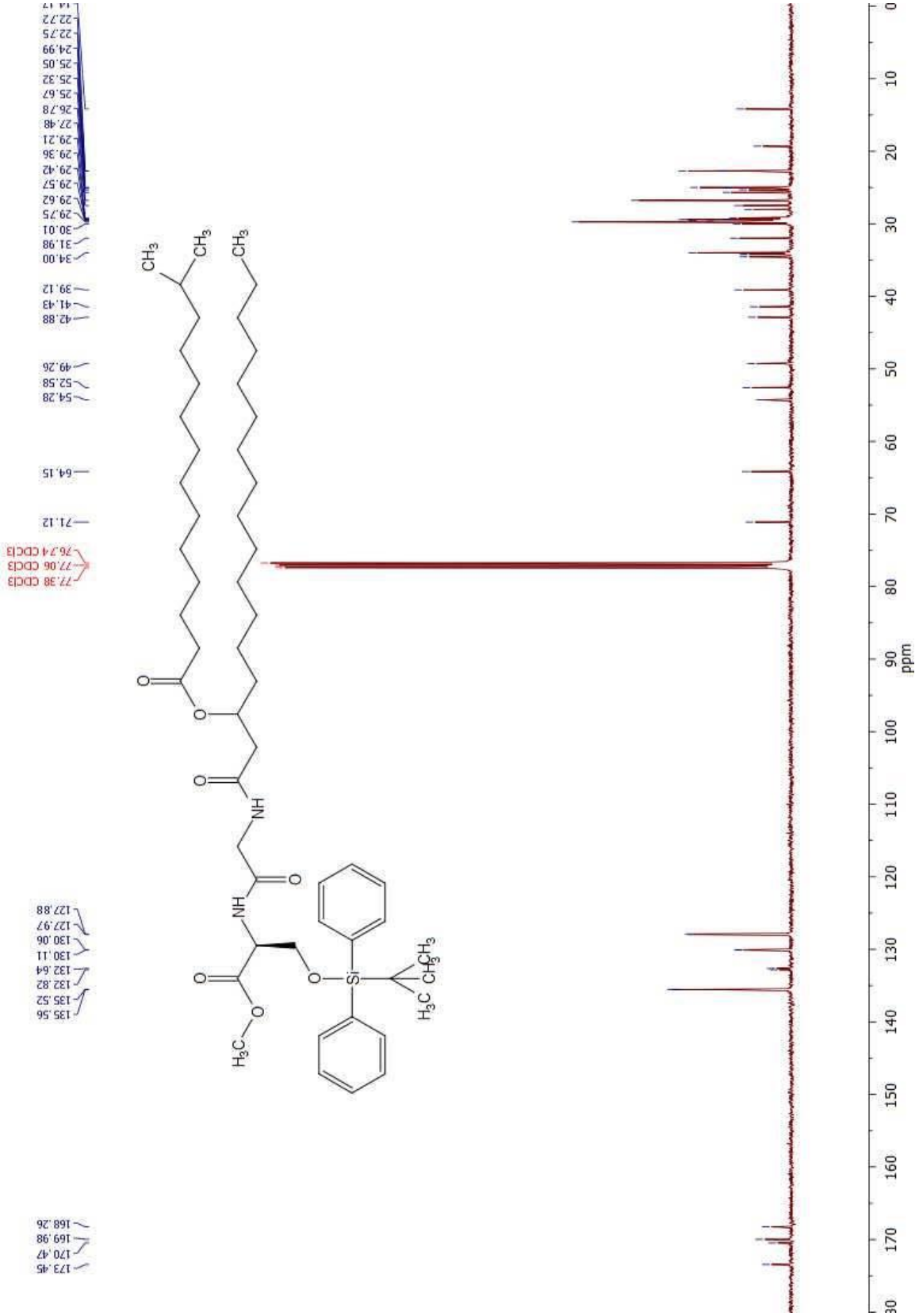
CH3
CH3
CH3
O
O
O
NH
NH
O
O
O
O
Si
H3C
CH3
CH3
H3C
ppm

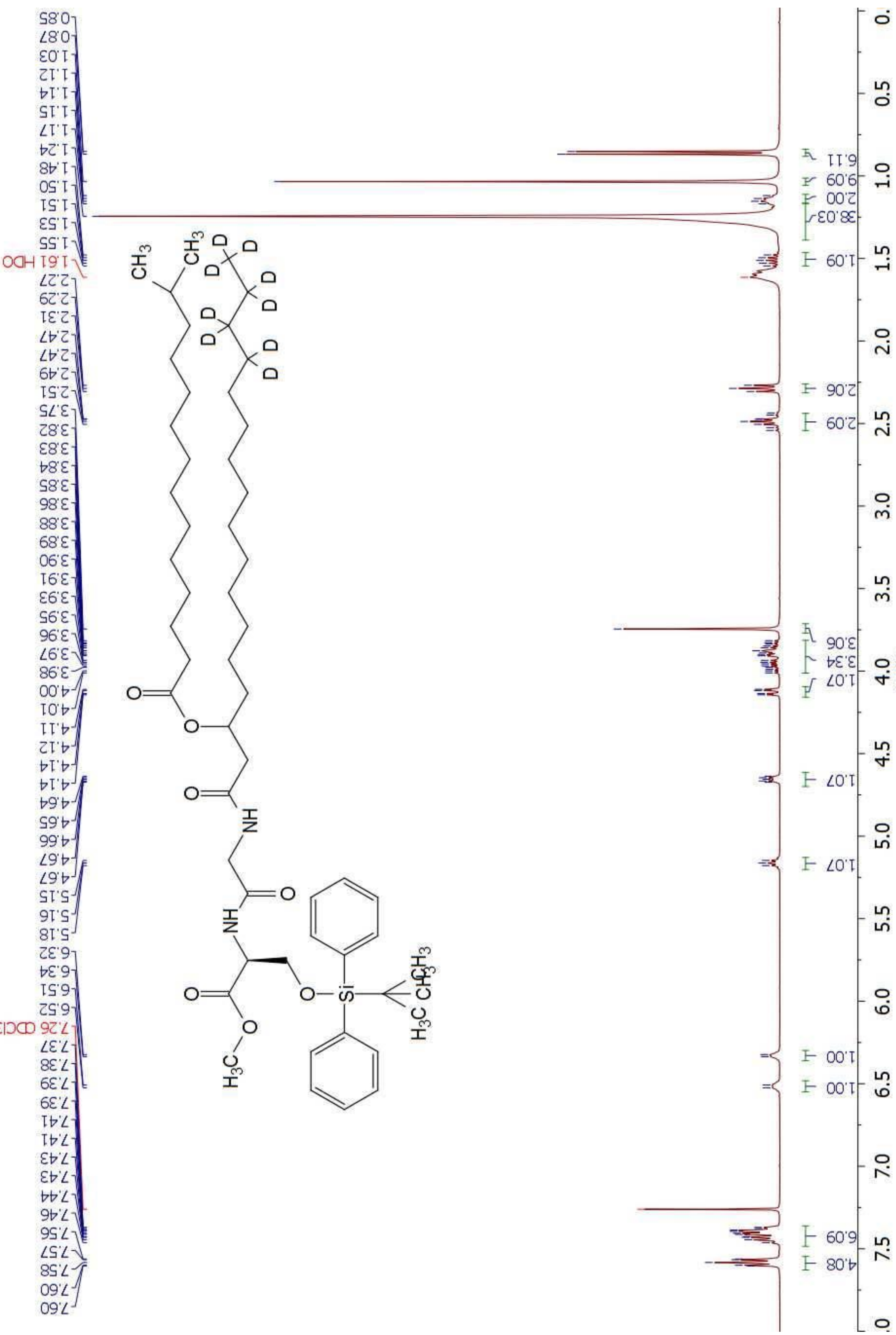

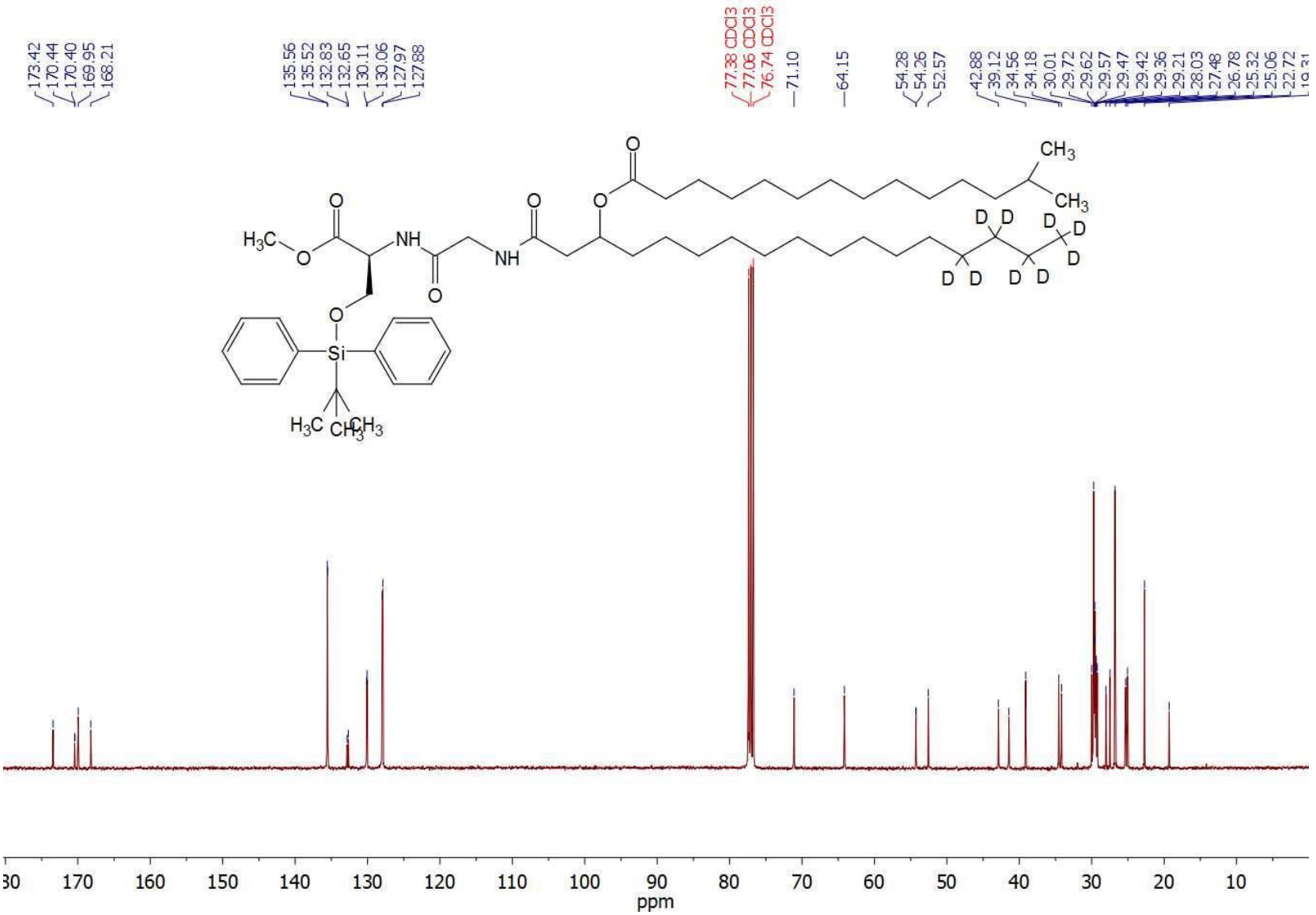
173.42
170.44
170.40
169.95
168.21
135.56
135.52
132.83
132.65
130.11
130.06
127.97
127.88
77.38 CDCl3
77.06 CDCl3
76.74 CDCl3
71.10
64.15
54.28
54.26
52.57
42.88
39.12
34.56
34.18
30.01
29.72
29.62
29.57
29.47
29.42
29.36
29.21
28.03
27.48
26.78
25.32
25.06
22.72
H3C
O
NH
NH
O
O
O
O
O
Si
CH3
CH3
H3C
CH3
CH3
D
D
D
D
D
D
D
D
D
D
170
160
150
140
130
120
110
100
90
80
70
60
50
40
30
20
10
ppm

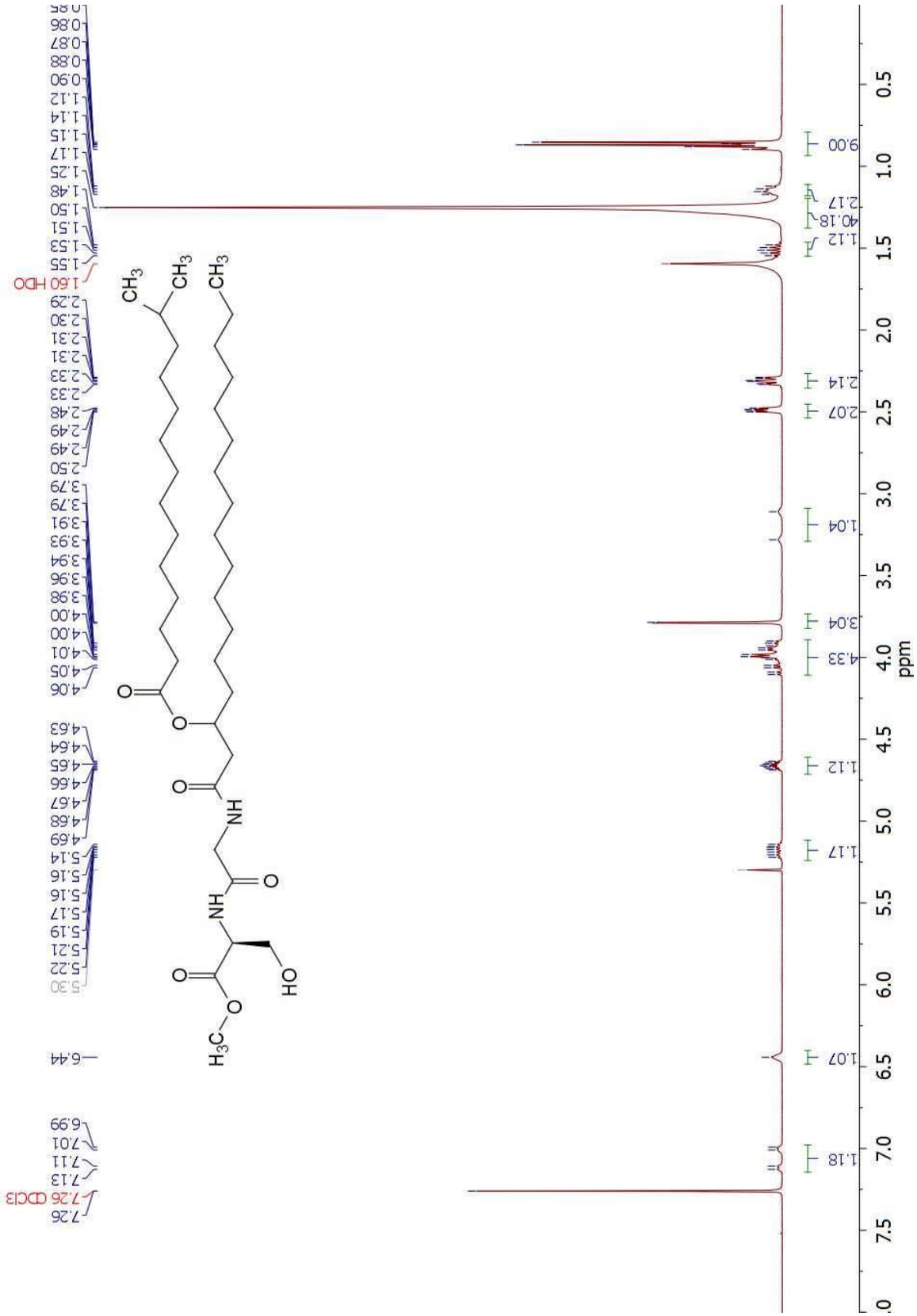
CH3
CH3
CH3
O
O
NH
O
NH
O
O
O
H3C
OH
7.26 CDCl3
6.44
1.60 HDO
9.00
2.17
40.18
1.12
2.14
2.07
1.04
3.04
4.33
1.12
1.17
1.07
1.18
ppm

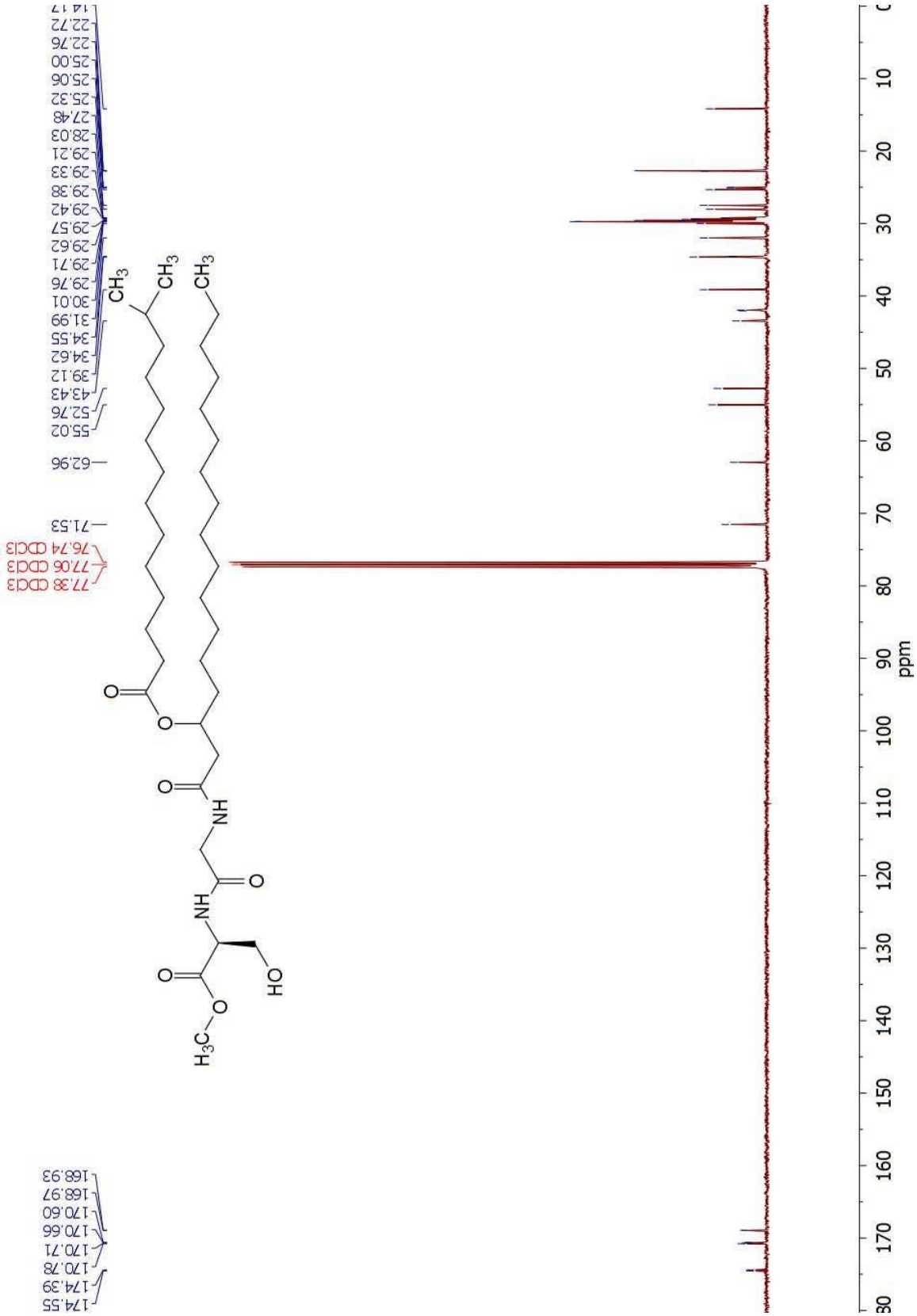
14.17
22.72
22.76
25.00
25.06
25.32
27.48
28.03
29.21
29.33
29.38
29.42
29.57
29.62
29.71
29.76
30.01
31.99
34.55
34.62
39.12
43.43
52.76
55.02
62.96
71.53
76.74 CDCl3
77.06 CDCl3
77.38 CDCl3
174.55
174.39
170.78
170.71
170.66
170.60
168.97
168.93
CH3
CH3
CH3
O
O
O
NH
O
NH
O
O
O
H3C
OH
ppm

7.26 CDCl3
H2O
ppm

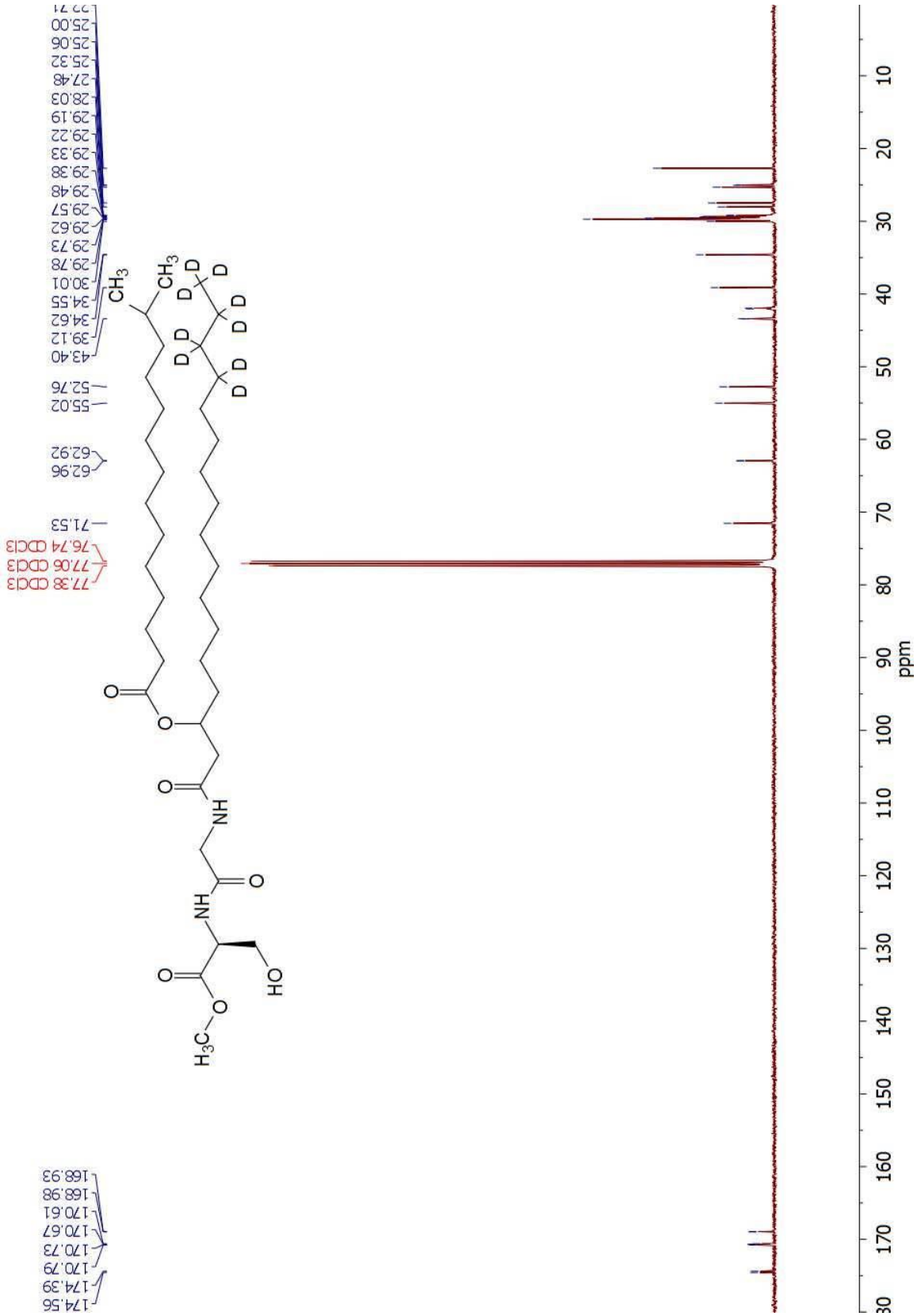
22.71
25.00
25.06
25.32
27.48
28.03
29.19
29.22
29.33
29.38
29.48
29.57
29.62
29.73
29.78
30.01
34.55
34.62
39.12
43.40
52.76
55.02
62.92
62.96
71.53
76.74 CDCl3
77.06 CDCl3
77.38 CDCl3
168.93
168.98
170.61
170.67
170.73
170.79
174.39
174.56
CH3
CH3
D
D
D
D
D
D
D
D
D
O
O
O
NH
NH
O
O
O
O
HO
H3C
10
20
30
40
50
60
70
80
90
100
110
120
130
140
150
160
170
ppm

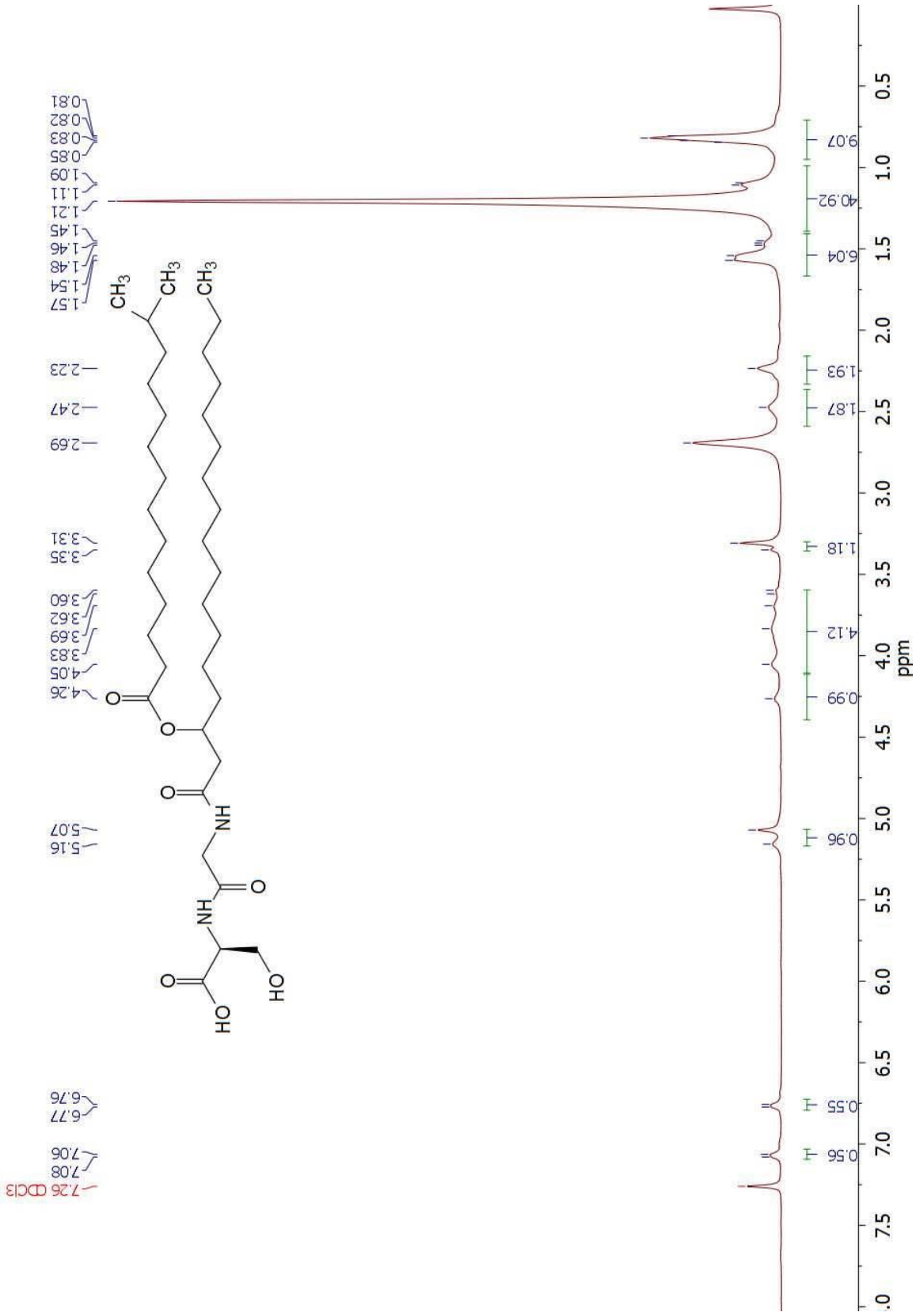
7.26 CDCl3
7.08
7.06
6.77
6.76
5.16
5.07
4.26
4.05
3.83
3.69
3.62
3.60
3.35
3.31
2.69
2.47
2.23
1.57
1.54
1.48
1.46
1.45
1.21
1.11
1.09
0.85
0.83
0.82
0.81
CH3
CH3
CH3
O
O
O
NH
NH
O
O
HO
OH
9.07
40.92
6.04
1.93
1.87
1.18
4.12
0.99
0.96
0.55
0.56
ppm

7.26 CDCl3
7.10
7.08
6.79
6.77
5.17
5.09
4.30
4.07
3.86
3.72
3.61
3.39
3.32
2.52
2.27
2.25
2.24
2.14
1.59
1.56
1.50
1.48
1.47
1.22
1.13
1.11
0.84
0.82
CH3
CH3
D
D
D
D
D
D
D
D
O
O
O
NH
NH
O
O
HO
OH
6.00
2.01
30.33
1.09
4.03
2.19
1.98
1.19
4.07
0.80
1.18
0.50
0.56
ppm

1.5 References

1. Turnbaugh, P. J.; Ley, R. E.; Hamady, M.; Fraser-Liggett, C. M.; Knight, R.; Gordon, J. *Nature* **2007**, 449, 804–810.
2. Peterson, J.; Garges, S.; Giovanni, M.; McInnes, P.; Wang, L.; Schloss, J. A.; Bonazzi, V.; McEwen, J. E.; Wetterstrand, K. A.; Deal, C.; Baker, C. C.; Di Francesco, V.; Howcroft, T. K.; Karp, R. W.; Lunsford, R. D.; Wellington, C. R.; Belachew, T.; Wright, M; Giblin, C.; David, H.; Mills, M.; Salomon, R.; Mullins, C.; Akolkar, B.; Begg, L.; Davis, C.; Grandison, L.; Humble, M.; et al. *Genome Res.* **2009**, 19, 2317–2323.
3. Sender, R.; Fuchs, S.; Milo, R. *Cell* **2016**, 164, 337-340.
4. Cho, I.; Blaser, M. J. *Nature Rev*. **2012**, 260-270.
5. Goldmuntz, E.; Penn, A. S. U.S. Departmant of Health and Human Services, Office of Women's Health, **2010**, 1-12.
6. Bell, E.; Bird, L. *Nature* **2005**, 435, 583.
7. National Multiple Sclerosis Society, www. Nationalmssociety.org
8. Polman, C. H.; Reingold, S. C.; Banwell B.; Clanet, M. Cohen, J. A.; Filippi, M.; Fujihara, K.; Havrdova, E.; Hutchinson, M.; Kappos, L.; Lublin, F. D.; Montalban, X.; O'Connor, P.; Sandberg-Wollheim, M.; Thompson, A. J.; Waubant, E.; Weinshenker, B.; Wolinsky, J. S. *Ann. Neurol.* **2011**, 69, 292–302.
9. Goldenberg, M. M. *Pharm. Therap*. **2012**, 37, 175-184.
10. Weinshenker B. C. *Neurol. Clin*. **1996**, 142, 1–308.
11. Broadley, S. A.; Deans, J.; Sawcer, S. J.; Clayton, D.; Compston, D. A. S. *Brain*, **2000**, 123, 1102-1111.
12. Proal, A. D.; Albert, P. J.; Marshall, T. G. *Cur. Opin. Rheumat*. **2013**, 25, 234-240.

13. Humphrey L. L.; Fu, R.; Buckley, D. I.; Freeman, M.; Helfand, M. *Gen. Intern. Med*. **2008**, 23, 2079.

14. (a) Holt, S.C.; L. Kesavalu, L.; Walker, S.; Genco. C.A. *Periodontol. 2000,* **1999**, *20*, 168-238. (b) Socransky, S. S.; Haffajee, A. D. *J. Periodontol*. **1992**, 63, 322-331.

15. (a) Al-Khafagee, N. S.; Al-Rubiae, F. M.; Witwit, L. J.; Al-Dahmoshi, H. O. *Int. J. Dent. Res. Dev*. **2013**, 3, 1-6. (b) Condorelli, F.; Scalia, G.; Cali, G.; Rossetti, B.; Nicoletti, G.; Lo Bue, A. M. *J. Clin. Microbiol*. **1998**, 36, 2322-2325.

16. Griffen, A. L.; Becker, M. R.; Lyons, S. R.; Moeschberger, M. L.; Leys, E. J. *J. Clin. Microbiol*. **1998**, 36, 3239-3242.

17. Wegner, N.; Wait, R.; Sroka, A.; Eick, S.; Nguyen, K.; Lundberg, K.; Kinloch, A.; Culshaw, S.; Potempa, J.; Venables, P. J. *Arth. Rheum*. **2010**, 62, 2662-2672.

18. Shapira, L.; Ayalon, S.; Brenner, T. *J. Periodontol*. **2002**, 73, 511-516.

19. Medzhitov, R. *Nat. Rev. Immunol*. **2001**, 1, 135-145.

20. (a) Medzhitov, R.; Preston-Hurlburt, P.; Janeway, C. A. *Nature,* **1997**, 388, 394-397. (b) Aderem, A.; Uleitch, R. J. *Nature,* **2000**, 406, 782-787.

21. Miranda-Hernandez, S.; Baxter, A. G. Am. *J. Clin. Exp. Immunol*. **2013**, 2, 75-93.

22. Fletcher, J. M.; Lalor, S. J.; Sweeney, C. M.; Tubridy, N.; Mills, K. H. G. *Clin. Exp. Immunol*. **2010**, 162, 1-11.

23. Hashimoto, M.; Asai, Y.; Ogawa, T. *Int. Immunol*. **2004**, 16, 1431-1437.

24. Nichols, F. C.; Housley, W. J.; O'Conor, C. A.; Manning, T.; Wu, S.; Clark, R. B. Am. J. Pathol. 2009, 175, 2430-2438.

25. Jain, S.; Coats, S. R.; Chang, A. M.; Darveau, R. P. *Infect. Immun*. **2013**, 81, 1277-1286.

26. Nichols, F. C.; Bajrami, B.; Clark, R. B.; Housley, W.; Yao, X. Infect. Immun. 2012, 80, 860-874.

27. Clark, R. B.; Cervantes, J. L.; Maciejewski, M. W.; Farrokhi, V.; Nemati, R.; Yao, X.; Anstadt, E.; Fujiwara, M.; Wright, K.T.; Riddle, C.; La Vake, C.J.; Salazar, J.C.; Finegold, S.; Nichols, F.C. *Infect Immun.* **2013**, 81, 3479-3489.

28. Farrokhi, V.; Nemati, R.; Nichols, F. C.; Yao, X.; Anstadt, E.; Fujiwara, M.; Grady, J.; Wakefield, D.; Castro, W.; Donaldson, J.; Clark, R. B. *Clin. Transl. Immunol*. **2013**, 2, 1-7.

29. Uchida, I.; Yoshida, K.; Kawai, Y.; Takase, S.; Itoh, Y.; Tanaka, H.; Kohsaka, M.; Imanaka, H. *J. Antibiot*. **1985**, 38, 1476.

30. (a) Kawai, Y.; Yano, I.; Kaneda K. *Eur. J. Biochem.* **1988**, 171, 73-80. (b) Kawai, Y.; Akagawa, K. *Infect. Immun*. **1989**, 57, 2086-2091. (c) Kawai, Y.; Kaneda, K.; Morisawa, Y.; Akagawa, K. *Infect. Immun*. **1991**, 59, 2560-2566.

31. Yoshida, K.; Iwami, M.; Umehara, Y.; Nichisawa, M.; Uchida, I.; Kohsaka, M.; Aoki, H.; Ianaka, H. *J. Antibiot*. **1985**, 38, 1469.

32. Nemoto, T. Ojika, M.; Takahata, Y.; Andoh, T.; Saagami, Y. *Tetrahedron*, **1998**, 54, 2683-2690.

33. Wang, Y.H.; Nemati, R.; Anstadt, E.; Liu, Y.; Son, Y.; Zhu, Q.; Yao, X.; Clark, R.B.; Rowe, D.W.; Nichols, FC. *Bone* **2015**, 81, 654-661.

34. Uchida, I.; Yosida, K.; Kawai, Y.; Takase, S.; Itoh, Y.; Tanaka, H.; Kohsaka, M.; Imanaka, H. *Chem. Pharm.* Bull. **1985**, 33, 424-427.

35. Murray, D. H.; Prokop, J. *J. Pharm. Sci.* **1965**, 54, 1468.

36. Shiozaki, M,; Deguchi, N.; Mochizuki, T. *Tet. Lett*. **1996**, 37, 3875-3876. (b) Shiozaki, M.; Deguchi, N.; Ishikawa, T.; Haruyama, H.; Kawai, Y.; Nishijima, M. *Tet. Lett*. **1998**, 39, 4497-4500. (c) Shiozaki, M.; Deguchi, N.; Mochizuki, T.; Wakabayashi, T.; Ishikawa, T.; Haruyama, H.; Kawai, Y.; Nishijima, M. *Tet*. **1998**, 54, 11861-11876.

37. Shioiri, T.; Terao, Y.; Irako, N.; Aoyama, T. *Tet*. **1998**, 54, 15701-15710.

38. Brooks, D. W.; Lu, L. D-L.; Masamune, S. *Angew. Chem. Int. Ed. Engl.* **1979**, 18, 72.

39. Takikawa, H.; Muto, S.; Nozawa, D.; Kayo, A.; Mori, K. *Tet. Lett*. **1998**, 39, 6931-6934.

40. Holmquist. C. R.; Roskamp, E. J. *J. Org. Chem.* **1989**. *54*, 3258-260.

41. (a)Mun, J.; Onorato, A.; Nichols, F.C.; Morton, M.D.; Saleh, A.I.; Welzel, M.; Smith, M.B. *Org. Biomol. Chem.* **2007***, 5*, 3826-3833. (b) Shioiri, T.; Irako, N. *Tetrahedron* **2000**, 56, 9129-9142.

42. (a) Bobbitt, J.M.; Flores, M.C.L. *Heterocycles* **1988***, 27*, 509. (b) Ma, Z.; Bobbitt, J.M. *J. Org. Chem.* **1991**, *56*, 6110.

43. (a) Sugai, T.; Ohta, H. *Tetrahedron Lett.* **1991**, *32*, 7063-7064. (b) Sugai, T.; Ritzén, H.; Wong, C.H. *Tetrahedron: Asymmetry* **1993**, *4*, 1051.

44. Takikawa, H.; Nozawa, D.; Kay, A.; Muto, S.-e.; Mori, K. J. *Chem. Soc., Perkin Trans. I* **1999**, 2467-2477.

45. (a) Dale, J. A.; Dull, D. L.; Mosher, H. S. *J. Org. Chem*. **1969**, 34, 2543–2549. (b) Dale, J.A.; Mosher, H.S. *J. Am. Chem. Soc.* **1973**, 95, 512-519.

46. Borthwick, A.D. *Chem. Rev*. **2012**, 3641-3716.

47. Shute, R. E.; Rich, D. H. J. Chem. Soc., *Chem. Commun*. **1987**, 15, 1155-1156.

48. Lovric, M.; Cepanec, I.; Litvic, M.; Bartolincic, A.; Vinkovic, V. *Croatica Chemica Acta CCACAA* **2007**, 80, 109-115.

49. Dietz, C.; Hart, T. K.; Nemati, R.; Yao, X.; Nichols, F. C.; Smith, M. B. *Tetrahedron*, **2015**, 72, 7557-7569.

50. (a) Bergbreiter, D. E.; Whitesides, G. M. *J. Org. Chem*. **1975**, 40, 779-782. (b) Cahiez, G.; Chaboche, C.; Jezequel, M. *tetrahedron* **2000**, 56, 2733-2737.

51. Rishi G.; Vaswani, A.; Chamberlin, R. *J. Org. Chem.* **2008**, 73,1661-1681.

52. Bartoli, G.; Antonio, G. D.; Fiocchi, R.; Giuli, S.; Marcantoni, E.; Marcolini, M. *Synthesis* **2009**, 6, 951-956.

53. Kiviranta, P.H.; Leppaenen, J.; Rinne, V.M.; Suuronen, T.; Kyrylenko, O.; Kyrylenko, S.; Kuusisto, E.; Tervo, A.J.; Jaervinen, T.; Salminen, A.; Poso, A.; Wallen, E.A.A. *Bioorg. Med. Chem. Lett.* **2007**, 17, 2448-2451.

54. Kim, H.I.; Graupe, M.; Oloba, O.; Koini, T.; Imaduddin, S.; Lee, T.R.; Scott S. Perry, S.S. *Langmuir* **1999**, 15, 3179-3185.

55. (a) Stein, J.; Budzikiewicz, H. *Zeit. Naturforschung, B* **1987**, 42, 1017-1020.

56. Irako, N.; Shioiri, T. *Tetrahedron Lett.* **1998**, 39, 5793-5796.

57. Bowler, J.; Lilley, T. J.; Pittam, J. D.; Wakeling, A. L. *Steroids* **1989**, 54, 71–99.

58. Savile, C. K.; Reed, D. W.; Meesapyodsuk, D.; Covello, P. S.; Buist, P. H. J. *Chem. Soc., Perkin Tran*s. **2001**, 1, 1116-1121.

59. Veken, B. J. van der; Odeurs, R.O.; Brown, A.; Mckean, D. C.; Morrisson, A. R. *J. Mol. Str.*, **1986**, 147, 57-66.

60. (a) Jorapur, Y. R.; Chi, D. Y. *J. Org. Chem*. **2005**, 70, 10774-10777. (b) Chandrasekhar, S.; Shyamsunder, T.; Chandrashekar, G.; Narsihmulu, C. *Synlett* **2004**, 3, 522- 524.

61. Paul, B.; Das, D.; Ellington, B.; Marsh, E. N. G. *J. Am. Chem. Soc*. **2013**, 135, 5234-5237.

62. Mai, A.; Rotili, D.; Tarantino, D.; Ornaghi, P.; Tosi, F.; Vicidomini, C.; Sbardella, G.; Nebbioso, A.; Miceli, M.; Altucci, L.; Filetici, P. *J. Med. Chem*. **2006**, 49, 6897-6907.
63. Steve Oh, M.S. *Slideshow: A Visual Guide to Multiple Sclerosis* WebMD, 2005, Reviewed April 13, 2016.

Synthesis of Nitroimidazole Indocyanine Green Dye Conjugates for Targeting Hypoxia in Tumor Cells for Near Infrared Fluorescence Frequency Domain Optical Tomography

2.1 Introduction

2.1.1 Cancer

In 2016 there is an expected 1.6 million new cases of cancer and nearly 600 thousand cancer deaths, which contributes to the second most common cause of death in the United States.[1] Cancer refers to over a hundred different diseases that are characterized as abnormal and unregulated cell growth. Cells in the human body are constantly being recycled by programmed cell death, apoptosis, and then replaced by cellular division. Of the estimated 100 trillion cells in an average adult, 50-70 billion cells are turned over each day. Within this process there is a probability of reproductive error, which can develop damaged DNA or gene mutations that leads to cancer. Some of the main causes include UV/nuclear radiation, carcinogenic chemicals, infections, internal factors, and poor health.

Commonly, a cell has a mechanism in place to correct mutations by either fixing the damaged DNA, or triggering apoptosis so the cells cannot multiply. When this fails, defective genes are passed on and the cells begin to multiply at an uncontrollable rate. These cells form abnormal growths in tissues called neoplasms, or more often referred to as tumors. Tumors show "the six hallmarks of cancer": evading apoptosis, sell-sufficiency in growth signals, insensitivity to anti-growth signals, tissue invasion and metastasis, limitless replicative potential, and sustained angiogenesis.[2] Over time, the tumor cells develop malignancy and obtain the ability to metastasis

to other parts of the body through blood vessels or the lymph system. Once cancer has the ability to migrate throughout the body, it is considered stage 4 cancer and chances of remission drastically decrease.[3] For this reason, tumor detection and eradication is of utmost concern in the fight against cancer.

2.1.2 Tumor Hypoxia

Once tumors grow to between 2-3 mm in size, they start to develop a tumor-specific microenvironment due to quick and uncontrolled growth. The growths are said to be hypoxic as low oxygen levels, pH, and glucose concentration are observed.[4] Tumor hypoxia is a direct result from the accelerated growth rate of cancer cells not allowing for proper angiogenesis, blood vessel formation. Without proper blood flow, oxygen levels and nutrient supplies diminish compared to healthy tissues. Mutated cells have the ability to adapt by altering their metabolism to the environment but healthy cells do not and will eventually die.

The cancer cells left in the hypoxic region start to exhibit a slow growth rate due to rapidly proliferating distal cancer cells not allowing the profusion into the tumor. This decrease in profusion often causes ineffectiveness of common chemotherapy drugs.[5] Alternatively, radiation therapy is used to produce reactive oxygen species within the cells that will damage DNA and lead to cell death. However, hypoxia decreases the effectiveness due to low oxygen concentration. The longer a tumor remains, its resistance to anticancer drugs and the probability of the cells gaining the ability to metastasis will increase. For this reason, determining if a tumor is hypoxic and monitoring the effectiveness of chemotherapy or radiation treatments is vital to the fight against cancer.

2.1.3 Detecting & Imaging Hypoxia

The ineffectiveness of chemotherapy regimens and radiotherapy on hypoxic tumors creates the demand for safe procedures for detection and monitoring of such growths. Invasive procedures were among the first diagnostic tools for sampling tissues from infected areas and are still used on a limited basses today. Polarographic oxygen microelectrodes can be inserted into the tumors to directly quantify the levels of hypoxia from measuring partial pressure of oxygen.[4,6] However, they are limited only to accessible tumors, mainly on surface areas of the body, such as cervix, head, and neck tumors.[7]

Non-invasive procedures offer alternatives to hypoxia imaging and are not limited to depth of the tumors while also being inherently safe measurements. Magnetic resonance imaging (MRI) and positron emission tomography (PET) are techniques that allow physicians to visualize tissue properties. To date, recent advances have allowed for the ability of both PET and MRI imaging to simultaneously scan for tumors within the body.[8] This allows more accuracy in treatment planning, monitoring, and evaluation of response to radiation therapy.

PET imaging can be used for measuring several metabolic processes in the body associated with tumor growth.[9] Most commonly, a 3-dimensional detector is used to measure gamma rays that are emitted by a exogenous tracer. The tracer is injected into the body and the detector measures its concentration as it localizes in the body. The structure of the tracer dictates what biological activity or function can be measured. The most common method for measurement of hypoxic tissue uses tracers encompassing nitroimidazoles. 2-nitroimidazole is

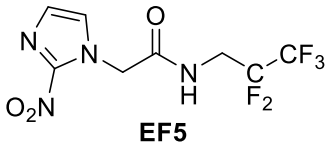

EF5

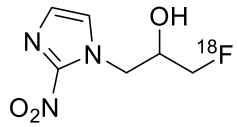

^{18}F-FAZA

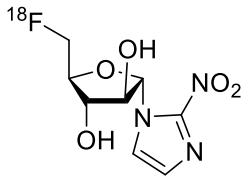

^{18}F-FMISO

known to undergo intracellular metabolism in which a nitroreductase reduces the nitro moiety. The reduced compound can then bond with proteins within the cell, and as a result increases the retention time. The reverse reaction is directly dependent on the oxygen concentration and is minimal in hypoxic environments.[10] Examples of the tracers are shown. The F-18 labeled derivative of EF5 is being studied for its effectiveness to study brain tumors due to its propensity to cross the blood brain barrier.[11] The other two derivatives, ^{18}F-FAZA and ^{18}F-FMISO, take advantage of their high levels of biodiversity that makes it easy to get into tumor cells. As the metabolism progresses, the compound will concentrate in hypoxic tissue and release positrons that will build a picture of the tumor with PET imaging.

MRI is a type of imaging that takes advantage of the science of nuclear magnetic resonance (NMR). When some atomic nuclei are applied to a magnetic field they can absorb and emit distinct radio frequencies. Based on the frequency, a conclusion can be drawn about the environment of the atomic nuclei is in. MRI scans take advantage of the abundance of NMR active hydrogen nuclei in the body. Mostly, the hydrogen atoms in the body exist in water and fat molecules. As a result, MRIs can image the microanatomy of a tissue and distinguish the density or organization of intra/extracellular space that is indicative of tumor growth.[12] Contrast agents can also be introduced to the body that can measure blood flow as it relates to permeability and perfusion. Hypoxic tumors can be indirectly illuminated by such contrast agents due to their poor vascular network and densely distributed cellular network.

Both non-invasive procedures discussed are widely used, however they do inherently possess some disadvantages and limitations. Some of these include as unfavorable imaging characteristics, such as high background counts and limited contrast ratio from hypoxic tumors to

normal tissues. Also, the high cost of these procedures make in unfeasible for routine imaging and drives the need for a cheap, safe, and non-invasive alternative.

Optical imaging is a non-invasive, low cost, and extremely safe alternative biological imaging. Near infrared (NIR) frequency domain optical tomography (FDOT) offers a highly sensitive technique for imaging targets within the body. A NIR fluorescent probe is administered, and the irradiation with NIR light allows for the collection of the emitted fluorescence signals from the fluorochrome. PET tracers are limited to a single decay event per molecule for imaging. A single fluorescent probe can produce absorb and emit nearly a hundred million photons per second for imaging. The released fluorescence signals are collected by detectors or a charge coupled device (CCD) camera for construction of the 3D imaging. The near-Infrared window of 650 to 900 nm allows for maximum depth penetration of light because there is minimal absorbance and high scattering by biological tissue. Hemoglobin and water are the major contributors of light absorption within the body. Figure 5 demonstrates the fact that absorbing factors are at a minimum in the NIR range. This technique is capable of imaging targets at depths up to several centimeters from the skin surface. It is noteworthy that bone and muscular tissues do slightly diminish the penetration of light. However, several studies demonstrated the ability of NIR fluorochromes to be coupled with targeting agents to efficiently

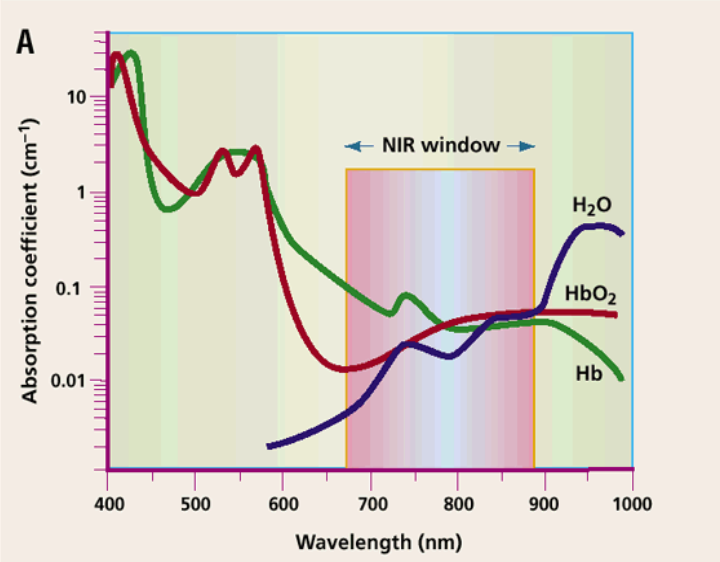

Figure 5. NIR window for optical imaging[13]

image receptors.[13] The main difficulty is developing a fluorescence dye and altering it with targeting moieties, to effectively image hypoxic tissue.

2.1.4 The Combination of Indocyanine Green Dye and Nitroimidazole for Optical Imaging

Indocyanine green (ICG) is the only FDA approved fluorescence imaging agent for patient use. It is used for determining the function of cardiac and hepatic processes as it readily binds to plasma in the blood. The application of ICG is hindered slightly by the problems of a low quantum yield and quick loss of fluorescence after binding to proteins in circulating blood.[14] However, its low toxicity and easy wash out rates gives ICG the ability to be a suitable scaffold for a fluorescence probe to be tailored towards targeting hypoxic tumors.

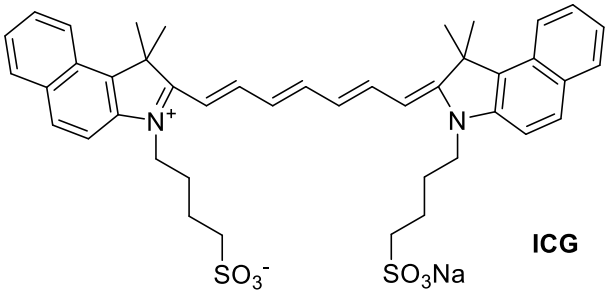

Nitroimidazole derivatives have been used as common moieties when targeting hypoxic cells of an organism since its potential was discovered by Varghese *et al.*[15] Specifically, 2-nitroimidazole has been incorporated into several radiosensitizers and hypoxia targeting prodrugs.[16] The sensitivity towards hypoxic cells is attributed to an enzyme mediated reduction of the nitro group by nitroreductase enzymes in the absence of oxygen. The reduction potentials for nitroimidazoles are shown in figure 6. 2-Nitroimidazole inherently has the highest reduction potential and therefore is the most widely used to target hypoxic cells. This

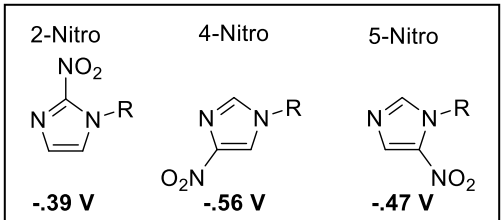

Figure 6. Reduction Potentials of Nitroimidazoles

reduced imidazole ring is susceptible to nucleophilic addition from cellular macromolecules to form long lasting binding adducts. The proposed mechanism for hypoxia specificity is shown in part a of figure 7.

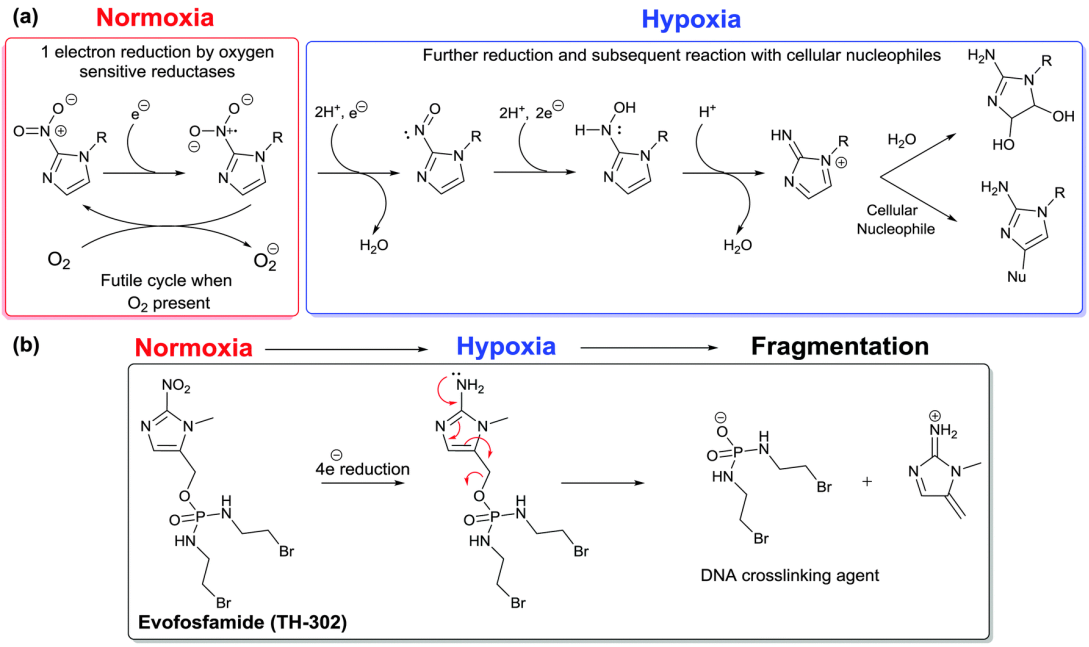

Figure 7. Mechanism proposed for 2-nitroimidaze selectivity towards hypoxic cells.[17]

Studies *in vivo* reveal the sensitivity towards hypoxia of 2-nitroimidazole is due to the bioactive reduction is dependent on oxygen concentration. In a normoxia environment the initial one electron activation reduction to a nitro radical is in competition with reverse reaction of O_2 oxidation. The reaction is highly reversible and high oxygen concentrations dictates the equilibrium between the two reactions making further reduction impossible because oxidation back to the parent nitro compound is inevitable. In Hypoxia, nitro radicals are further reduced by a nitroreductase to the nitroso derivative, and eventually to the hydroxyl-amine. Acid catalyzed dehydration creates a cyclic imine that is susceptible towards binding of certain nucleophilic proteins and locking the compound within the cell. A specific enzyme for the reductions is

unknown, however one-electron reductases such as NADPH–nitroreductases, NADPH–cytochrome P450 reductase, cytochrome b5 reductase, aldehyde dehydrogenase, and xanthine oxidase, and two-electron reductases such as DT-diaphorase have been acciociated.[18]

With a suitable fluorophore, nitroimidazole can be used to deliver and retain a fluorescent probe in hypoxic cells. ICG lacks a reactive functional group that can efficiently couple with targeting agents. Fortunately the development of ICG bis-carboxylic acid (**1**) has been achieved, while retaining all desirable characteristics of the parent ICG dye.[19] Figure 8 shows how the carboxylic acid derivative can be built upon to increase its sensitivity towards hypoxic cells.

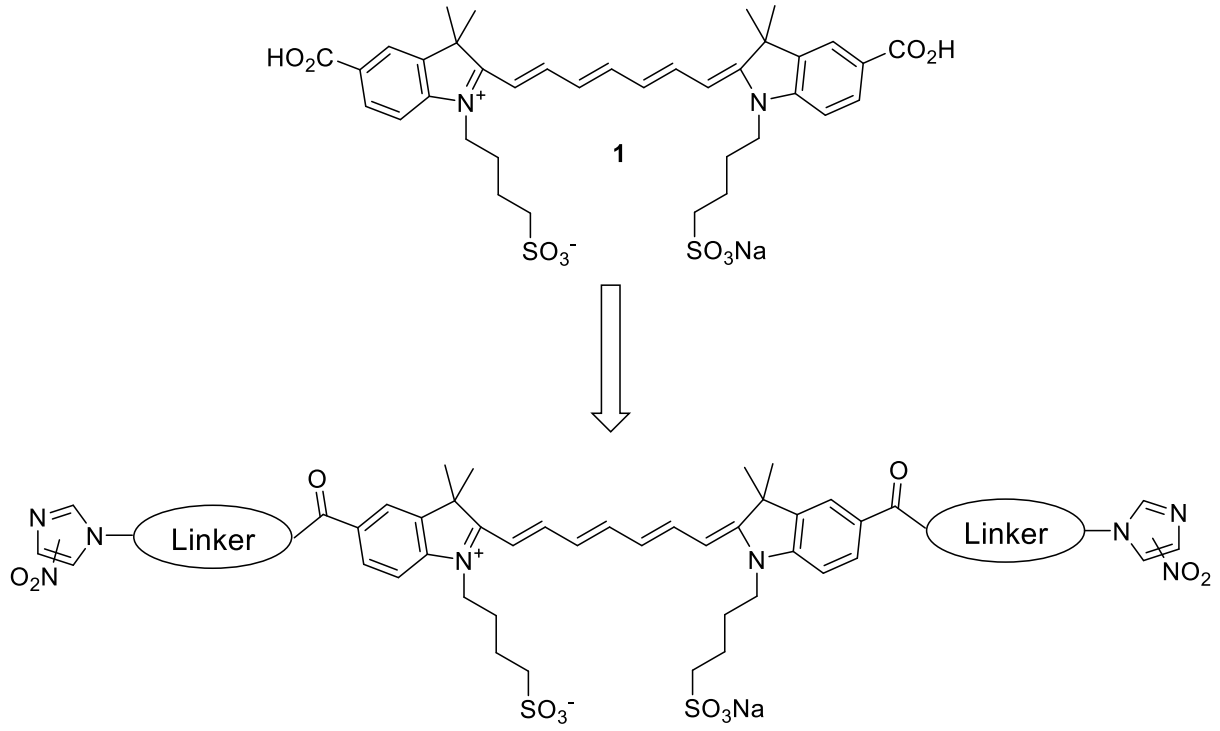

Figure 8. Proposed Structure for Fluoresence Hypoxia Probe

2.1.5 Development of ICG Dye Conjugates

The Smith group has developed a method for coupling nitoimidazoles to ICG bis-carboxylic acid **1**. Connecting the two fragments together with an appropriate linker was of the first priority. The first-generation protocol involved the incorporation of an ethanolamine linker in route to synthesizing dye conjugate (**2**).[20]

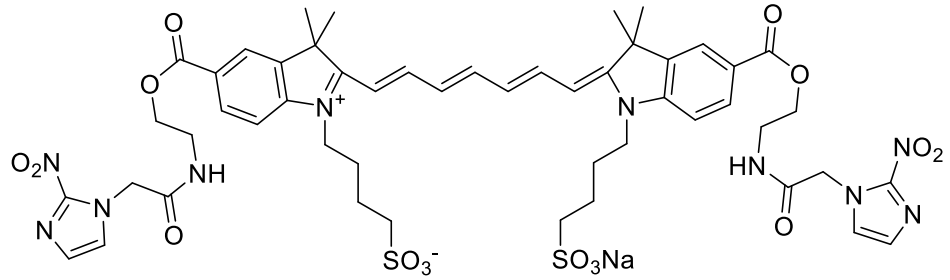

2-nitroimidazole ethanolamine (2)

The first generation targeted fluorophores showed great sensitivity in breast cancer cells treated under hypoxic conditions *in vitro*.[21] The cells fluorescence intensities were integrated to revealed a ratio between hypoxia per normoxia conditions are 2.5 for 2-nitroimidazole (**2**) treated cells and 1.2 for ICG (**1**) treated cells. These results were also verified *in vivo* using a murine model, which involved 4TI mammary cancer cells grown in balb/c mice.[22] The targeted dye **2** displayed a two-fold higher fluorescence at the hypoxic tumor site when compared to normal sites. Hypoxic sights showed no difference in flouresence when treated with the untargeted dye **1**. It is also noteworthy for later discussion that the 4-nitroimidazole derivative of **2** revealed minimal differences in fluorescence at the tumor when compared to the nomoxia tissues. An attempt to increase the bioavailability of the dye lead to the development of a "2nd generation dye conjugate" (**3**).[23]

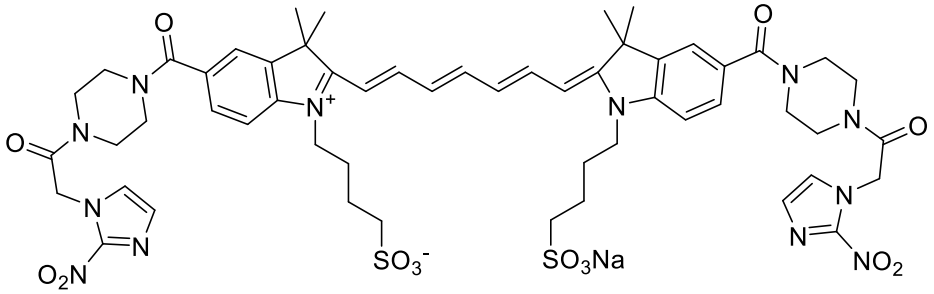

2-nitroimidazole piperazine ICG (3)

The linker of **3** was changed to a piperazine ring instead of the presumed to be labile ethanolamine linker used previously. The new linker is not believed to exhibit any direct influence on the targeting of hypoxia. However, the more robust piperazine moiety is presumed to be more metabolically stable because of the two secondary amide linkages. Increasing the number of carbon atoms and diminishing the polarity slightly, leads to greater solubility in tissue. We presume that for these reasons, the bioavailability is greatly increased. This increased bioavailability leads to a higher probability of the 2-nitroimidazole dye conjugate to perfuse into hypoxic cells, undergoing enzymatic reduction, and irreversibly binding to macromolecule nucleophiles. Since the reduction is selective towards hypoxia, this leads to an enhanced fluorescence intensity in cancerous tumors compared to other tissues. When compared *in vivo*, the fluorescence intensity of **3** was measured to be twice that of **2** in the tumor tissue (figure 9).[23]

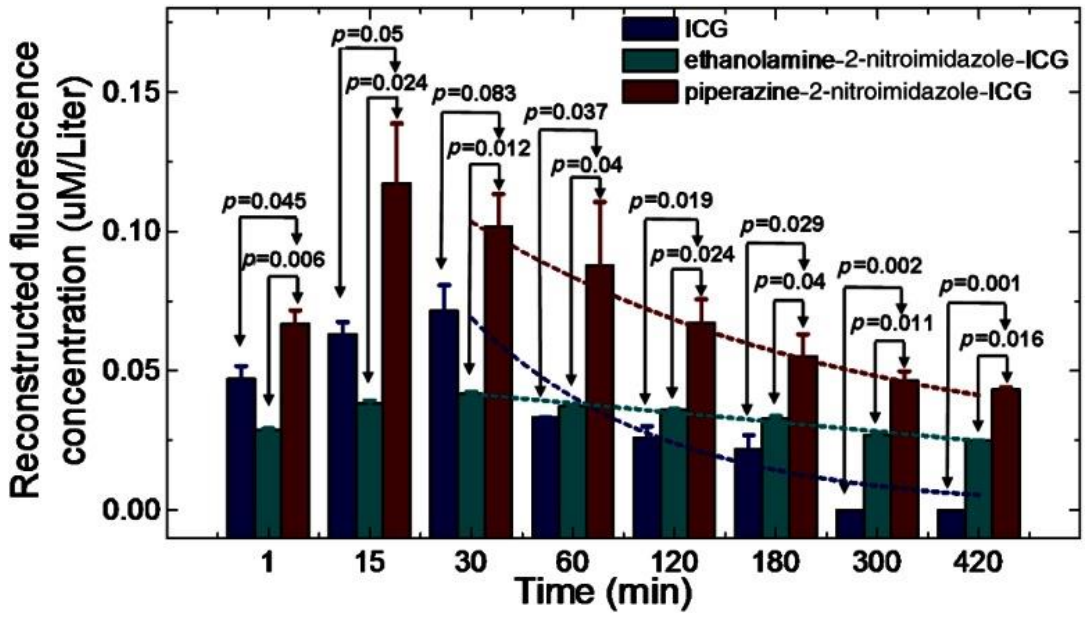

Figure 9. Fluoresence Intensity of 1st and 2nd Generation Dyes in Hypoxic Tumors

This work has demonstrated the effectiveness of coupling the fluorophore ICG with a known hypoxia-targeting agent to optically image cancerous tumors. Table 1 displays the optical properties of the synthesized dyes and comparison to the parent FDA approved ICG. The wavelengths of absorbance and emission all fall into the desired window for imaging human tissue. However the quantum yield, the ratio of emitted photons to absorbed photons, is considered very low in all cases. The introduction of the piperazine linker did slightly increase the quantum yield, but the dye conjugate is still low. This diminished florescent yield leads to the requirement of higher doses of dye for proper imaging. In addition, the toxicity of the dye conjugate is unknown.

The depth at which the dye conjugates can image will also be effected since the dye itself will inherently lose a large percentage of photons. For these reasons, there is a need for improvement upon the system.

Dye	λ_{abs} (nm)	λ_{em} (nm)	Extinction Coefficient ($M^{-1}cm^{-1}$)	Quantum Yield (Φ)
FDA approved ICG	780	807	115,000	0.0120
ICG bis-carboxylic acid (**1**)	755	790	220,920	0.0728
2-Nitroimidazole-ethanolamine-ICG (**2a**)	760	790	159,141	0.0420
2-Nitroimidazole-piperazine-ICG (**3**)	760	790	229,543	0.0825

Table 1. Optical Properties of ICG, ICG bis-carboxylic acid, and 1st & 2nd Generation Dye Conjugates

2.2 Results & Discussion

2.2.1 Synthesis of Nitroimidazole Piperazine ICG Dye Conjugates

With the aim of optically imaging hypoxic tissues that are indicative of cancerous tumors, our lab set out a goal of linking nitroimidazole, a known hypoxia targeting agent, to an indocyanine green (ICG) dye, which is a FDA approved fluorophore used as a medical diagnostic tool. Using a targeting moiety on a dye allows for selective imaging of desired regions while avoiding healthy tissues. The main priorities of the project include: (1) coupling the two compounds together with a linker that is stable in a biological system, (2) insure that the fluorescence properties of the dye remain useful, and (3) the nitroimidazole moiety is still efficient in targeting hypoxic cells.

To achieve the first priority, our lab identified ICG bis-carboxylic acid (**1**) as a suitable candidate to link with the targeting agent. It was first synthesized by *Lindsey et al* and the dye-conjugate showed great retention of optical properties, with a 5-fold increase of quantum yield, when compared to its parent compound ICG.[19a] The two carboxylic acid groups give a worthy branching point to which the targeting agent can be coupled. Our synthesis is shown in scheme 10.

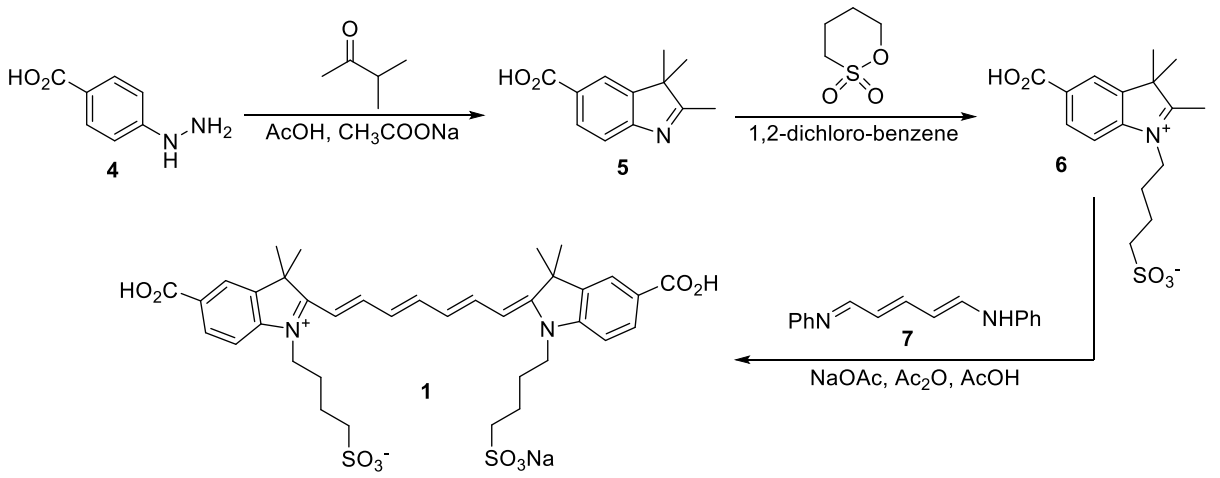

Scheme 10. Synthesis of ICG bis-carboxylic Acid (**1**)

Compound **1** was prepared by a straightforward synthesis as it was previously reported by Lindsey et al.[19a] Starting with commercially available *p*-hydrazinobenzoic acid (**4**), treatment with 3-methyl-2-butanone gave indole **5**, via a Fischer indole synthesis. Subsequent heating at reflux with butanesultone in 1,2-dichlorobenzene gave a zwitterion **6**. The assembly of dye **1** was completed by condensation of two equivalents of **6** with the commercially available glutacondianil hydrochloride (**7**). The synthesis of ICG bis-carboxylic acid (**1**) has a 55% overall yield through 3 steps and is routinely completed in gram scale.

To produce the target dye we envisioned a convergent synthesis in which the targeting agent is connected to the linker and then coupled together with dye **1**. The preparation of the targeting agent portion is shown in scheme 11.

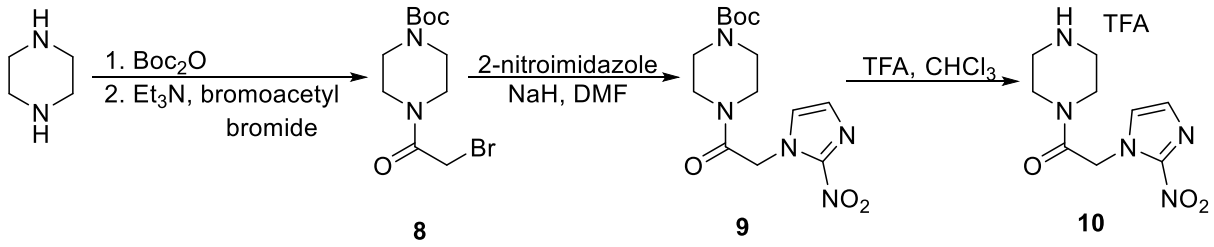

Scheme 11. Synthesis of 2-nitroimidazole Piperazine Fragment (**10**)

When designing this portion of the synthesis the main concern was to carry the expensive 2-nitroimidazole through as few synthetic steps as possible. Building upon the linker was therefore a logical plan compared to linearly from the imidazole ring. Stoichiometric protection of piperazine with di-*tert*-butyl dicarbonate gave half protected Boc-piperazine via a literature protocol.[24] Subsequent acyl substitution of the free amine with bromoacetyl bromide gave **8**. Coupling the 2-nitroimidazole linker was achieved via S_N2 of the primary halide to produce compound **9**. Deprotection of the Boc protected amine was achieved by stirring with trifluoroacetic acid, followed by crystallization to produce TFA salt **10** in a 27% yield from piperazine.[25]

The TFA salt **10** was coupled to ICG dye **1** using PyBOP as the coupling reagent. BOP reagents have demonstrated great efficiency when coupling secondary amino groups to acids and ByBOP is specifically used to minimize the amount of hazardous biproducts.[26] The synthesis is shown in scheme 12, producing 2-nitroimidazole-piperazine-ICG (**3**) in 28% yield.[27]

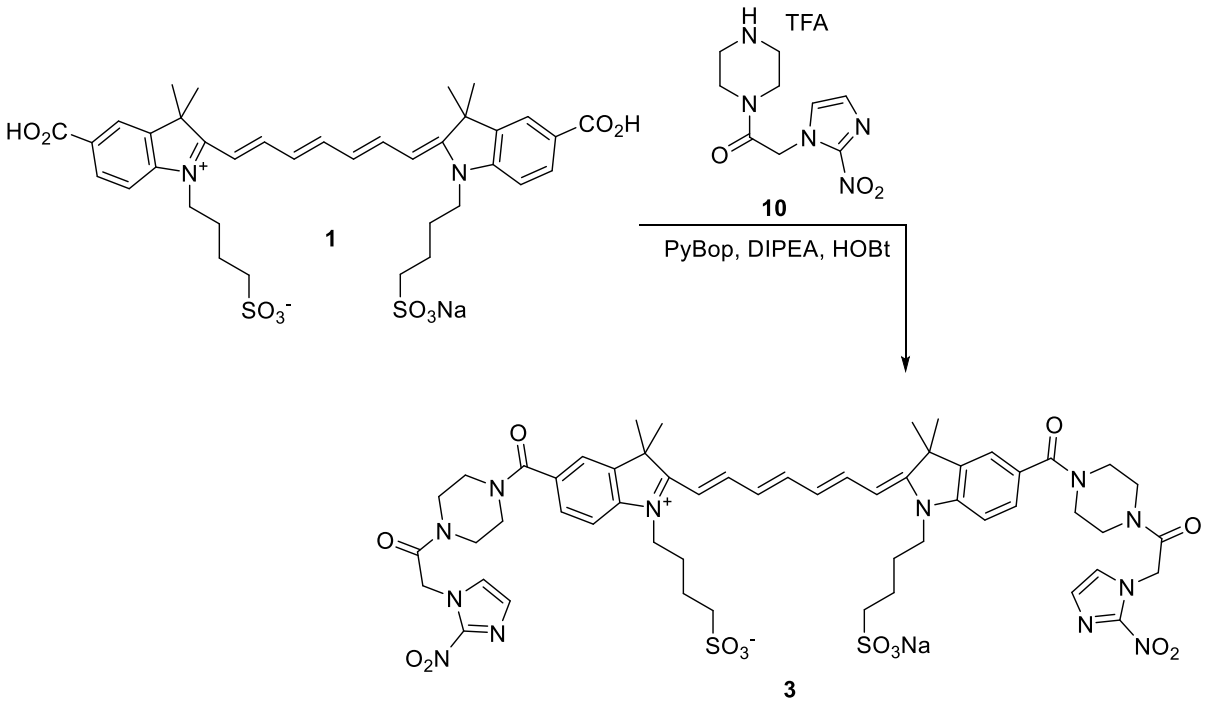

Scheme 12. Synthesis of 2-Nitroimidazole Piperazine ICG (**3**)

The low yield of the coupling procedure is due to the production of half loaded dye (single equivalence of **10** coupling to **1**) and the extreme difficulty of purification. Both the half loaded and fully loaded dyes exist in a mixture of rotational isomers that elute off of reverse phase columns in a wide overlapping range. For this reason multiple purification attempts are needed in small scales to achieve pure material. This is a problem that has yet to be solved. With an extreme amount of effort we managed to purify a large quantity of mostly pure material for toxicity testing. The results are expected in the near future, however stress tests did show minimal discomfort in mice injection experiments.

With the costly price of 2-nitroimidazole, $354.00 per gram (Sigma-Aldrich CAS=527-73-1), and the low yields in mind, our lab set out to try and produce the cheaper fluorescence dye **13**. Using 4-nitroimidazole, $1.86 pure gram (Sigma-Aldrich CAS=3034-38-6), should greatly decrease the cost. A literature search revealed that the 4-nitro does still retain hypoxia targeting properties with a minimal decrease in efficiency, but there is some concern of increased toxicity.[28] Scheme 13 displays the synthesis of 4-Nitroimidazole Piperazine ICG (**12**).

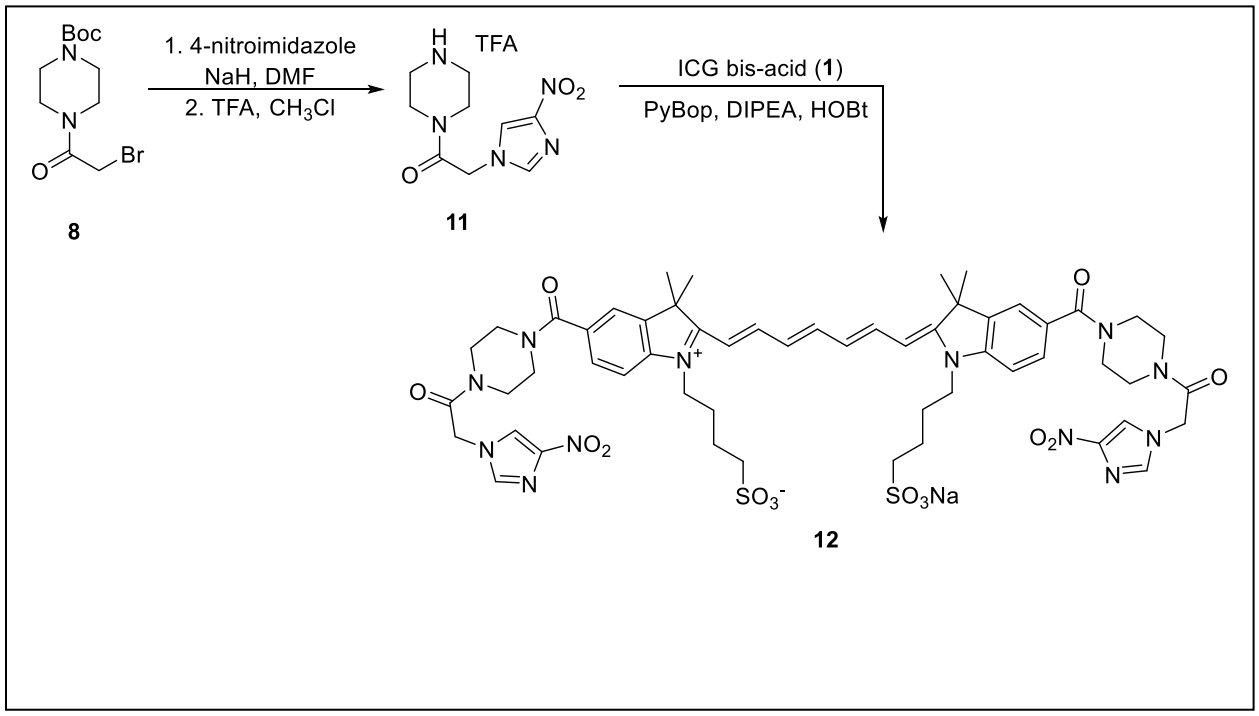

Scheme 13. Synthesis of 4-Nitroimidazole Piperazine ICG (**12**)

Dye Conjugate **12** was synthesized in the identical straight forward manner as known targeting dye **3** with similar yields.[29] The only difference is the incorporation of 4-nitroimidazole instead of 2-nitroimidasole. The two dyes used for *in vivo* studies to test the hypothesis that 4-nitroimidazole will still target hypoxic cells. For good measure, a control dye, a derivative with just imidazole linked to ICG, was synthesized to analyze the effect of having no targeting moiety on our synthetic dyes. The lack of a nitro group would create a unsuitable substrate for macromolecule binding within the cell. Scheme 14 shows the synthesis of imidazole-piperazine-ICG (**14**), a non-targeting second generation dye.

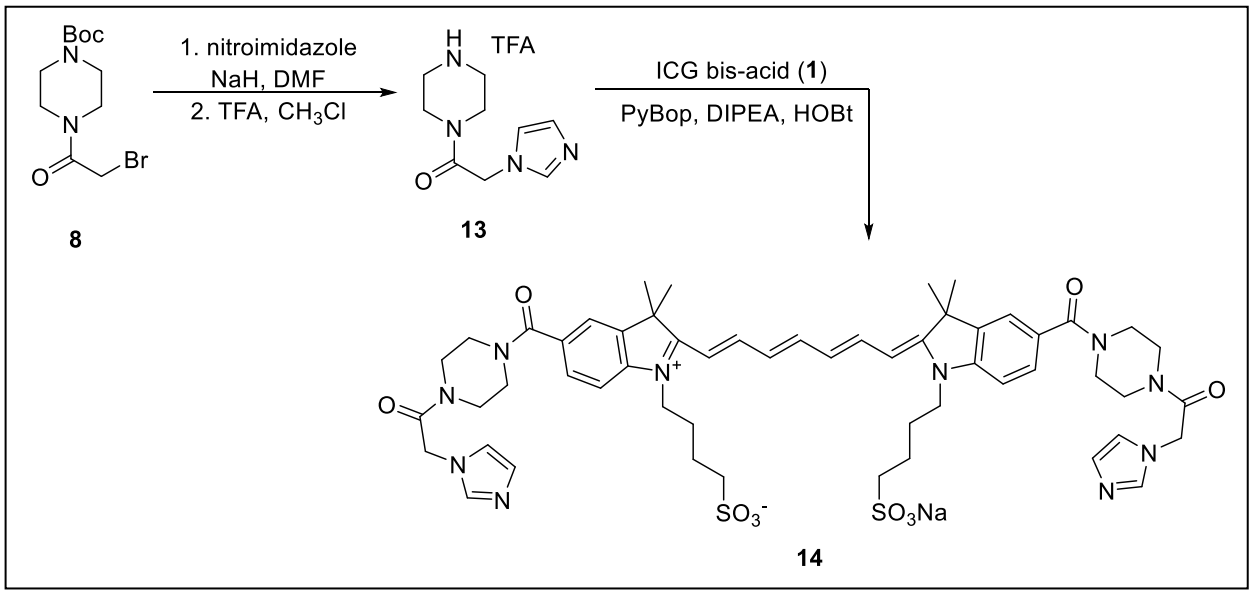

Scheme 14. Synthesis of imidazole-piperazine-ICG (**14**)

Again the synthesis followed identical synthetic methodology with just the substitution of imidazole to couple with the linker.[29] The only modification in the procedure was the duration of time and stoichiometry in which we allowed the substitution reaction of imidazole with intermediate **8**. The absence of a nitro moiety on the imidazole ring displayed a higher reactivity of the second nitrogen and yielded undesired di-substituted imidazole. Stirring the reaction for a shorter amount of time and increased equivalence of imidazole gave the proper substitution. Coupling of **13** with synthetic **1** produced ICG dye conjugate **14** to be used as a control for optical imaging experiments.

2.2.2 Hypoxia Targeting Evaluation of Nitroimidazole Piperazine ICG Dye Conjugates

Upon completion of the synthesis of the second generation dyes, *in vivo* testing was done in mice with hypoxic tumors.[29] The protocol used a murine model, which involved 4TI mammary

cancer cells grown in balb/c mice. The tumors were grown on top of the right leg until diameter was approximately 7-8 mm. All injections were administered intravenously through retro-orbital venous sinus. The tumor was then imaged at designated time intervals and the measured fluorescence intensity for each imaging experiment were averaged and compared.

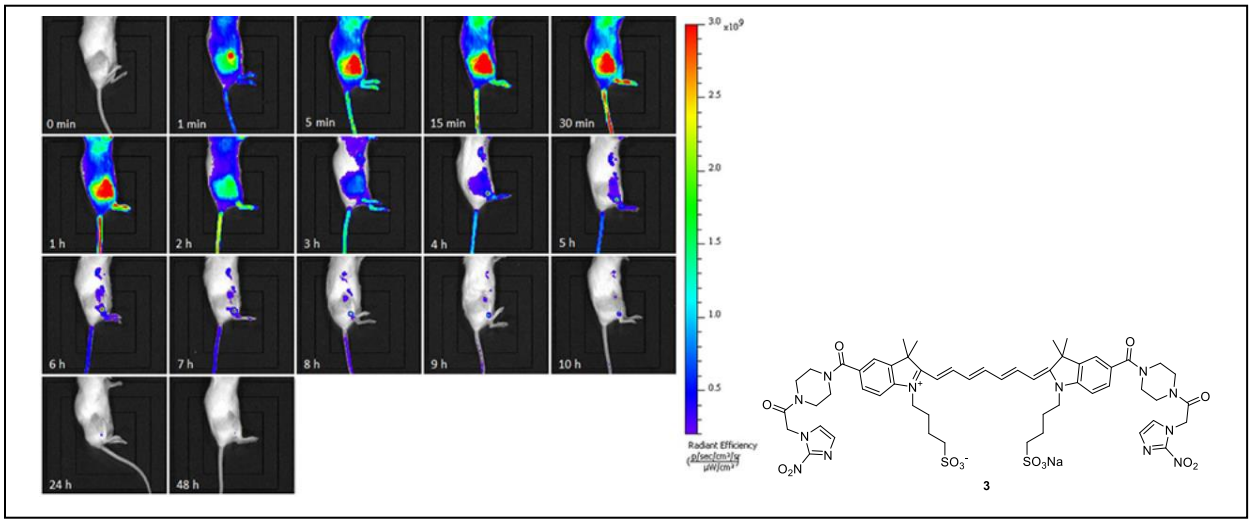

Figure 10. *In vivo* Fluorescence of 2-Nitroimidazole-Piperazine-ICG (**3**)

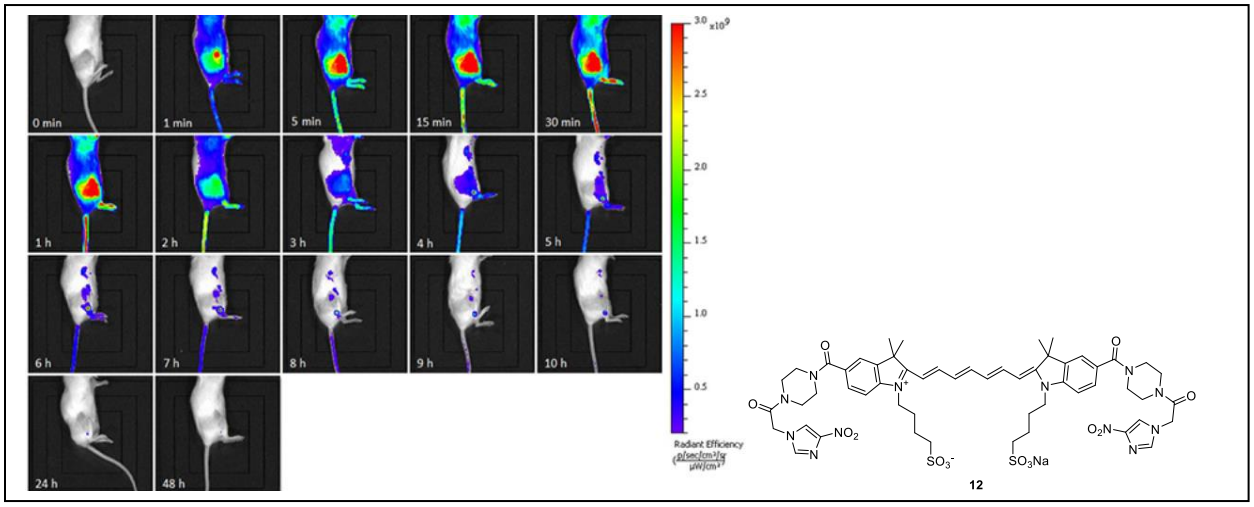

Figure 11. *In vivo* Fluorescence of 4-Nitroimidazole-Piperazine-ICG (**12**)

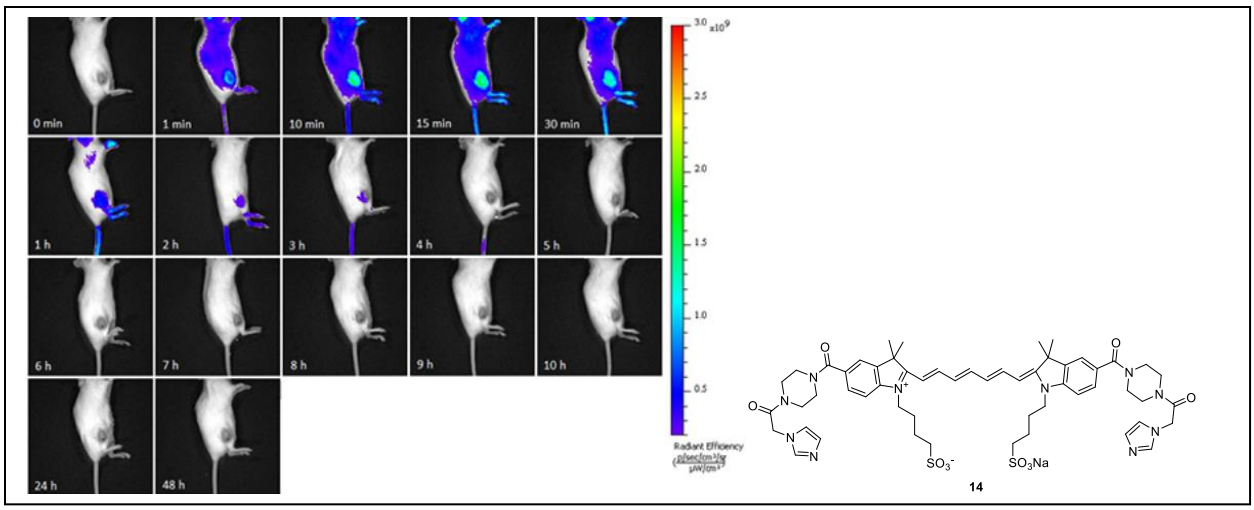

Figure 12. *In vivo* Fluorescence of Imidazole-Piperazine-ICG (**14**)

Figures 10, 11, and 12 shows images obtained over 48 h post injection of ICG dye conjugates **3**, **12**, and **14** respectively. Each image is averaged fluorescence distribution of a mouse injected with 100 μL of a 25 μM concentration of designated dye. The images show rapid uptake of the dye-conjugates in the tumor, as well as widespread distribution in the mouse. Washout rates in each case are rapid throughout the body, however **3** and **12** are retained in the tumor for a prolonged time relative to **14**. This is indicative of the need for a nitroimidazole moiety to target and irreversibly bind to hypoxic cells. Interestingly with identical injection concentrations, **12** appears to accumulate and retain in the tumor at higher concentrations for longer amount of time compared to **3**. Figure 13 is a graphical example of the maximum radiant efficiency for **3**, **12**, and **14** within the tumors vs. time. This is an aim to demonstrate the wash out rates of the three dye conjugates.

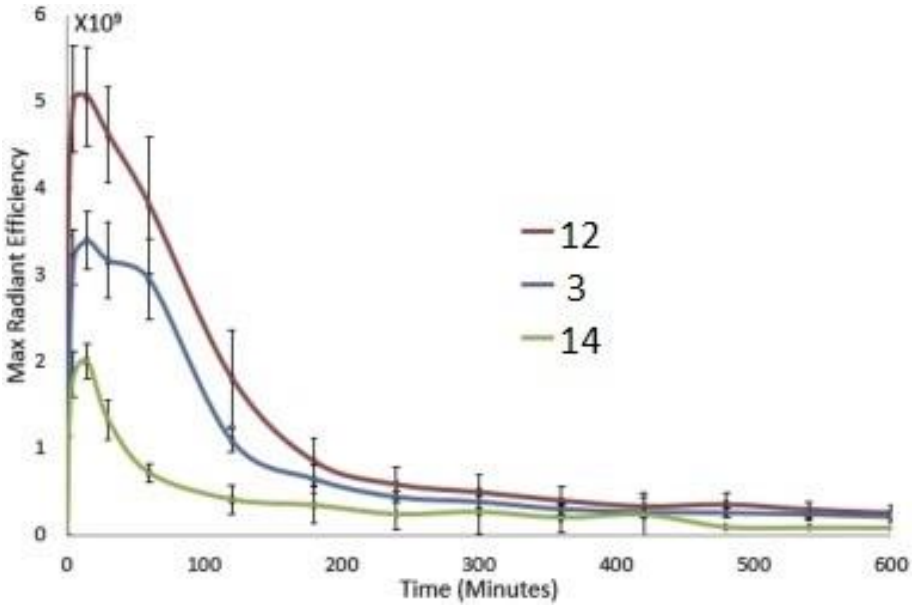

Figure 13. Graphical Representation of Maximum Radiant Efficiencies for 2nd Generation Dye Conjugates Over Time

The in vivo imaging reveals that all three dye conjugates go into the tumors extremely fast, therefore displaying a high level of biodiversity. The maximum intensity for imaging is around 15 minutes. Non-targeted dye **14** washes out of the tumor extremely fast as expected due to a lack of a binding potential. Targeted dyes **3** and **12** seem to wash out of the tumors at similar rates. This is most likely due to the cellular metabolism being identical for bound ICG dye conjugates. 4-Nitroimidazole-piperazine-ICG (**12**) has a higher fluorescence intensity in the tumor with the same injection volume and concentration when compared to 2-nitroimidazole-piperazine-ICG (**3**). Since the quantum yield of **12** is slightly lower then **3**, it implies that the 4-nitro derivative is actually slightly better at targeting hypoxia in our fluorescence probe system. The optical properties of all three second generation dyes are shown in Table 2.

Dye	λ_{abs} (nm)	λ_{em} (nm)	Extinction Coefficient ($M^{-1}cm^{-1}$)	Quantum Yield (Φ)
FDA approved ICG	780	807	115,000	0.0120
ICG bis-carboxylic acid (**1**)	755	790	220,920	0.0728
Nitroimidazole-piperazine-ICG (**14**)	755	790	204,100	0.0610
2-Nitroimidazole-piperazine-ICG (**3**)	755	790	229,543	0.0825
4-Nitroimidazole-piperazine-ICG (**12**)	755	790	207,519	0.0711

Table 2. Optical Properties of 2nd Generation Dye Conjugates

2.2.3 Synthesis of Rigid ICG Dye Conjugate

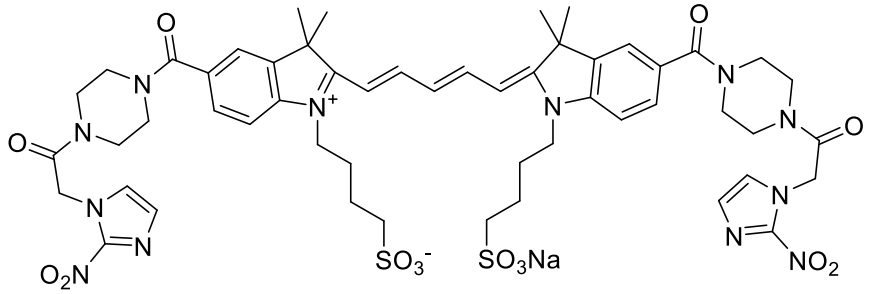

15

In an attempt to rigidify the dye conjugates and potentially increase the optical properties, *Mohammad et al* synthesized several ICG derivatives by altering the polyene chain.[30] The theory was that an introduction of a ring into the chain or shortening it would decrease the rotation around the C-C bonds. The rotational isomers of ICG derivatives can quench absorbed energy and diminish the release of fluorescence. The result is a probe with a low quantum yield and a poor tool for fluorescence imaging. Only one of the newly synthesized dyes revealed a large increase in quantum yield and was worth exploring further. This gave birth to the idea of a "3rd generation dye conjugate" (**15**). The deletion of 2 carbons to a pentamethine polyene chain is only difference

between the 2nd and 3rd generation of dye conjugates. This minor difference leads to a restriction of rotation around the polyene chain due to an increased steric clash between the sulfate side chains. The synthesis of **15** and its precursor bis-carboxylic acid **18** is shown in figure 14.[31]

The production of the shorten anilide **17** was achieved via condensation reaction of the bis(dimethyl acetal) of propanedial (**16**) with aniline in the presence of aqueous HCl. Reacting 2 equivalence of indole **6** with **17** produced "rigid ICG di-acid" (**18**). Coupling the di-acid with

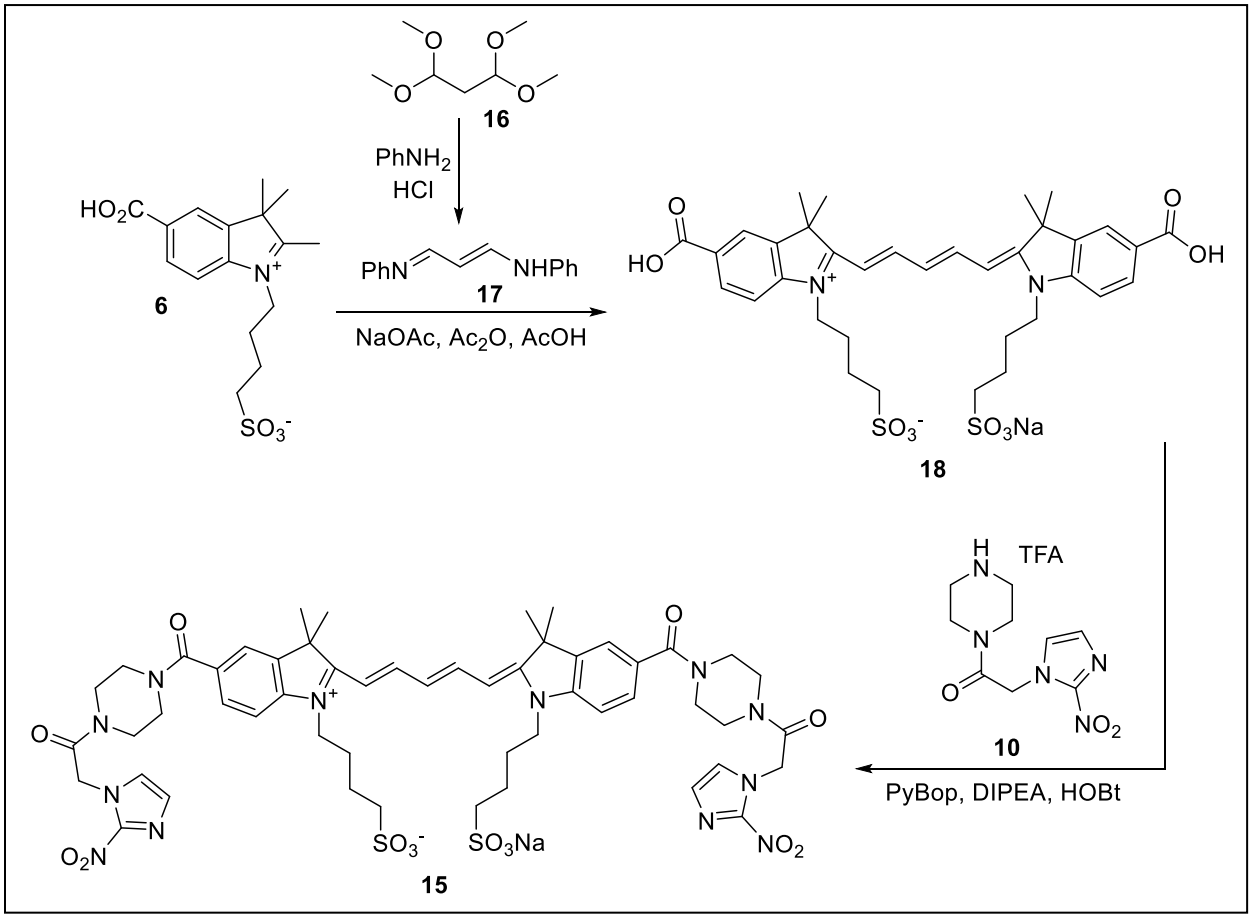

Scheme 15. Synthesis of 3rd Generation Dye Conjugate

targeting agent **10** synthesized 2-nitroimidazole-piperazine-rigid-ICG (**15**). Brief stability studies with UV light radiation showed nearly a 4-fold slower degradation half-life compared to the ICG counterparts. A small negative is that the max absorbance and fluorescence wavelengths displayed

a slight blue shift, however still fall in the ideal window for tissue imaging. The quantum yield of **15** and **18** greatly improved and are shown in table 3 with ICG comparisons.[31]

Dye	λ_{abs} (nm)	λ_{em} (nm)	Extinction Coefficient ($M^{-1}cm^{-1}$)	Quantum Yield (Φ)
FDA approved ICG	780	807	115,000	0.0120
ICG bis-carboxylic acid (**1**)	755	790	220,920	0.0728
2-Nitroimidazole-piperazine-ICG (**3**)	755	790	229,543	0.0825
Rigid bis-carboxylic acid (**18**)	655	672	262,000	0.403
2-Nitroimidazole-piperazine-rigid (**15**)	653	670	268,000	0.467

Table 3. Optical Properties of 3rd Generation Dye Conjugate

2.2.4 Hypoxia Targeting Evaluation of Rigid ICG Dye Conjugates

Evaluation of third generation dye's hypoxia imaging capabilities was done the same way as the previous *in vivo* studies.[31] Figure 15 shows the graphical representation of fluorescence intensity in the tumor over the course of a 48 hour period. The rigid dyes **15** and **18** were compared to second generation **3** and ICG bis-carboxylic acid (**1**). As expected the rigid analogs showed a superior fluorescence detectability for hypoxic tumors *in vivo*. This was expected due to the nearly 5-fold increase in quantum yield when compared to previous generation. Targeted dye conjugate **15** showed a slower diminishment of fluorescence when compared to **3**. This is likely the effect of increased stability of the rigid dyes.

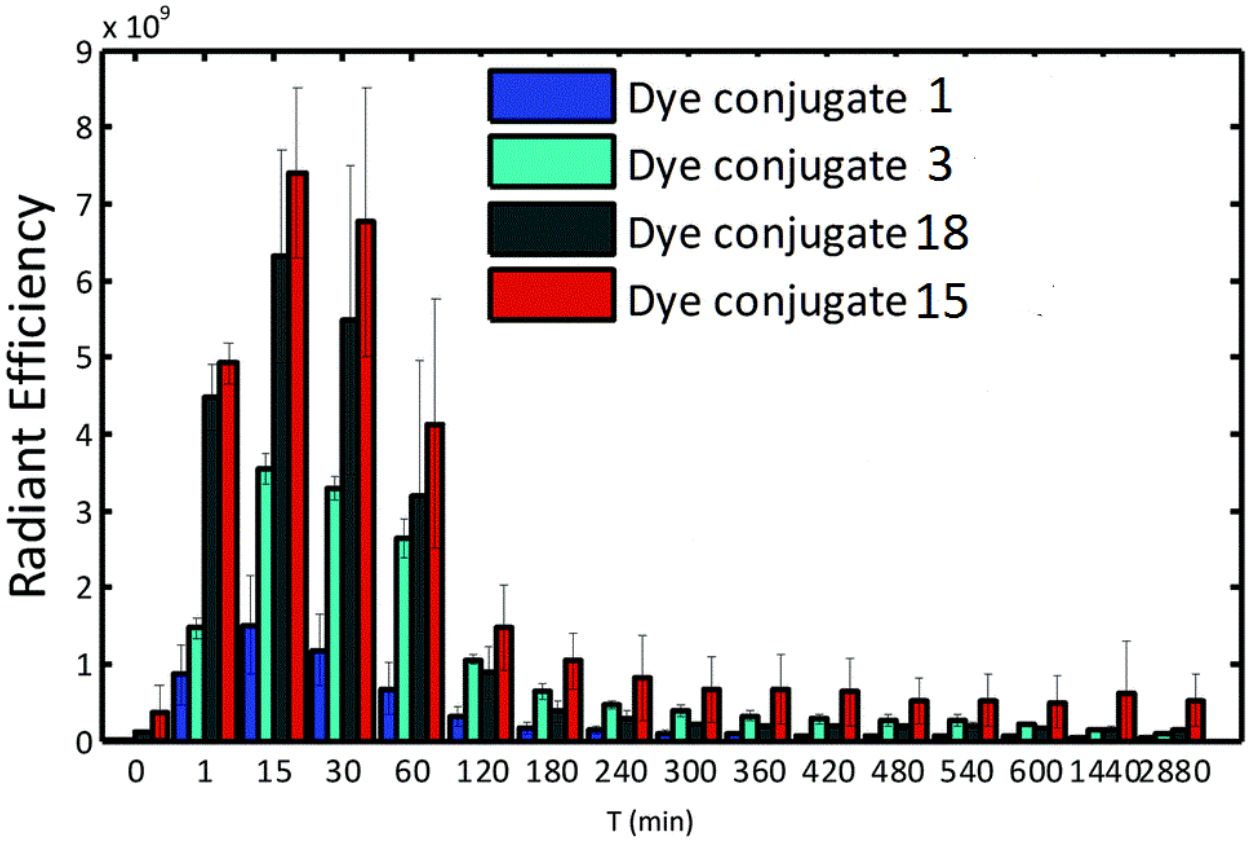

Figure 14. *In vivo* Fluoresence Efficiency of 3rd Generation Dyes

2.2.5 Synthesis of Biotin Derivative

It is important in our work to demonstrate proof that our dye conjugates are binding to targets in the cell and possibly understand the identity of that protein. Immunoprecipitation is a technique in which isolation of a protein is attained by selectively binding an antigen to the target protein. An antibody can bind the antigen and be used to separate the protein from others. An avidin-biotin pull down is a specific version of this.[32] Bioactive molecules can be labeled with a biotin moiety (biotinylation) and bound to their respective proteins. Avidin then attaches to the biotin and easily co-purified with the targeted protein. Applying this chemistry to the nitroimidazole dye conjugates could elucidate the specific protein binding of the compounds. For this reason biotinylated unsymmetrical dye conjugate **16** was designed.

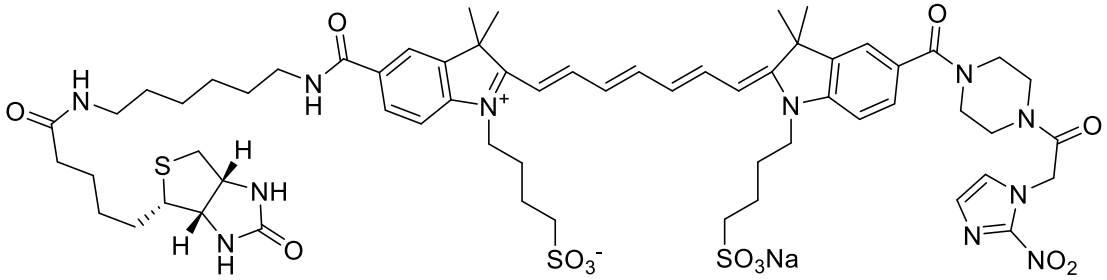

16

An unsymmetrical dye conjugate's synthesis is not as straight forward as the symmetrical targeted dye conjugates. Coupling bis-carboxylic acid ICG (**1**) with just one equivalence of targeting agent leads to a mixture of fully loaded (two targeting agents attached) and half loaded (one targeting agent attached). The mixtures are difficult to separate and deems the synthetic strategy useless. A way around this is by the production half methyl ester ICG **18**. Treatment of indole acid **6** with oxalyl chloride in methanol produced indole methyl ester **17**. One equivalence of each **6** and **17** can be coupled together to produced **18** with stepwise introduction of each indole. Then coupling the free acid with targeting agent **10** would produce half loaded dye **19**. Unfortunately all attempts at saponification of the methyl ester failed due to the degradation of the dye. One idea that was not tried is the use of an esterase. Without easy accessibility to a library of enzymes, we changed routes to synthesis biotinylated **16**.

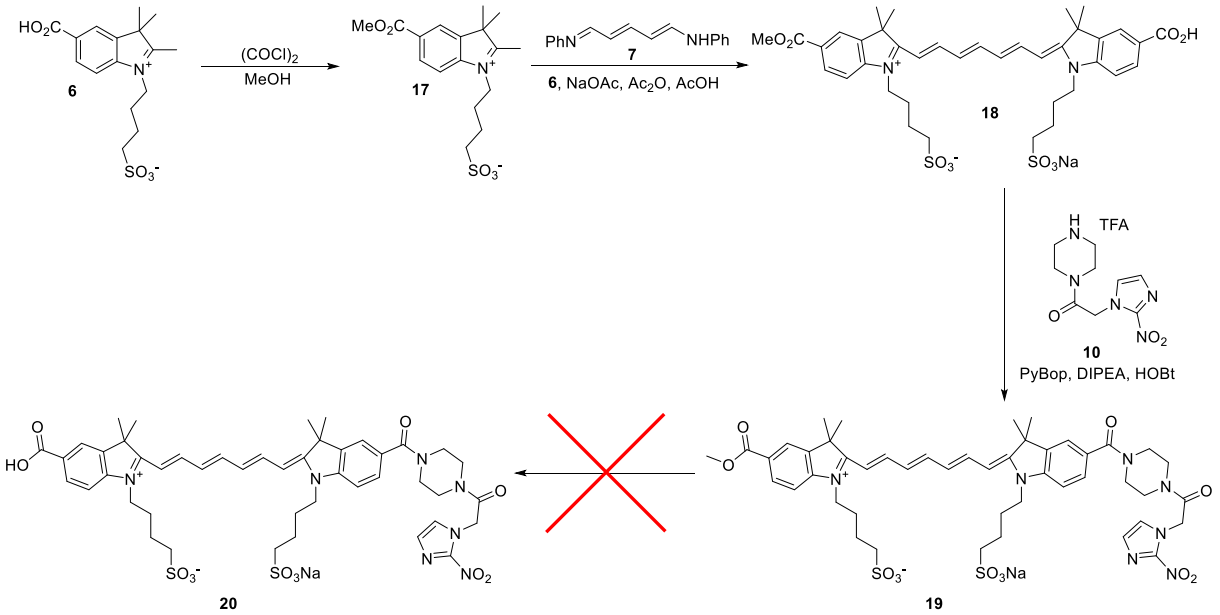

Scheme 16. Attempted Synthesis of Biotinylated ICG Dye Conjugate via Half Methyl Ester ICG di-acid

Attaching a biotin moiety to an earlier intermediate of the dye synthesis was a successful strategy. Biotin compound **21** was coupled to indole **5** to produce biotin-indole **22**.[33] Reaction with 1,4-butane sultone produced **23**, that could be linked to indole **6** with anilide **7** through a stepwise addition of each indole. This produced biotinylated dye **24** in an easily purified fashion. Final coupling with targeting agent **10** gave biotin dye conjugate **16**. This product has been verified and awaits being applied to tumor cells for the "avidin pull down" experiment.

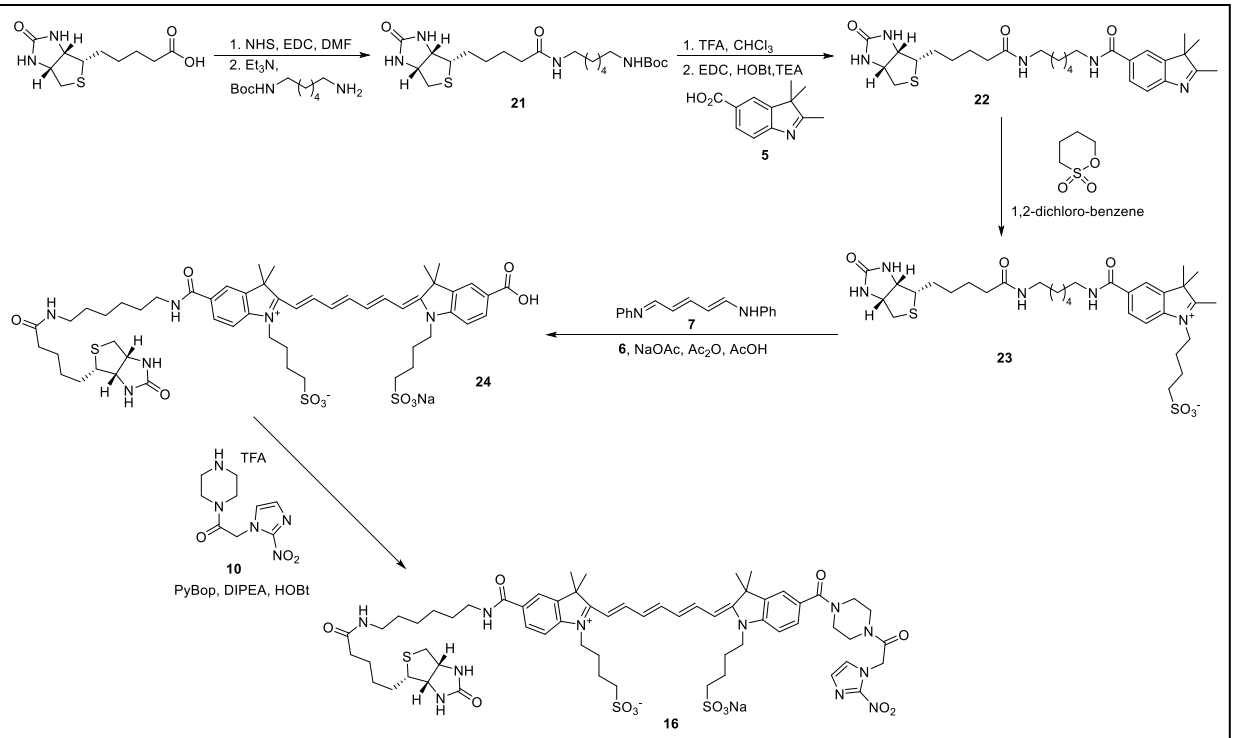

Scheme 17. Successful Synthesis of Biotinylated Dye Conjugate

2.2.6 Present Research & Future Work

Our current efforts are aimed towards the once again restrict the rotation around the polyene unit of our dye conjugates. The rigid dyes showed an excellent increase in quantum yield, however the blue shift fluorescence is a negative effect that may decrease tissue penetration. An SAR study has begun on the effects of the dye's optical properties by increasing the steric bulk attached to the indole rings. This would be in the form of increasing the size of the methyl groups on compound **1** (circled in red in figure 18). Preliminary studies are producing derivatives of the ethyl, pentyl and benzyl variety by incorporating them into the fisher indole synthesis. One possible structure that is highly interesting is macrocycle **26**. The bridged bicyclic ring system is thought to be possible through ring closing metathesis of **25** or a derivative aimed towards a different ring

construction. Shown is just a generic olefin coupling, but this could be envisioned through other completely different derivatives for ring closer. The aim is to try and lock the polyene unit into as strict of a formation as possible and increase the dyes quantum yield.

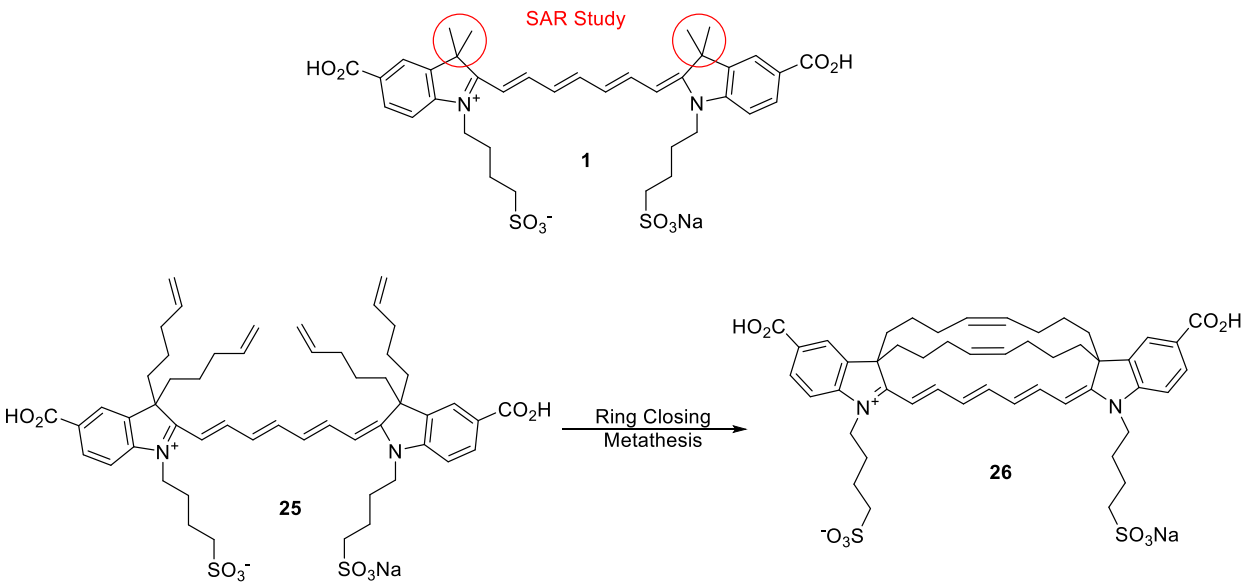

Figure 15. Current SAR Study towards a New Generation of Dye Conjugates

2.3 Experimental

All glassware was oven-dried, and all reactions were performed under a nitrogen atmosphere. All chemicals were purchased from the Sigma-Aldrich Chemical Co., and used without further purification unless otherwise noted. Tetrahydrofuran (THF) was distilled from sodium benzophenone ketyl, methylene chloride (dichloromethane, DCM) was distilled from calcium hydride, and dimethylformamide (DMF) was distilled *in vacuo* from calcium hydride. Ethyl acetate (EtOAc), methanol (MeOH), and diethyl ether were used as obtained from the vendor.

Thin-layer chromatography was done on Sorbent Technologies aluminum-backed TLC plates with fluorescent indicator and 0.2 mm silica gel layer thickness, and *p*-anisaldehyde or phosphomolybdic acid were used as developing agents. Column chromatography was done using 60 Å porosity, 32-63 μm silica gel. ^{1}H and ^{13}C NMR were collected on a Bruker Avance 300 (300.13 MHz ^{1}H, 75.48 MHz ^{13}C), Bruker DRX-400 (400.144 MHz ^{1}H, 100.65 MHz ^{13}C) or a Bruker Avance 500 (500.13 MHz ^{1}H, 125.65 MHz ^{13}C). Chemical shifts are reported in ppm downfield from tetramethylsilane (TMS) in the following format chemical shift, multiplicity (s=singlet, d=doublet, t=triplet, q=quartet, m=multiplet). Coupling constants are reported in Hz. Mass spectrometry data was collected on a HP 5870B GC/MSD mass spectrometer with an HP-1 column, and high resolution MS and MS/MS spectra were obtained by direct infusion into a QTOF mass spectrometer, QSTAR Elite from Sciex (Foster City, CA) or directly by using AccuTOF™ DART, JEOL (Peabody, MA). Multiple reaction monitoring (MRM) transitions were selected based the MS/MS spectra. IR spectra were taken on FT/IR-410/C031560585 JASCO and Nexus 670 FT-IR E.S.P, neat, unless otherwise stated. All melting points to an upper limit of 270 °C

were obtained using a Uni-melt capillary melting point apparatus or Digimelt MPA160. For products described as waxy solid or semi-solids, melting points could not be obtained.

Repeated efforts to obtain the ^{13}C NMR of dye conjugates failed to give a spectrum. We examined the possibility of aggregation, rotamers, relaxation time, and low concentration due to solubility issues. All of these issues can lead to poor ^{13}C NMR spectra. Attempts to obtain ^{13}C NMR spectra at 25 °C failed, and we heated the samples to 55 °C to promote deaggregation. We also explored different solvents, including CD_3OD, $(CD_3)_2CO$, D_2O. We examined extended delay (relaxation) times up to 10 to 15 s, as well as long acquisition times (up to 24 hours). None of these experiments led to a ^{13}C NMR. We have attempted indirect ^{13}C experiments, including HSQC, HMBC, and CIGAR. The problem is likely due to low solubility, coupled with the low isotope percentage of 13C relative to ^{12}C versus the high percentage of ^{1}H, but we do not have a definitive answer to this problem. No experiments have been successful, so only ^{1}H NMR data is provided.

It is noted that the commercial ICG obtained from SigmaAldrich, as well as derivatives prepared in our laboratory is a mixture of isomers as determined by high-performance liquid chromatography analysis. This mixture is undoubtedly a mixture of E/Z isomers of the polyene linker. No attempt was made to separate this mixture into the component stereoisomers, and in all cases, the mixture was used for in vivo studies. To the best of our knowledge, such mixtures are used in all biological studies that involve ICG.

2,3,3-Trimethyl-3H-indole-5-carboxylic acid, (5)

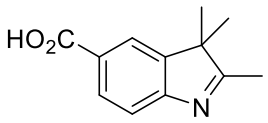

5

A 100 mL round-bottumed flask was charged with 4-hydrazinobenzoic acid (4.892 g, 32.2 mmol), 3-methylbutan-2-one (4.82 g, 45.1 mmol), sodium acetate (5.28 g, 64.4 mmol), and glacial acetic acid (50 mL). The mixture was stirred for 1 h and then heated at reflux overnight. The solvent was removed under reduced pressure to a sludge and then crystalized from 10% MeOH (80mL). The resulting precipitate was filtered and dried to yield **5** (3.66 g, 18.0 mmol, 55.9%) as a tan solid.[20] ^{1}H NMR (400 MHz, Chloroform-*d*) δ 8.13 (dd, *J* = 8.1, 1.7 Hz, 1H), 8.04 (d, *J* = 1.7 Hz, 1H), 7.63 (d, *J* = 8.1 Hz, 1H), 2.36 (s, 3H), 1.36 (s, 6H). ^{13}C NMR (101 MHz, Chloroform-*d*) δ 192.5, 171.0, 158.1, 145.9, 131.0, 126.4, 123.4, 119.9, 54.1, 23.0, 15.8.

5-Carboxy-1-(d-sulfobutyl)-2,3,3-trimethyl-3H-indolium betaine, (6)

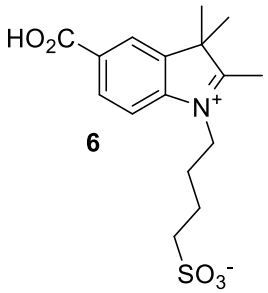

6

A mixture of **5** (3.66 g, 18.0 mmol) and 1,4-butanesultone (10.1 mL, 99.0 mmol) in 1,2-dichlorobenzene (80 mL), was created under a nitrogen atmosphere. The mixture was heated at reflux overnight. The reaction solution was cooled to room temperature and the red precipitate was filtered, rinsed with acetone, and dried to give **6** (4.90 g, 14.4 mmol, 80.2 %).[20] ^{1}H NMR (400

MHz, CD_3OD) δ 8.40 (d, *J* = 1.3 Hz, 1H), 8.34 (dd, *J* = 8.4 Hz, 1H), 8.07 (d, *J* = 8.4 Hz, 1H), 4.63 (t, *J* = 7.8 Hz, 2H), 4.43 (s, 3H), 2.93 (t, *J* = 7.1 Hz, 2H), 2.24-2.16 (m, 2H), 2.02-1.95 (m, 2H), 1.68 (s, 6H). ^{13}C NMR (101 MHz, CD_3OD) δ 201.1, 167.9, 145.3, 143.6, 133.7, 132.3, 125.6, 116.8, 56.2, 51.0, 27.3, 23.2, 22.6.

N-(2-Hydroxyethyl)-2-(4-nitro-1H-imidazol1-yl)acetamido-ICG, (1)

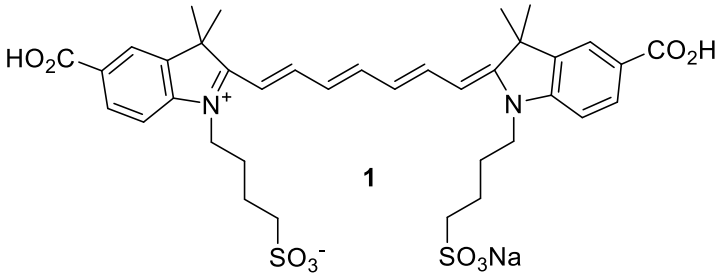

Indolium salt **6** (3.85 g, 11.3 mmol) and N-[5-(Phenylamino)-2,4-pentadienylidene]aniline monohydrochloride (1.79 g, 6.29 mmol) was added to a 100 mL round-bottomed flask. Then acetic anhydride (60 mL) and glacial acetic acid (36 mL) were added and stirred at room temperature. This solution was treated with sodium acetate (1.64 g) and then heated to reflux for 45 min. The blue solution was then cooled to room temperature before being poured into hot anhydrous ether (150 mL). The solution was cooled in the refrigerator overnight, and the green precipitate was vacuum filtrated and washed with ether. The product was recrystallized from a 1:4 mixture of water and propanol to yield **1** (2.94 g, 3.85 mmol, 68 %) as a green powder.[20] ^1H NMR (400 MHz, DMSO-*d6*) δ 12.96 (bs, 1H), 8.08 (d, J = 7.3 Hz, 2H), 7.97 (d, J = 7.3, 2H), 7.84 (m, 2H), 7.52 (d, J = 9.1 Hz, 2H), 7.47 (s, 1H), 6.48 (m, 4H), 4.15-4.06 (m,4H), 3.86 (s, 3H), 1.73 (s, 8H), 1.63 (s, 12H). ^{13}C NMR (101 MHz, DMSO-*d6*) δ 167.7, 166.6, 147.1, 142.0, 131.3, 125.6, 124.0, 123.8, 52.8, 51.4, 49.4, 41.8, 27.7, 26.8, 23.2.

Tert-butyl piperazine-1-carboxylate

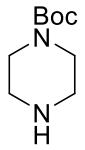

A solution of di-tert-butyl dicarbonate (3.80 g, 17.4 mmol) in CH_2Cl_2 (50 mL) was added dropwise to a stirring solution of piperazine (3.00 g, 34.8 mmol) in CH_2Cl_2 (60 mL) at room temperature and stirred for 16 h. The solvent were removed under reduced pressure and the residue dissolved in water (50 mL). The aqueous solution was extracted with methylene chloride (4 × 75 mL) and all the organic extractions were combined, dried over anhydrous magnesium sulfate, and concentrated to get tert-butyl piperazine-1-carboxylate as a white solid (1.5 g, 8.05 mmol, 34.7 %).[24] ^{1}H NMR (400 MHz, $CDCl_3$) δ 3.37 (m, 2 H), 2.79 (m, 2 H), 1.72 (bs, 1 H), 1.44 (s, 9 H) ppm. ^{13}C NMR (101 Hz, CDCl3) δ 154.3, 79.8, 45.6, 44.5, 28.8 ppm.

Tert-butyl 4-(2-bromoacetyl) piperazine-1-carboxylate, (8)

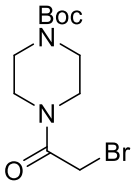

8

Triethylamine (2.8 mL, 20.3 mmol) was added to a stirring solution of tert-butyl piperazine-1-carboxylate (3.44 g, 18.4 mmol) in dry dichloromethane (100 mL) at 0°C and stirred for 15 min. Bromoacetyl bromide (1.8 mL, 20.3 mmol) was added dropwise at 0°C, and the resulting mixture was stirred at room temperature overnight. Reaction progress was monitored by TLC, and after

disappearance of the starting material, the mixture was concentrated and purified via column chromatography (hexanes:ethyl acetate 20%) to give tert-butyl 4-(2-bromoacetyl) piperazine-1-carboxylate (**8**, 3.36 g, 10.9 mmol, 59.3%) as a white solid. Mp: 95-97°C.[24] ^{1}H NMR (400 MHz, Chloroform-*d*) δ 3.86 (s, 2H), 3.63–3.56 (m, 2H), 3.56–3.46 (m, 4H), 3.46–3.41 (m, 2H), 1.47 (s, 9H). ^{13}C NMR (101 MHz, Chloroform-*d*) δ 165.6, 154.6, 80.6, 46.7, 42.1, 28.5, 25.7.

Tert-butyl 4-(2-(2-nitro-1 H-imidazol-1-yl)acetyl) piperazine-1-carboxylate, (9)

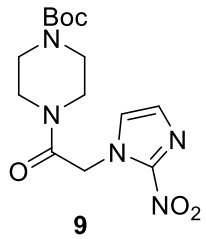

9

Commercially available 2-nitroimidazole (0.100 g, .885 mmol) was dissolved in 2 mL of freshly distilled DMF, under N_2, and cooled to 0°C. Sodium hydride (0.042 g, .106 mmol) was added to the reaction and stirred for 30 min before a dropwise addition of tert-butyl 4-(2-bromoacetyl)piperazine-1-carboxylate (**8**, 0.272 g, .885 mmol) dissolved in 2 mL of DMF. The mixture was slowly warmed to room temperature and stirred overnight. The reaction was concentrated under reduced pressure and then addition of 10 mL of water caused a white precipitate to form. The solid was filtered and dried under reduced pressure overnight to afford tert-butyl 4-(2-(4-nitro-1Himidazol-1-yl)acetyl)piperazine-1-carboxylate (**9**, 0.280 g, .825 mmol, 93%). Mp: 197-199°C.[27] ^{1}H NMR (400 MHz, Chloroform-*d*) δ 7.20 (s, 1H), 7.07 (s, 1H), 5.23 (s, 2H), 3.65–3.55 (m, 4H), 3.54–3.44 (m, 4H), 1.48 (s, 9H). ^{13}C NMR (101 MHz, Chloroform-*d*) δ 163.5, 154.5, 145.3, 128.3, 127.2, 80.7, 50.9, 45.1, 42.5, 28.5.

tert-Butyl 4-(2-(4-nitro-1H-imidazol-1-yl)acetyl)piperazine-1- carboxylate

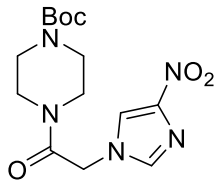

Commercially available 4-nitroimidazole (0.55 g, 4.9 mmol) was dissolved in 2 mL of freshly distilled DMF, under N_2, and cooled to 0°C. Sodium hydride (0.14 g, 5.9 mmol) was added to the reaction and stirred for 30 min before a dropwise addition of tert-butyl 4-(2-bromoacetyl)piperazine-1-carboxylate (1.50 g, 4.9 mmol) dissolved in 2 mL of DMF. The mixture was slowly warmed to room temperature and stirred overnight. Addition of 10 mL of water caused a white precipitate to form. The solid was filtered and dried under reduced pressure overnight to afford tert-butyl 4-(2-(4-nitro-1Himidazol-1-yl)acetyl)piperazine-1-carboxylate (1.26 g, 3.7 mmol, 76%).[29] Mp: 197-199 °C. ^{1}H NMR (400 MHz, $CDCl_3$) δ 7.82-7.81 (d, *J* = 1.5 Hz, 1H), 7.45-7.44 (d, *J* = 1.4 Hz, 1H), 4.86 (s, 2H), 3.65-3.63 (m, 2H), 3.56-3.54 (m, 2H), 3.50-3.47 (m, 4H), 1.48 (s, 9H). ^{13}C NMR (101 MHz, $CDCl_3$) δ 163.1, 154.6, 148.2, 137.1, 120.9, 81.1, 48.8, 45.0, 42.5, 28.5. HRMS (ESI-TOF): [M+H] Calc'd for $C_{14}H_{22}N_5O_5$ *m/z* 340.1621. Found *m/z* 340.1607.[29]

tert-Butyl 4-(2-(1H-imidazol-1-yl)acetyl)piperazine-1- carboxylate

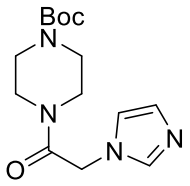

Commercially available imidazole (0.33 g, 4.9 mmol) was dissolved in 2 mL of freshly distilled DMF, under N_2, and cooled to 0°C. Sodium hydride (0.14 g, 5.9 mmol) was added to the reaction and stirred for 30 min before a dropwise addition of tert-butyl 4- (2-bromoacetyl)piperazine-1-carboxylate (1.50 g, 4.9 mmol) dissolved in 2 mL of DMF. The mixture was slowly warmed to room temperature and stirred overnight. Addition of 10 mL of water caused a white precipitate to form. The solid was filtered and dried under reduced pressure overnight to afford tert-butyl 4-(2-(1H-imidazol-1-yl)acetyl)piperazine-1-carboxylate (0.97 g, 3.3 mmol, 67%).[29] Mp: 147-149°C. ^{1}H NMR (400 MHz, Chloroform-*d*) δ 7.50 (s, 1H), 7.10 (s, 1H), 6.95 (s, 1H), 4.78 (s, 2H), 3.61 (d, *J* = 5.3 Hz, 2H), 3.49–3.39 (m, 6H), 1.47 (s, 9H). ^{13}C NMR (101 MHz, Chloroform-*d*) δ 164.9, 154.5, 138.1, 129.9, 120.1, 80.8, 48.2, 45.1, 42.2, 28.5. HRMS (ESI þ TOF): [M þ H] þ Calc'd for $CH_{23}N_4O_3$ m/z 295.1770. Found, m/z 295.1751.

4-(2-(2-Nitro-1H-imidazole-1-yl)acetyl)piperazin-1-ium trifluoroacetate, (10)

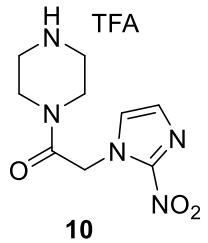

10

A solution of trifluoroacetic acid (1 mL) and chloroform (6 mL) was cooled to 0°C under a nitrogen atmosphere. tert-Butyl 4-(2-(2-nitro-1H-imidazol-1-yl)acetyl)piperazine-1-carboxylate (0.280 g, 0.823 mmol) dissolved in 3 mL of chloroform was added dropwise via cannula. The solution was slowly warmed to room temperature and stirred overnight. The reaction was concentrated in vacuo to a crude oil that was crystalized from ethyl acetate. The product was isolated by vacuum filtration and dried under reduced pressure to yield 4-(2-(2-nitro-1H-imidazole-1-yl)acetyl)piperazin-1-ium tri-fluoroacetate (**10**, 0.214 g, 0.636 mmol, 77%).[27] ^{1}H NMR (400 MHz, D2O) δ7.58 (s, 1 H), 7.40 (s, 1 H), 5.68 (s, 2 H), 4.08 (t, J ¼ 4 Hz, 2 H), 4.03 − 4.00 (m, 2 H), 3.59 (t, J ¼ 4 Hz, 2 H), 3.50-3.47 (m, 2 H); ^{13}C NMR (100 MHz, D2O) δ166.9, 163.3, 162.9, 162.6, 149.0, 129.2, 128.4, 121.0, 118.1, 115.2, 112.2, 51.3, 43.3, 42.2, 39.6; HRMS Calcd C10H14F3N5O5 240.1096, found 240.1149.

4-(2-(4-Nitro-1H-imidazole-1-yl)acetyl)piperazin-1-ium trifluoroacetate, (11)

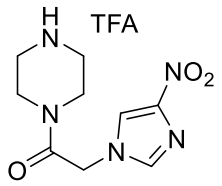

11

A solution of trifluoroacetic acid (1 mL) and chloroform (6 mL) was cooled to 0 C under a nitrogen atmosphere. tert-Butyl 4-(2-(4- nitro-1H-imidazol-1-yl)acetyl)piperazine-1-carboxylate (0.250 g, 0.73 mmol) dissolved in 3 mL of chloroform was added dropwise via cannula. The solution was slowly warmed to room temperature and stirred overnight. The reaction was concentrated in vacuo to a crude oil that was crystalized from ethyl acetate. The product was isolated by vacuum filtration and dried under reduced pressure to yield 4-(2-(4-nitro-1H-imidazole-1-yl)acetyl)piperazin-1-ium tri- fluoroacetate 9b (0.193 g, 0.55 mmol, 74%).[29] mp: 228e229 C; 1 H NMR (400 MHz, D2O) d 8.20 (bs, 1H), 7.79 (bs, 1H), 5.32 (s, 2H), 3.92e3.89 (m, 4H), 3.47e3.37 (m, 4H); 13C NMR (100 MHz, CDCl3) d 166.6, 163.4, 163.0, 162.5, 162.0, 146.7, 138.7, 123.5, 118.7, 49.0, 42.9, 41.7, 39.2; HRMS (ESI-TOF): [M þ H] þ Calc'd for C9H14N5O3 m/ z 240.1096. Found, m/z 240.1100.

4-(2-(1H-Imidazole-1-yl)acetyl)piperazin-1-ium trifluoroacetate, (13)

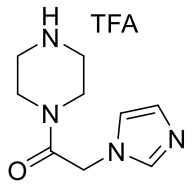

13

A solution of trifluoroacetic acid (1 mL) and chloroform (6 mL) was cooled to 0 C under a nitrogen atmosphere. tert-Butyl 4-(2- (1H-imidazol-1-yl)acetyl)piperazine-1-carboxylate (0.250 g, 0.85 mmol) dissolved in 3 mL of chloroform was added dropwise via cannula. The reaction mixture was slowly warmed to room temperature, stirred overnight, and concentrated in vacuo to a crude oil that was crystalized from ethyl acetate. The product was isolated by vacuum filtration and dried under reduced pressure to yield 4-(2-(1H-imidazole-1-yl)acetyl)piperazin-1-ium trifluoroa cetate 9a (0.161 g, 0.52 mmol, 61%).[29] mp: 129e130 C; 1 H NMR (400 MHz, D2O) d 8.76 (s, 1H), 7.53 (s, 1H), 7.46 (s, 1H), 5.43 (s, 2H), 3.90e3.87 (m, 4H), 3.44e3.41 (m, 2H), 3.36e3.34 (m, 2H); 13C NMR (100 MHz, CDCl3) d 166.0, 163.4, 163.0, 136.5, 123.6, 119.8, 118.0, 115.1, 50.1, 42.9, 41.8, 41.7, 39.3; HRMS (ESI þ TOF): [MCF3COO þ H] Calc'd for C9H15N4O m/z 195.1246. Found, m/z 195.1231.

Sodium 4-((Z)-2-((2E,4E,6E)-7-(3,3-dimethyl-5-(4-(2-(2-nitro- 1H-imidazol-1-yl)acetyl)cyclo-hexane-1-carbonyl)-1-(4- sulfonatobutyl)-3H-indol-1-ium-2-yl)hepta-2,4,6-trien-1-ylidene)- 3,3-dimethyl-5-(4-(2-(2-nitro-1H-imidazol-1-yl)acetyl) cyclohexane-1-carbonyl)indolin-1-yl)butane-1-sulfonate, (3)

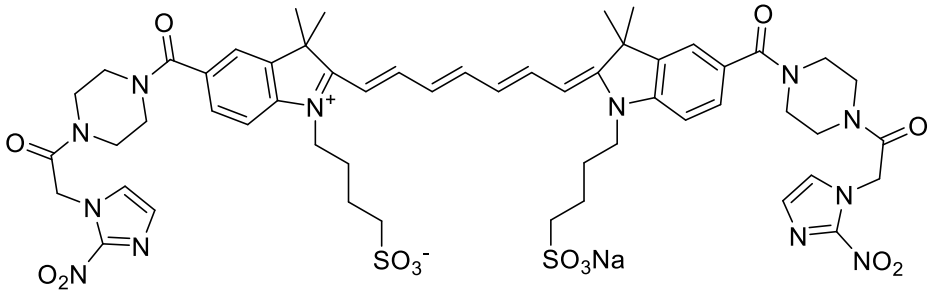

3

A stirred solution of ICG bis (carboxylic acid) (**1**, 0.139 g, 0.182 mmol) in dry DMF (2 mL) at 0°C was treated with benzotriazol-1-yl-oxytripyrrolidinophosphonium hexafluorophosphate (0.208 g, 0.400 mmol), 1-hydroxybenzotriazole (0.054 g, 0.400 mmol), and diisopropylethylamine (69.9 μL, 0.400 mmol) in that order, and stirred at 0°C for 15 min. At this time, 2-(2-nitro-1H-imidazol-1-yl)-1-(piperazin-1-yl)ethanone, TFA salt (**10**, 0.135 g, 0.400 mmol) was added and the resulting mixture stirred at room temperature for 48 h. The DMF was evaporated and the resulting solid was purified using C18 reverse phase column chromatography to yield compound **3** as an amorphous green solid (0.044 g, 0.037 mmol, 20.0%).[27] ^{1}H NMR (400 MHz, D2O): δ7.84 (t, J ¼ 12 Hz, 2 H), 7.57 (s, 2 H), 7.45 (bs, 5 H), 7.35–7.33 (m, 2 H), 7.27 (s, 2 H), 6.57 (t, J ¼ 12 Hz, 2 H), 6.29 (d, J ¼ 12 Hz, 2 H), 5.57 − 5.51 (m, 4 H), 4.15 (bs, 4 H), 3.86 − 3.52 (m, 16 H), 2.97 (t, J ¼ 8 Hz, 4 H), 1.99 − 1.97 (m, 4 H), 1.91 − 1.87 (m, 4 H), 1.61 (bs, 12 H). HRMS Calcd protonated formula C55H67N12O14S2 1183.4341, found 1183.4399.

Sodium 4-((Z)-2-((2E,4E,6E)-7-(3,3-dimethyl-5-(4-(2-(4-nitro- 1H-imidazol-1-yl)acetyl)cyclo-hexane-1-carbonyl)-1-(4- sulfonatobutyl)-3H-indol-1-ium-2-yl)hepta-2,4,6-trien-1-ylidene)- 3,3-dimethyl-5-(4-(2-(4-nitro-1H-imidazol-1-yl)acetyl) cyclohexane-1-carbonyl)indolin-1-yl)butane-1-sulfonate, (12)

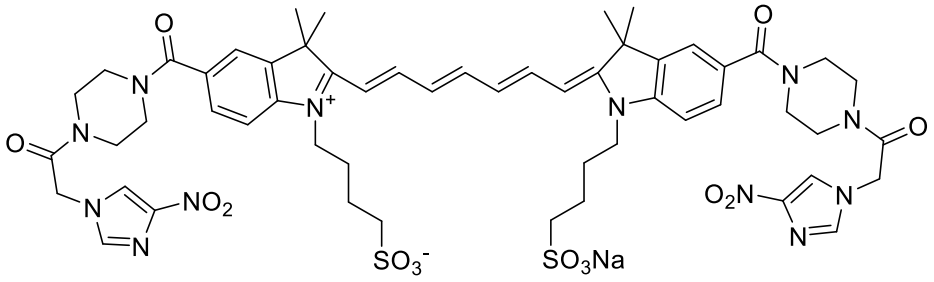

12

A total of (0.150 g, 0.197 mmol) of 2 was dissolved in 1 mL freshly distilled DMF under N2 and cooled to 0 C. The reaction was then charged with pyBop (0.220 g, 0.0423 mmol), HOBt (0.065 g, 0.423 mmol), DIPEA (0.074 mL, 0.423 mmol) and stirred for 15 min before the addition 4-nitroimidazole piperazine TFA (0.149 g, 0.423 mmol). The solution was warmed to room temperature and let stir overnight. The solvent extensively removed and the resulting sold was washed with EtOAc (15 mL), chloroform (15 mL), and acetonitrile (15 mL) before being recrystallized from methanol/ diethyl ether. The crude material was purified by C18 reverse phase chromatography to yield 6 as a green solid (0.049 g, 0.041 mmol, 21%).[29] mp: decomposed >250 C; 1 H NMR (400 MHz, D2O) d 8.26 (s, 2H), 7.92 (t, J ¼ 12 Hz, 2H), 7.81 (s,2H), 7.75 (s, 2H), 7.69 (s, 2H), 7.72e7.48 (m, 4H), 6.65e6.59 (m, 2H), 6.51 (d, J ¼ 8 Hz, 2H), 5.21 (bs, 4H), 4.11 (m, 4H), 3.58 (m, 16H), 1.80e1.71 (m, 8H), 1.68 (s, 12H); HRMS (ESI-TOF): [M-Na]- Calc'd for C55H65N12O14S2 m/z 1181.4185. Found, m/z 1181.4174.

Sodium 4-((Z)-2-((2E,4E,6E)-7-(3,3-dimethyl-5-(4-(2-(1Himidazol-1-yl)acetyl)cyclohexane-1-carbonyl)-1-(4- sulfonatobutyl)-3H-indol-1-ium-2-yl)hepta-2,4,6-trien-1-ylidene)- 3,3-dimethyl-5-(4-(2-(1H-imidazol-1-yl)acetyl)cyclohexane-1- carbonyl)indolin-1-yl)butane-1-sulfonate, (14)

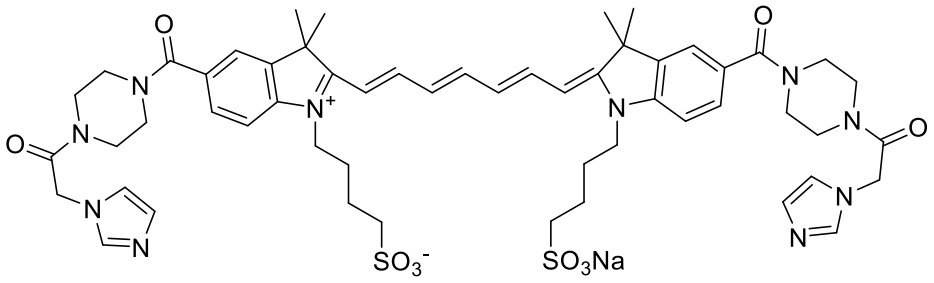

14

A total of (0.301 g, 0.39 mmol) of 2 was dissolved in 1 mL freshly distilled DMF under N2 and cooled to 0 C. The reaction was then charged with pyBop (0.45 g, 0.86 mmol), HOBt (0.117 g, 0.86 mmol), DIPEA (0.200 mL, 0.1.18 mmol) and stirred for 15 min before the addition imidazole piperazine TFA (0.266 g, 0.86 mmol). The solution was warmed to room temperature and let stir overnight. The solvent extensively removed and the resulting sold was washed with EtOAc (15 mL), chloroform (15 mL), and acetonitrile (15 mL) before being recrystallized from methanol/diethyl ether. The crude material was purified by C18 reverse phase chromatography to yield 5 as a green solid (0.065 g, 0.0058 mmol, 15%).[29] mp: decomposed >250 C; 1 H NMR (400 MHz, D2O) d 7.92 (t, J ¼ 12 Hz, 2H), 7.69 (s,2H), 7.51 (d, J ¼ 16 Hz, 6H), 7.06 (s, 2H), 7.05e6.95 (m, 1H), 6.87 (s, 2H), 6.62 (t, J ¼ 12 Hz, 2H), 6.50 (d, J ¼ 12, 2H), 5.06 (s, 4H), 4.10 (bs, 4H), 3.57 (bs, 16H), 1.77 (m, 8H), 1.67 (s, 12H); HRMS (ESITOF): [M-Na]- Calc'd for C55H67N10O10S2 m/z 1091.4483. Found, m/z 1091.4456.

Sodium 4-[2-[(1E,3E,5Z)-7-[1,1-dimethyl-3-(4-sulfonatobutyl)- indol-2-ylidene]penta-1,3-dienyl]-1,1-dimethylindol-3-ium-3-yl]- butane-1-sulfonate, (18)

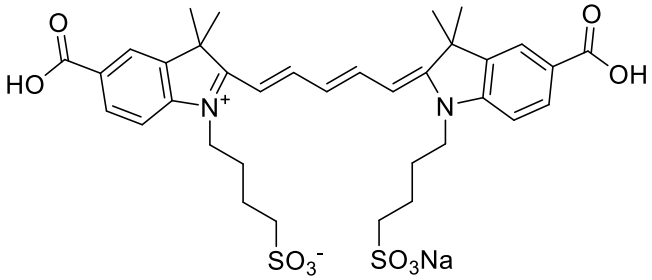

18

A vigorously stirred solution of 3-(5-carboxy-2,3,3-trimethyl-3H-indolium-1-yl)propane-1-sulfonate (6, 0.14 g, 0.41 mmol) and 7 (0.05 g, 0.19 mmol) in acetic anhydride (1 mL) and acetic acid (0.5 mL) was treated with sodium acetate (0.054 g, 0.66 mmol) and heated at reflux (120 °C) for 45 min. The reaction mixture was cooled to ambient temperature and anhydrous diethyl ether (5 mL) was added. The resulting precipitate was isolated by vacuum filtration to give a crude solid that was recrystallized (methanol : water) to give 8 as a blue solid (0.09 g, 0.12 mmol, 63%);22 mp: decomposition at 287 °C; 1 H NMR (400 MHz, CD3OD) δ 12.92 (bs, 2H), 8.43 (t, J = 13 Hz, 2H), 8.17 (s, 2H), 8.00 (d, J = 8.4 Hz, 2H), 7.53 (d, J = 8.4 Hz, 2H), 6.71 (t, J = 12.4 Hz, 1H), 6.50 (d, J = 13.7 Hz, 2H), 4.15 (bs, 4H), 1.18–1.76 (m, 8H), 1.73 (s, 12H).[31] 13C NMR (100 MHz, CD3OD) δ 175.7, 169.2, 156.8, 147.4, 142.8, 132.3, 128.7, 128.6, 124.6, 112.0, 106.0, 51.7, 50.4, 45.1, 27.9, 27.2, 23.5; 13C NMR (100 MHz, MeOD) d 175.7, 169.2, 156.8, 147.4, 142.8, 132.3, 128.7128.6, 124.6, 112.0, 106.0, 51.7, 50.4, 45.1, 27.9, 27.2, and 23.5 ppm. HRMS (TOF): [M + H]+ Calc'd for C35H43N2O10S2 m/z 715.2359. Found, m/z 715.2321.

Sodium 4-((Z)-2-((2E,4E)-5-(3,3-dimethyl-5-(4-(2-(2-nitro-1Himidazol-1-yl)acetyl)-piperazine-1-carbonyl)-1-(4-sulfonatobutyl)- 3H-indol-1-ium-2-yl)penta-2,4-dien-1-ylidene)-3,3-dimethyl-5- (4-(2-(2-nitro-1H-imidazol-1-yl)acetyl)piperazine-1-carbonyl)indolin- 1-yl)butane-1-sulfonate, (15)

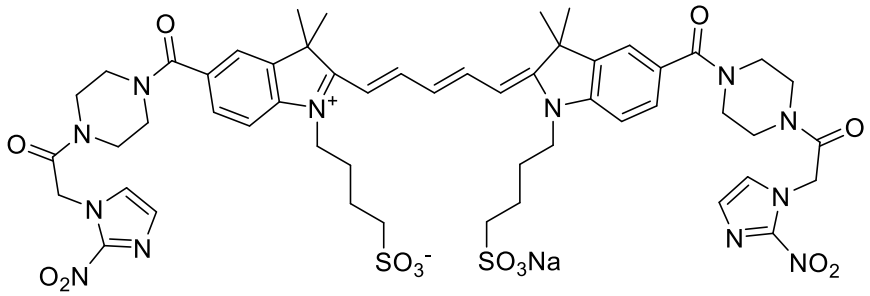

15

A total of 78 mg (0.149 mmol) of PyBOP was added to a stirring solution of bis-(carboxylic acid) 8 (50 mg, 0.0068 mmol) in dry DMF (2 mL) at 0 °C. This solution was subsequently treated with HOBt (hydroxybenzotriazole, 20 mg, 0.149 mmol), followed by diisopropylethylamine (DIPEA, 0.026 mL, 0.149 mmol). This mixture was stirred for 15 min before the addition of 2-nitroimidazole piperazine 11 (54 mg, 0.149 mmol) followed by stirring at room temperature for 48 h in the dark. The DMF was removed by air-drying to yield a thick blue oil and further concentrated in vacuo overnight. The crude mixture was recrystallized from methanol (15 mL) via the dropwise addition of diethyl ether (50 mL), and the resulting blue solid was washed with acetonitrile (2 × 25 mL), ethyl acetate (2 × 25 mL), and chloroform (2 × 25 mL). The crude was purified by C18 reverse phase column chromatography (H2O : MeOH) to yield 12 (25 mg, 0.021 mmol, 31%) as a blue solid.[31] mp: decomposed to black residue >250 °C; 1 H NMR (400 MHz, D2O) d 8.17 (m, 3H), 7.71 (s, 2H), 7.63 (d, J = 8 Hz, 2H), 7.55 (s, 2H), 7.50 (d, J = 8, 1H), 7.38 (s, 1H), 6.76 (t, 2H), 6.47 (d, 2H), 5.64 (bs, 4H), 4.27 (bs, 4H), 3.66–4.05 (bs, 16H), 3.06 (t, 4H),

2.10 (m, 4H), 1.97 (m, 2H), 1.80 (bs, 9H), 1.44 (m, 3H); HRMS (ESI-TOF): [M − Na]− Calc'd for m/z C53H63N12O14S2 1155.4034. Found, m/z 1155.4028.

2.4 NMR Spectrum

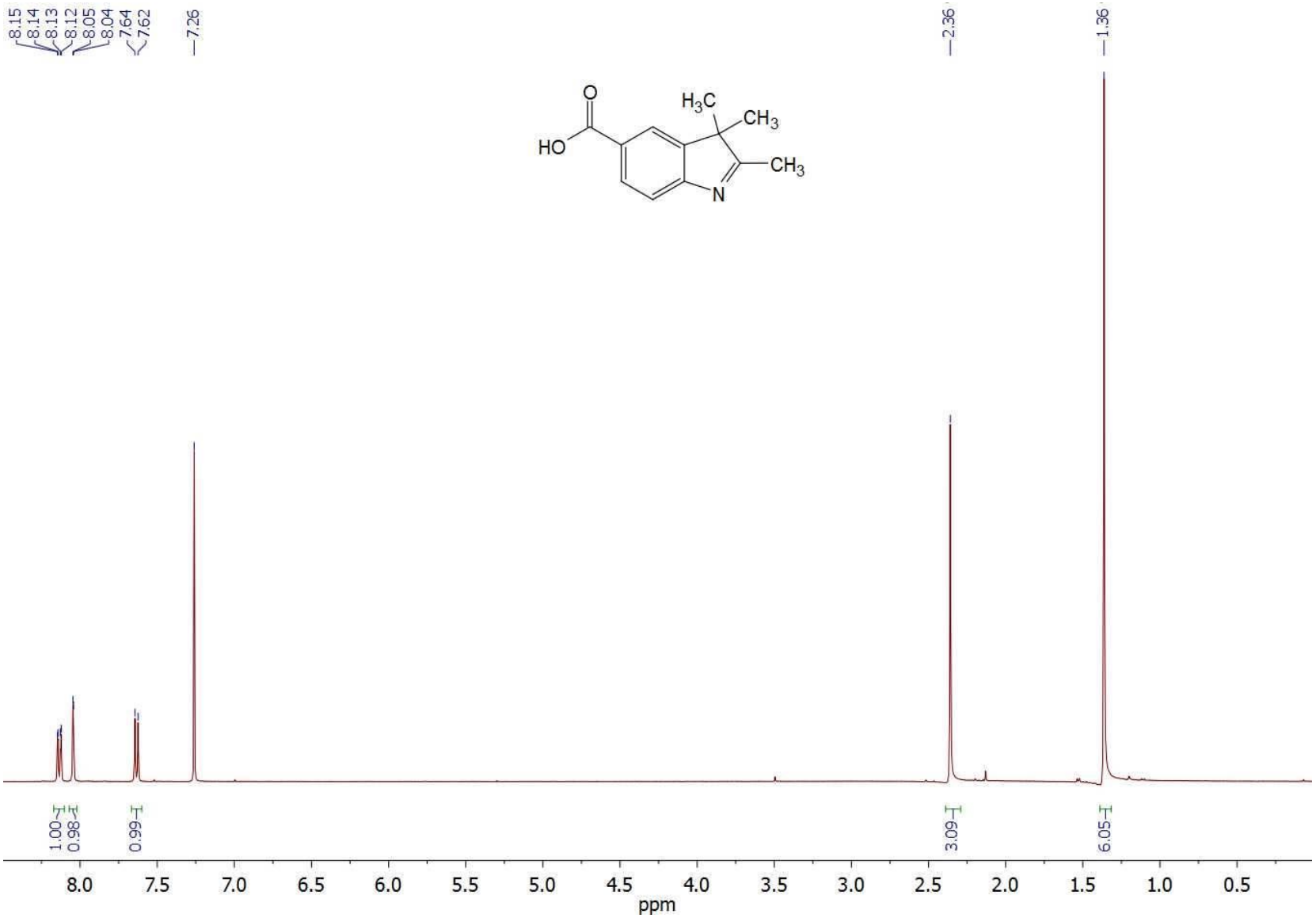
8.15
8.14
8.13
8.12
8.05
8.04
7.64
7.62
7.26
2.36
1.36
O
HO
H3C
CH3
CH3
N
1.00
0.98
0.99
3.09
6.05
8.0
7.5
7.0
6.5
6.0
5.5
5.0
4.5
4.0
3.5
3.0
2.5
2.0
1.5
1.0
0.5
ppm

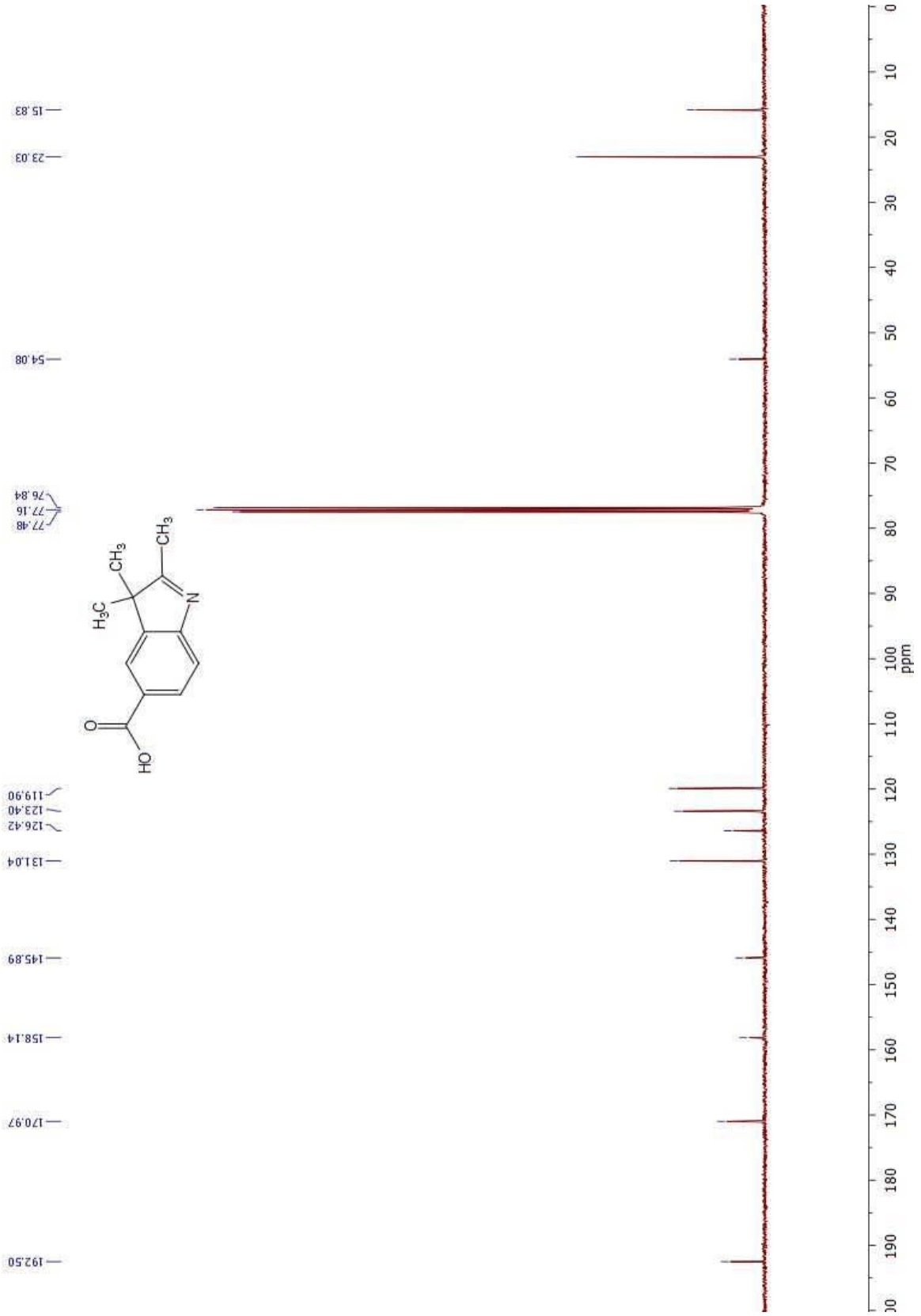
192.50
170.97
158.14
145.89
131.04
126.42
123.40
119.90
77.48
77.16
76.84
54.08
23.03
15.83
CH3
CH3
H3C
N
O
HO
ppm

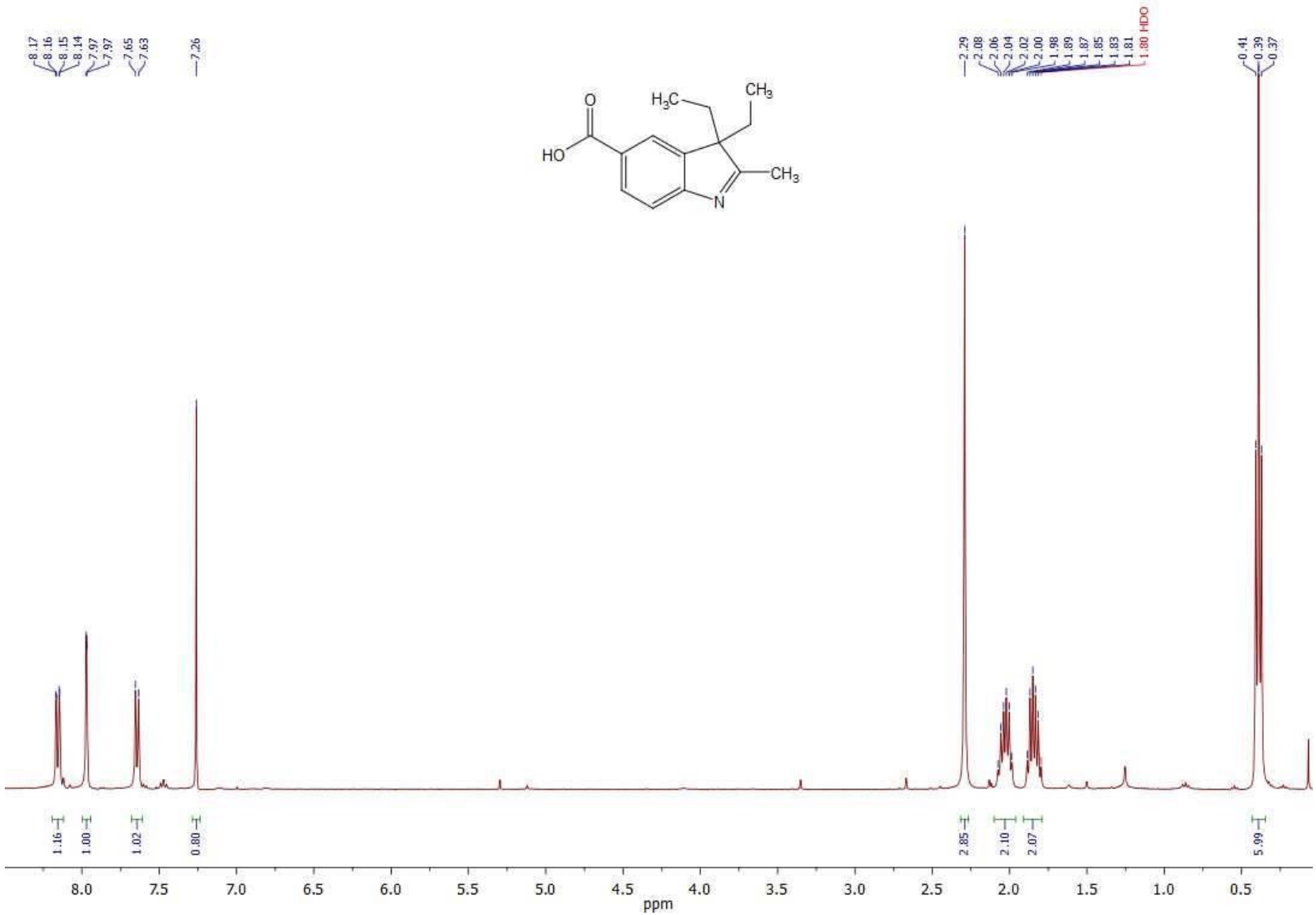
8.17
8.16
8.15
8.14
7.97
7.97
7.65
7.63
7.26
2.29
2.08
2.06
2.04
2.02
2.00
1.98
1.89
1.87
1.85
1.83
1.81
1.80 HDO
0.41
0.39
0.37
O
HO
H3C
CH3
CH3
N
1.16
1.00
1.02
0.80
2.85
2.10
2.07
5.99
8.0
7.5
7.0
6.5
6.0
5.5
5.0
4.5
4.0
3.5
3.0
2.5
2.0
1.5
1.0
0.5
ppm

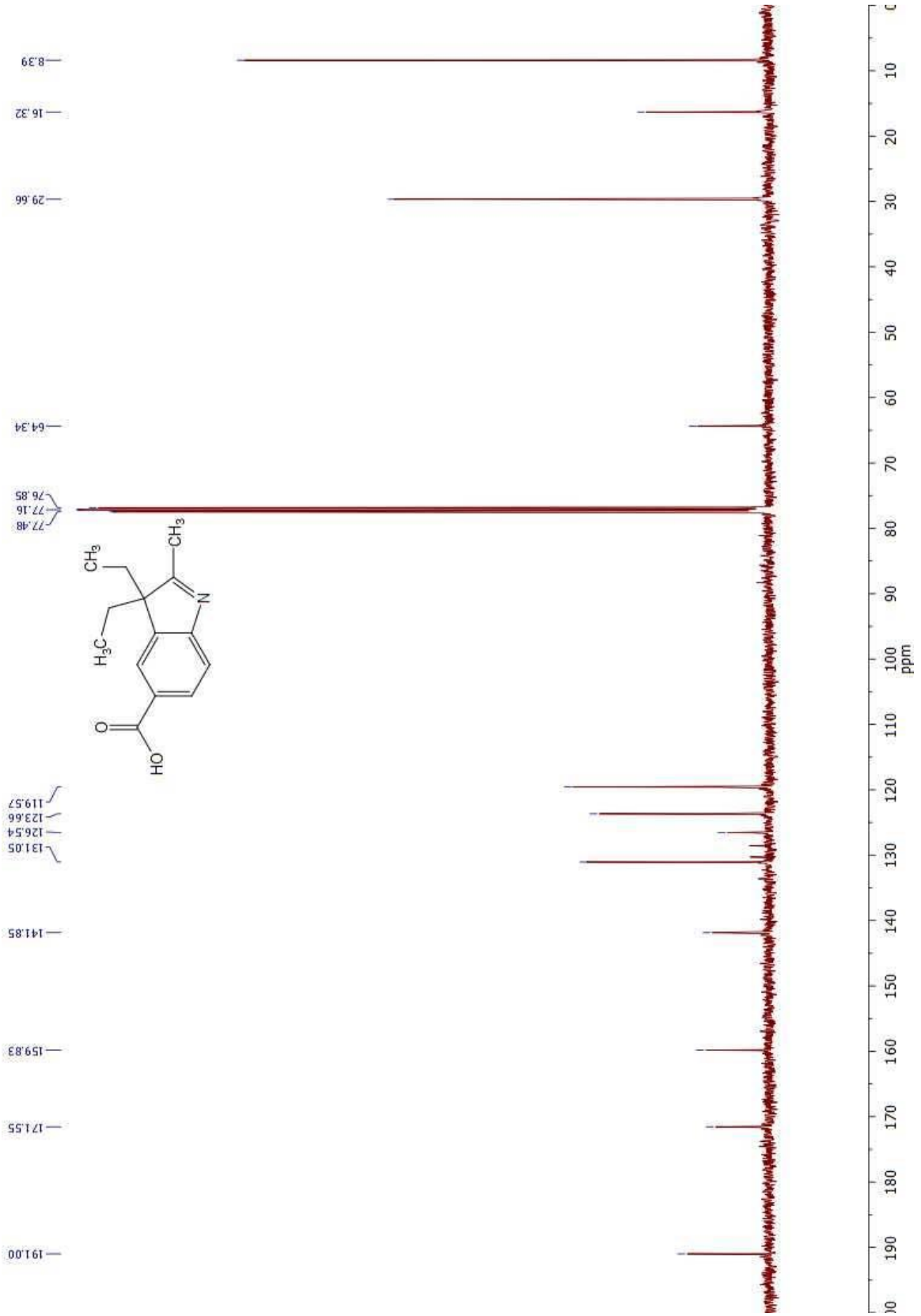
8.39
16.32
29.66
64.34
76.85
77.16
77.48
119.57
123.66
126.54
131.05
141.85
159.83
171.55
191.00
CH3
CH3
H3C
N
O
HO
ppm

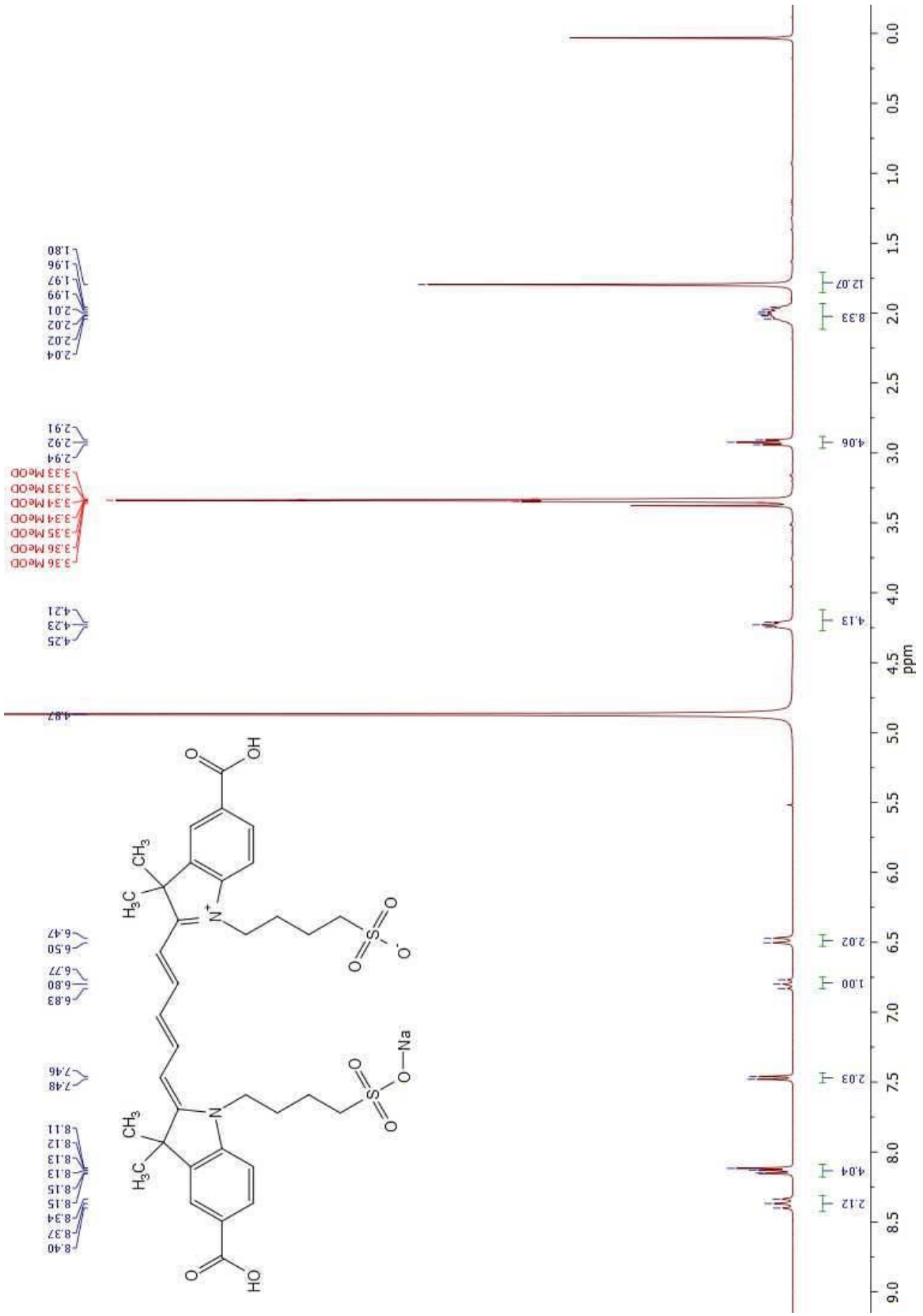
ppm
0.0
0.5
1.0
1.5
2.0
2.5
3.0
3.5
4.0
4.5
5.0
5.5
6.0
6.5
7.0
7.5
8.0
8.5
9.0
12.07
8.33
4.06
4.13
2.02
1.00
2.03
4.04
2.12
4.87
4.25
4.23
4.21
3.36 MeOD
3.35 MeOD
3.34 MeOD
3.34 MeOD
3.33 MeOD
3.33 MeOD
2.94
2.92
2.91
2.04
2.02
2.02
2.01
1.99
1.97
1.96
1.80
6.83
6.80
6.77
6.50
6.47
7.48
7.46
8.40
8.37
8.34
8.15
8.15
8.13
8.13
8.12
8.11
CH3
H3C
N+
S
O
O-
Na
OH
HO

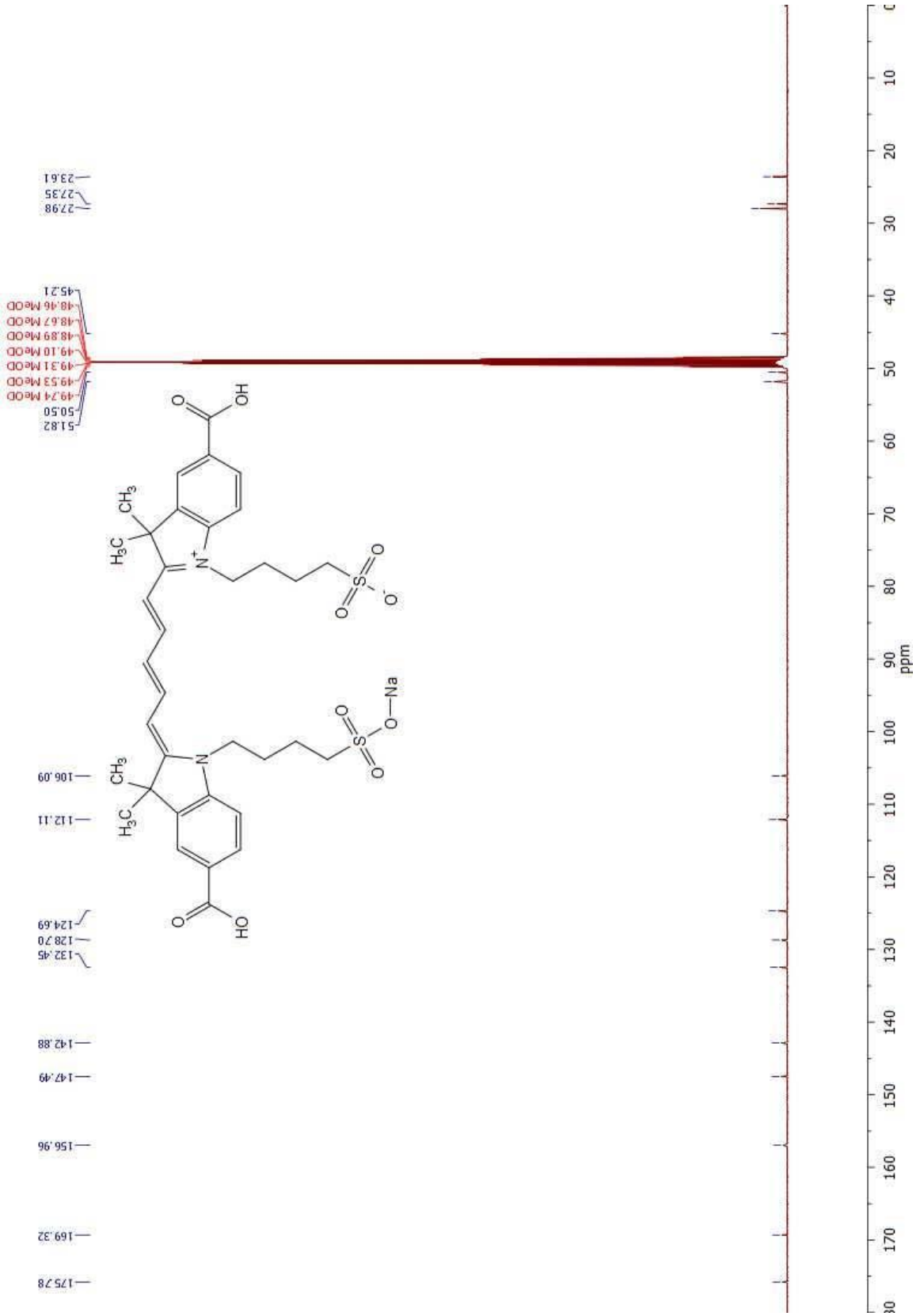
ppm
HO
O
OH
O
CH3
H3C
N+
S
O
O
O-
N
S
O
O
O—Na
CH3
H3C
HO
O
OH
O
23.61
27.35
27.98
45.21
48.46 MeOD
48.67 MeOD
48.89 MeOD
49.10 MeOD
49.31 MeOD
49.53 MeOD
49.74 MeOD
50.50
51.82
106.09
112.11
124.69
128.70
132.45
142.88
147.49
156.96
169.32
175.78

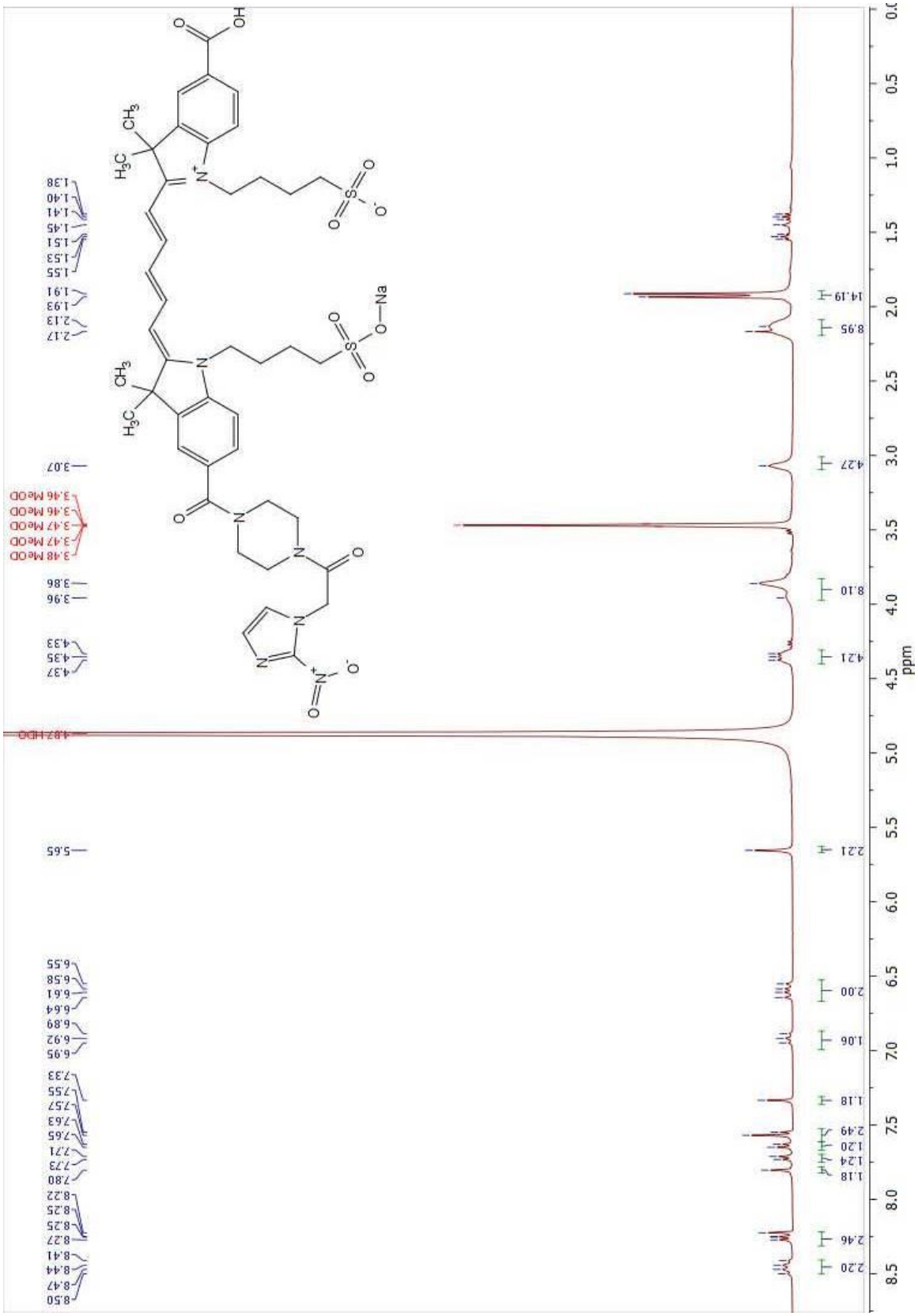

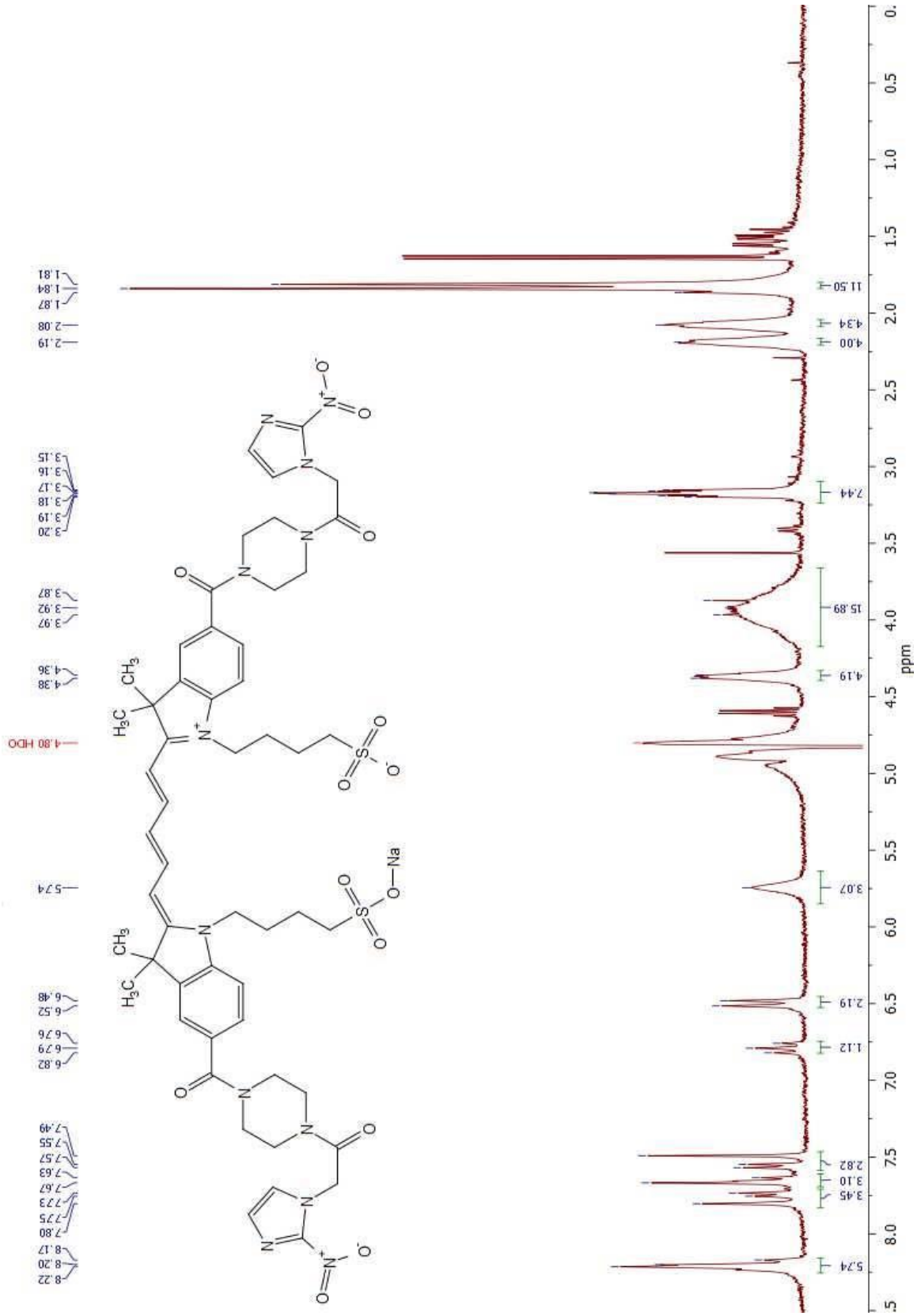

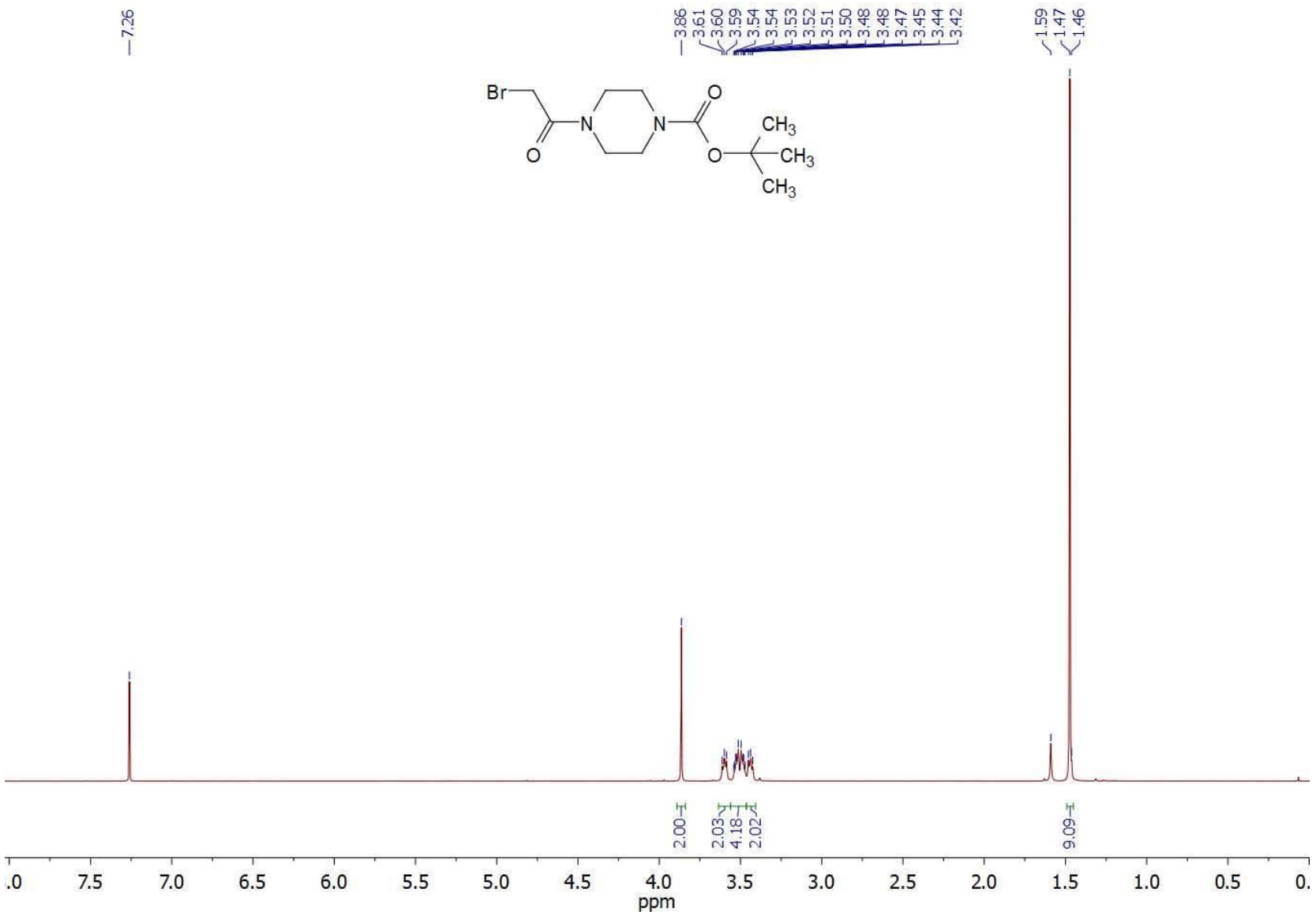
7.26
3.86
3.61
3.60
3.59
3.54
3.54
3.53
3.52
3.51
3.50
3.48
3.48
3.47
3.45
3.44
3.42
1.59
1.47
1.46
Br
O
N
N
O
O
CH3
CH3
CH3
2.00
2.03
4.18
2.02
9.09
ppm

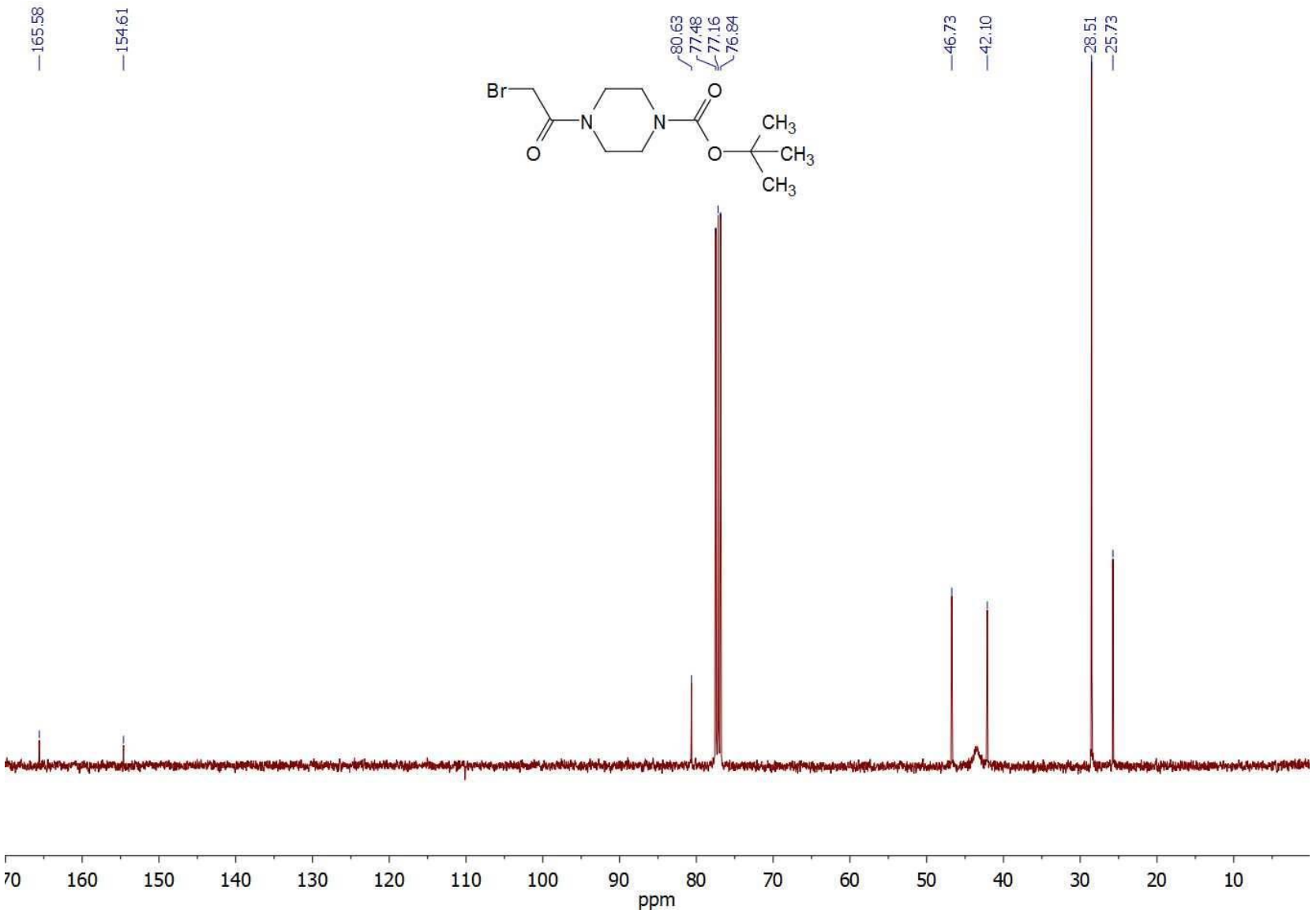
165.58
154.61
80.63
77.48
77.16
76.84
46.73
42.10
28.51
25.73
Br
N
N
O
O
O
CH3
CH3
CH3
70
160
150
140
130
120
110
100
90
80
70
60
50
40
30
20
10
ppm

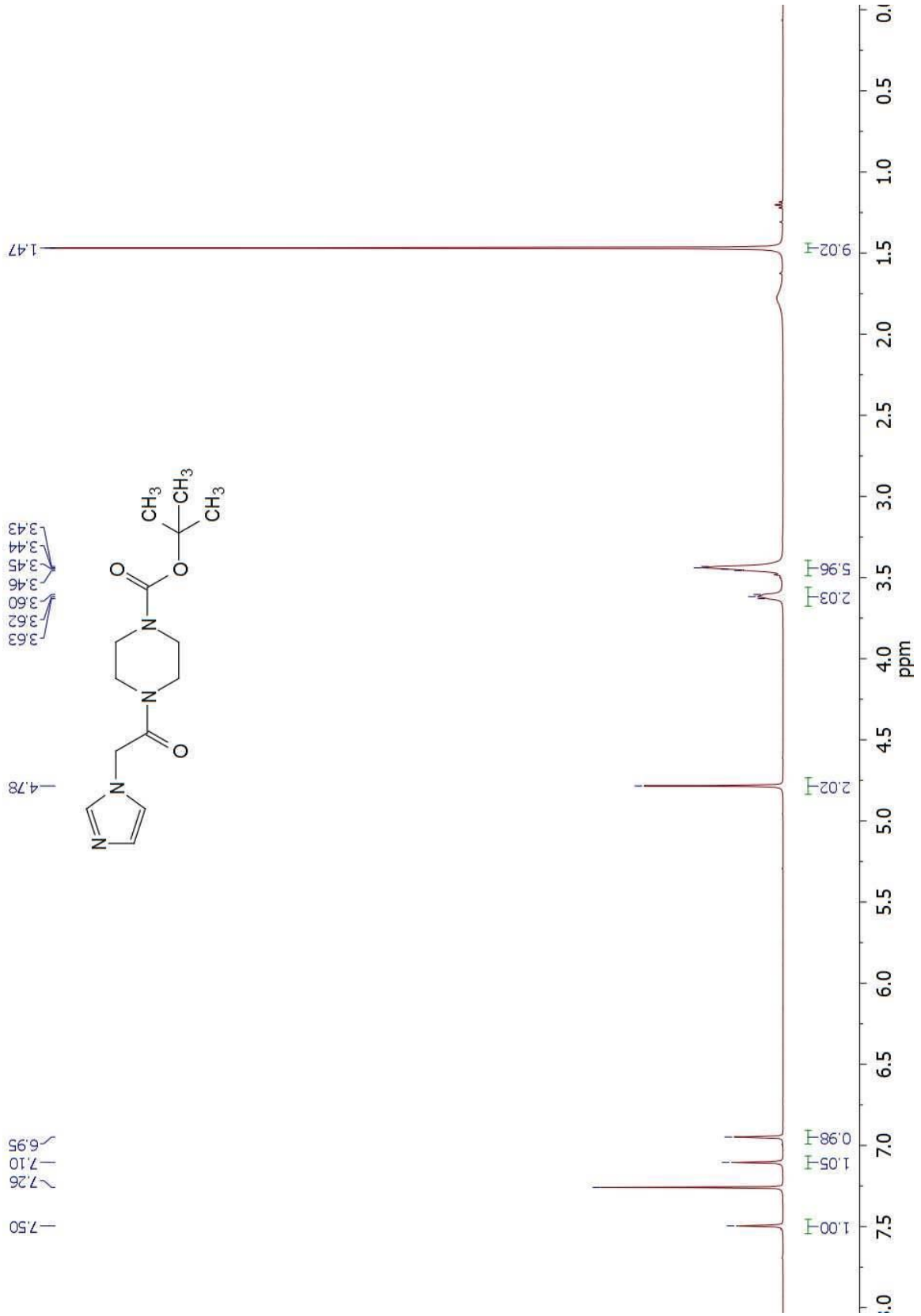
1.47
3.63
3.62
3.60
3.46
3.45
3.44
3.43
4.78
7.50
7.26
7.10
6.95
9.02
5.96
2.03
2.02
1.00
1.05
0.98
ppm

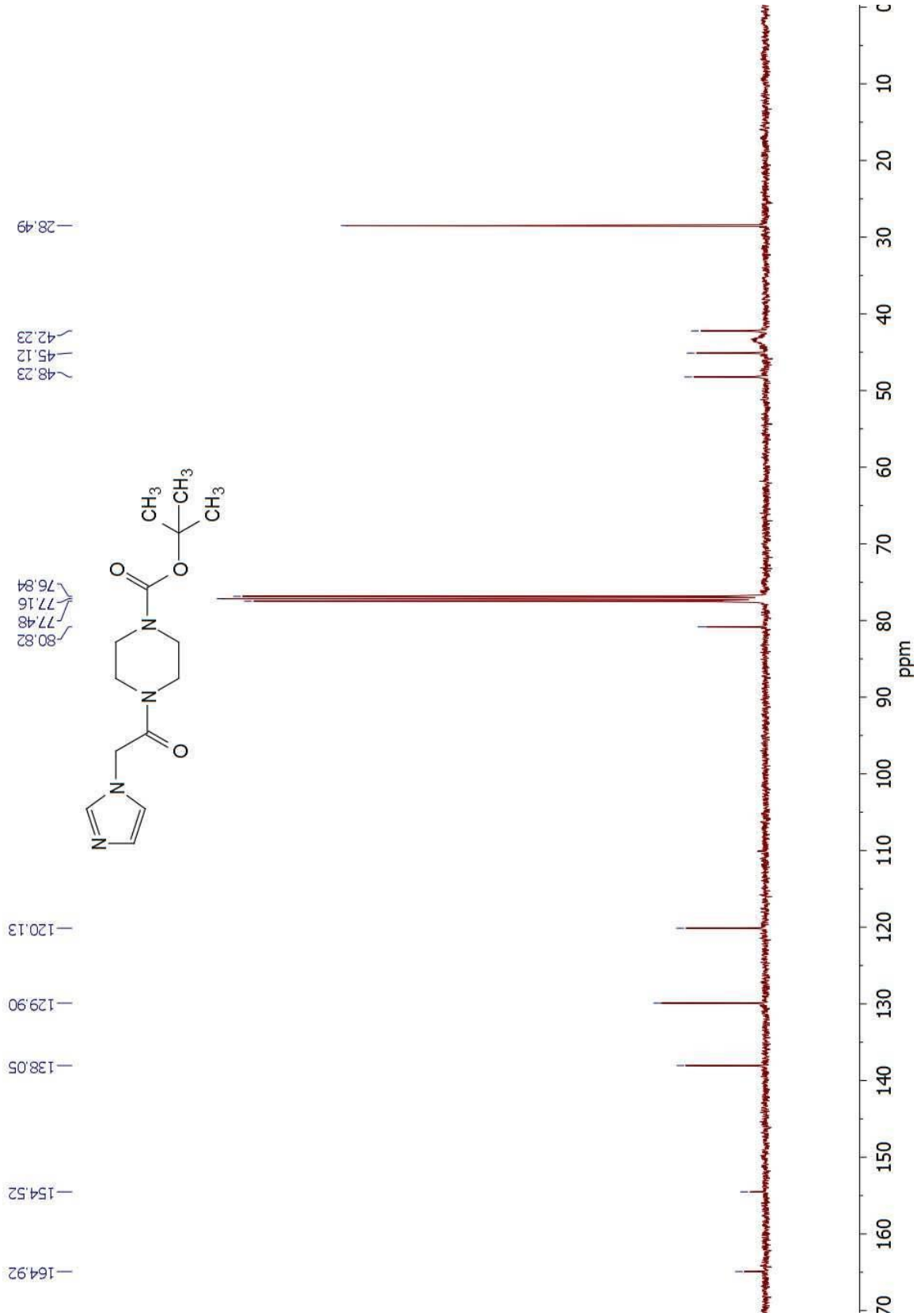
28.49
42.23
45.12
48.23
76.84
77.16
77.48
80.82
120.13
129.90
138.05
154.52
164.92
ppm

1.48
1.57
9.14
3.38
3.47
3.47
3.52
3.59
3.61
4.00
4.09
5.23
1.98
7.07
7.20
7.26
0.93
0.91
ppm

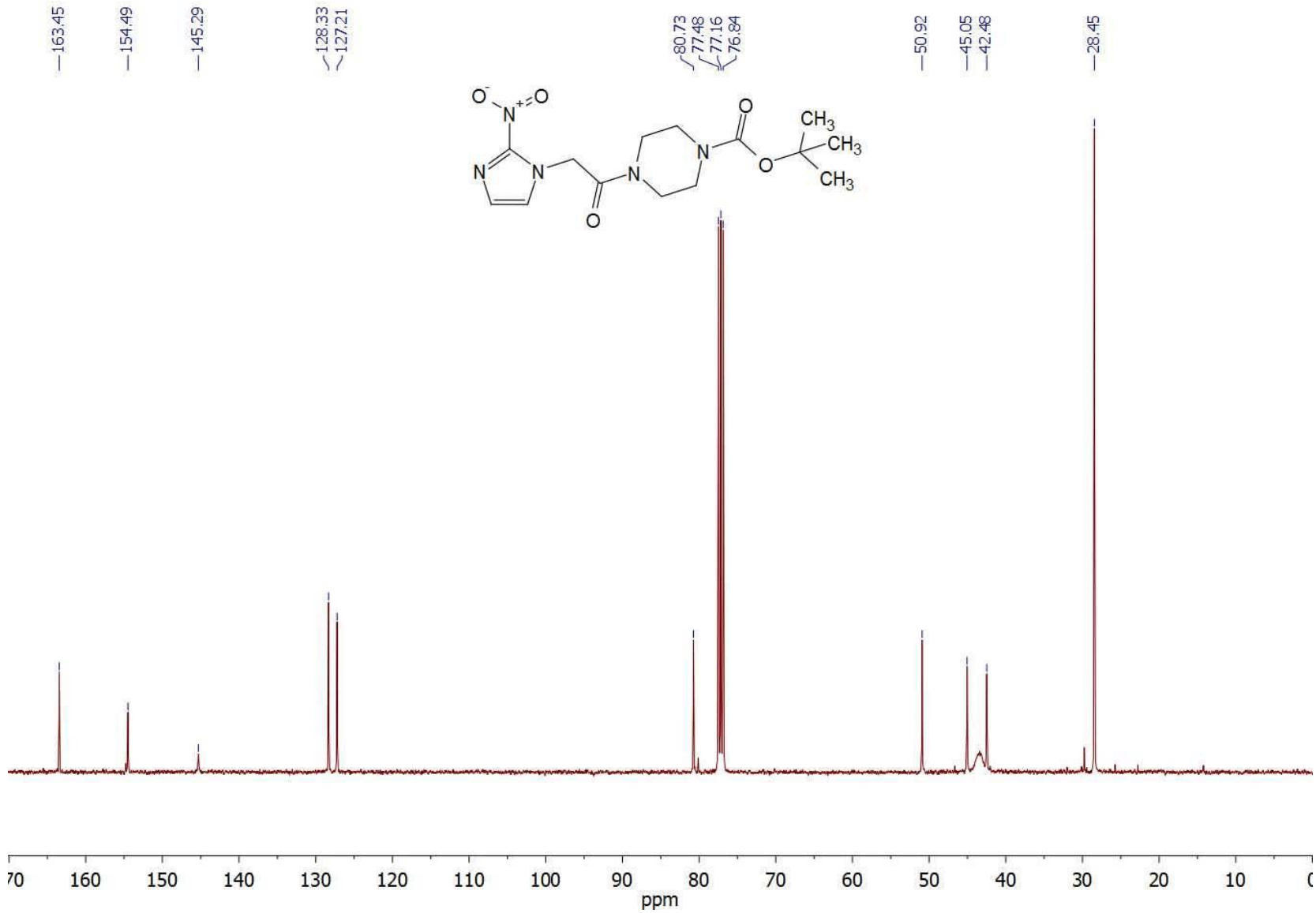
163.45
154.49
145.29
128.33
127.21
80.73
77.48
77.16
76.84
50.92
45.05
42.48
28.45
ppm

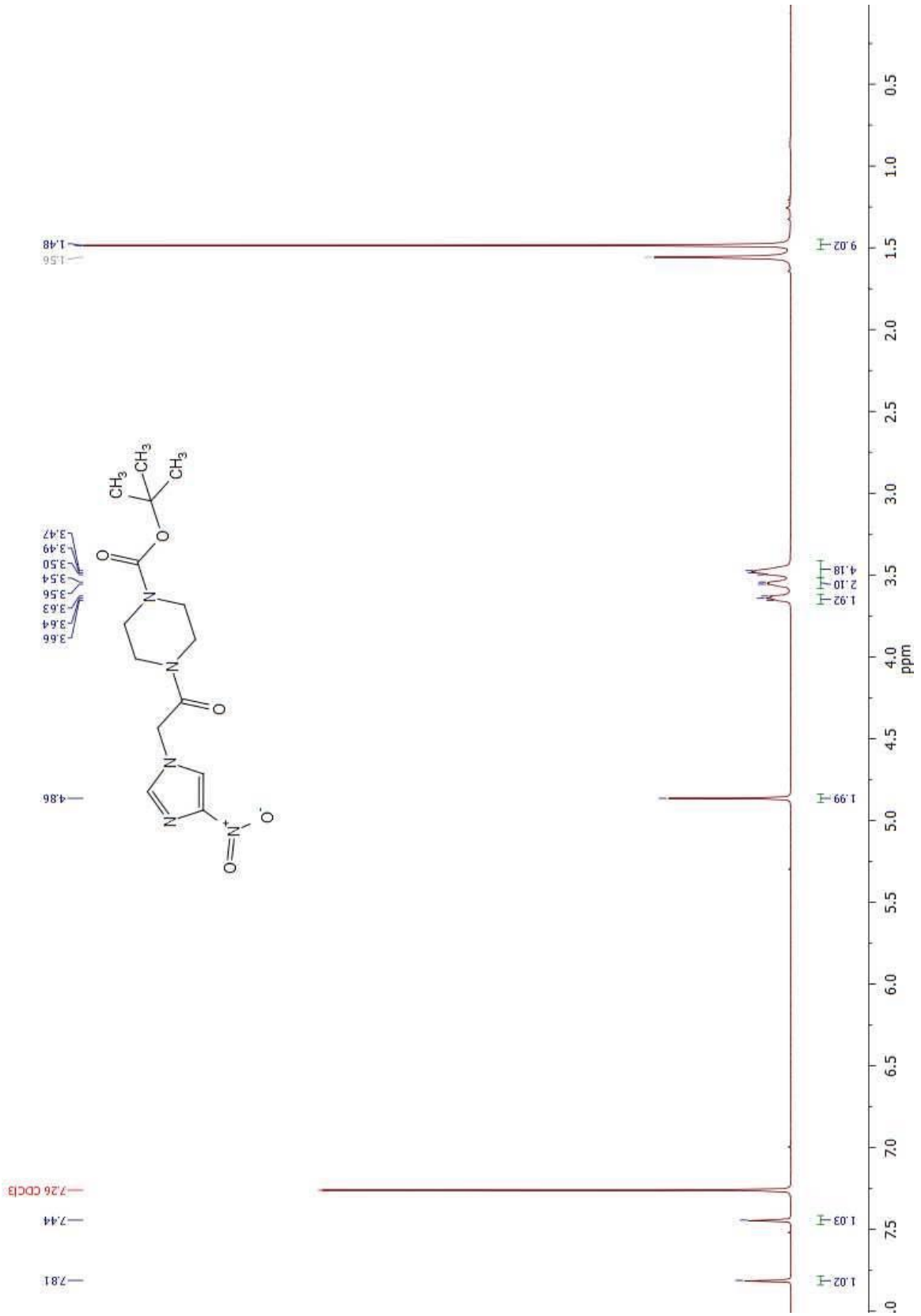
1.48
1.56
4.86
3.66
3.64
3.63
3.56
3.54
3.50
3.49
3.47
7.81
7.44
7.26 CDCl3
9.02
1.99
4.18
2.10
1.92
1.03
1.02
ppm

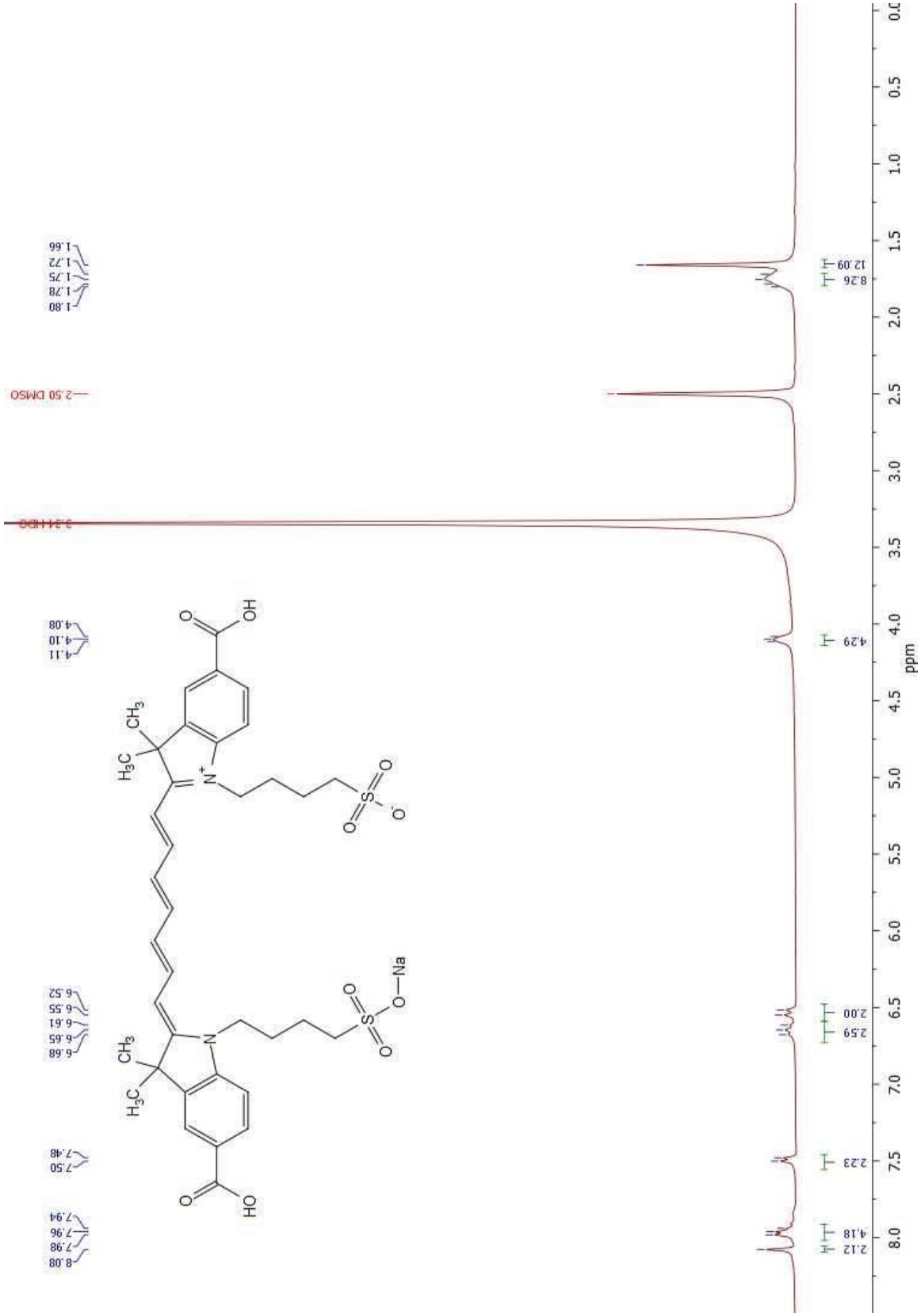
ppm
0.0
0.5
1.0
1.5
2.0
2.5
3.0
3.5
4.0
4.5
5.0
5.5
6.0
6.5
7.0
7.5
8.0
2.12
4.18
2.23
2.59
2.00
4.29
12.09
8.26
1.80
1.78
1.75
1.72
1.66
2.50 DMSO
3.31 HDO
4.11
4.10
4.08
6.68
6.65
6.61
6.55
6.52
7.50
7.48
8.08
7.98
7.96
7.94
OH
O
CH3
H3C
N+
S
O
O-
Na

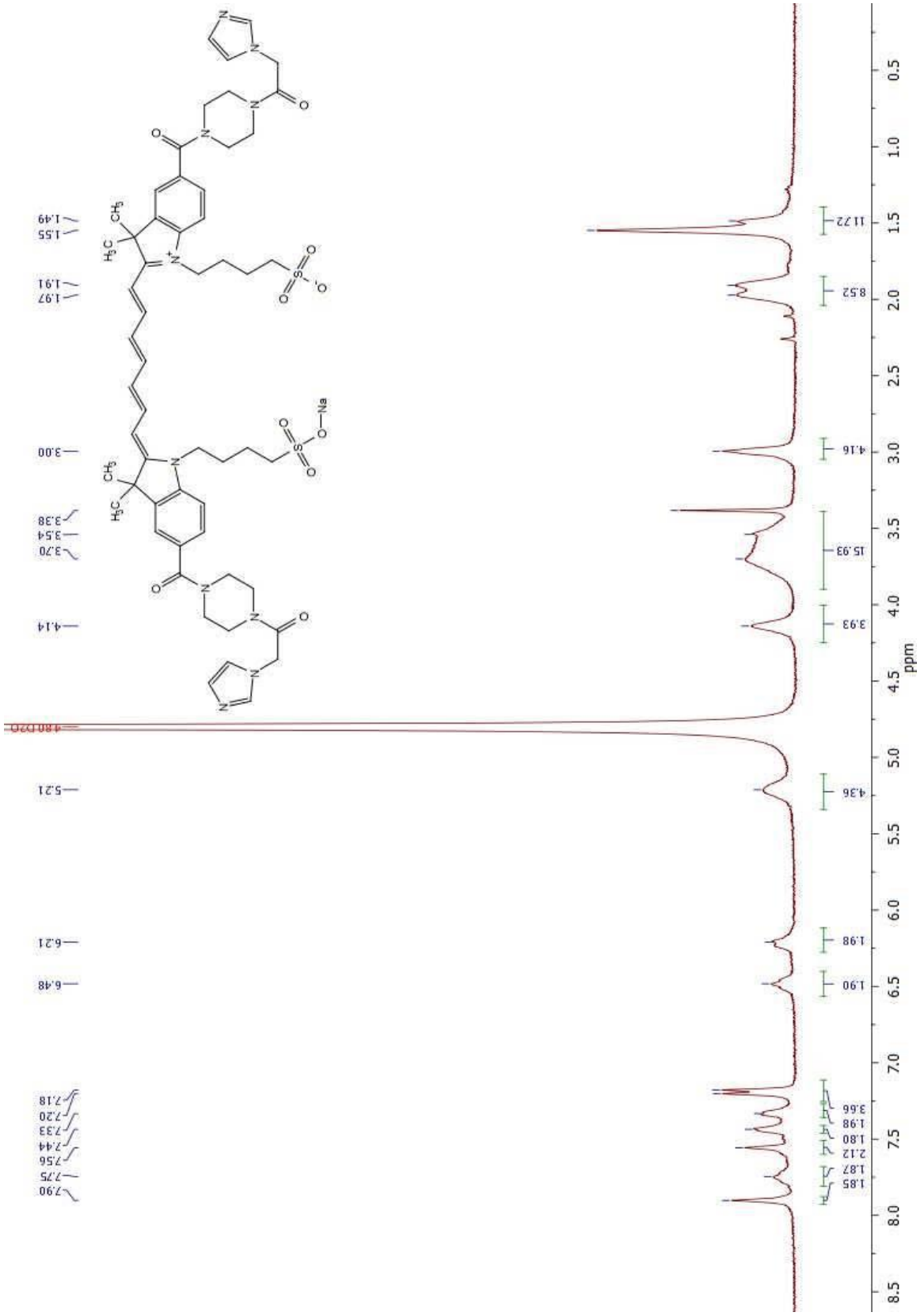
ppm

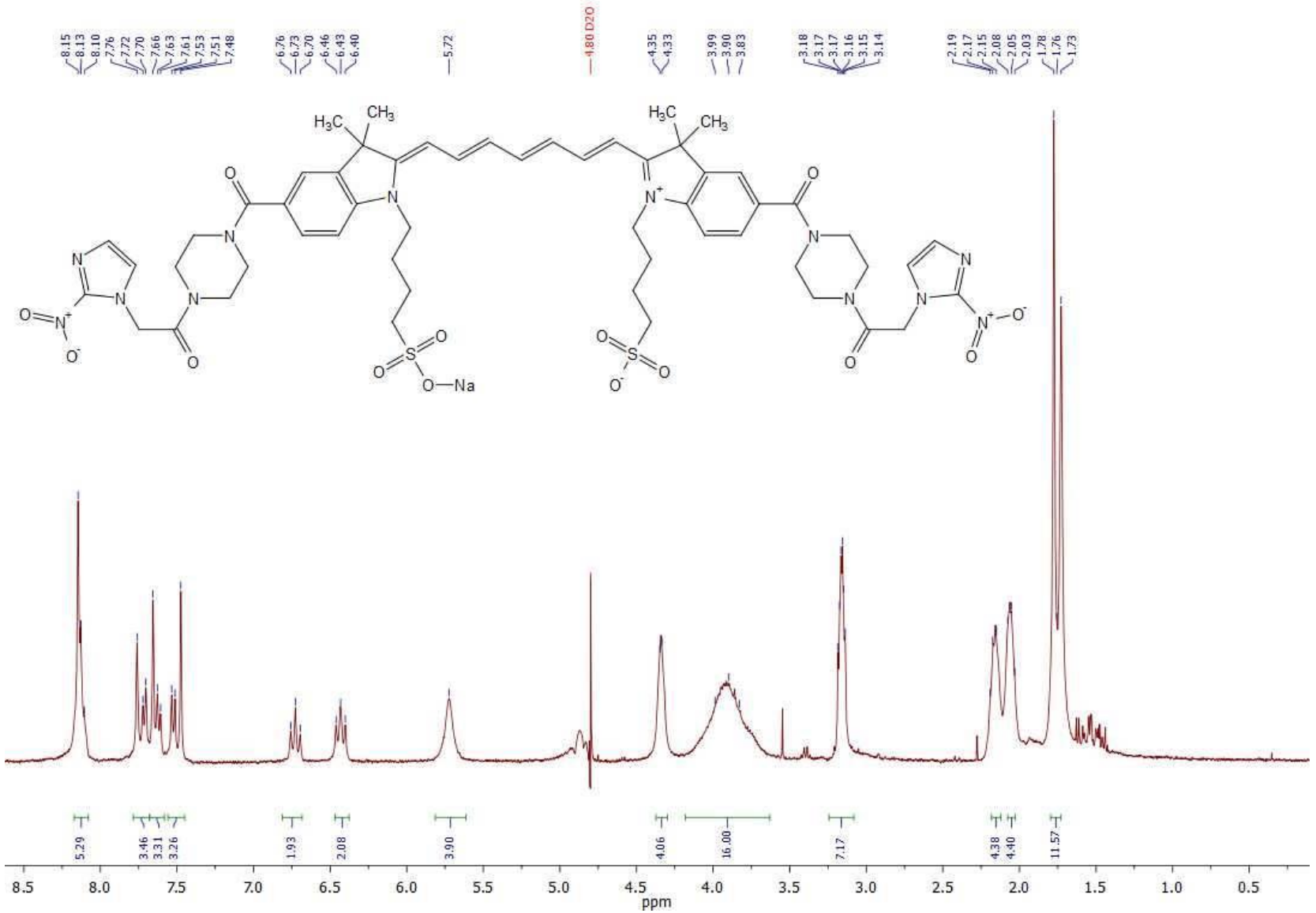
8.15
8.13
8.10
7.76
7.72
7.70
7.66
7.63
7.61
7.53
7.51
7.48
6.76
6.73
6.70
6.46
6.43
6.40
5.72
4.80 D2O
4.35
4.33
3.99
3.90
3.83
3.18
3.17
3.17
3.16
3.15
3.14
2.19
2.17
2.15
2.08
2.05
2.03
1.78
1.76
1.73
5.29
3.46
3.31
3.26
1.93
2.08
3.90
4.06
16.00
7.17
4.38
4.40
11.57
8.5
8.0
7.5
7.0
6.5
6.0
5.5
5.0
4.5
4.0
3.5
3.0
2.5
2.0
1.5
1.0
0.5
ppm

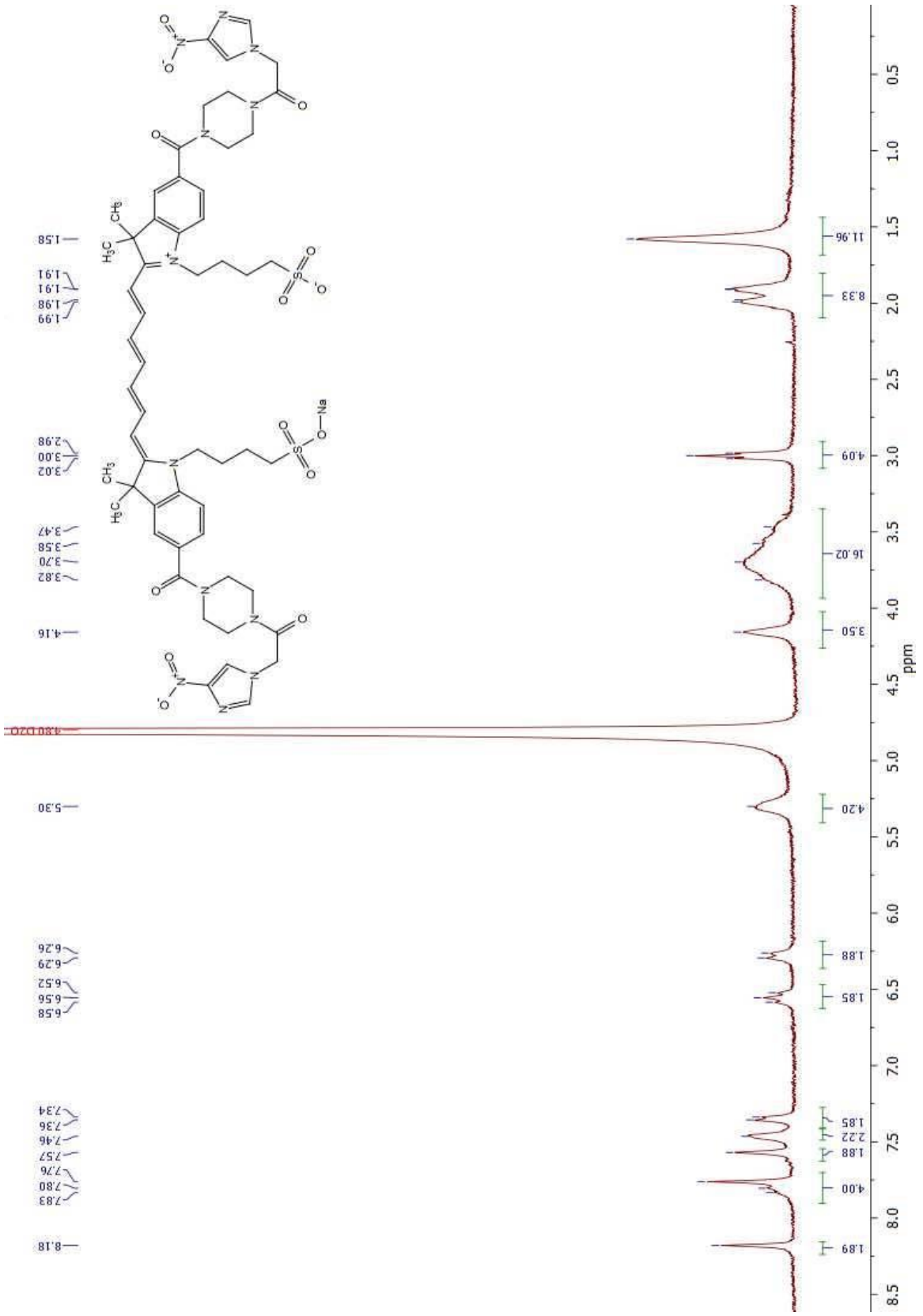
ppm

2.5 References

1. American Cancer Society. Cancer Facts & Figures 2016. Atlanta: American Cancer Society; **2016**.
2. Hanahan, D.; Weinberg, R. A. **2000**, *Cell*, 100, 57–70.
3. Thippeswamy, R.; Noronha, V.; Krishna, V.; Joshi, A.; Bal, M. M.; Purandare, N.; Rangarajan, V.; Pramesh, C. S.; Jiwnani, S.; Prabhash, K. *Indian J. Med. Paediatr. Oncol*. **2013**, 34, 121-125.
4. Raleigh, J. A.; Dewhirst, M. W.; Thrall, D. E. *Sem. Rad. Oncol*. **1996**, 6, 37-43.
5. Moulder, J. E.; Rockwell, S. *Cancer Metast. Rev* **1987**, 5, 313-341.
6. Cater D. B.; Silver I. A. *Acta. Radio.* **1960**, 153, 233-256.
7. Stone H. B.; Brown J. M.; Phillips T. L.; Sutherland R. M. *Radiat. Res*. **1993**, 136, 422-434.
8. Thorwarth, D.; Leibfarth, S.; Monnich, D. Clin. Transl. Imaging 2013, 1, 45-51.
9. Nestle U, Weber W, Hentschel M, Grosu AL (2009) Biological imaging in radiation therapy: role of positron emission tomography. Phys Med Biol 54:R1–R25
10. Vavere, A. L.; Lewis, J. S. Dalton Trans. 2007, 4893-4902.
11. Ziemer, L. S.; Evans, S. M.; Kachur, A. V.; Shuman, A. L.; Cardi, C. A.; Jenkins, W. T.; Karp, J. S.; Alavi, A.; Dolbier Jr., W. R.; Koch, C. J. *Eur. J. Nuc. Med. Mol. Imag*. **2003**, 30, 259-266.
12. van der Heide UA, Houweling AC, Groenendaal G, Beets-Tan RG, Lambin P (2012) Functional MRI for radiotherapy dose painting. Magn Reson Imaging 30:1216–1223.
13. Weissleder, R. *Nature Biotechnology* **2001**, 19, 316 – 317.

14. (a) Guo, Z.; Park, S.; Yoon, J.; Shin, I. *Chem. Soc. Rev*. **2014**, 43, 16–29. (b) Corlu, A.; Choe, R.; Durduran, T.; Rosen, M. A.; Schweiger, M.; Arridge, S. R.; Schnall, M. D.; Yodh, A. G. *Opt. Express* **2007**, 15, 6696–6716. (c) Aldrich, M.; Davies-Venn, C.; Angermiller, B.; Robinson, H.; Chan, W.; Kwon, S.; Sevick-Muraca, E. M. *Lymphat. Res. Biol*. **2012**, 10, 20–24. (d) Rockwell, S.; Dobrucki, I. T.; Kim, E. Y.; Marrison, T.; Vu, V. T. *Curr. Mol. Med*. **2009**, 9, 442-458.

15. Varghese, A. J.; Gulyas, S.; Mohindra, J. K. *Cancer Res*., **1976**, 36, 3761–3765.

16. (a) Kling, J. *Nat. Biotechnol*., **2012**, 30, 381. (b) Varia, M. A.; Calkins-Adams, D. P.; Rinker, L. H.; Kennedy, A. S.; Novotny, D. B.; Fowler, W. C.; Raleigh, J. A. Gynecologic Oncology 1998, 71, 270-277. (c) Kizaka-Kondoh, S.; Konsse-Nagasawa, H. *Cancer Sci*. **2009**, 100, 1366-1373.

17. Elmes, R. B. P. Chem. Commun. 2016, 52, 8935-8956.

18. (a) Melo T.; Ballinger J. R.; Rauth A. M. *Biochem. Pharmacol*. **2000**, 60, 625–634. (b) Wang Y.; Gray J. P.; Mishin V.; Heck D. E.; Laskin D. L.; Laskin J. D. *Free Radic. Biol. Med* **2008**, 44, 1169–1179. (c) Kizaka-Kondoh, S.; Konsse-Nagasawa, H. *Cancer Sci.* **2009**, 100, 1366–1373.

19. (a) Lindsey, J. S.; Brown, P.A.; Siesel, D. A. *Tetrahedron* **1989**, 45, 4845-4866. (b) Terpetschning, E.; Szmacinski, H.; Ozinskas, A.; Lakowicz, J. R. *Anal. Biochem*. **1994**, 217, 197-204. (c) Licha, K.; Riefke, B.; Ntziachristos, V.; Becker, A.; Chance, B.; Semmler, W. *Photochem. Photobio*. **2000**, 72, 392-398.

20. Pavlik, C.; Biswal, N. C.; Gaenzler, F. C.; Morton, M. D.; Kuhn, L. T.; Claffey, K. P.; Zhu, Q.; Smith, M. B. *Dyes and Pigments* **2011**, 89, 9–15.

21. Biswal, N. C.; Pavlik, C.; Smith, M. B.; Kuhn, L. T.; Claffey, K. P.; and Q. Zhu, Biomedical Optics, OSA Technical Digest (CD), paper JMA92, Optical Society of America **2010**.

22. Biswal, N. C.; Pavlik, C.; Smith, M. B.; Aguirre, A.; Xu, Y.; Zanganeh, S.; Kuhn, L. T.; Claffey, K. P.; Zhu, Q. *J. Biomed. Optics* **2011**, 16, 066009.

23. Xu, Y.; Zanganeh, S.; Mohammad, I.; Aguirre, A.; Wang, T.; Yang, Y.; Kuhn, L.; Smith, M. B.; Zhu, Q. *J. Biomedical Optics* **2013**, 18, 066009.

24. G. Barker, P. O'Brien, and K. R. Campos, *Org. Lett*. **2010**, 12, 4176–4179.

25. Imaeda, Y.; Kuroita, T.; Sakamoto, H.; Kawamoto, T.; Tobisu, M.; Konishi, N.; Hiroe, K.; Kawamura, M.; Tanaka, T.; Kubo, K. *J. Mad. Chem*. **2008**, 51, 3422-3436.

26. Wang, Z.; Gu, C.; Colby, T.; Shindo, T.; Balamurugan, R.; Waldmann, H.; Kaiser, M.; van der Hoorn, R. A. *Nature Chem. Bio*. **2008**, 4, 557-563.

27. Xu, Y.; Zanganeh, S.; Mohammad, I.; Aguirre, A.; Wang, T.; Yang, Y.; Kuhn, L.; Smith, M. B.; Zhu, Q. *J. Biomed. Opt*. **2013**, 18, 066009.

28. (a) Fitzpatrick, D. A.; Heindel, N. D.; Egolf, R. A.; Walton H. *Radiat Res* **1989**, 117,47-58. (b) Stratford, I. J.; Williamson, C.; Hardy, C. *Brit. J. Cancer* **1981**, 44, 109-116. (c) Chan, P. K. L.; Skov, K. A.; James, B. R. *Int J Radiat Biol* **1987**, 52, 49-55.

29. Abuteen, A.; Zhou, F.; Dietz, C.; Mohammad, I.; Smith, M. B.; Zhu, Q. *Dyes and Pigments*, **2016**, 251-260.

30. Mohammad, I.; Stanford, C.; Morton, M.; Zhu, Q.; Smith, M. B. *Dyes and Pigments*, **2013**, 99, 275-283.

31. Feifei, Z.; Zanganeh, S.; Mohammad, I.; Dietz, C.; Abuteen, A.; Smith, M. B.; Zhu, Q. *Org. Biomol. Chem*. **2015**, 13, 11220-11227.

32. Dundas, C. M.; Demonte, D.; Park, S. *Appl. Microbiol. Biotechnol*. **2013**, 97, 9343-9353.

33. Brglez, J.; Ahmed, I.; Niemeyer, C. M. *Org. Biomol. Chem*. **2015**, 13, 5102-5104.